Univerza v Ljubljani
Zdravstvena fakulteta

6TH 2021 SOCRATIC LECTURES

SOCRATIC LECTURES

6TH INTERNATIONAL SYMPOSIUM, LJUBLJANA, SLOVENIA, DECEMBER 11, 2021

PEER REVIEWED PROCEEDINGS

EDITED BY: VERONIKA KRALJ-IGLIČ

UNIVERSITY OF LJUBLJANA, FACULTY OF HEALTH SCIENCES

Socratic lectures
6th International Minisymposium, Ljubljana, December 11, 2021
Peer Reviewed Proceedings

Edited by Prof. Veronika Kralj-Iglič, Ph.D.
Reviewers: Karin Schara, M.D., Ph.D., Prof. Rok Vengust, M.D., Ph.D.

Published by: University of Ljubljana Press
For the publisher: Gregor Majdič, The Rector
Issued by: University of Ljubljana, Faculty of Health Sciences
For the issuer: Andrej Starc, The Dean

Design: Anna Romolo
Image on the front page: Lupe; Photo: Eva Osolnik

First Digital edition.
Publication is available online in PDF format at: https://www.zf.uni-lj.si/images/stories/datoteke/Zalozba/Sokratska_6.pdf

DOI: 10.55295/PSL.2021.D

Publication is free of charge.

Ljubljana, 2022

Kataložni zapis o publikaciji (CIP) pripravili v Narodni in univerzitetni knjižnici v Ljubljani
COBISS.SI-ID 97123587
ISBN 978-961-7128-20-8 (PDF)

The members of the Organizing Committee of Socratic Lectures: Jasna Dokl Osolnik, Vladimira Erjavec, Tjaša Griessler Bulc, Marija Holcar, Aleš Iglič, Monika Jenko, Boštjan Kocjančič, Tara Kostanjšak, Veronika Kralj-Iglič, Tomaž Lampe, Vid Lisjak, Boris Mankowsky, Gabriella Pocsfalvi, Anita Prelovšek, Anna Romolo, Karin Schara, Duško Spasovski, Polonca Trebše

Program

Socratic Symposium December 11, 2021, 10:00 – 20:00 (Ljubljana time)

Plenary lecture

10:00 - 10:45 **Antonella Bongiovanni, Italy:** Green bioparticles for cross-kingdom communication: a drug delivery platform designed by nature

11.00 - 13.00 Scientific sections

Section 1: Medicine organized and moderated by **Karin Schara** and **Boris Mankowsky**

11.00 - 11.30 **Boris Mankowsky, Ukraine:** Neuropathy and the brain
11.30 - 12.00 **Karin Schara, Slovenia:** Neuropathic diabetic foot
12.00 - 12.30 **Iris Marolt, Slovenia:** Approach to diabetic foot during/beyond coronavirus pandemic
12.30 - 13.45 **Marija Ipavec, Slovenia:** Experience with above knee endoprosthesis
13.45 - 14.00 **Maja Penko, Slovenia:** Evaluation of walking and running biomechanics with accelerometers in transtibial amputee

Section 2: Veterinary Medicine organized and moderated by **Vladimira Erjavec** and **Tara Kostanjšak**

11.00 - 11.20 **Metka Šimundić, Slovenia:** Internistic problems of brachicephalic dogs
11.20 - 11.40 **Žiga Žgank, Alenka Nemec, Vladimira Erjavec, Slovenia:** Blood lactate, body temperature and pulse before, during and after submaximall excercise in dogs with brachycephalic obstructive syndrome.
11.40 - 12.00 **Vladimira Erjavec, Barbara Lukanc, Croatia:** Surgical treatment of brachycephalic syndrome
12.00 - 12.20 **Tara Kostanjšak, Croatia:** Postoperative care in brachycephalic dogs
12.20 - 12.40 **Ana Smajlović, Croatia:** Heat stroke in barchycephalic dogs
12.40 - 13.00 **Vladimira Erjavec, Alenka Nemec Svete, Croatia:** Selected parameters of venous blood gas analysis in brachycephalic dogs with brachycephalic obstructive airway syndrome before and after surgical treatment

Section 3: Orthopaedics organized and moderated by **Boštjan Kocjančič** and **Duško Spasovski**

11.00 - 11.30 **Drenka Trivanović, Germany:** Bone marrow adipose tissue in hip bones: identification of progenitors, transcriptome and metabolic profile
11.30 - 11.45 **Torsten Blunk, Germany:** 3D Bioprinting of mesenchymal stromal cells in hyaluronic acid-based bioinks for cartilage regeneration
11.45 - 12.00 **Duško Spasovski, Serbia:** Treatment of cartilage degeneration with stem cells
12.00 - 12.15 **Matej Daniel, Czech Republic:** Modeling of hip fracture due to internal forces
12.15 - 12.30 **Boštjan Kocjančič, Slovenia:** Perspective of orthopaedic surgeon on blood saving
12.30 - 12.45 **Fabio Valenti, Slovenia:** The effect of somatosensory stimulation on quiet standing or balance control
12.45 - 13.00 **Klara Smolič, Slovenia:** The influence of foot type and footwear on performance in sports shooting

Section 4: Biocompatible materials organized and moderated by **Monika Jenko** and **Tomaž Lampe**

11.00 - 11.30 **Monika Jenko, Drago Dolinar, Slovenia:** Biomaterials and their biocompatibility in endoprosthetics

11.30 - 12.00 **Barbara Šetina Batič, Slovenia:** Imaging of materials with Scanning Electron Microscope

12.00 - 12.15 **Julija Balon, Slovenia:** Corrosion resistance of titanium implants with TiO2 coating

12.15 - 12.30 **Zala Jan, Slovenia:** Effect of corund on HUVEC and MG-63 cells

12.30 - 13.00 **Aljaž Muršec, Slovenia:** Frequancy of amputations and prosthetic care of dogs and needs for animal prosthetics specialists

Section 5: Ecology organized and moderated by **Tjaša Griessler Bulc** and **Polonca Trebše**

11.00 - 11.45 **Lara Čižmek, Ana Martić, Rozelindra Čož-Rakovac, Polonca Trebše, Croatia:** Evaluation of antioxidant activity of three different brown macroalgae by implementing electrochemistry and spectrophotometry: Correlation and future prospects

11.45 - 12.30 **Anja Vehar, Ana Kovačič, Nadja Hvala, David Škufca, Marjetka Levstek, Marjetka Stražar, Andreja Žgajnar Gotvajn, Ester Heath, Slovenia:** Fate of bisphenols during conventional wastewater

12.30 - 13.00 **Nina Lekše, Tjaša Griessler Bulc, Andreja Žgajnar Gotvajn, Slovenia:** Oil extraction of microplastics from communal dewatered sludge.

Section 6: Physics organized and moderated by **Aleš Iglič**

11.00 - 11.30 **Irene Cannata, Italy:** Hundred years from the Nobel prize for the discovery of the law of photoelectric effect.

11.30 - 12.00 **Raj Kumar Sadhu, Israel:** Theoretical model of efficient phagocytosis driven by curved membrane proteins and active cytoskeleton forces

12.00 - 12.15 **Luka Mesarec, Slovenia:** The Big Bang theory

12.15 - 12.30 **Mitja Drab, Slovenia:** Numerical studies of surfactant and vesicle interactions

12.30 - 12.45 **Samo Penič, Slovenia:** Experimental measurement of bending elasticity of phospholipid vesicles by non-invasive method

12.45-13.00 **Gregor Hojkar, Slovenia:** Use of Markov/Gibbs random fields in segmentation and noise analysis of two-dimensional images

Section 7: Extracellular Vesicles organized and moderated by **Marija Holcar** and **Gabriella Pocsfalvi**

11.00 - 11.15 **Ana Paulina Ramos Juarez, Italy:** Heterogeneity of plasma derived vesicles and their separation into discrete subpopulations

11.15- 11.30 **Tecla Marangon, Ireland:** Mesenchymal Stem cell derived EVs and their role in bone regeneration

11.30 – 11.45 **Ivana Sedej, Slovenia:** Urinary extracellular vesicles as biomarkers of kidney allograft injury

11.45 – 12.00 **Tina Levstek, Slovenia:** Urinary extracellular vesicles and their miRNA cargo in patients with Fabry disease

12.00 – 12.15 **Ula Štok, Slovenia:** Overview of extracellular vesicles in antiphospholipid syndrome

12.15 - 12.30 **Saša Koprivec, Slovenia:** Extracellular vesicles from canine mesenchymal stem cells and their potential applications in veterinary therapy

12.30 – 12.45 **Anja Černoša, Slovenia:** Fungal Extracellular Vesicles: What we (don't) know

12.45 – 13.00 **Marko Jeran, Slovenia:** Small cellular particles from European spruce

Section 8: Science meets art organized and moderated by **Jasna Dokl Osolnik** and **Anita Prelovšek**

13.00 - 13.20 **Elena Ernstovna Komarova, Alla Shapovalova Ozdural, Russia**: Semiotic and trans-cultural aspects of Bach's music in St. John's passion

13.20 - 13.40 **Petra Stipančić, Slovenia:** Archeologic treasures of the Museum of Dolenjska

13.40 - 14.00 **Špela Šubic, Barbara Predan, Slovenia:** The pioneering research practices of designer Janja Lap

14.00 - 14.20 **Larina Griessler, Irena Samide, Slovenia:** Transcultural aspects in Lili Novy's life and work

14.20 - 14.40 **Nelfi Paliska, Slovenia:** Europe on the edge of precipice - Lehár, Ahtik and Wulz

20.00 Closing Ceremony

Concert of organist Roberta Schmid, Italy, at Francescan Church of Assumption, Prešernov trg, Ljubljana

Program

J.S. Bach Choral Ich ruf zu dir, Herr Jesu Christ BWV 639
J.S. Bach Toccata and Fugue in D minor BWV 565
J. Pachelbel Ciacona in F minor
P. A. Yon Toccatina for flute
E. Gigout Toccata in B minor
M. Mussorgsky Old castle (from Pictures at an exhibition – trancription of J. Guillou)
J.G. Rheinberger Passacaglia
L. Boellmann Suite Gothique op.25: Introduction-Choral, Menuet Gothique, Prière a Notre Dame, Toccata

Editorial

The 6.th symposium Socratic Lectures was the fourth one taking place online. Focusing on students, the online teaching of Biophysics and Biomechanics was found to be convenient for physical problem solving. Furthermore, online presentations supported scientific excellence as we could invite the world top experts on the fields for literally no material input. The colleagues generously donated their lectures, in the spirit of Socrates. As every time since 2008 when Socratic lectures were organized for the first time, I was amazed and grateful for the willingness that brought these gifts to the colleagues and in particularly, to students. Evident from the program, this symposium exceeded all previous ones in number and diversity of scientific sections. Also we were wellcoming contributions from two national museums: Museum of Architecture and Design and Museum of Dolenjska. According to chairpersons, the quality of contributions was very high and the atmosphere was inspiring. There were some technical issues with Zoom which resulted in delay, however, this did not seem to spoil the good mood of the participants. The number of participants at the plenary lecture by dr. Antonella Bongiovanni from Palermo and a cumulative number of participants at the scientific sections oscillated around 160 while at the »Art meets science« section it oscillated around 50. Traditionally, music was a part of the Socratic lectures and during the pandemics, the performances took place online. This time, music was performed at the Franciscan Church of Assumption in Ljubljana, live, by organist Roberta Schmid. Although meeting online has its advantages as regards professional impact, we miss the vicinity of our colleagues and friends. Likewise, consuming raw music without electrical processing is precious, and those who came to the concert were lucky to have this oportunity. We have received 25 contributions to the Proceedings and 5 posters.

One may wonder how come such good outcome of the Socratic lectures, in spite of difficulties that the participants had to overcome, the peculiarities in learning and in scientific work, fear and loss due to pandemics and its economic effects. I think that it has something to do with energy of the participants that is keeping the spirit above the chaos and depression. It is amazing how sometimes a single event may turn things to better. During preparation for Socratic lectures and while they took place, a life of a small dog named Lupe (on the cover) was saved. The puppy, just few weeks old was abandoned on the street in Kosovo, but rescued by Eva Osolnik who offered her home. However, it took considerable effort to overcome obstacles posed by the rules and procedures to bring the dog to Ljubljana with all required attributes. With the help of veterinary doctors dr. Metka Šimundić, prof. dr. Vladimira Erjavec and Boštjan Korenjak, and with great input of Jasna Dokl Osolnik, the outcome contributed significantly to the success of the symposium. It presented a proof of the power of good which is a bright spot that should keep us struggling.

For any contribution to Socratic Lectures, we remain grateful,

Veronika Kralj-Iglič and Anna Romolo

CONTENTS

POSTERS

LIST OF OBJECTS WITH INSCRIPTIONS DEPICTED IN FIGURES

Objects and photos are kept in Dolenjski muzej Novo mesto

Univerza v Ljubljani
Zdravstvena fakulteta

6TH 2021 SOCRATIC LECTURES

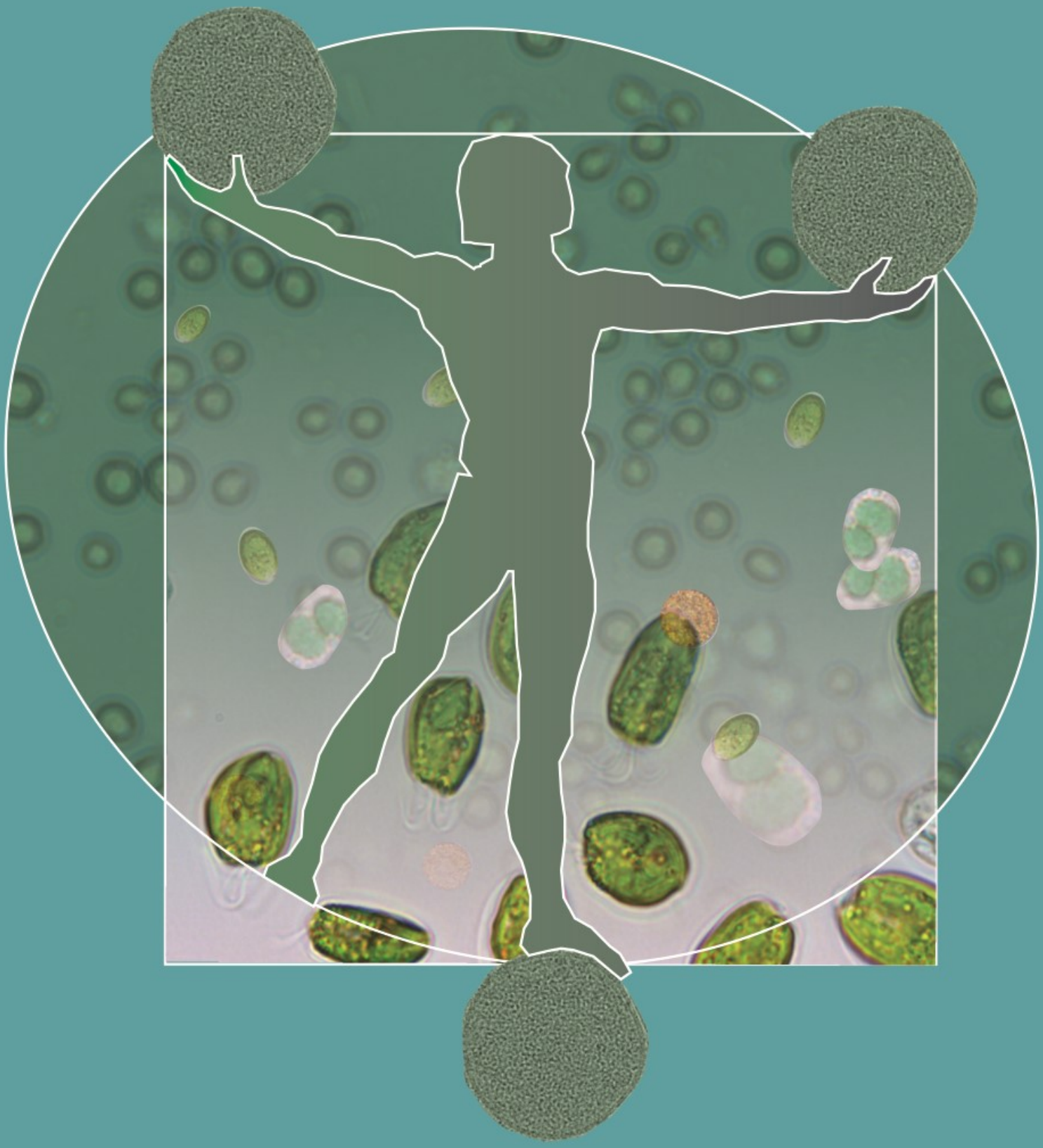

Scientific contribution/Original research/Invited lecture

Selected Parameters of Venous Blood Gas Analysis in Brachycephalic Dogs with Brachycephalic Obstructive Airway Syndrome before and after Surgical Treatment

Erjavec V[1], Nemec Svete A[1,*]

1. University of Ljubljana, Veterinary Faculty, Small Animal Clinic, Ljubljana, Slovenia
* Correspondence: Alenka Nemec Svete; alenka.nemecsvete@vf.uni-lj.si

Abstract:
Brachycephalic dog breeds, such as Pug, English and French Bulldogs and Boston Terrier belong to a group of breeds characterized by a severe shortening of the muzzle and thus the underlying bones, as well as a more modest shortening and widening of the skull. These breeds are prone to a conformation-related disorder known as brachycephalic obstructive airway syndrome (BOAS). Among consequences of the upper airway abnormalities is not only hypoxia, but also redued clearance of carbon dioxide. The aim of the present study was to evaluate selected parameters (pH, partial pressure of carbon dioxide, bicarbonate concentration and base excess) of venous blood gas analysis in brachycephalic dogs with BOAS before and one month after surgical treatment of BOAS. Sixty-two BOAS patients with different severity grades of BOAS were enrolled in the study. Patients were classified as grade 1, grade 2, and grade 3 based on the decrease in the radius of the airway at the level of the nasopharynx, oropharynx, laryngopharynx, and larynx after soft palate surgery. Contrary to our expectations, surgical treatment had no effect on selected venous blood gas parameters in any of the grades of BOAS. However, selected venous blood gas parameters deviated from the normal range before and after surgical treatment, indicating respiratory acidosis in our BOAS patients. Based on the results we may conclude that venous blood gas analysis could help in assessing the health status of brachycephalic dogs with BOAS.

Keywords: Brachycephaly; Brachycephalic obstructive airway syndrome; Dogs; Respiratory acidosis; Surgery; Venous blood gas analysis

Citation: Erjavec V, Nemec Svete A. Selected parameters of venous blood gas analysis in brachycephalic dogs with brachycephalic obstructive airway syndrome before and after surgical treatment. Proceedings of Socratic Lectures. 2021; 6: 1-6. https://doi.org/10.55295/PSL.2021.D.001

1. Introduction

Brachycephalic dog breeds, including Pug, English and French Bulldogs and Boston Terrier belong to a group of breeds characterized by a severe shortening of the muzzle and thus the underlying bones, as well as a more modest shortening and widening of the skull. In recent years, brachycephalic breeds have become increasingly popular companion dog breeds. Their popularity may be due to the similarity between the head shape of brachycephalic dogs and that of human infants. However, brachycephalic breeds have been shown to be generally less healthy than non-brachycephalic breeds and have shorter lifespan (Fawcett et al., 2018; Packer et al., 2019; O'Neill et al., 2020). Artificial selection for extreme brachycephaly has resulted in deformation of the upper airway tract leading to obstruction as the soft tissues have not shortened in proportion to the length of the skull. Brachycephalic dogs are prone to a conformation-related disorder known as brachycephalic obstructive airway syndrome (BOAS) (Packer et al., 2015; Liu et al., 2017; Fawcett et al., 2018; Packer et al., 2019). Clinical signs of BOAS include inspiratory dyspnoea, snoring, stertor and stridor, panting, stress, exercise and heat intolerance, cyanosis, and even syncopal episodes, gastrointestinal problems, and disturbed sleep patterns (Meola, 2013; Roedler et al., 2013; Dupre and Heidenreich, 2016; Packer et al., 2019). Treatment of affected dogs can be surgical or conservative, with the latter including medical treatment, weight management, and keeping patients cool, calm and with low physical activity (Torrez and Hunt, 2010; Meola, 2013; Dupre and Heidenreich, 2016). However, conservative treatment can only temporarily improve clinical signs and is thus merely palliative. Surgical treatment, which includes widening of the stenotic nares, staphylectomy and, in selected cases, ventriculectomy (sacculectomy) to improve airflow through the rima glottidis, is therefore recommended in most BOAS-affected dogs (Torrez and Hunt, 2010; Dupre and Heidenreich, 2016). Brachycephalic dogs have additional systemic complications (Meola, 2013; Mellema and Hoareau, 2014; Fawcett et al., 2018; O'Neill et al., 2020). Among consequences of the BOAS is not only hypoxia, but also redued clearance of carbon dioxide. Systemically healthy brachycephalic dogs have been found to have hypertension and significantly higher arterial partial pressure of carbon dioxide ($PaCO_2$) and significantly lower arterial partial pressure of oxygen (PaO_2) and arterial haemoglobin oxygen saturation (SaO_2) compared to non-brachycephalic breeds (Hoareau et al., 2012; Arulpagasam et al., 2018). Significantly lower SaO_2 (Dias et al., 2016; Arulpagasam et al., 2018) and PaO_2 (Canola et al., 2018) were reported in brachycephalic dogs with BOAS compared to non-brachycephalic dogs. On the other hand, no significant difference in arterial pH, PaO_2, bicarbonate (HCO_3^-) concentration and $PaCO_2$ was reported between BOAS-affected dogs and non-brachycephalic dogs (Dias et al., 2016; Arulpagasam et al., 2018). Arterial blood gas analysis is the gold standard for evaluating hypoxemia in patients with respiratory disorders. Peripheral venous blood gas analysis has been proposed as an alternative to arterial blood gas analysis for hypercapnia and metabolic disturbances, such as acidosis (Byrne et al., 2013). Nowadays, the venous blood gas analysis is increasingly used by veterinary practitioners, thus providing important information regarding acid-base status and ventilation (Ilkiw et al., 1991). Arterial blood sampling in conscious BOAS patients is risky due to their breathing difficulties resulting from upper airway obstruction (Hendricks, 1992; Arulpagasam et al., 2018). In BOAS patients, both arterial and venous blood gas analysis can be useful. If an arterial blood sample cannot be obtained, a venous blood sample may provide useful information about pH, HCO_3^- and PCO_2 levels in these patients (Hendricks, 1992). To the authors' knowledge, only three studies have been published reporting results of arterial blood gas analysis in BOAS patients (Dias et al., 2016; Arulpagasam et al., 2018; Canola et al., 2018), but there are none reporting results of venous blood gas analysis in these patients. Therefore, the aim of this study was to evaluate selected parameters of venous blood gas analysis (pH, PCO_2, HCO_3^-, base excess (BE)) in brachycephalic dogs with different severity of BOAS before and after surgical treatment of BOAS.

2. Materials and Methods

2.1. Dogs

A total of 62 client-owned dogs diagnosed with BOAS were included in the study. At the time of initial presentation, the history of the dogs was collected using a questionnaire about behaviour, health, and lifestyle. All the dogs that had any signs of concurrent disease or received any therapy or vaccination within the previous month were excluded from the study. Brachycephalic obstructive airway syndrome diagnosis was carried out based on clinical signs of upper airway obstruction and anatomical abnormalities, as has been described elsewhere (Dupre and Heidenreich, 2016; MacPhail and Fossum, 2019). Patients were classified as grade 1, grade 2, and grade 3 based on the decrease in the radius of the airway at the level of the nasopharynx, oropharynx, laryngopharynx, and larynx after soft palate surgery. Grade 1 patients had no or very mild narrowing of the airways, grade 2 patients had 50% decrease in airways radius and grade 3 patients had almost complete airway obstruction at the level of one or more of the following anatomic regions: nasopharynx, oropharynx, laryngopharynx and/or larynx. The patients' health status was assessed by history, physical examination, and blood tests including complete blood count with white blood cell differential count (data not shown), serum biochemical analyses (data not shown), and venous blood gas analyses (only selected parameters presented in the manuscript). The patients with BOAS were scheduled for surgical treatment under general anaesthesia. Stenotic nares were enlarged surgically by rhinoplasty. A horizontal wedge excision technique was used for excising part of ala nasi with a No. 11 scalpel blade. To oppose the wedge margins two to four simple interrupted sutures using synthetic absorbable monofilament suture material Glycomer 631 (Biosyn 4/0, Covidien, Dublin, Ireland) were placed. To correct both the excessive length and excessive thickness of the soft palate, folded flap palatoplasty was performed in all dogs. A portion of oropharyngeal mucosa and underlying soft tissue was excised using a Surgitron Radiolase II (Ellman International, Inc., Hicksville, NY, USA). The formal written consent of the owner was obtained before the dogs entered the study. All procedures complied with the relevant Slovenian governmental regulations (Animal Protection Act UL RS, 43/2007).

2.2. Blood collection and blood gas analysis

Venous blood samples were collected twice from BOAS patients via the central venous catheter, 2 hours (± 15 minutes) before premedication and oxygenation (before surgical treatment) and one month after surgical treatment. Blood samples for venous blood gas analyses were collected into blood gas syringes containing lithium heparin (Sarstedt, Numbrecht, Germany) and analysed immediately (less than 5 minutes) after collection using a blood gas analyser (RAPIDPoint 500, Siemens, Munich, Germany). The pH and PCO_2 were corrected for rectally measured body temperature.

2.3. Statistical analysis

Data were analysed using commercial software (IBM SPSS 25.0, Chicago, Illinois, USA). The Shapiro-Wilk test was performed to test whether the data were normally distributed. According to the results of normality tests, parametric (one-way ANOVA with Tukey Honestly Significant Difference post hoc test; pH, PCO_2, HCO_3^-, BE) or non-parametric (Kruskal-Wallis test followed by multiple comparisons and Bonferroni correction; age, weight, body condition score (BCS)) tests were used to compare the parameters between the dog groups. Paired t-test was used to compare selected parameters of venous blood gas analysis (pH, PCO_2, HCO_3^-, BE) before and after surgery. The significance level was set at 5%.

3. Results

Selected parameters of venous blood gas analysis were evaluated before and after surgical treatment in 62 BOAS patients classified into grade 1 (10 dogs), grade 2 (26 dogs), and grade 3 (26 dogs) (Table 1). Patients in grade 1 were the youngest; however, we found no significant difference in age, nor in body weight and BCS between the groups of BOAS patients. French Bulldogs were the most common breed. These dogs accounted for 31 of the 62 cases.

Table 1. Baseline characteristics of brachycephalic dogs in different grades of brachycephalic obstructive airway syndrome (BOAS).

	Grade 1	Grade 2	Grade 3	All BOAS patients
Number	10	26	26	62
Sex (female/male)	3/7	12/14	8/18	23/39
Age (years) Median IQR	 1.29 0.73 – 3.60	 2.54 1.33 – 3.71	 3.04 1.65 – 5.75	 2.58 1.40 – 4.75
Weight (kg) Median IQR	 8.2 5.8 – 12.3	 10.0 8.7 – 12.4	 10.1 8.4 – 11.8	 10.0 8.3 – 12.1
BCS Median IQR	 3.0 3.0 – 3.0	 3.0 3.0 – 4.0	 3.0 3.0 – 4.0	 3.0 3.0 – 4.0
Breeds	4 FB, 4 ST, 1 BST, 1 EB	13 FB, 6 P, 5 BST, 1 EB, 1 ST	14 FB, 6 P, 5 BST, 1 ST	31 FB, 12 P, 11 BST, 6 ST, 2 EB

IQR=interquartile range (25th to 75th percentile); BCS=body condition score; EB=English Bulldog; FB=French Bulldog; P=Pug; BST=Boston Terrier; ST=Shih-Tzu.

Selected parameters of venous blood gas analysis before and after surgery, as well as the corresponding reference intervals established in canine venous blood samples (Bachmann, et al. 2018) using the same analyser as in our study, are shown in Table 2. We found no significant difference in any of the selected blood gas parameters between the different grades of BOAS before and after surgical treatment.

Table 2: Selected venous blood gas parameters (mean ± standard deviation) of brachycephalic dogs in different grades of brachycephalic obstructive airway syndrome (BOAS) before and after surgical treatment.

	pH	PCO_2 (mmHg)	HCO_3^- (mmol/L)	BE (ecf) (mmol/L)
Grade 1 Before After	 7.342 ± 0.053 7.337 ± 0.523	 44.26 ± 7.54 44.97 ± 6.97	 22.74 ± 1.43 22.91 ± 1.33	 -2.51 ± 1.23 -2.48 ± 1.16
Grade 2 Before After	 7.336 ± 0.037 7.335 ± 0.046	 43.57 ± 5.85 43.59 ± 7.76	 22.84 ± 2.23 22.59 ± 2.09	 -2.61 ± 2.61 -2.94 ± 2.16
Grade 3 Before After	 7.323 ± 0.066 7.335 ± 0.037	 47.90 ± 9.18 46.54 ± 7.57	 23.59 ± 2.68 23.73 ± 2.68	 -2.07 ± 2.95 -1.78 ± 2.57
REF	7.352 – 7.450	28.6 – 44.7	18.1 – 26.3	-6.70 – 1.50

REF=reference interval (Bachmann et al., 2018); PCO_2 = partial pressure of carbon dioxide; HCO_3^-= bicarbonate concentration; BE (ecf)=base excess in extracellular fluid

4. Discussion

The present study is the first that reports selected parameters of venous blood gas analysis in brachycephylic dogs with different grades of BOAS before and one month after surgical treatment. Therefore, our results were compared only to the published reference values of venous blood gas parameters determined in healthy dogs (Bachmann et al., 2018).

Although expected, we found no significant difference in any of the selected blood gas parameters when comparing them before and one month after surgical treatment in any of the groups of BOAS patients. These results suggest that surgical treatment had no effect on selected venous blood gas parameters or that the effect may not have been apparent because of the too short time after surgery. It may be that it would be more useful to take the blood samples six months after surgery. The mean values of pH were below the lower limit of the reference range (Bachmann et al., 2018) before and after surgical treatment in all groups of BOAS patients, indicating acidosis. Furthermore, the mean values of PCO_2 exceeded the upper value of the reference range (Bachmann et al., 2018) in grade 3 of BOAS before and after surgical treatment and in grade 1 after surgery, indicating hypercapnia. High PCO_2 values obtained in BOAS patients could be due to hypoventilation in these dogs as a result of upper airway obstruction. The results of our study indicate the presence of respiratory acidosis in our BOAS patients. As reported by Hendricks (1992), chronic respiratory acidosis could be present in BOAS. On the other hand, the mean values of bicarbonate and BE, a quantity reflecting only the non-respiratory (metabolic) component of acid-base disturbances, remained within the reference intervals in all groups of BOAS patients before and after surgery. Based on our results, we may summarize that the changes in selected venous blood gas parameters found in our BOAS patients are indicative of respiratory acidosis and that these parameters are not affected by surgical treatment of BOAS. In addition to routine haematological and biochemical analyses, venous blood gas analysis could help in assessing the health status of brachycephalic dogs with BOAS. It is known that there are breed-specific anatomical airway differences between different brachycephalic breeds such as pugs and bulldogs, so the response to surgery can be unpredictable and breed-specific. Pugs have a significantly smaller rima glottidis than French Bulldogs, 82% of them have nasopharyngeal turbinates, they also have a higher prevalence of laryngeal collapse (96%), all of which may negate the surgical benefit. Therefore, further studies with a larger number of dogs are needed to evaluate the effect of breed on venous blood gas parameters and to assess whether surgical treatment of BOAS affects venous blood gas parameters in individual brachycephalic breeds.

5. Conclusions

Surgical treatment of BOAS had no effect on selected venous blood gas parameters in any of the grades of BOAS one month after surgery. Selected venous blood gas parameters deviated from the normal range before and after surgical treatment, indicating respiratory acidosis in our BOAS patients. Venous blood gas analysis could help in assessing the health status of brachycephalic dogs with BOAS.

Funding: This research was supported by Slovenian Research Agency (research program No. P4-0053).

Institutional Review Board Statement: All procedures complied with the relevant Slovenian governmental regulations (Animal Protection Act UL RS, 43/2007).

Conflicts of Interest: The authors declare no conflict of interest.

Acknowledgements: The authors thank Rebeka Turk and Luka Šparaš for the processing of the collected blood samples.

References

1. Arulpagasam S, Lux C, Odunayo A, et al. Evaluation of pulse oximetry in healthy brachycephalic dogs. J Am Anim Hosp Assoc. 2018; 54: 344–350. DOI 10.5326/JAAHA-MS-6654
2. Bachmann K, Kutter APN, Jud Schefer R, Sigrist NE. Determination of reference intervals and comparison of venous blood gas parameters using a standard and nonstandard collection method in 51 dogs. SAT. 2018; 160: 163–170. DOI: 10.17236/sat00150
3. Byrne AL, Bennett M, Pace NL, Thomas P. Peripheral venous blood gas analysis versus arterial blood gas analysis for the diagnosis of respiratory failure and metabolic disturbances in adults (Protocol). Cochrane Database Syst Rev. 2013; 11: CD010841. DOI: 10.1002/14651858.CD010841
4. Canola RAM, Sousa MG, Braz JB, et al. Cardiorespiratory evaluation of brachycephalic syndrome in dogs. Pesq Vet Bras. 2018; 38: 1130–1136. DOI: 10.1590/1678-5150-PVB-5376
5. Dias MLM, Morris CFM, Moreti BM, et al. Anatomical, Cardiovascular, and Blood Gas Parameters in Dogs with Brachycephalic Syndrome. Acta Sci Vet. 2016; 44: 1356. DOI: https://doi.org/10.22456/1679-9216.80932
6. Dupre G, Heidenreich D. Brachycephalic Syndrome. Vet Clin Small Anim. 2016; 46: 691–707. https://doi.org/10.1016/j.cvsm.2016.02.002
7. Fawcett A, Barrs V, Awad M, et al. Consequences and Management of Canine Brachycephaly in Veterinary Practice: Perspectives from Australian Veterinarians and Veterinary Specialists. Animals (Basel). 2019; 9. DOI: 10.3390/ani9010003
8. Hendricks JC. Brachycephalic airway syndrome. Vet Clin North Am Small Anim Pract. 1992; 22: 1145–1153. DOI:10.1016/s0195-5616(92)50306-0
9. Hoareau GL, Jourdan G, Mellema M, Verwaerde P. Evaluation of arterial blood gases and arterial blood pressures in brachycephalic dogs. J Vet Intern Med. 2012; 26: 897–904. DOI: 10.1111/j.1939-1676.2012.00941.x
10. Ilkiw JE, Rose RJ, Martin IC. A comparison of simultaneously collected arterial, mixed venous, jugular venous and cephalic venous blood samples in the assessment of blood-gas and acid-base status in dog. J Vet Intern Med. 1991; 5: 294–298. DOI: 10.1111/j.1939-1676.1991.tb03136.x
11. Liu NC, Troconis EL, Kalmar L, et al. Conformational risk factors of brachycephalic obstructive airway syndrome (BOAS) in pugs, French bulldogs, and bulldogs. PLoS One. 2017; 12: e0181928. DOI: 10.1371/journal.pone.0181928
12. MacPhail C, Fossum TW, Surgery of the upper respiratory system. In: Fossum TW, editor. Small animal surgery, 5th edn. Philidelphia, Pennsylvania, Elsevier. 2019; pp. 833–883.
13. Mellema MS, Hoareau GL. Brachycephalic syndrome. In: Silverstein DC, Hopper K, editors. Small animal critical care medicine, 2nd edn. St. Louis, Missouri, Elsevier. 2003; pp. 104–106.
14. Meola SD. Brachycephalic airway syndrome. Top Companion Anim Med. 2013; 28: 91–96. DOI: 10.1053/j.tcam.2013.06.004
15. O'Neill DG, Jackson C, Guy JH, et al. Epidemiological associations between brachycephaly and upper respiratory tract disorders in dogs attending veterinary practices in England. Canine Genet Epidemiol. 2015; 2: 10. DOI: 10.1186/s40575-015-0023-8
16. O'Neill DG, Pegram C, Crocker P, et al. Unravelling the health status of brachycephalic dogs in UK using multivariable analysis. Sci Rep. 2020; 10: 17251. DOI: 10.1038/s41598-020-73088-y
17. Packer RMA, Hendricks A, Tivers MA, Burn CC. Impact of facial conformation on canine cealth: Brachycephalic Obstructive Airway Syndrome. PLoS One. 2015; 10: e0137496. DOI: 10.1371/journal.pone.0137496
18. Packer RMA, O'Neill DG, Fletcher F, Farnworth MJ. Great expectations, inconvenient truths, and the paradoxes of the dog-owner relationship for owners of brachycephalic dogs. Plos One. 2019; 14: e0219918. DOI: 10.1371/journal.pone.0219918
19. Roedler FS, Pohl S, Oechtering GU. How does severe brachycephaly affect dog's lives? Results of a structured preoperative owner questionnaire. Vet J. 2013; 198: 606–610. DOI: 10.1016/j.tvjl.2013.09.009
20. Torrez CV, Hunt GB. Results of surgical correction of abnormalities associated withbrachycephalic airway obstruction syndrome in dogs in Australia. J Small Anim Pract. 2006; 47: 150–154. DOI: 10.1111/j.1748-5827.2006.00059.x

Scientific contribution/Original research/Invited lecture

Blood Lactate, Body Temperature and Heart Rate During Submaximal Exercise in Dogs with Brachycephalic Obstructive Airway Syndrome: A Preliminary Study

Žgank Ž[1], Nemec Svete A[1], Erjavec V[1]*

1. University of Ljubljana, Veterinary Faculty, Small Animal Clinic, Ljubljana, Slovenia
* Correspondence: Vladimira Erjavec: vladimira.erjavec@vf.uni-lj.si

Abstract

The aim of the present preliminary study was to investigate how submaximal exercise affects blood lactate (BL) concentrations, body temperature (BT) and heart rate (HR) in dogs with brachycephalic obstructive airway syndrome (BOAS). Seven dogs with BOAS grade 2/3 and 3/3 were subjected to submaximal exercise on a treadmill. Each dog was subjected to training session that began with a 5-minute walk at a speed of 2.5 km/h and an incline of 0% and continued with a 5-minute walk at a speed of 2.5 km/h and at an incline of 5%. Heart rate, BT, and BL concentrations were measured before the start (T1), every 5 minutes during the test (T2, T3) and after 15 and 30 minutes of rest (T4, T5). Blood lactate concentrations at T3 and T5 were significantly lower ($P < 0.05$) than concentrations at T1. Heart rate and BT values at T2 and T3 were significantly higher ($P < 0.05$) than values at T1. Submaximal exercise resulted in a significant decrease in BL concentrations and a significant increase in BT and HR in dogs with BOAS. The results of this preliminary study can give us additional information about the severity of BOAS; however, further studies are needed to gain better insight into the physiological response of BOAS patients of individual breeds to submaximal exercise testing.

Keywords: Brachycephalic obstructive airway syndrome; Treadmill; Brachycephalic dogs; Blood lactate; Submaximal exercise test

Citation: Žgank Ž, Nemec Svete A, Erjavec V. Blood lactate, body temperature and heart rate during submaximal exercise in dogs with brachycephalic obstructive airway syndrome: a preliminary study. Proceedings of Socratic Lectures. 2021; 6: 8-13. https://doi.org/10.55295/PSL.2021.D.002

1. Introduction

The popularity of brachycephalic dogs has increased in recent years. This may be due to their distinct physical facial features, which resemble the facial features of a human baby and elicit the same positive emotions in adults. Breeds such as French and English bulldogs, pugs, and Boston terriers are examples of extremely brachycephalic breeds. They have a typically shaped head with a very short muzzle and a round, short and broad head (Ekenstedt et al., 2020). The soft tissues of the upper airway have not reduced in proportion to the skull length and these deformities lead to upper airway obstruction (Dupré and Heidenreich, 2016). These upper airway abnormalities cause a variety of clinical signs called brachycephalic obstructive airway syndrome (BOAS) (Lodato and Hedlund, 2012). BOAS is a progressive disease. Dogs with BOAS may present with clinical signs such as stertor, stridor, snoring, coughing, increased respiratory effort, exercise intolerance, hyperthermia, and collapse. These problems may be exacerbated in the presence of stress, physical activity, and high ambient temperatures (Meola et al., 2013).

In dogs with cardiac, respiratory, or neuromuscular disease, exercise tests (ET) is used to assess the severity of the disease. In dogs with BOAS, ET can help identify clinically relevant airway obstruction when clinical signs are mild or dynamic (Riggs et al., 2019). In sports medicine blood lactate (BL) is one of the most important biochemical parameters measured during exercise. In both human and animal athletes, such as horses and dogs, BL is used to determine the level of fitness and effort (Alves et al., 2020). It is a metabolite of the anaerobic glycolytic pathways (Rovira et al., 2018). It is produced continuously under anaerobic conditions and has at least three functions: a major energy source, the major gluconeogenic precursor, and a signalling molecule (Brooks, 2018). In dogs, physical activity leads to higher heath and therefore higher cardiovascular and thermoregulatory demand (Robbins et al., 2017). Measurement of HR and BT during exercise is useful for monitoring exercise intensity and may also be useful for detecting subclinical disease (Rovira et al., 2018). Monitoring HR during exercise is also useful for determining cardiac output and monitoring workload. Monitoring HR during rest periods can help determine physical fitness and metabolic status (Alves et al., 2020).

The aim of this study was to determine how submaximal exercise affects the levels of BL, HR, and BT in dogs with BOAS.

2. Materials and Methods

2.1. Animals

Seven client-owned brachycephalic dogs, prospectively recruited as BOAS patients were included in the study. The dogs were graded with BOAS grade 2/3 (n=2) and grade 3/3 (n=5). BOAS grade was based on clinical signs of upper airway obstruction and anatomical abnormalities (Erjavec et al., 2021).

Formal written consent of the owner was obtained before the dogs participated in the study. All procedures complied with the relevant Slovenian governmental regulations (Animal Protection Act UL RS, 43/2007).

2.2. Exercise test and measurements of BL concentration, HR, and BT

The exercise test was performed in the Laboratory of physiology, Faculty of sports, University of Ljubljana in a controlled climatic environment. The test was performed in two stages. The first stage was a 5-minute walk on a treadmill at a speed of 2.5 km/h and a 0% incline. The second stage was a 5-minute walk at a speed of 2.5 km/h at an inclination of 5%. There was a 1-minute break between both stages for measurements. After the exercise the dogs had 30 minutes of recovery time.

Heart rate, BT and BL concentrations were measured before the start (T1), after the first 5 minutes of exercise (T2), after 10 minutes (T3) of exercise, and after 15 minutes (T4) and 30 minutes of recovery (T5). Blood samples for measurement of BL concentrations were collected from the cephalic vein. Blood lactate concentration was measured immediately after blood was drawn using a portable device (Accutrend Plus, Roche Diagnostics

GmbH, Mannheim, Germany). Heart rate was measured by palpation of the femoral artery and counted for 15 seconds and then multiplied by four. Body temperature was measured rectally with digital thermometer (Microlife, Microlife AG, Widnau, Switzerland).

2.3. Statistical analysis

Data was analysed with commercial software (IBM SPSS 25, Chicago, Illinois, USA). Descriptive statistics were used to describe the basic features of the data. The Shapiro Wilk test was performed to test whether the data were normally distributed. According to the results of normality tests, repeated measures ANOVA with Bonferroni corrections (parametric test) was used to test for statistically significant differences in the measured parameters (BL concentrations, HR, BT) among different measuring points. Normally distributed data are reported as means ± standard deviation (SD); not normally distributed data are reported as medians and interquartile range (IQR – 25th to 75th percentile). A value of $P < 0.05$ was considered significant.

3. Results

In this preliminary study we evaluated 7 dogs of the following breeds: French bulldogs (n=6) and Boston terrier (n=1). Baseline characteristics of the evaluated dogs are summarised in **Table 1**.

Table 1. Baseline characteristics of brachycephalic obstructive airway syndrome patients.

Number of dogs	7
Sex (female/male)	1/6
Age (months); Mean ± SD	22.14 ± 12.41
Weight (kg); Mean ± SD	10.91 ± 1.23
BCS Median; IQR	3.0; 3.0 – 3.0

SD – standard deviation; BCS – body condition score; IQR – interquartile range (25th to 75th percentile).

Before, during and after submaximal exercise test, BL concentrations did not exceed reference ranges determined in dogs with the same portable device as in our study (Stevenson et al., 2007). Blood lactate concentrations (**Figure 1**) decreased significantly during the exercise testing. Compered to initial BL measurement at T1, significantly lower BL concentrations were observed at T3 ($P = 0.017$; after 10 minutes of exercise) and at T5 ($P = 0.002$; after 30 minutes of resting time). The lowest BL concentration was measured at the last measuring point (after 30 minutes of recovery), when it was significantly lower compared with the initial BL concentration ($P = 0.002$) and with the BL concentration measured at T2 ($P < 0.001$; 5 minutes after the start of the exercise test).

During exercise testing, the BT values (**Figure 2**) changed significantly. Body temperature values were significantly higher at measuring points T2 ($P = 0.016$) and T3 ($P = 0.001$) compared with the initial values of BT. Afterwards, BT decreased significantly, with the last BT values being significantly lower compared to the BT values measured at T4 ($P = 0.018$) and T3 ($P = 0.003$) measuring points.

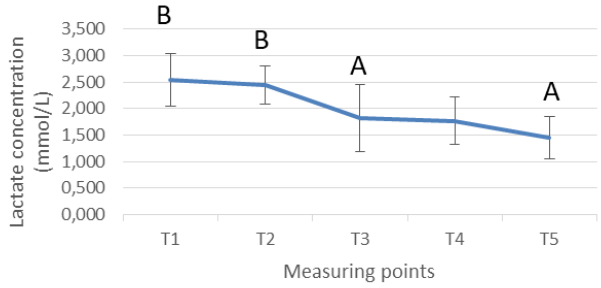

Figure 1. Blood lactate concentrations (mmol/L; mean ± standard deviation) before, during and after submaximal exercise test; A - significant ($P < 0.05$) difference compared to T1; B - significant ($P < 0.05$) difference compared to T5; T1 - BL concentration before the start of ET; T2 - BL concentration after 5 min of ET; T3 - BL concentration after10 minutes of ET; T4 - BL concentration after 15 minutes of rest; T5 - BL concentration after 30 minutes of rest.

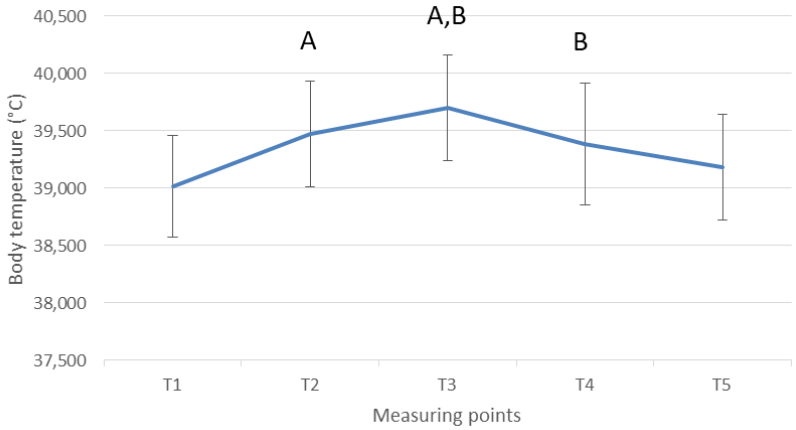

Figure 2. Body temperature (°C) values (mean ± standard deviation) before, during and after submaximal exercise test; A - significant ($P < 0.05$) difference compared to T1; B - significant ($P < 0.05$) difference compared to T5; T1 - BT before the start of ET; T2 - BT after 5 minutes of ET; T3 - BT after 10 minutes of ET; T4 - BT after 15 minutes of rest; T5 - BT after 30 minutes of rest.

The values of HR (**Figure 3**) showed the same pattern of changes as BT. Heart rate values were significantly higher at measuring points T2 ($P = 0.022$) and T3 ($P = 0.022$) compared with the initial values of HR. Afterwards, HR decreased significantly with the last HR values being significantly lower compared with the HR values measured at T4 ($P = 0.014$) and T3 ($P = 0.024$) measuring points.

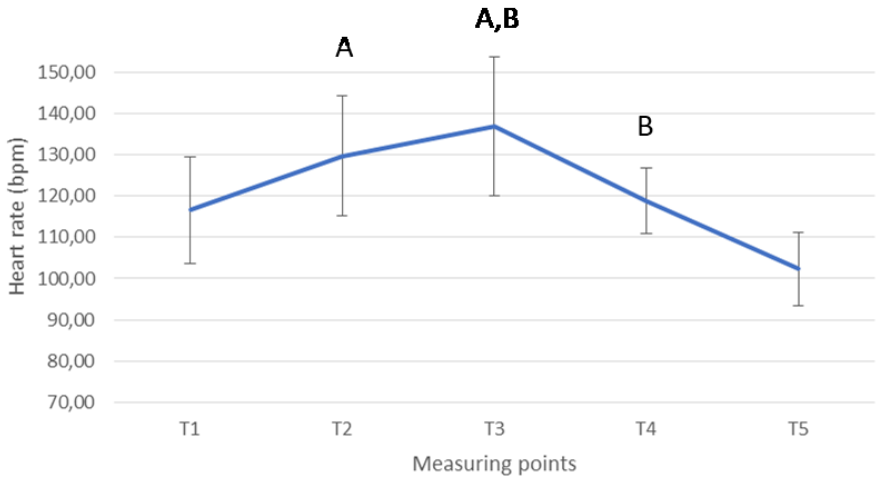

Figure 3. Heart rate values (bpm) (mean ± standard deviation) before, during and after submaximal exercise test; A - significant ($P < 0.05$) difference compared to T1; B - significant ($P < 0.05$) difference compared to T5; T1 - HR before the start of ET; T2 - HR after 5 minutes of ET; T3 - HR after 10 minutes of ET; T4 - HR after 15 minutes of rest; T5 - HR after 30 minutes of rest.

4. Discussion

In the present study we investigated blood lactate concentrations, body temperature, and heart rate in dogs with BOAS during a submaximal exercise test. Exercise resulted in a significant increase of HR and BT and a significant decrease in BL concentrations.

To the best of the authors' knowledge there are no published reports of BL concentrations in dogs with BOAS during a submaximal exercise test. However, there are few reports (Riggs et al., 2019; Lija-Maula et al., 2017) published on exercise testing in dogs with BOAS but none of these reports was a full objective evaluation of the dogs. In the study by Riggs et al. (2019) the dogs performed a 5-minute walk and a 3-minute trot test to assess the severity of upper respiratory disease. In the study by Lija-Maula et al. (2017) they used the 6-minute walk test and the 1000 metre walk test to objectively assess the severity of BOAS in English bulldogs.

Lactate level is an indicator of physical fitness, athletic performance, and disease in animals (Ferasin and Marcora, 2007). In our study BL concentrations were highest before the start of the test. However, blood lactate concentrations decreased significantly during the test and reached the lowest BL concentration at the last measuring point. During submaximal exercise, the accumulation of lactate is reduced (Brito Vieira et al., 2014). This can be attributed to increased oxidative capacity, reduced production of lactate and an increase in the rate of lactate removal. Lactate removal may be associated with an increase in the utilisation of other tissues such as liver, heart, kidneys, and skeletal muscle. It may also be due to the increase in gluconeogenesis in skeletal muscle cells and hepatocytes, its use by oxidative fibres or increased lactate transport through the sarcolemma (Brito Vieira et al., 2014). In human athletes, lactate concentrations decreased during long endurance exercises. The authors speculated that the decrease in BL concentration was probably caused by the fact that the working muscles produced less lactate due to the lower energy demand caused by the lower respiratory demand or that the trained respiratory muscles used more lactate as fuel for their own activity (Spengler et al., 1999). The latter might be the reason for a significant decrease in BL concentration in our study. Indeed, brachycephalic dogs suffer from laboured breathing, which may result in trained respiratory muscles that use lactate as fuel.

An increase in HR and BT was expected in this study. The increase in HR is the indicator of cardiovascular workload and the most important determinant of cardiac output and oxygen uptake (Rovira et al., 2018). We observed the same pattern of significant changes in HR and BT in our BOAS patients. Both parameters increased during the exercise test and were highest after the inclination part of the test, when workload was great-

est. Heart rate and BT began to decrease when the dogs were at rest. Despite a decrease in BT during rest, the values were still higher than BT before the start of the workload. This is due to the increased muscle load, which generates higher amounts of body heat (Rovira et al., 2018).

Our preliminary results warrant further studies with a larger number of BOAS patients to evaluate the physiological responses to submaximal exercise testing in individual brachycephalic breeds and to determine if surgical treatment of BOAS affects responses to this type of exercise.

5. Conclusions

The present study demonstrated that submaximal exercise of only 10 minutes duration caused a significant increase in HR and BT, and surprisingly, a significant decrease in BL concentrations. The results of this preliminary study may give us additional information about the severity of BOAS. However, further studies are needed to gain better insight into the physiological response of BOAS patients of individual breeds to submaximal exercise testing.

Funding: This research was supported by Slovenian Research Agency (research program No. P4-0053).

Institutional Review Board Statement: All procedures complied with the relevant Slovenian governmental regulations (Animal Protection Act UL RS, 43/2007).

Conflicts of Interest: The authors declare no conflict of interest.

Acknowledgements: The authors thank Janez Vodičar from Laboratory of Physiology, Faculty of Sports, University of Ljubljana, for providing the facilities and for help with the use of the equipment.

References

1. Alves JC, Santos AM, Jorge PI, Lafuente P. A protocol for the determination of the maximal lactate steady state in working dogs. J Sports Med Phys Fitness. 2020; 60: 942-946. DOI: 10.23736/S0022-4707.20.10305-0.
2. Brito Vieira WH, Halsberghe MJ, Schwantes ML et al. Increased lactate threshold after five weeks of treadmill aerobic training in rats. Braz J Biol. 2014; 74: 444-9. DOI: 10.1590/1519-6984.07912.
3. Brooks GA. The Science and Translation of Lactate Shuttle Theory. Cell Metab. 2018; 27(4):757-785. DOI: 10.1016/j.cmet.2018.03.008.
4. Dupré G, Heidenreich D. Brachycephalic Syndrome. Vet Clin North Am Small Anim Pract. 2016; 46, 691–707. DOI: 10.1016/j.cvsm.2016.02.002.
5. Ekenstedt KJ, Crosse KR, Risselada M. Canine Brachycephaly: Anatomy, Pathology, Genetics and Welfare. J Comp Pathol. 2020; 176: 109-115. DOI: 10.1016/j.jcpa.2020.02.008.
6. Erjavec V, Vovk T, Svete AN. Evaluation of Oxidative Stress Parameters in Dogs with Brachycephalic Obstructive Airway Syndrome Before and after Surgery. J Vet Res. 2021; 65(2):201-208. DOI: 10.2478/jvetres-2021-0027.
7. Ferasin L, Marcora S. A pilot study to assess the feasibility of a submaximal exercise test to measure individual response to cardiac medication in dogs with acquired heart failure. Vet Res Commun. 2007; 31: 725-37. DOI: 10.1007/s11259-007-3566-7.
8. Lilja-Maula L, Lappalainen AK, Hyytiäinen HK et al. Comparison of submaximal exercise test results and severity of brachycephalic obstructive airway syndrome in English bulldogs. Vet J. 2017; 219: 22-26. DOI: 10.1016/j.tvjl.2016.11.019
9. Lodato DL, Hedlund CS. Brachycephalic airway syndrome: pathophysiology and diagnosis. Compend Contin Educ Vet. 2012; 34: E3.
10. Meola SD. Brachycephalic airway syndrome. Top Companion Anim Med. 2013; 28: 91-6. DOI: 10.1053/j.tcam.2013.06.004.
11. Riggs J, Liu NC, Sutton DR, et al. Validation of exercise testing and laryngeal auscultation for grading brachycephalic obstructive airway syndrome in pugs, French bulldogs, and English bulldogs by using whole-body barometric plethysmography. Vet Surg. 2019; 48: 488-496. DOI: 10.1111/vsu.13159.
12. Environmental and Physiological Factors Associated With Stamina in Dogs Exercising in High Ambient Temperatures. Front Vet Sci. 2017; 4: 144. DOI: 10.3389/fvets.2017.00144.
13. Rovira S, Munoz A, Benito M. Effect of exercise on physiological, blood and endocrine parameters in search and rescue-trained dogs. Vet Med. 2008; 53: 333–346. DOI:10.17221/1860-VETMED
14. Spengler CM, Roos M, Laube SM, Boutellier U. Decreased exercise blood lactate concentrations after respiratory endurance training in humans. Eur J Appl Physiol Occup Physiol. 1999; 79: 299-305. DOI: 10.1007/s004210050511.
15. Stevenson CK, Kidney BA, Duke T, et al. Evaluation of the Accutrend for lactate measurement in dogs. Vet Clin Pathol. 2007; 36: 261-266. DOI: 10.1111/j.1939-165x.2007.tb00221.x

Scientific contribution/Original research/Invited lecture

Anaesthetic Management for Dogs Treated Surgically for Brachycephalic Syndrome: A Preliminary Study

Lukanc B[1], Nemec Svete A[1], Erjavec V[1] *

1. University of Ljubljana, Veterinary Faculty, Small Animal Clinic, Ljubljana, Slovenia
* Correspondence: Barbara Lukanc; barbara.lukanc@vf.uni-lj.si

Abstract:
Brachycephalic breeds have various health problems due to anatomic abnormalities that represented brachycephalic obstructive airway syndrome (BOAS). BOAS is characterized by stenotic nostriles, an elongated soft palate, aberrant nasal conche, everted laryngeal saccules, laryngeal collapse and hypoplastic trachea and is clinically observed by dyspnea, stridor, exercise intolerance and vomiting. Staphylectomy and resection of the ala nasi for surgical treatment of BOAS was performed in 30 brachycephalic dogs (BOAS group) (14 French bulldogs, 9 Boston terriers, and 7 pugs). There were two control groups, a group of 15 non-brachycephalic dogs and a group of 11 brachycephalic dogs that did not have surgery associated with BOAS. The dogs in the BOAS group had significantly higher body temperature compared to the control group of brachycephalic dogs, but not compared to the group of non-brachycephalic dogs. Internal diameter of the endotracheal tube was significantly smaller in the BOAS group and in the control group of brachycephalic dogs compared with the group of non-brachycephalic dogs. The time of extubation after general anaesthesia was significantly longer in the BOAS group compared to both control groups. The brachycephalic dogs for surgical correction of BOAS should be provided with gastroprotectives, antiemetics, dexamethasone and analgesics before surgery, sedation should be minimal to achieve earlier recovery from anaesthesia and spontaneous breathing without support. After surgery of the BOAS, dogs should be provided with non-steroidal analgesics, gastroprotectives and metoclopramide, they should be restrained from vigorous playing and exercise for at least 10 days.

Keywords: Brachycephalic dog; Anaesthesia; Brachycephalic obstructive syndrome

Citation: Lukanc B, Nemec Svete A, Erjavec V. Anaesthetic management for dogs treated surgically for brachycephalic syndrome: a preliminary study. Proceedings of Socratic Lectures. 2021; 6:15-21. https://doi.org/10.55295/PSL.2021.D.003

1. Introduction

Brachycephalic dogs are characterised by severe shortening of the facial and nasal bones, resulting in upper airway deformity (Downing and Gibson, 2018). These include narrowed nostrils, elongated soft palate, hypoplastic trachea, laryngeal collapse, and eversion of the laryngeal saccules (O'Dwyer, 2017). These anatomic features result in upper airway obstruction (Doxey and Boswood, 2004) and brachycephalic obstructive airway syndrome (BOAS) (O'Dwyer, 2017). BOAS is clinically manifested by dyspnea, stridor, snoring, disturbed sleep patterns, exercise intolerance, and syncope. Two-thirds of brachycephalic dogs also have stridor at rest and 90% snore during sleep (Roedler et al., 2013). In severe cases, BOAS can lead to acute pulmonary oedema (Downing and Gibson, 2018). Forceful inspiration against an obstruction can increase negative intrapleural pressure, the pressure is transmitted to the interstitium and alveoli causing an increase in the hydrostatic gradient. Fluid transudate from the pulmonary capillaries to the pulmonary interstitium occurs, resulting in pulmonary oedema. Elevated negative pressures result in an increase in venous return to the right side of the heart, increasing pulmonary artery pressure while decreasing left ventricular function and increasing afterload. Pulmonary blood volume and pulmonary venous pressure increase, leading to an increase in hydrostatic pressure and oedema formation (Lang et al., 1990). To alleviate these respiratory signs in brachycephalic breeds, surgical treatment such as resection of the ala nasi and resection of the soft palate (staphylectomy) is often required (Aron and Crowe, 1985). This procedure is performed under general anaesthesia.

Due to upper airway problems and difficult breathing, many brachycephalic dogs often have gastrointestinal abnormalities such as regurgitation, vomiting, gastroesophageal reflux, cardial atony, gastritis, gastric retention, distal oesophagitis and pyloric hyperplasia, stenosis and atony, and duodenal inflammation (Poncet et al., 2006; Gruenheid et al., 2018). Clinical signs of gastroesophageal reflux include ptyalism, regurgitation, and vomiting (Poncet et al., 2006).

The aim of our study was to investigate the anaesthetic management of brachycephalic dogs, focusing on specific anaesthetic procedures to avoid potential complications before, during, and after anaesthesia.

2. Materials and Methods

In our preliminary study, 30 brachycephalic dogs (BOAS group), 21 males (M), 9 females (F), including 14 French bulldogs (FB), 9 Boston terriers (BST), and 7 pugs were included for surgical treatment of BOAS. Staphylectomy was performed by folded flap palatoplasty (FFP) and resection of ala nasi was performed by vertical edge alaplasty. There were two control groups, a group of 15 (7M, 8F) non-brachycephalic dogs and a control group of 11 (6M, 5F) brachycephalic dogs (FB, BST and pugs) that underwent surgery unrelated to BOAS.

Clinical examinations of the dogs were performed on the day of surgery without sedation. Dogs were presented with respiratory and gastrointestinal signs but were otherwise healthy.

Food was withheld for 14 hours and water for two hours before anaesthesia. Before premedication, the dogs were given maropitant (Prevomax 10 mg/ml, Eurovet Animal Health B.V., AE Bladel, The Netherlands) 1 mg/kg intravenously, pantoprazole (Nolpaza 40 mg, Krka, Nova mesto, Slovenia) (0.78 - 1.18) mg/kg intravenously, metoclopramide (Vomend 5 mg/ml, Eurovet Animal Health BV, AE Bladel, The Netherlands) 0.17 - 0.26 mg/kg subcutaneously, dexamethasone (Dexamethason Krka 4 mg/ml, Krka, Novo mesto, Slovenia) (0.09 - 0.16) mg/kg intramuscularly.

Before premedication and induction, dogs were preoxygenated with 100% oxygen (2 – 3) l/min using the flow-by technique. Premedication included butorphanol (Butomidor 10 mg/ml, Richter Pharma, Wels, Austria) (0.12 - 0.33) mg/kg and midazolam (Midazolam Accord 1mg/ml, Accord Healthcare, Poland Sp.z.o.o., Pabianice, Poland) (0.045 -

0.14) mg/kg intravenously (3 – 55) minutes before intravenous induction with propofol (Propomitor 10 mg/ml, Orion Corporation Orion Pharma, Espoo, Finland). Propofol was titrated (2.1 - 13.1 mg/kg) for (5 – 20) minutes during endoscopic examination of the larynx and trachea, in the meantime oxygen was administered by flow-by (2 – 3) l/min as close as possible to the dog's mouth. The dogs were intubated with a cuffed endotracheal tube and endoscopic examination of the nasopharynx was performed. Anaesthesia was maintained with isoflourane (Isoflurine 1000 mg/g, Chemical Iberica PV, Espana) in 100% oxygen. Before surgical incision, the dogs were administered carprofen (Rycarfa 50 mg/ml, Krka, Novo mesto, Slovenia) (3.2 - 4.1) mg/kg intravenously. The eyes were lubricated to prevent drying and corneal damage. Surgery of ale nasi and soft palate was performed.

When the dogs were awake after surgical correction of the upper airway, the BOAS group of dogs were given buprenorphine (Bupredine Multidose 0.3 mg/ml, La Vet Beheer BV, TV Oudewater, The Netherlands) (0.01-0.02) mg/kg was administered intravenously to the group BOAS. Six hours after the first dose of dexamethasone, the same dose of dexamethasone was repeated intramuscularly

For home care, dogs received carprofen (Rycarfa, Krka, Novo mesto, Slovenia) 2 mg/kg orally for 5 to 7 days, metoclopramide (Reglan 10 mg, Alkaloid, Skopje, Macedonia) 0.2 mg/kg twice daily, 14 days, esomeprazole (Nexium 20 mg, AstraZeneca UK Limited, Cheshire, Great Britain) 1 mg/kg, twice daily, 14 days.

Data were analyzed with commercial software (IBM SPSS 25.0, Chicago, Illinois, USA). Descriptive statistics were used to describe the basic features of the data. The Shapiro-Wilk test was performed to test whether the data were normally distributed. A one-way ANOVA with Tukey HSD post hoc test in the case of a normal distribution of the data or a Kruskal-Wallis test followed by multiple comparison and Bonferroni correction in the case of non-normal distribution of the data were used to test for statistically significant differences in the measured parameters (age, weight, pulse, body temperature, internal diameter of endotracheal tube, time of extubation after general anaesthesia) between the groups of BOAS patients (FB, BST, pugs), as well as between the group of all BOAS patients (all BOAS breeds combined), the group of non-brachycephalic dogs, and a control group of brachycephalic dogs. The data that were normally distributed are reported as means ± SDs; the data that were not normally distributed are reported as medians and IQR (IQR - 25th to 75th percentile). A value of $p < 0.05$ was considered significant.

3. Results

Baseline characteristics of groups of patients and control dogs, and measured parameters are summarized in **Table 1**.

Groups of BOAS patients (FB, BST, and pugs) did not differ in pulse, internal diameter of endotracheal tube, the time of extubation after general anaesthesia and body temperature; FB had significantly higher weight than BST ($P = 0.013$) and pugs ($P = 0.010$). Furthermore, FB were significantly younger than BST ($P = 0.043$) and pugs ($P = 0.026$). All dogs in BOAS group had significantly higher body temperature in comparison to control group of brachycephalic dogs ($P = 0.024$), but not in comparison to group of non-brachycephalic dogs (**Table 1**).

Internal diameter of endotracheal tube was significantly smaller in BOAS group ($P < 0.001$) and control group of brachycephalic dogs ($P = 0.002$) in comparison to group of non-brachycephalic dogs. But there was no significant difference in ID of endotracheal tube between BOAS group and control group of brachycephalic dogs (**Table 1**).

The time of extubation after general anaesthesia was significantly longer in BOAS group compared to group of non-brachycephalic dogs ($P < 0.001$) and control group of brachycephalic dogs ($P = 0.029$) (**Table 1**).

Heart rate (HR) in FB ranged from 100 bpm to 140 bpm (median 126 bpm), in BST ranged from 88 bpm to 160 bpm (median 120 bpm) and in pugs from 96 bpm to 190 bpm (median 120 bpm) (**Table 1**).

The time of extubation after general anaesthesia was significantly longer in BOAS group compared to the group of non-brachycephalic dogs ($P < 0.001$) and control group of brachycephalic dogs ($P = 0.029$) (**Table 1**).

The dogs in BOAS group were significantly younger compared to the group of non-brachycephalic dogs ($P = 0.020$) (**Table 1**).

Table 1: Selected parameters in different breeds of brachycephalic dogs and in different groups of dogs.

		Age (months)	Weight (kg)	Number of dogs n (F/M)	Tempera-ture (° C)	HR (bpm)	ID endotra-cheal tube (mm)	Extubation time after the end of surgery (min)	Duration time of anaesthe-sia (min)
		Median (IQR)	Mean ± SD		Mean ± SD	Median (IQR)	Median (IQR)	Median (IQR)	Median (IQR)
FB		16.0(11.0 – 35.5)	11.7± 2.2	14 (11/3)	38.8 ± 0.5	126(100–131)	6.0 (5.5 – 6.0)	23 (19 – 31)	65 (54 – 80)
BST		55.0(36.5 – 86.0)	9.2 ± 1.6	9 (7/2)	38.5 ± 0.5	120(100–139)	5.5 (5.0 – 5.8)	20 (15 – 30)	85 (60 – 98)
Pug		73-0(33.0 – 93.0)	8.9 ± 1.4	7 (3/4)	38.5 ± 0.6	120(110–172)	6.0 (5.5 – 6.0)	20 (15 – 20)	60 (50 – 65)
BOAS group (14 FB + 9 BST + 7 pugs)		38.0(15.0 – 73.8)	10.3± 2.2	30 (21/9)	38.7 ± 0.5	120(100–136)	5.8 (5.5 – 6.0)	10 (16 – 30)	65 (55 – 80)
Group of nonbrachi-cephalic dogs		117.0(14.0 –148.0)	8.9 ± 1.9	15 (7/8)	38.6 ± 0.4	110(88 – 122)	7.5 (7.0 – 8.0)	7 (5 – 13)	55 (40 – 90)
Control group of brachicephalic dogs		86.0 (42.0 – 118.0)	10.5± 2.0	11 (6/5)	38.2 ± 0.6	120(92 – 120)	6.0 (5.4 – 6.6)	12 (10 – 17)	90 (60 – 100)

ID – internal diameter in mm; IQR interquartile range - 25th-75th percentile, F-female, M-male, FB-French bulldog, BST-Boston terrier, n-number of dogs, HR-heart rate, bpm-beats per minute, a - significantly ($P = 0.0024$) higher compared to control group of brachycephalic dogs; b - significant difference compared to BOAS group ($P < 0.001$) and compared to control group of brachycephalic dogs ($P = 0.002$); c – significant difference compared to group of non-brachycephalic dogs ($P< 0.001$) and compared to control group of brachycephalic dogs ($P = 0.029$).

4. Discussion

Anaesthesia of brachycephalic dogs is thought to pose a greater risk compared to other dog breeds because the airway is abnormal in brachycephalic dogs (Gruenheid M, et al., 2018). During the preanesthetic evaluation, it is important to obtain a thorough history and perform a detailed clinical examination to identify possible preexisting comorbidities and risk factors for the individual patient (Downing and Gibson, 2018). This is beneficial in assessing the risk of anaesthesia. In some patients, anaesthesia can be delayed if the problems can be resolved prior to anaesthesia. Brachycephalic dogs with BOAS have a reduced capacity for heat dissipation by painting because of their anatomic abnormalities. Therefore, maintaining normothermia during the perioperative period and postoperatively is critical to avoid respiratory distress (Downing and Gibson, 2018). It is important to reduce stress and consecutive hyperthermia in dogs before and after anaesthesia. At the Veterinary Faculty we leave nervous and agitated dogs under the supervision of their owners until premedication. When accompanied by their owners, they remain calm.

Due to high negative intrathoracic pressure, these dogs have a high prevalence of gastroesophageal reflux, which is associated with an increased risk of oesophagitis and aspiration pneumonia (Shaver et al., 2017). Poncet et al. (2006) recommended that dogs undergoing upper airway surgery receive concomitant gastroprotectives and prokinetics postoperatively to prevent vomiting and aspiration pneumonia and improve prognosis.

The severity of respiratory and gastrointestinal signs was positively correlated in French bulldogs, males, and heavy brachycephalic dogs (Poncet et al., 2006).

Brachycephalic dogs have increased vagal tone compared with non-brachycephalic dogs, which could contribute to the development of bradycardia during general anaesthesia (Doxey and Boswood, 2004). No dog in our study required treatment for bradycardia.Brachycephalic breeds have learned to compensate for their breathing insufficiencies, but sedated and anaesthetized animals cannot compensate for laboured breathing, so the anesthetist should pay attention to their breathing (O'Dwyer, 2017). It is important to administer only as much sedation as necessary and to avoid excessive sedation and relaxation of pharyngeal muscle tone, which leads to relaxation with consequent worsening airway obstruction and hypoventilation. If acute and complete respiratory obstruction occurs, it is necessary to proceed directly with general anaesthesia (Murrel, 2016). For sedation, we used butorphanol and midazolam mixed together and administered slowly intravenously for up to 5 minutes to control the effect of sedation. When the dogs lay down and fell asleep, we stopped titrating the drugs. Preoxygenation should be used before induction to prolong the time of desaturation after apnoea which is desirable in dogs with respiratory disorders and when endotracheal intubation may be difficult and delayed (McNally et al., 2009). If the preoxygenation represent a stress and may exacerbate respiratory difficulties than preoxygenation poses a greater risk than benefit. Five minutes before and during intravenous sedation, dogs were preoxygenated with 100% oxygen to fill the alveoli with a higher than normal oxygen concentration. Guidelines for selection of endotracheal tube size in dogs are based on normal body weight. However, these guidelines cannot be used for brachycephalic dogs (Reminga and King, 2017), which is consistent with our findings that the ID of the endotracheal tube was significantly smaller in all dogs of brachycephalic breeds. However, in the BOAS group, pugs had the lowest body weight, but BST had the smallest endotracheal tube. Therefore, endotracheal tubes with different internal diameters should be prepared before sedation and induction of general anaesthesia. In brachycephalic dogs, endotracheal tubes should be shorter than in non-brachycephalic dogs. In addition, equipment for aspiration of saliva, mucous or regurgitated content should be prepared before premedication of brachycephalic dogs. There was no significant difference in the size of the endotracheal tube between the BOAS group and the control group of brachycephalic dogs, which may indicate that difficult breathing in brachycephalic breeds is mainly caused by airway obstruction by soft tissue rather than by the diameter of the trachea. This was also confirmed by the markedly improved breathing of brachycephalic dogs after nose and soft palate surgery. During recovery, brachycephalic dogs should be positioned in sternal recumbency with the head elevated, neck extended, and tongue pulled rostrally from the mouth to keep the airway open (Downing and Gibson, 2018). Extubation of the endotracheal tube should be delayed as long as possible and should not be done while dogs are still sedated (Adshead, 2014). Dogs should not be extubated until muscle tone returns and they are able to hold their head up independently. The time to extubation after general anaesthesia was significantly longer in the BOAS group than in the two control groups. Therefore, it is important for the anesthetist to have sufficient time for brachycephalic dogs to recover, especially when the dogs are anaesthetized for surgical correction of BOAS. The anesthetist also needs more time before the start of anaesthesia to prepare all medications and equipment needed for general anaesthesia of brachycephalic dogs.

When dogs are fully awake and breathing well for several hours without needing supplemental oxygen, they are stable enough to be discharged to home care.

When brachycephalic dogs are sedated for various reasons, they must be monitored closely for upper airway obstruction. The postoperative period is the most common time for a dog to die. Most dogs die within 3 hours of the end of the procedure (Brodbelt et al., 2008).

However, some dogs become very agitated, stressed, and even hyperthermic when left in the cage during the postoperative period. Therefore, we advise leaving them in the hospital unit under the supervision of their owner until they are stable enough to go

home. In very rare cases, when dogs are extremely agitated, even when accompanied by their owner, they need to be sedated to calm them down. Before discharge, dogs are given analgesics and cortisone, but not sedation.

Corrective surgery of the upper airway in brachycephalic dogs is beneficial to reduce postanaesthetic complications when subsequent surgical and diagnostic procedures are anticipated (Doyle et al., 2020). Despite all the anaesthetics risks and potential complications during and after the surgical procedure, we strongly encourage owners to have their dog with BOAS undergo upper airway surgery early in life, as it will greatly improve the dog's breathing and well-being.

5. Conclusions

When anaesthetizing brachycephalic dogs, we use minimal sedation to achieve earlier recovery from anaesthesia. It has been our experience that the dogs are much calmer when they are with their owner. When we keep them separated from their owner in the clinic, they are so agitated that most of them require sedation.

Brachycephalic dogs for surgical correction of BOAS should be given gastroprotectives, antiemetics, dexamethasone, and analgesics. They should be fasted at least 12 hours before anaesthesia to prevent vomiting.

For anaesthesia, we should prepare a narrower and shorter endotracheal tube than in non-brachycephalic dogs of the same weight, as well as an aspirator for possible aspiration of saliva, mucus, and blood from the mouth and trachea.

Extubation time for brachycephalic dogs is much longer in brachycephalic dogs than in non-brachycephalic dogs.

After BOAS surgery dogs should be discharged home with nonsteroidal antiinflammatory drugs, gastroprotectives, and metoclopramide. They should be restrained from vigorous playing and exercise for at least 10 days.

Funding: This research was supported by Slovenian Research Agency (research program No. P4-0053).

Institutional Review Board Statement: All procedures complied with the relevant Slovenian governmental regulations (Animal Protection Act UL RS, 43/2007).

Conflicts of Interest: The authors declare no conflict of interest.

References

1. Adshead S. Reducing the risk of anaesthetic complications in patients with brachycephalic obstructive airway syndrome. Vet Nurse. 2014; 5: 78–87. https://doi.org/10.12968/vetn.2014.5.2.78
2. Aron DN, Crowe DT. Upper airway obstruction. General principles and selected conditions in the dog and cat. Vet Clin North Am Small Anim Pract. 1985; 15: 891-891. DOI: 10.1016/s0195-5616(85)50101-1
3. Brodbelt DC, Blissitt KJ, Hammond RA, et al. The risk of death: the confidential enquiry into perioperative small ani¬mal fatalities. Vet Anaesth Analg. 2008; 35: 365–373. DOI: 10.1111/j.1467-2995.2008.00397.x
4. Downing F, Gibson S. Anaesthesia of brachycephalic dogs. J Small Anim Pract. 2018; 59: 725–733. DOI: 10.1111/jsap.12948
5. Doxey S, Boswood A. Differences between breeds of dog in a measure of heart rate variability. Vet Rec. 2004; 154: 713–717. DOI: 10.1136/vr.154.23.713
6. Doyle CR, Aarnes TK, Ballash GA, et al. Anesthetic risk during subsequent anesthetic events in brachycephalic dogs that have undergone corrective airway surgery: 45 cases (2007-2019). J Am Vet Med Assoc. 2020; 7: 744-749. DOI: 10.2460/javma.257.7.744
7. Gruenheid M, Aarnes TK, McLoughlin A et al. Risk of anesthesia-related complications in brachycephalic dogs. J Am Vet Med Assoc. 2018; 253: 301-306. DOI: 10.2460/javma.253.3.301
8. Lang SA, Duncan PG, Shephard DA, et al. Pulmonary oedema associated with airway obstruction. Can J Anaesth. 1990; 37: 210-218. DOI: 10.1007/BF03005472
9. McNally EM, Robertson SA, Pablo LS. Comparison of time to desaturation between preoxygenated and nonpreoxygenated dogs following sedation with acepromazine maleate and morphine and induction of anesthesia with propofol. Am J Vet Res. 2009; 70: 1333-1338. DOI: 10.2460/ajvr.70.11.1333
10. Murrel J. Pre-anaesthetic medication and sedation. In: Duke-Novakovski T, de Vries M, Seymour C, editors. BSAVA Manual of Canine and Feline Anaesthesia and Analgesia. 3rd edn. BSAVA, Gloucester UK. 2016; pp. 170-189. DOI: 10.22233/9781910443231.13
11. O'Dwyer L. Anaesthesia for the Brachycephalic Patient. WSAVA 2017 Congress proceedings 2017, Copenhagen, Denmark 25th - 28th September. Available from https://www.vin.com/apputil/content/defaultadv1.aspx?id=8506297&pid=20539&

12. Poncet CM, Dupre GP, Freiche VG, et al. Long-term results of upper respiratory syndrome surgery and gastrointestinal tract medical treatment in 51 brachycephalic dogs. J Small Anim Pract. 2006; 47: 137-142. DOI: 10.1111/j.1748-5827.2006.00057.x
13. Reminga C, King LG. Oxygenation and Ventilation. In: Kirby R, Linklater A, editors. Monitoring and intervention for the critically ill small animal. The rule of 20. Wiley Blackwell, UK 2017; pp. 109-136.
14. Roedler FS, Pohl S, Oechtering GU. How does severe brachy¬cephaly affect dog's lives? Results of a structured preopera-tive owner questionnaire. Vet J. 2013; 198: 606–610. DOI: 10.1016/j.tvjl.2013.09.009
15. Shaver SL, Barbur LA, Jimenez DA, et al. Evaluation of gastroesoph¬ageal reflux in anesthetized dogs with brachycephalic syndrome. J Am Anim Hosp Assoc. 2017; 53: 24-31. DOI: 10.5326/JAAHA-MS-6281

Scientific contribution/Original research/Invited lecture

Surgical Treatment of Brachycephalic Syndrome in Dogs

Erjavec V[1,*], Lukanc B[1]

1. University of Ljubljana, Veterinary Faculty, Small Animal Clinic, Ljubljana, Slovenia
* Correspondence: Vladimira Erjavec; vladimira.erjavec@vf.uni-lj.si

Abstract:
Brachycephalic breeds are becoming increasingly popular, despite various health problems due to a number of congenital anatomical features that differ from those of mesaticephalic breeds. Morphologic anomalies of the upper airway are primary (stenotic nostrils and elongated soft palate) and secondary due to increased airway resistance, negative intraluminal pressure and turbulent airflow. A total of 32 client-owned dogs of brachycephalic breeds were examined during the study period. The dogs were divided into 3 groups based on the severity of airway obstruction. All dogs underwent alaplasty and soft palate surgery, sacculectomy was performed in only 3 dogs. Based on the results of the questionnaire completed by owners before and 2 weeks after surgery, respiratory signs, gastrointestinal signs, exercise intolerance, and sleep disturbance improved in dogs in all groups of brachycephalic syndrome after surgery. It is important that veterinarians, as professionals, make the public aware of the potential problems associated with exaggerated brachycephalic characteristics. It is important that owners of a dog diagnosed with brachycephalic syndrome seek surgical treatment early in the affected dog's life. The owners of brachycephalic dogs should not perceive the clinical signs related to conformational inherited disorders as "normal" for the breed.

Citation: Erjavec V, Lukanc B. Surgical treatment of brachycephalic syndrome in dogs. Proceedings of Socratic Lectures. **2021; 6:** 23-29. https://doi.org/10.55295/PSL.2021.D.004

Keywords: Brachycephalic syndrome; Surgical treatment; Dogs; Staphylectomy; Alaplasty

1. Introduction

Brachycephaly in dogs is the result of years of artificial selection for a short head shape. Originally, the brachycephalic phenotype was selected for fighting, but more recently brachycephalic breeds have been selected as pets with appealing appearance (Ekenstedt et al., 2020).

Brachycephalic syndrome (BS) has been identified in many brachycephalic breeds, including French and English bulldogs, pugs, Boston terriers, Shih-tzu, Pekingese, and Lhasa Apso (Trappler and Moore, 2011) and includes a variety of clinical signs such as loud upper respiratory sounds (stridor, stertor), sniffing, dyspnea, sleeping disorders, intolerance to exercise and heat, cyanosis, gastrointestinal signs, and in severe cases, fainting and occasionally death (Wykes, 1991; Poncet et al., 2005; Riecks et al., 2007; Roedler et al., 2013).

Morphologic anomalies of the upper airway are divided into primary and secondary. Primary anomalies include stenotic nostrils in which the nostril is deformed, and the opening is reduced to a vertical slit (Dupre and Heidereich, 2016), relative macroglossia (Ekenstedt et al., 2020), aberant or protruding nasal turbinates, narrow (naso)pharyngeal dimensions, an elongated soft palate, narrow laryngeal dimensions, and tracheal hypoplasia (Dupre and Heidereich, 2016; ter Haar and Sanches, 2017). As a result of increased airway resistance, negative intraluminal pressure, and turbulent airflow, secondary physical changes develop such as everted laryngeal saccules, everted tonsils, naso-pharyngeal collapse, and laryngeal, tracheal, and bronchial collapse (de Lorenzi et al., 2009), which may contribute to further obstruction (ter Haar and Sanches, 2017).

The initial diagnosis of brachycephalic syndrome is based on a combination of breed and clinical signs; further diagnostic imaging is recommended for therapeutic and prognostic reasons. Early diagnosis and surgical intervention of brachycephalic syndrome to improve airflow is important to prevent further deterioration and progression of secondary changes (Meola, 2013). Dogs with acute respiratory distress should be treated medically and preferably operated on at a later date after the edema and soft tissue inflammation have resolved. Treatment of affected dogs can be conservative (weight management and environmental modifications) or surgical. Several surgical techniques have been described to reduce the soft tissues at different levels.

The aim of our study was to evaluate the different anatomic changes in brachycephalic dogs and to assess the short-term outcome in dogs of different grades of dogs undergoing surgery for BS. In this article, we present our current surgical treatment of BS, which includes alaplasty and staphylectomy in all dogs and sacculectomy in selected cases.

2. Methods

A total of 32 dogs of brachycephalic breeds owned by clients were examined during the study period. After diagnosed with BS, 14 French bulldogs (FB), 9 pugs (P), 5 Boston terriers (BST), 3 English bulldogs (EB), and 1 Japanese Chin (JC) were included in the study.

A preoperative questionnaire on BS - related signs (respiratory signs, gastrointestinal signs, exercise intolerance, and sleep disturbance) was completed for each dog at initial presentation, and the same questionnaire was completed again two weeks after surgery. Diagnosis was based on clinical signs of upper airway obstruction, gastrointestinal clinical signs, and anatomic abnormalities, as described elsewhere (Dupre and Heidenreich, 2016). Formal written informed consent was obtained from the owner before the dogs participated in the study. All procedures complied with the relevant Slovenian governmental regulations (Animal Protection Act UL RS, 43/2007). The study

was evaluated and approved by the Ethical Committee on Animal Research of the Veterinary Faculty, University of Ljubljana. The dogs were scheduled for general anaesthesia during which endoscopic examinations and surgical treatments were performed.
Data was analysed with commercial software (IBM SPSS 25, Chicago, Illinois, USA). Descriptive statistics were used to describe the basic features of the data (age, weight, body condition score (BCS)). The Shapiro Wilk test was performed to test whether the data were normally distributed. According to the results of normality tests, Kruskal Wallis test followed by multiple comparisons and Bonferroni adjustment was used to test for statistically significant differences in age, weight and BCS among groups of BOAS patients. Data are reported as medians and interquartile range (IQR – 25th to 75th percentile). A value of $P < 0.05$ was considered significant.

3. Results

The dogs were classified into 3 grades according to the severity of obstruction at different anatomic levels, such as nasopharynx, oropharynx, laryngopharynx, and larynx, causing airway narrowing after soft palate surgery, as described elsewhere (Erjavec et al., 2021). Four dogs (1P, 3 FB) with no or minimal airway obstruction after nostril and soft palate surgery were classified as group 1, 16 dogs (3P, 3BST, 9FB, 1JC) with up to 50% airway obstruction after surgery were classified in group 2, and 12 dogs (5P, 3EB, 2BST, 2FB) with almost complete airway obstruction after surgery were classified in group 3. Baseline characteristics of the BOAS patients included in the individual groups are summarized in **Table 1**. We found no significant difference in age, weight and BCS among groups of BOAS patients. Evaluation of soft tissue anatomic changes revealed that all dogs (32/32) had stenotic nostrils and an overlong soft palate., everted tonsils were observed in 28/32 (87.5%) dogs, 24/32 (75%) dogs had obstructed choanae, aberrant conchae were present in 15/32 (46.9%) dogs, 23/32 (71.9%) had redundant soft tissue (edematous mucosa) protruding through the choanae, and 31/32 (96.9%) dogs had everted laryngeal saccules.

Table 1. Baseline characteristics in groups of brachycephalic obstructive airway syndrome patients.

	Grade 1	Grade 2	Grade 3
Number	4	16	12
Sex (female/male)	3/1	5/11	5/7
Age (years) Median IQR	 2.41 1.08–4.75	 2.88 1.14–7.11	 1.75 1.44–7.90
Weight (kg) Median IQR	 9.78 7.49–12.30	 10.20 7.78–12.53	 9.68 8.54–10.80
BCS Median IQR	 3.0 2.3–3.0	 3.0 3.0–4.0	 3.0 3.0–3.0

BCS, body condition score; IQR, interquartile range (25th to 75th percentile)

The dogs were intubated and the surgical procedure was performed under general anaesthesia with isoflurane (Isoflurine 1000mg/g, Chemical Iberica PV, Espana) in 100% oxygen. For surgery, each dog was placed in a sternal position. Resection of the nostrils was performed with a horizontal wedge excision of the dorsomedial and caudal part of the alae with a No. 11 scalpel blade. Few simple interrupted sutures with the synthetic

absorbable monofilament suture Glycomer 631 (Biosyn 4/0; Covidien, Dublin, Ireland) were placed to counteract the wedge margins (**Figure 1**).

Figure 1. Nostrils in Boston terrier left side open nostril after the surgery, right nostril closed to a vertical slit.

Because many brachycephalic dogs have an excessively thick and long soft palate, a folded flap palatoplasty (FFP) (Findji and Dupre, 2008) was performed in all dogs. A portion of the oropharyngeal mucosa and underlying soft tissue was removed using a Surgitron Radiolase II (Ellman International, Inc., Hicksville, NY, USA) (**Figure 2**). In 3 of the 32 dogs, a sacculectomy was also performed. For sacculectomy, the dogs were extubated, and the saccules were grasped with forceps and cut with scissors. Minimal bleeding occurred.

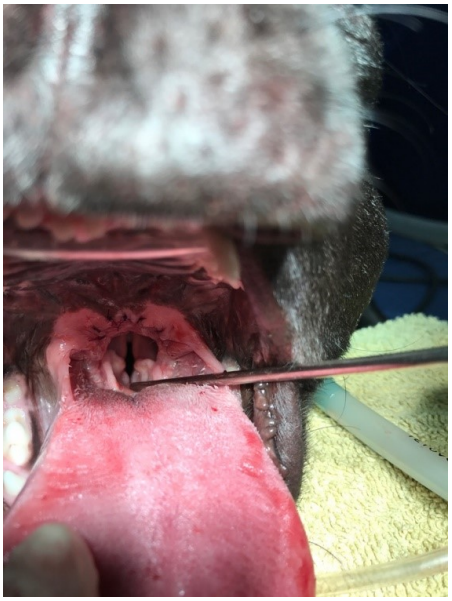

Figure 2. Soft palate after the folded flap palatoplasty surgery.

Based on the results of questionnaires completed by the owners, all clinical signs (respiratory signs, gastrointestinal signs, exercise intolerance, and sleep disturbance) in all groups of dogs improved two weeks after surgery. Before surgery, the most prominent clinical signs were respiratory problems and sleep disturbances; after surgery, sleep disturbances remained the most prominent clinical sign in all groups of dogs (Erjavec et al., 2021).

4. Discussion

Surgery should be performed early to prevent further deterioration and possible airway collapse, but the optimal time for surgery has not yet been determined. It has been recommended to be performed after 6 months of age (Dupre and Heidenreich, 2016) and even at the time of spay or castration (Trappler and Moore, 2011). At Veterinary Faculty in Ljubljana, both procedures are not combined. We recommend operating on the BS first and evaluating the result at a later neutering. In dogs not operated at a young age and suffering from brachycephalic syndrome, which are middle-aged (Haimel and Dupre, 2015) and older than 10 years, surgery can still improve clinical signs and should be performed in all dogs suffering from brachycephalic syndrome. It is not entirely clear which part of the obstructed airway is most responsible for the clinical signs of BS (Ekenstedt et al. 2020). In our study, all dogs had some degree of stenosis of the nostrils and all dogs had an elongated soft palate. These findings are high compared to other studies (Poncet et al. 2005; Torrez and Hunt, 2006; Fasanela et al. 2010) but are consistent with the study by Seneviratne et al. (2020). Several techniques have been described for the correction of stenotic nostrils, no technique is more recommended than another, they all aim to allow more air into the nasal cavity. There was never a serious complication during this surgery; however, there is always a lot of bleeding during the procedure. The nasopharynx was narrowed in 75% of dogs due to mucosal folds and/or an aberrant caudal turbinate, and an aberrant caudal turbinate was present in 26.9% of dogs. Studies show partial regrowth of the removed turbinates, so the long-term effects of turbinectomy need to be further investigated (Schuenemann and Oechtering, 2014). All dogs underwent FFP to shorten an excessively long and thick soft palate. The soft palate is shortened by retracting the caudal edge of the soft palate and folding it onto itself. With FFP, the surgical site is moved rostrally and possible edema of the wound may be less obstructive to the airway. Although it has been reported that up to 28% of dogs require a tracheostomy after surgical treatment of BS (Dupre and Heidereich, 2016), none of the dogs in our study required this. We hypothesise that the effect of this surgery is due to both the opening of the nasopharynx and the removal of the rima glottidis obstruction.

In many brachycephalic dogs, the tongue is 10 times denser than in mesaticephalic dogs (Jones et al. 2020), thick and excessively long (relative macroglossia), and displaces the soft palate further dorsally, which, together with hypertrophy of the nasopharyngeal mucosa (Ekenstedt et al., 2020), results in airway obstruction during nasal breathing. However, the tongue volume in pugs is smaller than in French and English bulldogs (Siedenburg and Dupre, 2021). In our study, we observed that the tongue in pugs is relatively longer than in other brachycephalic dogs and that it is not as thick and therefore does not contribute to breathing problems. To date, no surgical techniques to reduce the size of the tongue have been successful in treating BS.

Everted tonsils used to be treated with tonsillectomy, but this is no longer recommended because minimal or no effect was observed after tonsil removal (Poncet et al., 2005; Poncet et al., 2006). We have so far never removed tonsils for the treatment of BS. Laryngeal saccules can be surgically removed using a variety of instruments or devices, but the complication rate after removal is high, so routine removal is not recommended (Huges et al., 2018). At the Veterinary faculty we have removed them only when everted saccules contributed significantly to obstruction and when further anaesthesia would pose a high risk to the patient. The trachea may be congenitally hypo-plastic, with tracheal cartilages that touch or overlap. While this may exacerbate respiratory clinical signs, it is not considered a major cause BS (Ekenstedt et al., 2020) and does not affect

postoperative outcomes (Riecks et al., 2007). In addition, this condition cannot be treated surgically. Collapsed trachea and bronchi are the result of chronically increased airway pressure (ter Haar and Sanches, 2017) and, according to our observations, occur mainly in pugs.

Possible complications during surgery from BS and postoperatively include bleeding, vomiting, hyperthermia, aspiration pneumonia, respiratory problems due to soft tissue edema, or airway obstruction by saliva, mucus, and/or blood. Close patient monitoring is essential. Professional help must be sought immediately if there is retching, vomiting, or possible respiratory problems. Several techniques have been described for the correction of narrowed nostrils. No one technique is more recommended than another; they all aim to allow more air into the nasal cavity. Limited exercise (walks on a harness, no playing with other dogs) is recommended for at least one week after surgery to avoid the complications mentioned above.

5. Conclusions

Our study shows that respiratory signs, gastrointestinal signs, exercise intolerance, and sleep disturbance improved in dogs in all groups of BS after surgery. Nevertheless, surgery is recommended at an early age when BS is diagnosed because the more severe secondary physical changes may develop as a result of increased airway resistance, negative intraluminal pressure, and turbulent airflow. Surgical treatment of BS usually involves alaplasty and palatoplasty, and occasionally a sacculectomy may be performed.

Funding: This research was supported by Slovenian Research Agency (research program No. P4-0053).
Institutional Review Board Statement: All procedures complied with the relevant Slovenian governmental regulations (Animal Protection Act UL RS, 43/2007).
Conflicts of Interest: The authors declare no conflict of interest.
Acknowledgements: The authors thank Alenka Nemec Svete for her valuable suggestions and professional help in designing and finalising this paper.

References

1. De Lorenzi D, Bertoncello D, Drigo M. Bronchial abnormalities found in a consecutive series of 40 brachycephalic dogs. J Am Vet Med Assoc. 2009; 235: 835-40. DOI: 10.2460/javma.235.7.835.
2. Dupre G, Heidereich D. Brachycephalic Syndrome. Vet Clin Small Anim. 2016; 46: 691–707 http://dx.doi.org/10.1016/j.cvsm.2016.02.002
3. Ekenstedt KJ, Crosse KR, Risselada M. Canine Brachycephaly: Anatomy, Pathology, Genetics and Welfare. J Comp Pathol. 2020; 176: 109-115. DOI: 10.1016/j.jcpa.2020.02.008.
4. Erjavec V, Vovk T, Svete A. Evaluation of oxidative stress parameters in dogs with brachycephalic obstructive airway syndrome before and after surgery. J Vet Res. 2021; 65: 201-208. https://doi.org/10.2478/jvetres-2021-0027.
5. Findji L, Dupré G. Folded flap palatoplasty for treatment of elongated soft palates in 55 dogs. Eur J Companion Anim Pract. 2008; 19: 125–132.
6. Haimel G, Dupré G. Brachycephalic airway syndrome: a comparative study between pugs and French bulldogs. J Small Anim Pract. 2015; 56: 714-9. DOI: 10.1111/jsap.12408.
7. Fasanella FJ, Shivley JM, Wardlaw JL, et al. Brachycephalic airway obstructive syndrome in dogs: 90 cases (1991–2008). J Am Vet Med Assoc. 2010; 237: 1048–51. DOI: 10.2460/javma.237.9.1048
8. Haar G.ter, Sanchez RF. Brachycephaly-related diseases. In: Small Dogs – Big Problems, Veterinary Focus. 2017; 27: 15-22.
9. Hughes JR, Kaye BM, Beswick AR, Ter Haar G. Complications following laryngeal sacculectomy in brachycephalic dogs. J Small Anim Pract. 2018; 59: 16-21. doi: 10.1111/jsap.12763.
10. Jones BA, Stanley BJ, Nelson NC. The impact of tongue dimension on air volume in brachycephalic dogs. Vet Surg. 2020; 49 :512-520. DOI: 10.1111/vsu.13302.
11. Meola SD. Brachycephalic airway syndrome. Top Companion Anim Med. 2013; 28: 91–96. DOI: 10.1053/j.tcam.2013.06.004
12. Poncet CM, Dupré G, Freiche VG, et al. Prevalence of gastrointestinal tract lesions in 73 brachycephalic dogs with upper respiratory syndrome. J Small Anim Pract. 2005; 46: 273–9. DOI: 10.1111/j.1748-5827.2005.tb00320.x.
13. Poncet CM, Dupre GP, Freiche VG, Bouvy BM. Long-term results of upper respiratory syndrome surgery and gastrointestinal tract medical treatment in 51 brachycephalic dogs. J Small Anim Pract 2006; 47: 137–42. DOI: 10.1111/j.1748-5827.2006.00057.x

14. Riecks TW, Birchard SJ, Stephens JA. Surgical correction of brachycephalic syndrome in dogs: 62 cases (1991-2004). J Am Vet Med Assoc. 2007; 230: 1324-1328. DOI: 10.2460/javma.230.9.1324
15. Roedler FS, Pohl S, Oechtering GU. How does severe brachycephaly affect dog's lives? Results of a structured preoperative owner questionnaire. Vet J. 2013; 198: 606-610. DOI: 10.1016/j.tvjl.2013.09.00
16. Schuenemann R, Oechtering G. Inside the brachycephalic nose: conchal regrowth and mucosal contact points after laser-asisted turbinectomy. J Am Anim Hosp Assoc. 2014; 50: 237–46. DOI: 10.5326/JAAHA-MS-6086
17. Siedenburg JS, Dupré G. Tongue and Upper Airway Dimensions: A Comparative Study between Three Popular Brachycephalic Breeds. Animals (Basel). 2021; 11:662. doi: 10.3390/ani11030662.
18. Torrez CV, Hunt GB. Results of surgical correction of abnormalities associated with brachycephalic airway obstruction syndrome in dogs in Australia. J Small Anim Pract. 2006; 47:150–4. DOI: 10.1111/j.1748-5827.2006.00059.x
19. Trappler M, Moore K. Canine brachycephalic airway syndrome: surgical management. Compend Contin Educ Vet. 2011; 33:E1-7. PMID: 21870354.
20. Wykes PM. Brachycephalic airway obstructive syndrome. Probl Vet Med. 1991; 3: 188-97. PMID: 1802247.

Review

An Overview of the Latest Developments in the Treatment of Feline Hyperthyroidism with Radioactive Iodine ^{131}I

Ferjan P[1], Jeran M[2,3,*]

1. University of Ljubljana, Faculty of Veterinary Medicine, Ljubljana, Slovenia
2. University of Ljubljana, Faculty of Health Sciences, Laboratory of Clinical Biophysics, Ljubljana, Slovenia
3. University of Ljubljana, Faculty of Electrical Engineering, Laboratory of Physics, Ljubljana, Slovenia

* Correspondence: Marko Jeran; marko.jeran@fe.uni-lj.si

Abstract: Feline hyperthyroidism is a disorder resulting from excessive concentrations of thyroid hormones in the systemic circulation. Parenteral application of radioiodine ^{131}I is the treatment of choice, but it can cause iatrogenic hypothyroidism. To minimalize that risk, algorithms for individual doses and prognosis factors have been suggested. Treatment of hyperthyroidism can worsen a pre-existing renal condition, therefore, renal function should always be assessed pre-and post-treatment. To make this treatment more available and widespread, oral administration of ^{131}I has been suggested. This contribution reviews the latest contributions on this subject and compares them to what is already known about the treatment of feline hyperthyroidism with radioactive iodine.

Keywords: endocrinology, feline hyperthyroidism, treatment, radioiodine ^{131}I

Citation: Ferjan P, Jeran M. An overview of the latest developments in the treatment of feline hyperthyroidism with radioactive iodine ^{131}I. Proceedings of Socratic Lectures. 2021; 6: 31-36. https://doi.org/10.55295/PSL.2021.D.005

Publisher's Note: UL ZF stays neutral with regard to jurisdictional claims in published maps and institutional affiliations.

1. Introduction

Hyperthyroidism is a disorder resulting from excessive concentrations of triiodothyronine (T3) and/or thyroxine (T4) in the systemic circulation. Thyroid hormones have a wide variety of actions, most important being the metabolism of carbohydrates, proteins, lipids, and increasing overall sympathetic drive (Mooney et al., 2012). An increase in their concentration causes a hypermetabolic state, responsible for symptoms, seen in hyperthyroidism (Graves et al., 2017).

1.1. Etiology

The cause of feline hyperthyroidism is, most commonly, benign adenomatous hyperplasia of one (30%) or both (70%) lobes (Mooney et al., 2012). Thyroid carcinoma is a rare occurrence (Graves et al., 2017), except when the initial benign hyperplasia is not treated – then it can potentially turn malignant (Carney et al., 2016). The underlying etiology is still not completely understood (Mooney et al., 2012). Multiple factors could be causing the abnormal growth of cells. In some hyperthyroid cats, mutations in thyroid-stimulating hormone (TSH) receptors and G-protein have been detected, leading to decreased ability of cAMP inhibition, resulting in excess secretion of T3 and T4. Some studies have shown that goitrogens (polybrominated diphenyl ethers, PBDEs) in food and/or the environment, isoflavones from soy, and varying concentrations of iodine in food might be some of the factors (Carney et al., 2016).

1.2. Clinical manifestation

Hyperthyroidism usually affects middle-aged and older cats. The most common clinical signs, associated with excessive production of thyroid hormones are weight loss with normal or increased appetite, tachycardia, systolic murmurs and gallop rhythm of the heart, intermittent gastrointestinal disorders (vomiting and/or diarrhea), polyuria/polydipsia, irritability, and palpable goiter (Mooney et al., 2012).

1.3. Diagnosis

T4 is the main secretory product of the feline thyroid gland, therefore the diagnostic method of choice is measuring serum concentrations of total thyroxine (tT4) (Graves et al., 2017). Most hyperthyroid cats have elevated tT4 concentrations, however, around 10% of all cases have serum total T4 concentrations within the reference interval. Especially in the early stages or mild cases, concentrations can fluctuate (Mooney et al., 2012). Concurrent diseases, such as diabetes mellitus, hepatic diseases, chronic kidney disease (CKD), congestive heart failure, etc., can also lower tT4 levels. Rechecking cats with symptoms of hyperthyroidism but no increase in tT4 is indicated. Tests for free T4 (fT4) have high sensitivity, but poor specificity and tend to be expensive. fT4 can be increased in cats with occult hyperthyroidism and can, as a result, be used in diagnosing euthyroid patients. Thyroid scintigraphy is an extremely sensitive test for diagnosing hyperthyroidism. Thyroid uptake of pertechnetate or radioactive iodine correlates strongly with hyperthyroxinemia, but the test is limited by its availability. Scintigraphy can also be in use for cats undergoing thyroidectomy – identifying unilateral versus bilateral disease and ectopic (**Figure 1**) (Graves et al., 2017). Other diagnostic tests include serum TSH measurement, T3 suppression test, TSH, and TRH stimulation test (Mooney et al., 2012; Graves et al., 2017).

1.4. Treatment options

Medical management with methimazole or carbimazole inhibits thyroid hormone synthesis and release, but it is non-curative. It is recommended for either pre-operative (to decrease metabolic and cardiac complications) or long-term management. Surgical thyroidectomy is considered to be very effective and a treatment of choice, but can lead to

hypocalcemia if parathyroid glands are injured. Treatment with radioiodine 131I is usually considered the best treatment option for feline hyperthyroidism and will be the main topic of discussion in this contribution (Mooney et al., 2012). The research reviewed in this article outlines new approaches to the treatment that result in lower rates of iatrogenic hypothyroidism, thus making it safer. Alternative methods of ^{131}I administration are also suggested, possibly making the treatment more available. It also discusses how to deal with concurrent and post-treatment kidney damage.

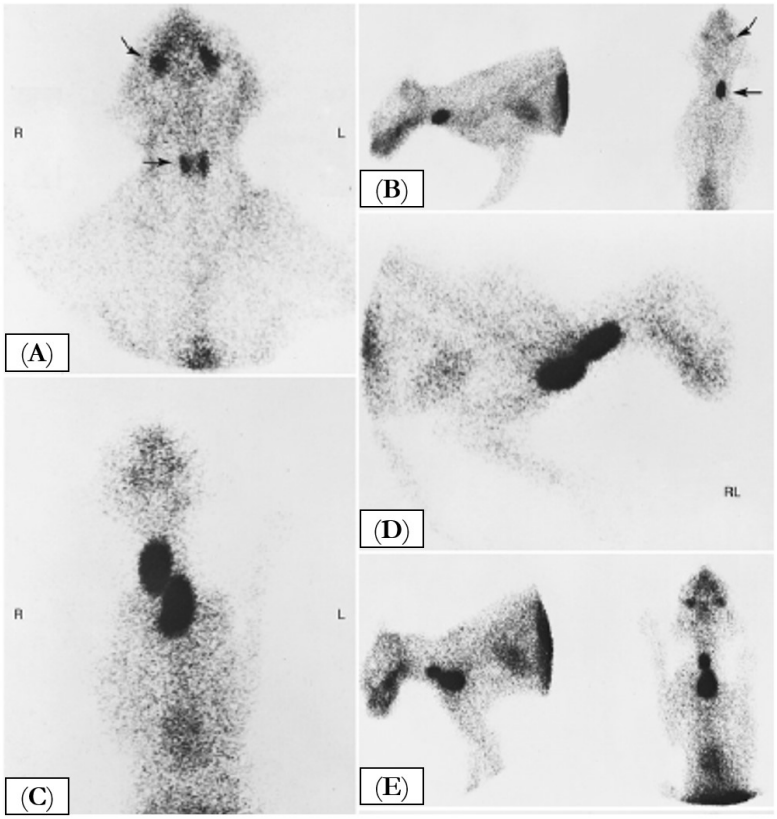

Figure 1. Thyroid scan (radioactive technetium – 99m) of a normal cat (A), thyroid scan of a cat with unilateral disease (B), thyroid scan of a cat with symmetric bilateral disease (C and D), thyroid scan of a cat with asymmetric bilateral disease (E). From Graves et al. (2017).

Thyroid hormones and thyroglobulin are the only iodinated organic molecules in the body, therefore any iodine, that comes into the body is taken to thyroid follicular cells. Radioiodine therapy exploits this process, using radioactive iodine isotope ^{131}I, which concentrates in thyroid tissue (Mooney et al., 2012). Radioiodine emits beta particles, that cause tissue damage and can only travel up to 2 mm, therefore are only locally destructive (Peterson et al., 2021a). It predominantly damages hyperactive cells (Graves et al., 2017). The main limitations of radioactive iodine treatment are the requirement for special licensure, isolation of cat from 3 days to 4 weeks after the treatment (Carney et al., 2016), and the possibility of developing hypothyroidism (Peterson et al., 2021a,b). T4 declines within the normal range in 4 – 12 weeks post-treatment, and the symptoms can persist for a few months (Graves et al., 2017).

2. Individualised dose and the prognosis factors

The long-term prognosis for cats, treated with ^{131}I is good. Median survival time is estimated to be from 24 months – 4 years. The most common causes of death in cats, treated with radioiodine are those normally associated with aging, such as malignancy and renal disease (Mooney et al., 2012). Euthyroidism in cats, treated with radioiodine, is not

always achieved. 5% to 10% of cats remain persistently hyperthyroid and 20% to 50% develop iatrogenic hypothyroidism (Peterson et al., 2021b).

A recent study, conducted by Peterson et al. (2021a, b), aimed to individualize the dosing algorithm of ^{131}I, and, as a result, minimize the risk of iatrogenic hypothyroidism (Peterson et al., 2021a). They also wanted to identify pretreatment factors, that could predict persistent hyperthyroidism and iatrogenic hypothyroidism after individualized treatment with ^{131}I (Peterson et al. 2021b).

They found that with the fixed-dose (3–5 mCi), iatrogenic hypothyroidism develops in 30–80% of cats within 6 months of treatments. By using an individualized algorithm, Paterson and Rishniw performed a prospective study that included 1400 hyperthyroid cats treated with ^{131}I (Peterson et al., 2021 a, b). Cats that fitted the criteria, underwent an evaluation, that included a complete physical examination, routine laboratory testing (CBC, serum biochemical profile, complete urinalysis), determination of serum tT4, T3, and TSH concentrations, and qualitative and quantitative thyroid scintigraphy (Peterson et al., 2021b). Thyroid scintigraphy was performed by injecting sodium ^{99m}Tc – pertechnetate (TcTU) intravenously, to classify the pattern of the disease (unilateral, bilateral, or multifocal disease) and to exclude thyroid carcinoma. They determined the volume of each thyroid tumor by calculating the percent thyroidal uptake of the injected TcTU (Peterson et al., 2021a).

Next, they assigned each of the parameters (T3 and T4 concentrations, TcTU, and thyroid volume) ^{131}I dose scores. The higher the parameter value was, the higher the dose score. For example, serum T_4 concentration of 15 µg/dL had a higher dose score than serum T_4 concentration of 6 µg/dL. This was done so there would be the same unit (mCi) for all of the parameters, which would simplify calculating the final dose (Peterson et al., 2021a).

The average ^{131}I dose score of all parameters combined was then calculated for each individual patient. To avoid overdosage, only 80% of this composite dose was used (Peterson et al., 2021a).

24 hours after administration, the percent of thyroidal ^{131}I uptake was determined, and based on that, an additional ^{131}I dose was calculated and added to reach an adequate radiation dose (200 µCi per cm^3) (Peterson et al., 2021a).

The average calculated final dose (dose, given on the first day plus the additional dose, given after 24 hours) was 1.9 mCi (ranging from 1.0–10.6 mCi). Almost all cats (1380) required an additional ^{131}I administration on day 2 (Peterson et al., 2021a). Based on serum concentrations of T4 and TSH at 6 to 12 months after treatment, they divided cats into 4 categories: euthyroid (1047 cats – 74.8%), overtly hypothyroid (57 cats – 4.1%), subclinically hypothyroid (240 cats – 17.1%), and persistently hyperthyroid (56 cats – 4%) (Peterson et al., 2021a, b).

The study identified several pretreatment factors, that would help predict which cats would develop iatrogenic hypothyroidism or remain persistently hyperthyroid. Cats that developed ^{131}I induced hypothyroidism were older, female, had a detectable TSH concentration, bilateral thyroid disease, milder severity, and a higher 24-hour percent ^{131}I uptake. Cats, that were more likely to remain hyperthyroid tended to be younger and have higher severity and lower ^{131}I uptake (Peterson et al., 2021b).

The study concludes that the calculated doses resulted in cure rates (percent of the cats that became euthyroid) similar or better to previously reported treatment rates but with much lower ^{131}I doses and that individualized doses of ^{131}I lower the prevalence of ^{131}I induced hypothyroidism (Peterson et al., 2021a).

If the patient becomes hypothyroiditic after the treatment, supplementation with levothyroxine might be needed, but it will also suppress pituitary TSH, which is needed to stimulate atrophied thyroid tissue. In those cases, it is of most importance to establish euthyroidism and avoid renal damage, while at the same time avoiding iatrogenic hypothyroidism (Carney, 2016). Monitoring of serum creatinine, tT4, and TSH is thus necessary (Carney, 2016). It was suggested that patients should be tested 30, 60, 90, and 180 days post-treatment (Carney, 2016).

3. ^{131}I administration

^{131}I is usually administered parenterally (Yu et al., 2020) – intravenously or subcutaneously (Graves et al., 2017). Oral iodine administration is also effective but is not often used, due to the possibility of vomiting after the administration, resulting in treatment failure. However, iodine for treatment p/o is cheaper and easier to obtain. There is limited recent literature about the outcome of fixed oral doses for radioiodine in cats, and there is little known about the bioavailability of radioiodine. A retrospective study, that was published in 2019 by Yu et al. (2020) aimed to describe the percentage of hyperthyroid cats treated with a fixed dose of 3.7 mCi radioiodine orally, that had tT4 concentrations within, below, or above the reference interval. The study included 227 cats, that had been treated using 3.7 mCi radioiodine capsules orally. Maropitant citrate (Cerenia, Zoetis) was administered at 1 mg/kg subcutaneously, to minimize the risk of vomiting over the next 24 hours. Cats were fasted 12 h before the therapy, as an additional precaution. Out of 277 cats, 161 had tT4 concentrations available at diagnosis and after the treatment and were included in the study. Out of those, 133 (82.6%) cats had tT4 concentrations within the reference interval, 4 (2.5%) had tT4 levels above the reference interval and 24 (14.9%) cats had tT4 concentrations below the reference interval. The study showed that the radioiodine dose should not necessarily be higher when it is administered orally (Yu et al., 2020). The dose used in this study was comparable or even lower than those usually used parenterally (Yu et al., 2020). The rate of resolution of hyperthyroidism was comparable with other studies, as were the rates of persistent hyperthyroidism and iatrogenic hypothyroidism (Yu et al., 2020).

4. Post-treatment renal insufficiency

In cats with hyperthyroidism, high serum thyroid hormone concentrations result in increased renal blood flow. That is due to decreased vascular resistance and increased cardiac output, which lead to an increased glomerular filtration rate. Treatment of hyperthyroidism decreases glomerular filtration rate (GFR) (Stock et al., 2017), leading to chronic kidney disease in 15–60% of cases in 6–8 months post-treatment (Graves TK, et al. 2017). Pre-treatment parameters could help predict post-treatment renal failure. Routinely used variables, such as serum urea and creatinine concentrations, urine specific gravity and proteinuria have low sensitivity and are influenced by cats hyperthyroid state (Stock et al., 2017). American College of Veterinary Internal Medicine (ACVIM) Panel recommends fully determining the renal status prior to hyperthyroidism treatment, using International Renal Interest Society (IRIS) staging guidelines, including determination of blood pressure, urine protein quantification, and body condition score. If azotemia develops post-treatment, IRIS Guidelines should be used for staging, treatment, and managing the disease (Carney et al. 2016). IRIS advises against leaving hyperthyroidism untreated to avoid kidney injury and an azotemic state (Carney et al. 2016). Elevated T4 can cause activation of the renin-angiotensin-aldosterone system, leading to increased cardiac output, volume overload, renal hypertension, ultimately progressing to CKD (Carney et al., 2016).

5. Discussion

Treatment with radioactive iodine ^{131}I is the most effective option of treatment for feline hyperthyroidism, resulting in a cure rate of 95% or higher (Carney et al, 2016). The general principle of treatment was to parenterally administer a fixed dose of ^{131}I, risking iatrogenic hypothyroidism. To avoid this complication, an estimation of a dose was used, which included severity of clinical disease, elevation in circulating tT4 concentration, and the size of goiter estimated by palpation (Graves et al. 2017). In 2021, a new algorithm was developed (Peterson et al, 2021a), that could be used to measure an individualized dose even more accurately, taking into account the concentration of thyroid hormones

pre-treatment, the uptake of sodium ^{99m}Tc – pertechnetate via thyroid scintigraphy, and thyroid volume. Lower doses resulted in lower incidents of iatrogenic hypothyroidism, while rates of euthyroidism stayed the same (Peterson et al, 2021a). Whilst successful, the downside might be the limited access to expensive nuclear equipment, used for thyroid scintigraphy and the radioiodine treatment itself.

A study by Peterson and Rishniw (2021b) has shown, that age, sex, TSH concentration, type of disease, and 24-hour percent ^{131}I uptake are significant prognosis factors for iatrogenic hyperthyroidism. Older, female cats, that had detectable TSH concentration, bilateral thyroid disease, milder severity, and a higher 24-hour percent ^{131}I uptake, were more likely to be hypothyroid after the radioiodine treatment (Peterson et al., 2021b). It was reported (Stock et al, 2017) that the treatment for hyperthyroidism can worsen the preexisting renal disease, therefore kidney function should be assessed pre- and post-treatment, using IRIS staging guidelines. The use of methimazole before radioiodine treatment has been suggested for patients with a high risk of iatrogenic hypothyroidism and CKD since it is reversible and can in some ways predict the risk of significant renal compromise (Carney et al. 2016). Either way, hyperthyroidism should not be left untreated (Carney et al. 2016).

^{131}I is usually administered parenterally, either intravenously or subcutaneously. Oral administration is cheaper and more widely available, but not usually used, due to the risk of vomiting, unpredictable resorption, and the concept, that a higher dose should be used (Yu et al., 2020). Recent studies (Yu et al., 2020) have shown, that when antiemetic agents are used, oral administration is successful with the same doses, that are used for parenteral treatment. Success rates were also comparable to those of parenteral treatment, but it remains unclear to what extent the resorption of ^{131}I is affected by the state of the gastrointestinal tract and its absorptive capacity. Those parameters are often changed in cats with hyperthyroidism, so further studies are needed to determine possible dose alterations and actual success rates.

Conflicts of Interest: The authors declare no conflict of interest.

References

1. Carney HC, Ward CR, Bailey SJ et al. 2016 AAFP Guidelines for the management of feline hyperthyroidism. J Feline Med Surg. 2016; 18: 400 – 416. DOI: 10.1177/1098612X16643252
2. Graves TK, Feline hyperthyroidism. In. Ettinger SJ, Feldman EC, Cote E, editors. Textbook of veterinary internal medicine. Elsevier, St. Louis, Missouri. 2017; pp. 4236 – 4255.
3. Mooney CT, Peterson M. Feline hyperthyroidism. In. Mooney CT, Peterson ME, editors. BSAVA manual of canine and feline endocrinology. BSAVA, Gloucester, United Kingdom. 2012; pp. 92 – 110. DOI: 10.22233/9781905319893.10
4. Peterson ME, Rishniw M. A dosing algorithm for individualized radioiodine treatment of cats with hyperthyroidism. J Vet Inetrn Med. Aug 2021a; 35: 2140 – 2151. DOI: 10.1111/jvim.16228
5. Peterson ME, Rishniw M. Predicting outcomes in hyperthyroid cats treated with radioiodine. J Vet Inetrn Med. 2021b: 1-10. DOI: 10.1111/jvim.16319
6. Stock E, Daminet D, Paepe D, et al. Evaluation of renal perfusion in hyperthyroid cats before and after radioiodine treatment. J Vet Inetrn Med. 2017; 31: 1658 – 1663. DOI: 10.1111/jvim.14852
7. Yu L, Lacorcia L, Finch S, Johnstone T. Assessment of treatment outcomes in hyperthyroid cats treated with an orally administered fixed dose of radioiodine. J Feline Med Surg. 2020; 22: 744 – 752. DOI: 10.1177/1098612X19884155

Scientific contribution/Original research/Invited lecture

Evaluation of the Antioxidant Activity of Three Different Brown Macroalgae by Implementing Electrochemistry and Spectrophotometry: Correlation and Prospects

Čižmek L[1], Martić A[1], Čož-Rakovac R[1], Trebše P[2,*]

1. Laboratory for Aquaculture Biotechnology, Division of Materials Chemistry, Ruđer Bošković Institute, Bijenička 54, 10000 Zagreb, Croatia
2. University of Ljubljana, Faculty of Health Sciences, Zdravstvena pot 5, 1000 Ljubljana, Slovenia

* Correspondence: Polonca Trebše; polonca.trebse@zf.uni-lj.si;

Abstract:
In this study, a comprehensive evaluation of the antioxidant activity of three brown macroalgae *Dictyota dichotoma*, *Dictyota fasciola*, and *Halopteris scoparia* from the Adriatic Sea (Croatia) by implementing electrochemical and spectrophotometrical measurements was performed. The aim was to find out if the used methods correlate with each other to obtain information about the present antioxidant activity. The samples were subjected to fractionation by solid-phase extraction (SPE) which allowed the separation of different polarity compounds. Voltammetry of microfilm immobilized on a glassy carbon electrode using square-wave voltammetry (SWV) was applied as an electrochemical method, and the obtained results were correlated to the results of four spectrophotometric methods, namely the reduction of the radical cation (ABTS), the 2,2-diphenyl-1-picryl-hydrazyl (DPPH) assay, the Folin–Ciocalteu, and the oxygen radical absorbance capacity (ORAC) assay. All methanolic fractions from three brown macroalgae showed higher antioxidant activity than the dichloromethane fractions. The highest activity was obtained for *H. scoparia* methanolic fraction with an IC_{50} concentration of 1.947 mg/mL. It was found that antioxidant activity obtained by SWV only correlates well to 1,1-diphenyl-2-picrylhidrazine (DPPH) radical assay ($R^2 = 0.83, p < 0.05$), while a good correlation was found between ABTS and ORAC assays ($R^2 = 0.\ 0.94$, $p < 0.05$). Correlations indicate that the synergistic effect of different compounds extracted from the samples impacted their antioxidant response. All three researched brown macroalgae have shown to be a potent source of natural antioxidants that could further be used in the research of oxidative stress-related diseases.

Keywords: Brown seaweeds; Marine organisms; Voltammetry; Extraction; Bioactivity

Citation: Čižmek L, Martić A, Čož-Rakovac R, Trebše P. Evaluation of antioxidant activity of three different brown macroalgae by implementing electrochemistry and spectrophotometry: Correlation and future prospects. Proceedings of Socratic Lectures. 2021; 6: 38-47. https://doi.org/10.55295/PSL.2021.D.006

1. Introduction

Marine macroalgae or seaweeds are in the last decade in a continuous focus of the scientific community, but even in the focus of a wider public as they are acknowledged as a valuable source of different bioactive compounds such as polyphenols, peptides, pigments, and polysaccharides that are associated with several health benefits and biological activities (Afonso et al., 2019; Cardoso et al., 2014; Cikoš et al., 2021). Evolutionary development of such a variety of natural compounds was enhanced by macroalgal adaptation to extreme marine conditions in terms of temperature, light, pressure, oxygen, salinity, as well as microbial and viral attacks, and toxicity (Ruocco et al., 2016; Zhao et al., 2018). Thus, the chemical composition of macroalgae varies considerably not only among different species but also within the same species that inhabited different ecosystems.

Brown algae are known for their accumulation of specific metabolites with great antioxidant potential, especially phenolic compounds phlorotannins, polysaccharides alginates, laminarans, and fucoidans with antiviral, anti-inflamatory, antitumoral, antithrombotic, and antioxidant activity (Rabanal et al., 2014) along with carotenoid fucoxanthin with antiproliferative effects on cancer cells (Afonso et al., 2019; Ktari et al., 2021). Brown algae *Dictyota dichotoma* and *Dictyota fasciola* belong to the Dictyotaceae family known for producing polyphenols, diterpenes, and sulfated polysaccharides, especially during stress conditions possessing the capacity of protecting the immune system and serving as scavengers of oxygen free radicals (Sathya et al., 2017), while the extracts of *Halopteris scoparia* have shown the potential to be used as a protective and preventive agent against human cancers (Güner et al., 2019).

Antioxidants are a highly heterogeneous group of chemical compounds, and many methods have been developed to evaluate the antioxidant potential of algae biomass extracts (Kohen et al., 2002; Prior et al., 2005). Most assays for the determination of antioxidant activity are based on chemical reactions of antioxidants with a probe, which has a different color depending on its redox state, followed by spectrophotometric measurement. The main disadvantage of this type of methods is that they are based on color formation, which can be problematic when applied to algal extracts due to high concentrations of colored chlorophylls and carotenoids, so a blank solution has to be measured for each tested sample and concentration. Also, the chemical assays measure only a fraction of the total antioxidant activity in the extract as the performed redox reactions have a specific redox potential (Goiris et al., 2012). Electrochemical (voltammetric) methods have been recognized as an alternative to chemical antioxidant assays (Čižmek et al., 2021; Goiris et al., 2012). Some of the benefits of voltammetric measurements are sensitivity (analysis of both lipophilic and hydrophilic extracts, and can be carried out on colored samples), rapidity, simplicity (no need for laborious sample preparation and simple equipment), and the capacity to directly measure the number of electrons transferred by an antioxidant. The obtained peak potentials detected in the voltammogram can be used as an indicator of the redox potential of major antioxidants present in the sample and their reducing power. Voltammetry provides quantitative information on the total antioxidant capacity of the sample given by the total area under the curve (AUC). This is especially important when crude samples are measured, in which usually several compounds with various oxidation potentials contribute to the AUC (Goiris et al., 2012; Haque et al., 2021).

In this study, we evaluated the antioxidant activity of two different fractions from three brown macroalgae. The primarily used method was square-wave voltammetry (SWV), followed by the reduction of the radical cation (ABTS), the 2,2-diphenyl-1-picryl-hydrazyl (DPPH) assay, the Folin–Ciocalteu, and the oxygen radical absorbance capacity (ORAC) assays. To correlate obtained results for antioxidant activity, Pearson's correlation coefficient was used.

2. Material and Methods

2.1. Chemicals

The standards of gallic acid (>97.5%), L-ascorbic acid (≥99%), DPPH (2,2-diphenyl-1-picrylhydrazyl), ABTS (diammonium salt of 2,2′-azino-bis(3-ethylbenzthiazolin-6-yl) sulfonic acid, >99.0%), dichloro-dihydro-fluorescein diacetate (≥97%, DCF-DA), AAPH (2,2-azobis (2-methylpropionamidine) dihydrochloride, 97%) and 2′,7′-dichloro fluorescin diacetate were purchased from Sigma-Aldrich (St. Louis, MO, USA).

Dimethyl sulfoxide (DMSO, p.a.), methanol (p.a.), ethanol (p.a.), hydrochloric acid (HCl, p.a.), sodium carbonate (Na_2CO_3, p.a.), dibasic sodium phosphate ($Na_2HPO_4*2H_2O$, p.a.), monobasic sodium phosphate ($NaH_2PO_4*H_2O$, p.a.) and Folin–Ciocalteu reagent were obtained from Kemika (Zagreb, Croatia) while potassium persulfate (>98%) was purchased from Scharlau, (Regensburg, Germany).

The solvents used for solid-phase extraction were of HPLC grade and were obtained from Honeywell (Charlotte, NC, USA).

2.2. Macroalgae samples and extraction procedure

Three brown marine macroalgae: *Dictyota dichotoma* (DIDI), *Dictyota fasciola* (DIFA), and *Halopteris scoparia* (HASC) were collected from the Adriatic Sea, transported, cleaned with distilled water several times, freeze-dried, and stored at 4◦C until further analysis. The extraction was performed on 5 g of each macroalgae sample with a mixture of solvents methanol (MeOH)/dichloromethane (DCM) (1:1, *v*/*v*), in an ultrasonic bath (Bandelin, Sonorex digiplus 560W, Germany) for 5 min. The extraction of each sample was repeated three times with centrifugation between each sonication. The supernatants were collected and mixed with C18 powder and then subjected to evaporation under nitrogen flow (5.0, Messer, Croatia). The SPE cartridges (C18, Agilent Bond Elut, Germany) were conditioned with methanol and ultrapure water, and afterward, the dry extracts were eluted using solvents with decreasing polarity (water>MeOH>DCM). Polar fraction F1 was discarded and was not analyzed within this study, while less polar fractions (F2 and F3) were collected and dried under nitrogen flow. Before the analysis, the fractions were dissolved with appropriate solvents, F2 fraction in MeOH and F3 fraction in DCM.

2.2. Electrochemical analysis

The electrochemical experiments were carried out in accordance with our recently published paper (Čižmek et al., 2021). Briefly, a computer-controlled PalmSens electrochemical system (Houten, the Netherlands) with PSTrace software was used with glassy carbon electrode (GC electrode, BASi, diameter 3 mm) as a working electrode, an Ag/AgCl (3 mol/L KCl) electrode as a reference electrode and a platinum wire as a counter electrode. All potentials were expressed *versus* Ag/AgCl (3 mol/L KCl) reference electrode. Cyclic (CV) and square-wave (SWV) voltammetry were performed on all samples in 0.1 mol/L phosphate buffer solution (PBS) as an electrolyte solution. Analysis of samples was performed by pipetting the known volume of obtained sample (5 µL) on the surface of the GC working electrode and left to dry at room temperature for a minute. Unless otherwise stated, all measurements were performed in triplicates. CV experiments on modified GC electrode were performed at a potential scan rate of 50 mV/s, while SWV was performed using a potential step increment of 2 mV and a square-wave amplitude of 20 mV. The frequency varied from 10 to 200 Hz. The change in pH value was also analyzed.

2.4. Spectrophotometric analysis

Antioxidant activity was evaluated by implementing four *in vitro* assays: reduction of radical cation assay (ABTS), 2,2-diphenyl-1-picrylhydrazyl-hydrate (DPPH) assay, oxygen radical absorbance capacity (ORAC) assay, and Folin-Ciocalteu method. All measurements were performed in triplicates on a spectrophotofluorimeter microplate reader (Infinite M200 PRO, TECAN, Switzerland) in the multi-well plate (96-well). By the

reactions with appropriate reagents, obtained fractions were tested for their antioxidant activity. Their color change, with regards to control or blank sample, was measured. The F2 and F3 fractions of each macroalga were prepared at a stock concentration of 10 mg/mL and appropriate dilutions of each sample were prepared for further analysis. A detailed description of all preformed methods can be found in recently published research (Radman et al., 2022).

2.5. Statistical analysis

The obtained values for evaluation of antioxidant activity are expressed as mean values with standard deviations of four replicates. The differences between the means were analyzed by Tukey's test of One-Way ANOVA using GraphPad Prism 8.0 (GraphPad Software Inc., San Diego, CA, USA). Values of $p < 0.05$ and lower were considered significantly different. Correlations and regression analysis describing the antioxidant activities between spectrophotometric methods (ABTS, DPPH, Folin-Ciocalteu, and ORAC assays) and voltammetric analysis (SWV) were conducted using the regression program in GraphPad Prism 8.0.

3. Results

3.1. Voltammetric analysis

In this research, square-wave voltammetry was employed to determine the antioxidant capacity of the dry residues of extracts from brown macroalgae samples immobilized on the surface of GCE and immersed into a 0.1 mol/L phosphate buffer solution. To evaluate their activity and optimal electrochemical response, a change in the pH values, ranging from 3 to 11, for all obtained extracts was tested. As can be seen from Figure 1a-f, the pH of the solution affects the voltammetric response of each sample, i.e., the oxidation current is strongly dependent on pH (data not shown). The potential of the lead peak for all samples was independent over the pH range. Voltamograms for fraction F2 for both Dictyota species (Fig. 1a and 1c) have similar electrooxidative response which consists of one oxidation peak at the potentials E_P = 0.704 V and E_P = 0.748 V *vs.* Ag/AgCl/3 mol/L KCl, respectively. The voltammogram of the dry residue of fraction F2 from the *H. scoparia* is rather different with a lead oxidation peak at the potential E_{P1} = 0.622 V and a "shoulder" peak at E_{P2} = 0.960 V which becomes more distinctive with a higher pH value (Figure 1e). As can be seen from Fig. 1b,d, and f, fractions F3 for all three samples are overall less electroactive than F2 fractions. For Dictyota species, DIDI F3 and DIFA F3, the most pronounced peak was observed at the potentials E_P = 0.878 V and E_P = 0.928 V at pH 7, respectively. Voltammogram for HASC F3 fraction is similar to voltammogram for its F2 fraction, but it can be observed that pH-value has a higher influence on its response, with the lead oxidation peak at the potential E_{P1} = 0.471 V and a "shoulder" peak at E_{P2} = 0.669 V at the most alkaline electrolyte, pH 11.

Under alkaline experimental conditions (pH 11), square-wave voltammograms were recorded by changing the frequency in the range from 10 to 200 Hz for all tested samples. The peak potential was highly dependent on the logarithm of frequency (10 Hz < f < 200 Hz) for all macroalgae extracts. Cyclic voltammograms of macroalgae extracts were recorded in PBS (pH 11) within the potential range from -0.5 to 1.2 V and at a scan rate of 50 mV/s as a support for the electrochemical mechanism of extracts (data not shown).

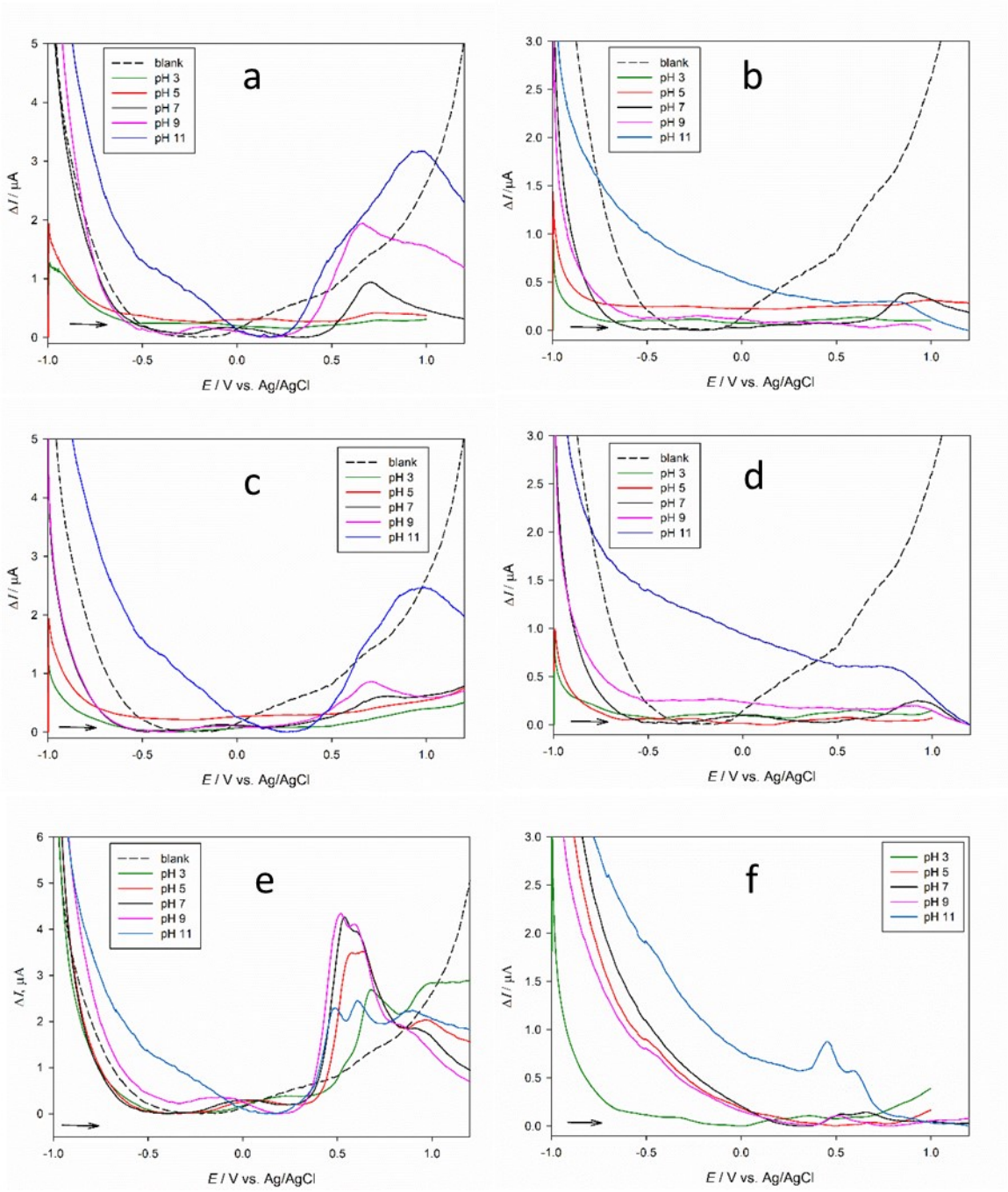

Figure 1. Square-wave voltammetric response curves obtained under different pH conditions for all samples: (**a**) *Dictyota dichotoma* (DIDI) F2, (**b**) DIDI F3, (**c**) *Dichtyota fasciola* (DIFA) F2, (**d**) DIFA F3, (**e**) *Halopteris scoparia* (HASC) F2, and (**f**) HASC F3 while immobilized on the surface of glassy-carbon electrode (GCE) and immersed in 0.1 M PBS. The frequency was 50 Hz, pulse amplitude was 20 mV, and the step potential was 2 mV.

To assess antioxidant activity using voltammetric analysis, the area under the curve (AUC) was integrated, the value of which represents an estimate of the total antioxidant activity of the extracts. To express total antioxidant capacity in gallic acid equivalents (GAE), a calibration was carried out in which AUC was plotted against different concentrations of the gallic acid standard (y = 581304x - 125.52). The highest antioxidant activity based on the AUC value was obtained for HASC F2 (0.396±0.032 mg/g GAE), followed by HASC F3 (0.234±0.080 mg/g GAE) > DIFA F2 (0.099±0.001 mg/g GAE) > DIFA

F3 (0.068±0.006 mg/g GAE) > DIDI F3 (0.050±0.002 mg/g GAE) > DIDI F2 (0.028±0.002mg/g GAE). Compared to HASC F2 antioxidant activity, HASC F3 showed 1.7 folds lower activity ($p < 0.001$), while on average 7 folds lower activity ($p < 0.001$) was obtained for all fractions of Dictyota species. No significant difference in antioxidant activity was observed between fractions of two Dictyota species.

3.2. Spectrophotometric analysis

Four other spectrophotometric methods regarding the assessment of antioxidant activity were employed, namely ABTS, DPPH, Folin-Ciocalteu, and ORAC assays, and diverse results were obtained. As depicted in Figure 2a, results of the DPPH assay, revealed the highest antioxidant activity for HASC F2 with the inhibition percentage around 35% for the concentration of 5 mg/mL, followed by DIDI F3 and DIFA F2 extract with inhibition percentages around 20%. When normalized per gram of the fraction, HASC F2 (9.411±2.436 mg AAE/g fraction) showed a significantly higher ($p < 0.0001$) antioxidant activity than all other fractions.

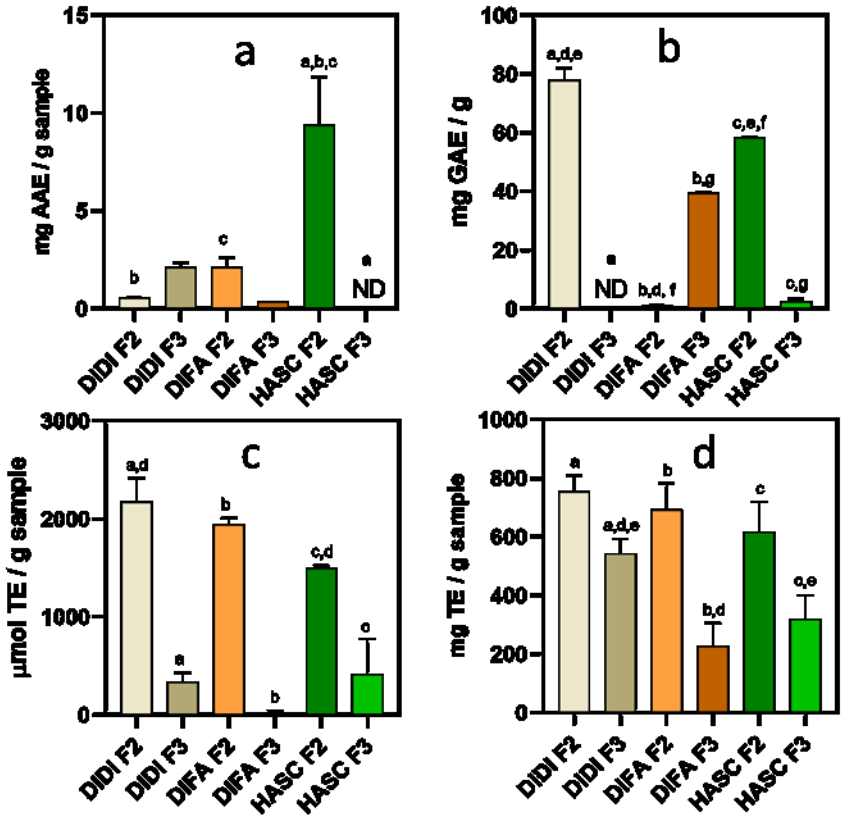

Figure 2. Radical scavenging effect of two less polar fractions from three *brown* macroalgae, *Dictyota dichotoma* (DIDI), *Dichtyota fasciola* (DIFA), and *Halopteris scoparia* (HASC), using (**a**) 2,2-diphenyl-1-picryl-hydrazyl (DPPH), (**b**) Folin-Ciocalteu (**c**) oxygen radical absorbance capacity (ORAC) and (**d**) reduction of the radical cation (ABTS) *in vitro* assays (mean ± SD; $n = 4$). Columns sharing the same letters indicate a significant difference between all samples ($p < 0.001$). ND - none determined.

The results using the Folin–Ciocalteu assay revealed high activity for two F2 fractions, DIDI F2 (77.84±4.19 mg/g GAE) and HASC F2 (58.26±0.22 mg/g GAE), moderate activity for DIFA F3 (39.47±0.52 mg/g GAE), low activity for HASC F3 (2.36±1.12 mg/g GAE) and DIFA F2 (1.13±0.32 mg/g GAE), while no activity was observed for DIDI F3.

Antioxidant activity of the different polarity fractions from brown macroalgae varied from 25 to 2500 µM/g TE by implementing the ORAC assay (Fig. 1c). Samples with a high ORAC activity were all three methanolic fractions: DIDI F2 (2175.18±246.73 µM/g

TE), DIFA F2 (1944.24±63.95 μM/g TE) and HASC F2 (1497.50±26.49 μM/g TE), while F3 fractions for all three samples exerted significantly lower activity ($p < 0.001$), as can be seen at Fig. 1c.

The fourth method implemented in this research was the reduction of the radical cation by implementing an ABTS assay (Fig 1d). Different concentrations of F2 and F3 for all algae were prepared in the range from 0.005 to 15 mg/mL to obtain IC_{50} curves. The IC_{50} values for both samples were calculated as shown in Table 1, with the corresponding confidence interval, slope, and coefficient of determination (R^2). As can be seen, the lowest IC_{50} value, i.e., the highest antioxidant activity was obtained for F2 of HASC, followed by F2 fractions of DIDI and DIFA which exhibited almost the same activity. Interestingly, IC_{50} values for fraction F3 of DIDI and DIFA could not be determined because the upper inhibition plateau could not be reached, while the IC_{50} value for HASC F3 is relatively high indicating lower antioxidant activity of this sample.

Table 1. Dose-inhibition results using the ABTS in vitro assay ($n = 4$) to obtain the half-maximal inhibitory concentration (IC_{50}) with the presented confidence intervals, Hillslope, and R^2 value.

Sample		IC_{50} value, mg/mL	Confidence interval	Hillslope	R^2 value
Dictyota dichotoma	F2	2.595	1.889 – 2.899	1.122	0.987
	F3	ND	-	-	-
Dictyota fasciola	F2	2.582	2.078 - 3.404	1.254	0.984
	F3	ND	-	-	-
Halopteris scoparia	F2	1.947	1.332 – 4.320	1.130	0.964
	F3	4.317	3.065 – 5.102	1.854	0.925

To evaluate the correlation between electrochemical (SWV) and spectrophotometric (ABTS, DPPH, Folin-Ciocalteu, and ORAC) methods for all samples, Pearson's correlation coefficient (Utakod et al., 2017) was applied. Multiple regression analysis between SWV and DPPH showed a good correlation. The Pearson's correlation coefficient for SWV *versus* DPPH was a positive value of 0.83 ($p < 0.05$). For other spectrophotometric methods, there was no correlation obtained with SWV. Additionally, a statistically significant ($p < 0.05$) high positive correlation between ABTS and ORAC with Pearson's correlation coefficient of 0.94 was observed. A medium positive correlation between ABTS *versus* DPPH and Folin-Ciocalteu methods was found with Pearson's correlation coefficients of 0.35 and 0.37, respectively. Also, a medium positive correlation between DPPH and Folin-Ciocalteu and ORAC assays was observed with Pearson's correlation coefficients of 0.29 and 0.30, respectively. Lastly, Pearson's correlation coefficient of 0.34 was obtained between results of ORAC and Folin-Ciocalteu assays.

4. Discussion

Numerous studies in the recent years have been focused on finding important bioactive compounds with antioxidative activity from natural sources such as marine organisms (Corsetto et al., 2020). Within this study, *in vitro* evaluation of the antioxidative activity of two fractions, methanolic (F2) and dichloromethanolic (F3) obtained from three brown macroalgae (DIDI, DIFA and HASC) was first performed by implementation of square-wave voltammetry (SWV) since voltammetric methods determine antioxidant activity by measuring the electrondonating capacity. This method has attracted some attention in the last decade because it provides fast and sensitive response and evaluation of antioxidant activity of extracts obtained from both macro- and microalgae samples (Goiris et al., 2012; Ragubeer et al., 2010; Ragubeer et al., 2012). However, it is still underexploited, probably due to the complex interpretation of the obtained results and the fact that extracted compounds need to be electroactive to provide a signal. In this rese-

arch, focus was on naturally occurring organic compounds in brown macroalgae, and since they could act as antioxidants through electron transfer, it was considered that they would be largely responsible for the antioxidant activity of analyzed samples. It is known that the oxidation potentials of compounds correlate with their antioxidant activity, i.e., samples with less positive oxidation potential possess higher radical scavenging activity (Hotta et al., 2002). As can be seen from Fig. 1b,d, and f, fractions F3 for all three samples are overall less electroactive, probably because the mostly non-polar molecules with small or none electroactivity are present in that fractions. (Ir)reversibility of reactions for all sample fractions was determined by changing the frequency and plotting the first peak P1 potential with the logarithm of frequency (10 Hz < f < 200 Hz). The linear dependence of oxidation peak potentials for all F2 and F3 fractions with the logarithm of frequency confirmed that these processes are irreversible (Mirčeski et al., 2007). Subsequently, by conducting the cyclic voltammetry (CV) in phosphate buffer solution (pH 11), all macroalgae showed lower sensitivity but confirmed the (ir)reversibility of these processes for each obtained peak. Because SWV yielded more and better-defined peaks than the CV, it was used for the determination of the antioxidant profile of these samples. The results of AUC were summarized and expressed as gallic acid equivalents for comparison with spectropohotmetric assays. Detailed electrochemical analysis of gallic acid by means of square-wave voltammetry (SWV) was performed in our recent study (Čižmek et al., 2021). The obtained results showed higher antioxidant activity for HASC F2 and F3 fractions than for DIDI and DIFA samples, i.e. most of the area that is quantified from the voltammograms of HASC has a lower oxidation potential, around 0.600 V (Fig. 1e,f).

Since antioxidants act by several mechanisms and a single assay cannot accurately reflect all of the antioxidants in a complex fraction (Antolovich et al., 2002; Gan et al., 2017) but also to evaluate used voltammetric method, in this research antioxidant activity was evaluated by employing additional four spectrophotometric methods. DPPH assay measures the antioxidant action via both single electron transfer (a SET mechanism) and by radical quenching (hydrogen atom transfer (HAT)), and is most commonly used method for estimation of total antioxidant activity. DPPH activity is relatively low when expressed per gram of extract for all tested fractions, while two Dictyota species showed simmilar activity, *H. scoparia* showed the highest activity, especially F2 fraction. Results of the DPPH assay for *D. dichotoma* are in agreement with other studies, athough the extraction and fractionation steps were different (Çelenk et al., 2016; El-Shaibany et al., 2020). When analyzing and correlating different extraction methods, El-Shaibany et al., 2020 found that the different polarity extracts showed different but low antioxidant activity, explained by complexity of their composition. Additionally, Çelenk et al., 2016 evaluated the antioxidant activities of 24 marine macroalgae, among which was *D. dichotoma*, and also observed lower antioxidant activity in the extract obtained by maceration in methanol for 10 days. Results obtained by Folin-Ciocalteu method revealed that this assay should not be considered as a measure of total phenolic content, but rather as the rate of overall antioxidant capacity, similar to ABTS assay because some nonphenolic compounds exhibit considerable reactivity toward Folin-Ciocalteu reagent (Everette et al., 2010; Sánchez-Rangel et al., 2013). Obtained results are in accordance with study evaluating six Dictyotales samples, among which were DIDI and DIFA extracted with methanol overnight (Ktari et al., 2021). Results also showed higher activity for DIDI than the DIFA sample. Implementation of ORAC and ABTS assays revealed similar antioxidant behavior of tested samples i.e. methanolic fraction of all three samples showed higher activity. Recently, Güner et al., 2019 analyzed three different extracts from *H. scoparia*, namely hexane, chloroform, and methanol extracts utilizing DPPH and ABTS assays. The results for methanol extracts were similar to the results of this study (lower activity by implanting DPPH assay, and higher inhibition percentage for ABTS assay).

The applied correlations using Pearson's correlation coefficient suggest that numerous compounds were extracted from each macroalga and consequently exhibited different modes of action, but also had a synergistic effect. Therefore, the lack of significant correlation between methods can be explained. However, this research provided infor-

mation that SWV can be used to assess the antioxidant activity of the macroalgae samples and implies the potential usage of voltammetry to quickly determine their antioxidant activity.

5. Conclusions

Three brown macroalgae *Dictyota dichotoma*, *Dictyota fasciola*, and *Halopteris scoparia* from the Adriatic Sea (Croatia) were investigated in this study with a respect to their antioxidant activity by implementing electrochemical and spectrophotometrical measurements. Fractionation by solid-phase extraction (SPE) allowed the separation of compounds of different polarities with the focus on less polar compounds. By implementing square-wave voltammetry (SWV), lower electrooxidation potential was obtained for all methanolic fractions. The highest overall antioxidant activity was observed for methanolic fraction F2 of *H. scoparia*, while both Dictyota species exert similar activity indicating a similar chemical composition. Correlation between voltammetric and spectrophotometric methods showed that electrochemical analysis can be used for the determination of antioxidant activity. Overall, these findings indicate the potential of brown macroalgae as a source of beneficial antioxidant agents in the different areas of industry. However, detailed chemical analysis and determination of a leading electrooxidation mechanism are still pending and will provide additional information necessary for the elucidation of such complex systems.

Funding: The authors acknowledge the finantial support from Slovenian Research Agency (ARRS), the research core funding No. P3-0388 (Mechanisms of health maintenance). This research was supported also by the Croatian Government and the European Union (European Regional Development Fund—the Competitiveness and Cohesion Operational Program—KK.01.1.1.01) funding it through the project Bioprospecting of the Adriatic Sea (KK.01.1.1.01.0002), granted to The Scientific Centre of Excellence for Marine Bioprospecting—BioProCro. One-month financial support for postdoctoral research at the Faculty of Health Sciences at Ljubljana, Slovenia, awarded to L. Čižmek by the Institute Ruđer Bošković is gratefully acknowledged.
Conflicts of Interest: The authors declare no conflict of interest.

1. Afonso NC, Catarino MD, Silva AMS, Cardoso SM. Brown macroalgae as valuable food ingredients. Antioxidants. 2019; 8: 365. DOI:10.3390/antiox8090365.
2. Antolovich M, Prenzler PD, Patsalides E, et al. Methods for testing antioxidant activity. Analyst. 2002; 122: 11–34. DOI: 10.1039/b009171p
3. Cardoso SM, Carvalho LG, Silva PJ, Pereira L. Bioproducts from seaweeds: A review with special focus on the Iberian Peninsula. Curr. Org. Chem. 2014; 18: 896-917. DOI: 10.2174/1385272818071405151541l6
4. Cikoš A-M, Flanjak I, Bojanić K, et al.,. Bioprospecting of coralline red alga *Amphiroa rigida* J.V. Lamouroux: Volatiles, fatty acids and pigments. Molecules. 2021; 26: 520. DOI:10.3390/molecules26030520.
5. Çelenk FG, Özkaya AB, Sukatar A. Macroalgae of Izmir Gulf: *Dictyotaceae* exhibit high in vitro anti-cancer activity independent from their antioxidant capabilities. Cytotechnology. 2016; 68: 2667–2676 . https://doi.org/10.1007/s10616-016-9991-0
6. Corsetto PA, Montorfano G, Zava S, et al. Characterization of antioxidant potential of seaweed extracts for enrichment of convenience food. Antioxidants 2020, 9: 249. DOI: 10.3390/antiox9030249.
7. Čižmek L, Bavcon Kralj M, Čož-Rakovac R, et al.Supercritical carbon dioxide extraction of four medicinal Mediterranean plants: Investigation of chemical composition and antioxidant activity. Molecules. 2021; 26: 5697. DOI: 10.3390/molecules26185697.
8. El-Shaibany A, AL-Habori M, Al-Maqtari T, Al-Mahbashi H. The Yemeni Brown Algae *Dictyota dichotoma* Exhibit High *In Vitro* Anticancer Activity Independent of Its Antioxidant Capability. BioMed Research International. 2020; 9 pages. https://doi.org/10.1155/2020/2425693
9. Everette JD, Bryant QM, Green, AM et al. Thorough study of reactivity of various compound classes toward the Folin−Ciocalteu reagent. J. Agric. Food Chem. 2010; 58: 8139–8144. DOI: 10.1021/jf1005935.
10. Gan J, Feng Y, He Z, et al. Correlations between antioxidant activity and alkaloids and phenols of Maca (*Lepidium meyenii*). J. Food Qual. 2017; 2017: 1–10. DOI: 10.1155/2017/3185945.
11. Goiris K, Muylaert K, Fraeye I, et al. Antioxidant potential of microalgae in relation to their phenolic and carotenoid content. J. Appl. Phycol. 2012; 24:1477–1486. DOI 10.1007/s10811-012-9804-6.

12. Güner A, Nalbantsoy A, Sukatar A, Yavaşoğlu NÜK. Apoptosis-inducing activities of *Halopteris scoparia* L. Sauvageau (Brown algae) on cancer cells and its biosafety and antioxidant properties. Cytotechnology. 2019; 71:687–704. DOI: 10.1007/s10616-019-00314-5.
13. Haque MA, Morozova K, Ferrentino G, Scampicchio M. Electrochemical methods to evaluate the antioxidant activity and capacity of foods: A review. Electroanalysis. 2021; 33: 1419-1435. DOI: 10.1002/elan.202060600.
14. Hotta H, Nagano S, Ueda M, et al. Higher radical scavenging activities of polyphenolic antioxidants can be ascribed to chemical reactions following their oxidation. Biochim. Biophys. Acta-Gen. Subj. 2002; 1572: 123–132. DOI: 10.1016/S0304-4165(02)00285-4.
15. Ktari L, Mdallel C, Aoun B, et al. Fucoxanthin and phenolic contents of six Dictyotales from the Tunisian coasts with an emphasis for a green extraction using a supercritical CO_2 method. Front. Mar. Sci. 2021; 8: 647159. DOI: 10.3389/fmars.2021.647159.
16. Kohen R, Nyska A. Oxidation of biological systems: oxidative stress phenomena, antioxidants, redox reactions, and methods for their quantification. Toxicol. Pathol. 2002; 30: 620−650. DOI: 10.1080/01926230290166724.
17. Mirčeski V, Komorsky-Lovrić Š, Lovrić M. Square-Wave Voltammetry: Theory and Application. 1st ed.; Springer: Heidelberg, Germany, 2007.
18. Prior RL, Wu X, Schaich K. Standardized methods for the determination of antioxidant capacity and phenolics in foods and dietary supplements. J. Agric. Food Chem. 2005; 53: 4290−4302. DOI: 10.1021/jf0502698.
19. Rabanal M, Ponce NMA, Navarro DA, et al. The system of fucoidans from the brown seaweed *Dictyota dichotoma*: Chemical analysis and antiviral activity. Carb. Pol. 2014; 101: 804– 811. DOI: 10.1016/j.carbpol.2013.10.019.
20. Radman S, Čižmek L, Babić S, et al. Bioprospecting of less-polar fractions of *Ericaria crinita* and *Ericaria amentacea*: Developmental toxicity and antioxidant activity. Mar. Drugs. 2022; 20: 57. DOI: 10.3390/md20010057.
21. Ragubeer N, Beukes DR, Limson JL. Critical assessment of voltammetry for rapid screening of antioxidants in marine algae. Food Chem. 2010; 121: 227−232. DOI: 10.1016/j.foodchem.2009.11.076.
22. Ragubeer N, Limson JL, Beukes DR. Electrochemistry-guided isolation of antioxidant metabolites from *Sargassum elegans*. Food Chem. 2012; 131: 286−290. DOI: 10.1016/j.foodchem.2011.08.037.
23. Ruocco N, Costantini S, Guariniello S, Costantini M. Polysaccharides from the marine environment with pharmacological, cosmeceutical and nutraceutical potential. Molecules. 2016; 21:551. DOI:10.3390/molecules21050551.
24. Sánchez-Rangel JC, Benavides J, Heredia JB, et al. The Folin–Ciocalteu assay revisited: Improvement of its specificity for total phenolic content determination. Anal. Methods. 2013; 5: 5990–5999. DOI: 10.1039/c3ay41125g.
25. Sathya R, Kanaga N, Sankar P, Jeeva S. Antioxidant properties of phlorotannins from brown seaweed *Cystoseira trinodis* Forsskå) C. Agardh. Arab. J. Chem. 2017; 10: S2608–S2614. DOI: 10.1016/j.arabjc.2013.09.039.
26. Utakod N, Laosripaiboon W, Chunhachart O, Issakul K. The efficiency and the correlation between testing methods on antimicrobial and antioxidant activities of selected medicinal essential oils. Int. Food Res. J. 2017; 24: 2616–2624.
27. Zhao C, Yang C, Liu B, et al. Bioactive compounds from marine macroalgae and their hypoglycemic benefits. Trends Food Sci. Technol. 2018; 72: 1-12. DOI: 10.1016/j.tifs.2017.12.001.

Scientific contribution/Original research

Oil Extraction of Microplastics from Communal Dewatered Sludge

Lekše N[1*], Griessler Bulc T[2], Žgajnar Gotvajn A[1]

1. University of Ljubljana, Faculty of Chemistry and Chemical Technology, Večna pot 113, SI-1000 Ljubljana
2. University of Ljubljana, Faculty of Health Sciences, Zdravstvena pot 5, SI-1000 Ljubljana

* Correspondence: Nina Lekše; nina.lekse11@gmail.com

Abstract:
Microplastics (MPs) as solid particles are found all over in the environment. Plastic particles, smaller than 5 mm are defined as MP and smaller than 1 µm as nanoplastic. One of main sources are communal wastewater treatment plants (WWTPs), that contribute to releasing MPs into the environment. Through outlet, MPs continue their way into surface waters and groundwaters or come in environment with sewage sludge that is disposed on farmland or other surfaces. There is still no standardized method for extracting plastic particles from environmental samples, so we investigated efficiency of oil extraction protocol (OEP). Since sludge consists of organic matter and it needs to be pre-treated before an extraction, Fenton's reagent was used to reduce organic matter. Before and after the extraction, particles were analysed with Fourier-transform infrared spectroscopy (FT-IR), where we discovered that a washing step after the extraction with 96% ethanol removes oil traces and other interferences. A recovery rate of MP particles was assessed by counting spiked plastic particles on filters after a vacuum filtration. The results showed that with OEP the recovery rate was on average 10% higher in pre-treated samples in comparison with samples without pre-treatment. We determined the highest recovery rate for bigger particles (1-5 mm) of polypropylene (PP), (86% ± 16% with OEP and 99% ± 4% with pre-treatment). The results reveal that the oil extraction can offer a cost-efficient, rapid and simple extraction method for MPs with high recovery rate especially for plastic particles with lower densities as PP and polystyrene (PS).

Keywords: Microplastics, communal wastewater treatment plants, sludge, oil extraction, pre-treatment, organic matter

Citation: Lekše N, Griesseler Bulc T, Žgajnar Gotvajn A. Oil extraction of microplastics from communal dewatered suldge. Proceedings of Socratic Lectures. 2021; 6: 49-55. https://doi.org/10.55295/PSL.2021.D.007

Introduction

Microplastics (MPs) as solid particles of anthropogenic origin are due to their lasting persistence and small weight found all over in the environment. Mainly, plastic particles, smaller than 5 mm are defined as MP and smaller than 1 µm as NP (Blair et al., 2019). MP is also classified into primary and secondary MP, where primary is intentionally made in small dimensions and being in those sizes also used, while secondary MP breaks down from bigger plastic waste, during its usage or after physical, chemical or biological processes (Carr et al., 2016; Talvitie et al., 2017). MP could pose a serious risk to environment. It could negatively affect aquatic environment and as persistent small size pollutant can be fast and easily transferred on long distances, where it can physically and chemically impact many organisms and it could be also transferred through food chain to humans (Anderson et al., 2016; Corradini et al., 2019). Particles of MP could be found in cosmetic and other products for personal hygiene, textile products and in many industrial processes (Carr et al., 2016). One of significant sources of MPs is a communal wastewater treatment plant (WWTP) (Sun et al., 2019), where MPs from households through outlet can continue their way mostly into surface waters and groundwaters or on farmland with sewage sludge disposal (Ngo et al., 2019).

Since MP could reach environment, not only with wastewater through the outlet, but also with sewage sludge, quantification and qualification of MP in the sludge, that is a complex mixture, reach with organic compounds, is highly important (Hurley et al., 2018). Various different procedures of MP extraction found in literature (Hurley et al., 2018; Lares et al., 2019) aggravate comparison between results. Despite many different procedures and results reported in the literature, main steps of procedures after sampling usually involve pre-treatment, extraction, identification and characterization (Hurley et al., 2018). High content of organic matter in waste sludge could hamper the efficiency of extraction of MPs and samples need to be pre-treated (Hurley et al., 2018; Li et al., 2020). Organic matter, microorganisms and other inorganic matter that are tied together by biopolymers make sludge samples additionally more difficult to process as for example soil samples (Zhang et al., 2020).

Different chemical methods for pre-treatment have several disadvantages; nitric acid (HNO_3) could physically and chemically change surface of MP and pre-treatment could take a long time (Li et al., 2020), alkaline digestion with sodium hydroxide (NaOH) and potassium hydroxide (KOH) could change size and shape of some type of plastics (PET) due to high pH (Dehaut et al., 2016; Cole et al., 2014). One of other possible methods is enzyme digestion that is expensive and could take days (Hurley et al., 2018; Cole et al., 2014; Mintenig et al., 2017). One of common pre-treatment methods is oxidation, using hydrogen peroxide (H_2O_2) that could lead to degradation of some polymers of MP and could change colour of MP, that could affect visual recognition (Nuelle et al., 2014). The alternative of H_2O_2 is Fenton's reagent. Presence of iron catalyst ($FeSO_4$), together with H_2O_2, allows rapid digestion of organic matter (Hurley et al., 2018; Dyachenko et al., 2017).

Most often used methos for MP extraction is separation based on difference of density, where MP float on the surface of solutions. Supernatant, together with MP is then filtrated (Hanvey et al., 2017). Solutions like sodium chloride (NaCl), zinc chloride ($ZnCl_2$) and sodium iodide (NaI) (Zhou et al., 2018; Han et al., 2019) are usually used, but are environmentally unfriendly, often hazardous and can be expensive (Nuelle et al., 2014; Imhof et al., 2012). As simple, fast and efficient method is also oil extraction procedure (OEP), due to lipophilic properties of plastics (Gies et al., 2018). Some researchers used olive, canola and castor oil for MP extraction from soil, where olive oil was the most efficient with the strongest affinity towards different types of polymers (Scopetani et al., 2020). It utilizes lipophilicity properties of plastics. By adding oil to organic matter MP can be efficiently extracted from sludge (Crichton et al., 2017).

The aim of the study was to develop rapid, easy and cost-efficient extraction method, that achieves high recovery rate in separating MP particles from sludge samples. The method was tested by counting MP particles on filter, that are after identified by FT-IR

analysis. The hypothesis was that different types and sizes of MP can impact the recovery rate of OEP prior the pre-treatment of sample with Fenton's reagent.

1. Methods

2.1 Sample collection and preparation

Sewage sludge samples were collected from WWTP after dewatering. Collected samples were stored in dark and cold place until further analysis. In comparison with other protocols and research, we did not dry sludge samples prior extraction, because drying turned dried sludge into a solid agglomerate, possibly because of high content of organic matter (Vermeiren et al., 2020). Target weight of dewatered sludge were 40 g of sample. For each experiment, sludge was added into a clean glass jar and spiked with prepared MP particles. We added 100 mL of deionized water and left it on the stirrer at 700 rpm and 40 °C for 10-15 min or until sample was homogenized. Three replicates were done for each experiment (n=9).

2.2 Spiking of microplastics

Sludge samples were spiked with MP particles in order to evaluate the MP recovery rate. MP particles were mechanically fragmented and sieved on small particles (smaller than 1 mm) and bigger particles (sized between 1 mm and 5 mm). We used polyvinyl chloride (PVC), polystyrene (PS), polypropylene (PP) and polyethylene terephthalate (PET), since most of them are one of the most common types of MP that are produced and found in the environment [27]. Particles were cut manually from PET bottle and PP and PS pot, while PVC particles were of industrial origin. Each particle of MP was picked by hand and carefully transferred into the sample. 10 pieces of each type and size of polymer was added in the sample, prior analysed by FTIR. Specific densities of selected types are listed in **Table 1**.

Table 1. Specific densities of selected polymers (Crichton E M, et al, 2017; Vermeiren P, et. al. 2020)

	PVC	PS	PP	PET
Density [g/cm³]	1.3-1.45	1.05	0.83-0.85	1.37

PVC: polyvinyl chloride, PS: polystyrene, PP: polypropylene, PET: polyethylene terephthalate

2.3 Removal of the organic matter

Since sludge contain high amount of organic matter, we used Fenton's reagent to reduce organic matter before the extraction procedure to increase recovery rate. As suggested by Vermeiren P, et. al. 2020, 20 mL of Fenton's reagent and 20 mL of 30% H_2O_2 was added in sample of 40 g with spiked MPs. The temperature was regulated with ice bath to avoid thermal degradation. Solution of catalyst was made of 3, 6 g of iron (ll) sulfate heptahydrate ($FeSO_4$ x $7H_2O$), 250 mL of deionized water and 1 mL of sulfuric acid (H_2SO_4). Three replicates were done (n=9).

2.4 Oil extraction protocol

Each sludge sample with spiked MP, after homogenization or after oxidation in case of pre-treatment, was transferred into separatory funnel (**Figure 1**). We added 100 mL of deionized water and shake by hand for 30 s. After that, we added 10 mL of olive oil to each sample. Funnel was sealed and shaken for 60 s by hand to ensure that sludge sample with spiked MP got into contact with olive oil thorough mixing of the sample. To ensure, that all MP particles and sample stays in the mixture, walls and lid of the funnel were rinsed with 200 mL of deionized water. After settling for 15 minutes, the lower aqueous and solid phase was let out from separation funnel into other clean separation funnel where 5 mL of oil was added, sealed and shaken by hand for 60 s. After settling and solid phase removal, oil layer, that remained in both funnels, was filtered using a vacuum filtration with Whatmann filters GF/C 47 mm. Lid and walls of the funnel were rinsed with

100 mL of deionized water and 100 mL of ethanol (EtOH, 96 %). Filters were carefully transferred to Petri dishes, covered and stored at 4 °C.

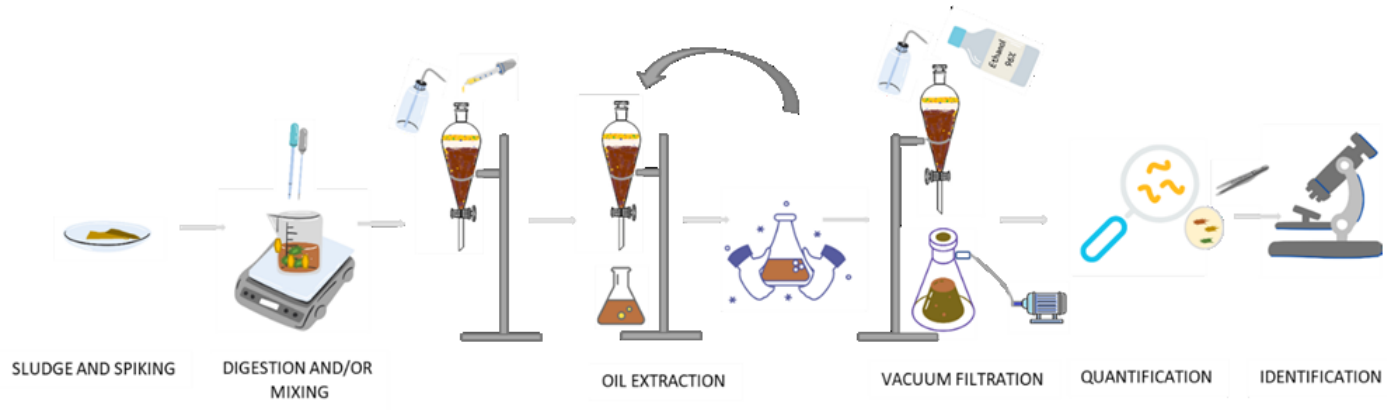

Figure 1. Steps of oil extraction procedure.

2.5 Quantification and identification

The extracted MP particles were visually quantified with magnifying lens and microscope Olympus CX43 on four times magnification. Visual identification of polymers is preliminary identification and it is the first step of polymer characterization. Particles were after extraction analysed with FTIR.

2.6 Details of sample characteristics

For dewatered sludge we determined moisture content and content of organic matter. Moisture content was established through the percentage loss while drying the sample at 105 °C for 12 h and content of organic matter through loss on ignition, while samples were heated to 550 °C for 4 h. Three replicates were done with 10 g of sludge and average value was calculated.

2. Results

After we counted and identified polymers, we determined the average recovery rate for samples that were oxidated with Fenton's reagent before OEP and samples where only OEP was done, for each type of MP and size. In the case that any other particle of MP was found in the sample it was not included in calculation of recovery rate. Recovery rate was higher for samples where oxidation of samples was performed before OEP for all types and sizes of MP. Average recovery rate with oxidation with Fenton's reagent prior OEP was on average 10% higher than OEP alone. Average recovery rate of all small polymer types (< 1 mm) reached 78% ± 17% with OEP and with additional oxidation 86% ± 9% while for bigger polymers (1-5 mm) 65% ± 32% with OEP and 75% ± 34% with oxidation. PVC with the highest density, had the lowest recovery rate. For bigger particles when only OEP was used it reached 19% ± 10%, while with oxidation, the recovery rate was higher, but still low (24% ± 12%) in comparison with plastics, that have lower densities. Small PVC particles reached higher average recovery rate 54% ± 30% with OEP and 77% ± 12% with pre-treatment. PP particles, with the lowest density, had the highest recovery rate for bigger particles and reached 99% ± 4% with oxidation and 86% ± 16% with only OEP. Small particles PP reached 93% ± 8% with OEP and 97% ± 5% with additional oxidation. Average recovery rates with SD are shown on **Figure 2**.

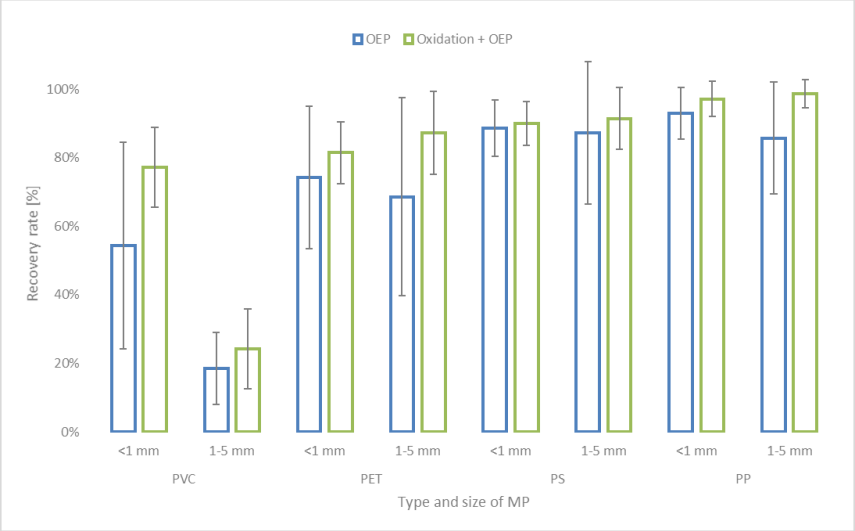

Figure 2. Recovery rate (mean + SD; n=9) of OEP with and without oxidation with Fenton's reagent

3.2 FTIR analysis

FT-IR analysis prior and after extraction have confirmed, that no chemical change occurred during the procedure (Figure 3, PVC polymer). It seems, that Ethanol efficiently removes oil from particles and does not affect FTIR spectra from polymers.

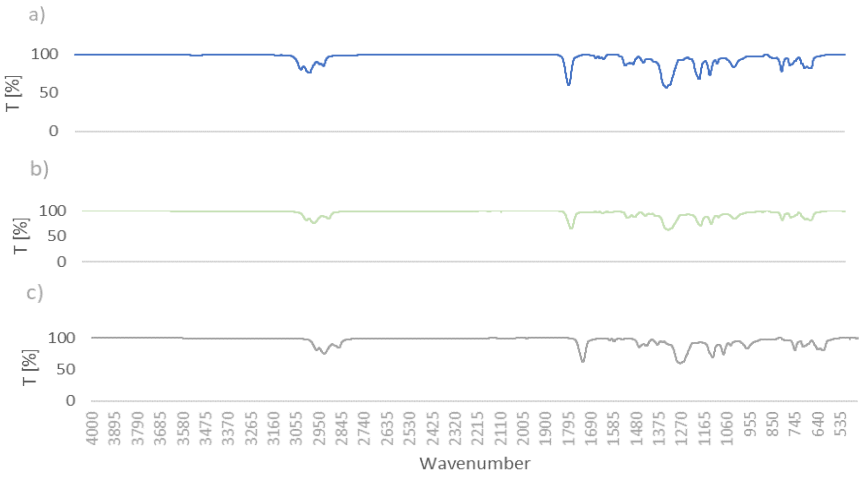

Figure 3. FTIR spectra from samples for PVC sample a) before extraction, b) after olive oil extraction c) after oxidation, followed by oil extraction protocol.

3. Discussion

Oxidation with Fenton's reagent improves recovery rate for all types of MP and it seems, that size of particles does not have impact on higher recovery rate, except with particles, that have higher densities as is PVC. Oxidation was shown as an important pre-step for oil extraction of MP in sludge samples with reducing organic matter and helps to avoid clogging the vacuum filters, slowing down the filtration and also quantification and identification of polymers is easier to miss, when oxidation is involved in the procedure.

No marked difference in recovery rate was discovered between different sizes of polymers, except with PVC, where the recovery rate was much higher (in average 36% with OEP and 53% with oxidation) with particles smaller than 1 mm. However, for polymers with higher densities, further experiments need to be done, since those polymers can be easily overseen because of small size and colours of MP with this approach. In the usage of OEP it is important, that the mixture is well mixed, so that all polymers

got into the contact with oil. The method is suitable for smaller particles than is the size of the outlet of the funnel, since it restricts the maximum size of MP and bigger particles could also clog the funnel as high content of organic matter. This is the reason, why pre-treatment is an important step prior OEP.

4. Conclusion

OEP is simple, reliable, rapid and cost-effective method for separation of polymer particles in environmental samples. It is a promising extraction method, since it reaches high recovery rate and is harmless to environment and humans. Nevertheless, further research needs to be done with particles of higher densities and bigger sizes than 1 mm. Currently there is no standardised procedure of treatment of environmental samples as it is sludge. Efficient and standardised extraction method of MP from sludge could unify results of further research and ensure comparable results between different research studies.

Funding: This research was supported by the Slovenian Research Agency (ARRS), the research programme of Chemical Engineering P2-0191 and Mechanisms of Health Maintenance P3-0388.

References

1. Anderson J C, Park B J, Palace V P. Microplastics in aquatic environments: Implications for Canadian ecosystems. Environ Pollut. 2016; 218: 269-280. DOI: 10.1016/j.envpol.2016.06.074.
2. Andrady A L. Microplastics in the marine environment. Mar Pollut Bull. 2011; 62(8): 1596-1605. DOI: 10.1016/j.marpolbul.2011.05.030.
3. Blair R M, Waldron S, Gauchotte-Lindsay C. Average daily flow of microplastics through a tertiary wastewater treatment plant over a ten-month period. Water res.2019; 163: 114909. DOI: 10.1016/j.watres.2019.114909.
4. Carr S A, Liu J, Tesoro A G. Transport and fate of microplastic particles in wastewater treatment plants. Water Res. 2016; 91: 174-182. DOI: 10.1016/j.watres.2016.01.002.
5. Corradini F, Meza P, Eguiluz R, Casado F, et al. Evidence of microplastic accumulation in agricultural soils from sewage sludge disposal. Sci Total Environ. 2019; 671: 411-420. DOI: 10.1016/j.scitotenv.2019.03.368.
6. Cole M, Webb H, Lindeque P K, Fileman E S, et al. Isolation of microplastics in biota-rich seawater samples and marine organisms. Sci Rep. 2014; 4: 4528. DOI: 10.1038/srep04528.
7. Crichton E M, Noël M, Gies E A, Ross P S. A novel, density-independent and FTIR-compatible approach for the rapid extraction of microplastics from aquatic environment. Anal Methods. 2017; 9: 1419-1428. DOI: 10.1039/C6AY02733D.
8. Dehaut A, Cassone A-L, Frere L, Hermabessiere L, et al. Microplastics in seafood: Benchmark protocol for their extraction and characterization. Environ Pollut. 2016; 215: 223-233. DOI: 10.1016/j.envpol.2016.05.018.
9. Dyachenko A, Mitchell J, Arsem N. Extraction and identification of microplastic particles from secondary wastewater treatment plant (WWTP) effluent. Anal Methods. 2017; 9: 1412-1418. DOI: 10.1039/c6ay02397e.
10. Gies E A, LeNoble J L, Noël M, Etemadifar A, et al. Retention of microplastics in a major secondary wastewater treatment plant in Vancouver, Canada. Mar Pollut Bull. 2018; 133: 553-561. DOI: 10.1016/j.marpolbul.2018.06.006.
11. Gong J, Xie P. Research progress in sources, analytical methods, eco-environmental effects, and control measures of microplastics. Chemosphere (Oxford). 2020; 254: 126790-126790. DOI: 10.1016/j.chemosphere.2020.126790.
12. Han X, Lu X, Vogt R D. An optimized density-based approach for extracting microplastics from soil and sediment samples. Environmental pollution. 2019; 254: 113009-113016. DOI: 10.1016/j.envpol.2019.113009.
13. Hanvey J S, Lewis P J, Lavers J L, Crosbie N D, et al. A review of analytical techniques for quantifying microplastics in sediments. Analytical methods, 2017; 9(9): 1369-1383. DOI: 10.1039/c6ay02707e.
14. Hurley R R, Liusher A, Olsen M, Nizzetto L. Validation of a Method for Extracting Microplastics from Complex, Organic-Rich, Environmental Matrices. Environ Sci Technol. 2018; 52: 7409-7417. DOI: 10.1021/acs.est.8b01517.
15. Imhof H K, Schmid J, Niessner R, Ivleva N P, et al. A novel, highly efficient method for the separation and quantification of plastic particles in sediments of aquatic environments. Limnology and oceanography, methods. 2012; 10(7): 524-537. DOI: 10.4319/lom.2012.10.524.
16. Lares M, Ncibi M C, Sillanpää M, Sillanpää M. Intercomparison study on commonly used methods to determine microplastics in wastewater and sludge samples. Environ Sci Pollut Res Int. 2019; 26(12): 12109-12122. DOI: 10.1007/s11356-019-04584-6.
17. Li X,Chen L, Ji Y, Li M, et al. Effects of chemical pretreatments on microplastic extraction in sewage sludge and their physicochemical characteristics. Water Res. 2020; 171: 115379. DOI: 10.1016/j.watres.2019.115379.

18. Mintenig S M, Int-Veen I, Löder M G J, Primpke S, et al. Identification of microplastic in effluents of waste water treatment plants using focal plane array-based micro-Fourier-transform infrared imaging. Water Res. 2017; 108: 365-372. DOI: 10.1016/j.watres.2016.11.015.
19. Ngo P L, Pramanik B K, Shah K, Roychand R. Pathway, classification and removal efficiency of microplastics in wastewater treatment plants. Environ Pollut. 2019; 255: 113326. DOI: 10.1016/j.envpol.2019.113326.
20. Nuelle M T, Dekiff J H, Remy D, Fries E. A new analytical approach for monitoring microplastics in marine sediments. Environ Pollut. 2014; 184: 161-169. DOI: 10.1016/j.envpol.2013.07.027.
21. Scopetani C, Chelazzi D, Mikola J, Leiniö V, et al.Olive oil-based method for the extraction, quantification and identification of microplastics in soil and compost samples. Sci Total Environ, 2020. 733: p. 139338. DOI: 10.1016/j.scitotenv.2020.139338.
22. Sun J, Dai X, Wang Q, M van Loosdrecht M C, et al. Microplastics in wastewater treatment plants: Detection, occurrence and removal. Water Res. 2019; 152: 21-37. DOI: 10.1016/j.watres.2018.12.050.
23. Talvitie J, Mikola A, Koistinen A, Setälä O. Solutions to microplastic pollution - Removal of microplastics from wastewater effluent with advanced wastewater treatment technologies. Water Res. 2017; 123: 401-407. DOI: 10.1016/j.watres.2017.07.005.
24. Vermeiren P, Munoz C, Ikejima K. Microplastics identification and quantification from organic rich sediments: A validated laboratory protocol. Environ Pollut. 2020; 262: 114298. DOI: 10.1016j.envpol.2020.114298.
25. Zhang Z, Chen Y. Effects of microplastics on wastewater and sewage sludge treatment and their removal: A review. Chemical engineering journal (Lausanne, Switzerland : 1996). 2020; 382: 122955-122971. DOI: 10.1016/j.cej.2019.122955.
26. Zhou Q, Zhang H, Fu C, Zhou Y. The distribution and morphology of microplastics in coastal soils adjacent to the Bohai Sea and the Yellow Sea. Geoderma. 2018; 322: 201-208. DOI: 10.1016/j.geoderma.2018.02.015.

Scientific contribution

Fate of Bisphenols During Conventional Wastewater Treatment

Vehar A[1,2], Kovačič A[1], Hvala N[3], Škufca D[1,2], Levstek M[4], Stražar M[4], Žgajnar Gotvajn A[5], Heath E[1,2,*]

1. Department of Environmental Sciences, Jožef Stefan Institute, Ljubljana, Slovenia
2. Jožef Stefan International Postgraduate School, Ljubljana, Slovenia
3. Department of Systems and Control, Jožef Stefan Institute, Ljubljana, Slovenia
4. Javno Podjetje Centralna čistilna naprava Domžale-Kamnik d.o.o., Domžale, Slovenia
5. University of Ljubljana, Faculty of Chemistry and Chemical Technology, Ljubljana, Slovenia

* Correspondence: Ester Heath; ester.heath@ijs.si

Abstract:
There is limited knowledge of the fate of bisphenols (BPs) during wastewater treatment and their emissions into the environment *via* effluent release or sludge disposal. In this study, BPA and its 15 substitutes in a municipal wastewater treatment plant were monitored. First, an analytical method for determining 16 BPs in the solid phase of activated sludge, based on solid-phase extraction and gas chromatography-mass spectrometry, was developed and validated. The method was then used to analyse composite samples from different compartments of a municipal wastewater treatment plant with sequencing batch reactor technology. BPs concentrations were then converted into mass flows and their removal from wastewater and adsorption to primary and secondary sludge was determined. On average, 12% of the BPs were adsorbed to primary sludge, 2% adsorbed to secondary sludge, 18% remained in the wastewater treatment plant effluent, and 68% were removed. In addition, their emissions into the environment were also evaluated and were 2 g day^{-1} of BPs *via* effluent release and 6 g day^{-1} *via* sludge disposal. The data shows that the emissions of BPs are not negligible, and for that reason, they should be monitored and considered.

Keywords: Bisphenol; Sludge; Wastewater; Mass balance

Citation: Vehar A, Kovačič A, Hvala N, Škufca D, Levstek M, Stražar M, Žgajnar Gotvajn A, Heath E. Fate of Bisphenols During Conventional Wastewater Treatment. Proceedings of Socratic Lectures. 2021; 6: 57-62. https://doi.org/10.55295/PSL.2021.D.008

Introduction

Bisphenols (BPs) are synthetic organic compounds used in the production of epoxy resins and polycarbonate, commonly, for example, in food contact materials, compact discs, construction materials, thermal paper, dental composites, medical equipment, water pipes, toys, sports equipment and dyes for synthetic clothes (Česen et al. 2018, Hu et al., 2019, Kovačič et al., 2019, Noszczyńska et al., 2018). BPA, the most common bisphenol, is a known endocrine-disrupting compound. The concern over the safety of BPA has resulted in its gradual replacement by other BPs. Since they all share a common structure of two hydroxyphenyl functionalities, the concern is that they may also share endocrine-disrupting potential (Kovačič et al., 2019).

Bisphenols can be commonly determined in surface- and groundwater, sea, sediments, soil and even dust and range from few ng L^{-1} or ng g^{-1} to few μg L^{-1} to μg g^{-1}. The primary source of BPs to the environment are wastewaters (WW), mainly from industrial effluents and, on a smaller scale, also municipal WW (Hu et al., 2019). BPs can enter municipal WW by, e.g., food contact material leaching and synthetic clothes washing, while they enter the industrial WW by, e.g., food processing industry, food contact material industry and dry-cleaners effluents. These wastewaters are treated at the municipal wastewater treatment plants (WWTP) and BPs are, according to their physicochemical parameters, removed from the aqueous phase to different extent: some are degraded or mineralised, some remain in the aqueous phase and are discharged with effluents to surface waters, while some get adsorbed to sludge, which can be used in land applications, landfilled or incinerated.

In order to fill some gaps regarding the behaviour of BPs in WWTP, this study has the following four aims: 1) development of the method for determining 16 BPs in sludge from WW treatment, 2) determination of the concentrations of BPs in real samples of WW and sludge at different points of WWTP, 3) determination of the adsorption of BPs onto the primary and secondary sludge, their removal from the WW and their removal during the anaerobic digestion of sludge, 4) evaluation of the emissions of BPs into the environment via effluent release or sludge disposal.

1. Methods

An analytical method for determining 16 BPs in sludge was developed and validated. First, sludge was sampled and prepared using centrifugation and lyophilization. BPs were then extracted from the sludge to the solvent using an ultrasonic bath and centrifugation. After that, solid-phase extraction (SPE) was performed, the eluate was dried and derivatized. Samples were then analysed using gas chromatography coupled with mass spectrometry.

Aqueous samples were prepared following the method of Kovačič et al. (2019). First, aqueous samples were filtered and then loaded into SPE cartridges. The eluate was dried, derivatized and analysed after the same procedure as sludge samples.

During the development of an analytical method for sludge, two types of SPE cartridges were tested: a) OASIS Prime HLB cartridges, based on water-wettable hydrophilic-lipophilic balanced copolymer and b) Affinimip® SPE Bisphenols cartridges, based on molecularly imprinted polymer, designed for the extraction of BPs. During the optimization of the method, recovery and repeatability were monitored. In case of Oasis Prime HLB cartridges different parameters were tested: 1) five extraction solvents, 2) two centrifugation parameters and two or three extraction repetitions, 3) extract cleaning with QuEChERS and filtration, 4) influence of acidification prior to loading, 5) five washing solutions and 6) five different elution solvents. In case of Affinimip® SPE Bisphenol cartridges, two protocols with small variations suggested by a manufacturer were tested. In the end, the method using Oasis Prime HLB cartridges was chosen, since it provided the highest recoveries and repeatability, while it was also cost and time effective. Finally, the

method performance was assessed regarding recovery, linearity, accuracy, the limit of detection and quantification, sensitivity, precision (method and instrumental repeatability) and the matrix effect.

WW and sludge sampling was performed at the Central Wastewater Treatment Plant Domžale-Kamnik, which has a capacity of 149,000 population equivalents. 24-hour composite samples of influent to the WWTP (WWTP_inf), influent to the primary settler (PSE_inf), effluent from the primary settler (PSE_eff) and with 24-hour delay effluent from the WWTP (WWTP_eff) were sampled. 6-hour composite samples of primary (PS) and secondary sludge (SS) were sampled, and one grab sample of anaerobically stabilised sludge (AS) was sampled on the same day (**Figure 1**).

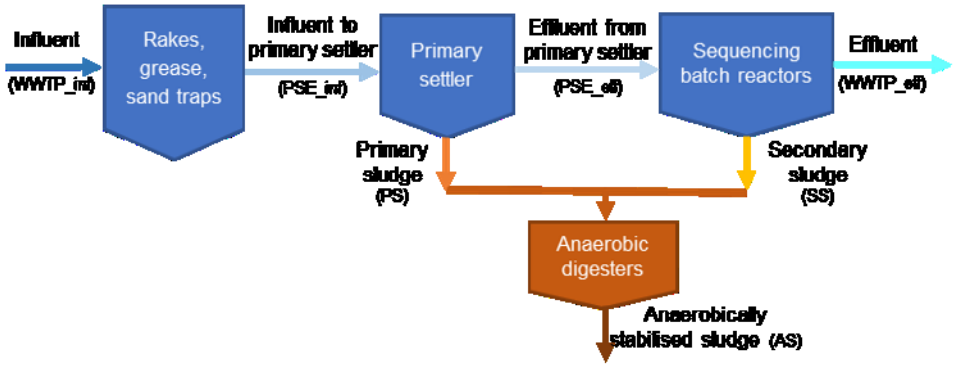

Figure 1. Scheme of a WWTP and the flows where samples were taken

2. Results

In the WW flows, BPA and BPS were the most abundant and 22BPF, 24BPF, 44BPF and BPE to a lesser extent (**Figure 2**). The concentration of BPs increased during the mechanical stage with the highest values in PSE_eff. All BPs in the WWTP_eff were below the limit of quantification (LOQ(BPA) = 18 ng L^{-1}, LOQ(15 BPs) = 2 ng L^{-1}) except BPA (79 ng L^{-1}), BPS (20 ng L^{-1}), BPBP (3 ng L^{-1}), 22BPF (3 ng L^{-1}) and BPAP (2 ng L^{-1}).

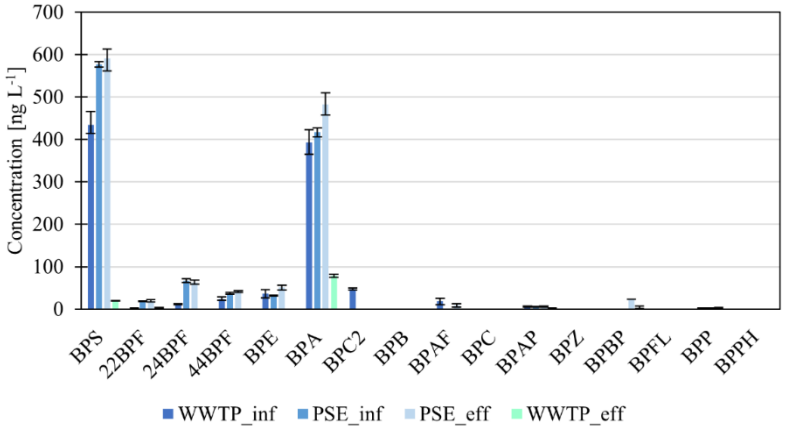

Figure 2. The concentrations of BPs in the WWTP_inf, PSE_inf, PSE_eff, WWTP_eff

In the sludge, the most abundant BPs were BPA and BPS, while 22BPF, 24BPF and 44BPF were present to a lesser extent (**Figure 3**). The highest concentrations of BPs were observed in the anaerobically stabilised sludge, compared to the primary and secondary sludge, where BPA reached 946 ng g^{-1} in the solid phase (SP) and 3248 ng L^{-1} in the aqueous phase (AP).

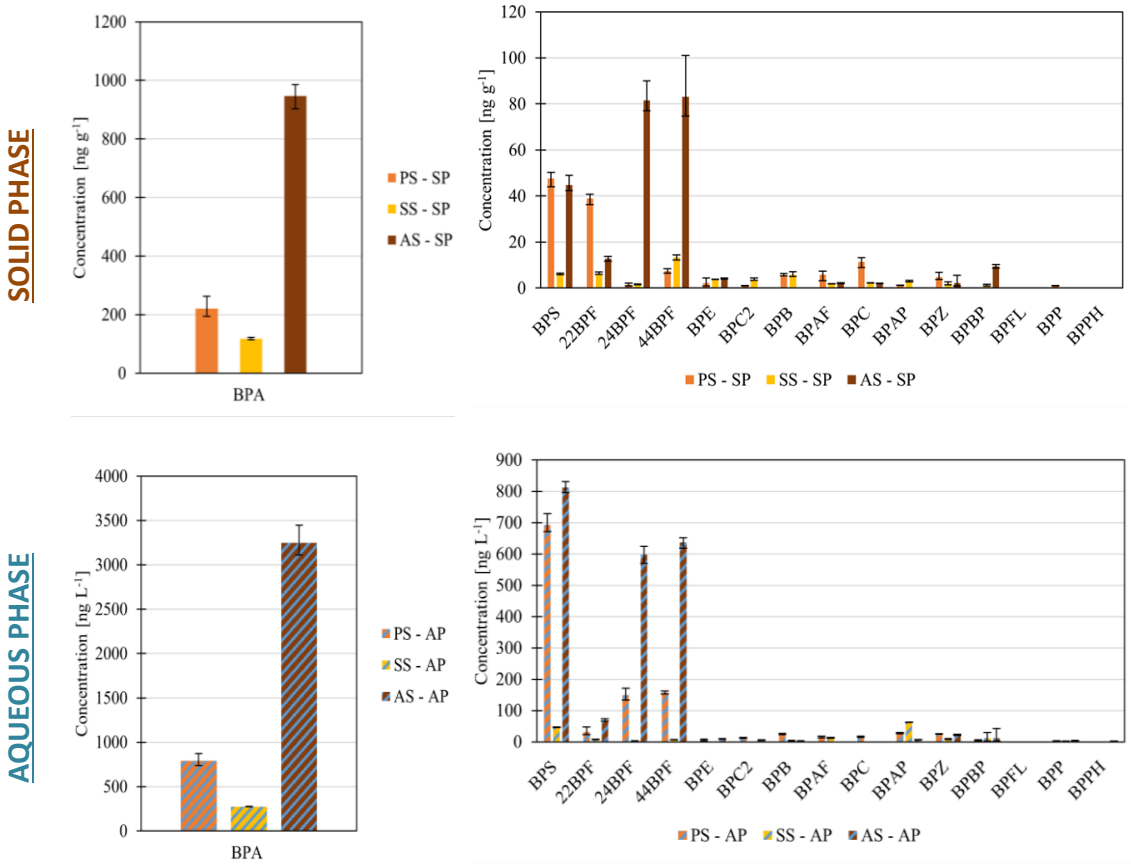

Figure 3. Levels of BPs in the solid (SP) and aqueous phase (AP) of primary (PS), secondary (SS), and anaerobically stabilised sludge (AS)

According to the calculated mass flows of BPs (**Figure 4**), BPA and BPS were again the most abundant in wastewater. The trend of mass flows rising through the mechanical stage of treatment with the maximum in the PSE_eff and the trend of maximal mass of BPs flows in the AS, lower in PS and the lowest in SS were present again.

Possible explanations for the increasing concentrations of BPs through the mechanical stage of treatment can be adsorption and later desorption of the compounds at different parts of the mechanical stage of WWTP. Besides, the concentrations of BPs in the solid particles in WW flows were not measured, since the content of solid particles is so low that is usually not determined. There are three possible reasons for the higher concentrations of BPs in the influent to the primary settler. The first could be receiving the external WW (septic tanks), which are delivered by trucks. The second could be the inflow of the wastewater from the deamonification process of the centrate, which comes from the mechanical thickening of the anaerobically stabilised sludge. The third reason could be the inflow of pretreated wastewater, which is a result of the treatment of hazardous and non-hazardous liquid waste in the electrocoagulation plant. All the above-mentioned types of WW go directly to the mechanical stage of WWTP.

One of the possible reasons for the higher amounts of BPs in the anaerobically stabilised sludge is its single grab sampling. Since its retention time is 30 days, determined concentrations cannot be directly related to the concentrations of BPs in primary and secondary sludge. The other reasons can be adsorption and later desorption of the compounds at the parts of the anaerobic reactor, deconjugation of conjugated compounds as well as addition of external sludge, going directly to anaerobic stabilisation.

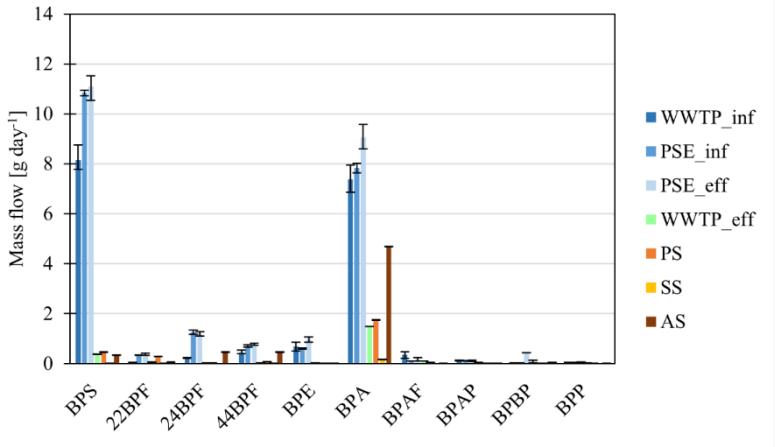

Figure 4. Mass flows of BPs in the selected wastewater flows and sludge

On average, 12% of the BPs were adsorbed to PS, 2% adsorbed to SS, 18% remained in the WWTP_eff, and 68% were removed (**Figure 5**). The lowest removal efficiency (29%) was observed for BPAF, a halogenated bisphenol, which is in agreement with the fact that compounds with strong C-F bonds are generally poorly biodegradable under aerobic conditions (Kovačič et al., 2019). The second-lowest removal efficiency was obtained for BPP, where the mass flows through the treatment system were relatively low. In case the concentrations were below the LOQ, the removal was calculated from the LOQ values.

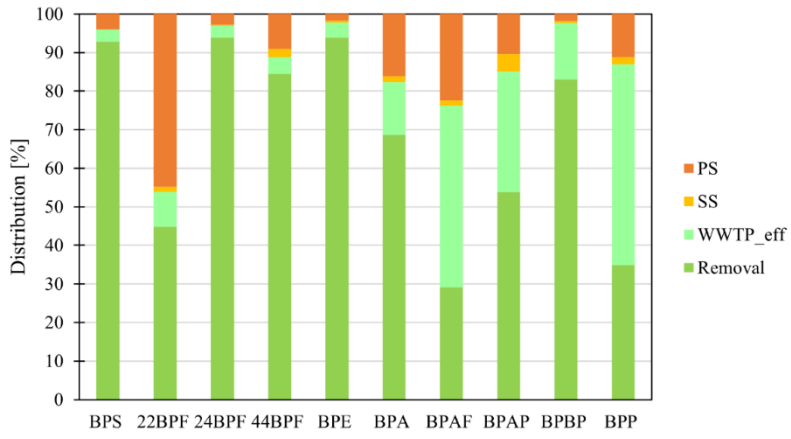

Figure 5. Distribution of BPs in primary (PS) and secondary sludge (SS), WWTP_eff and their removal (%)

Removal of BPs in anaerobic conditions was successful only for 6 BPs (**Figure 6, A**), on average 52%. The negative removal in anaerobic conditions was shown for 4 BPs (**Figure 6, B**), which means that the mass flows of BPs in sludge increased after the anaerobic digestion. The anaerobic removal of BPAF was the highest (79%) among all BPs, which was expected since halogenated compounds are known to be more biodegradable in anaerobic conditions.

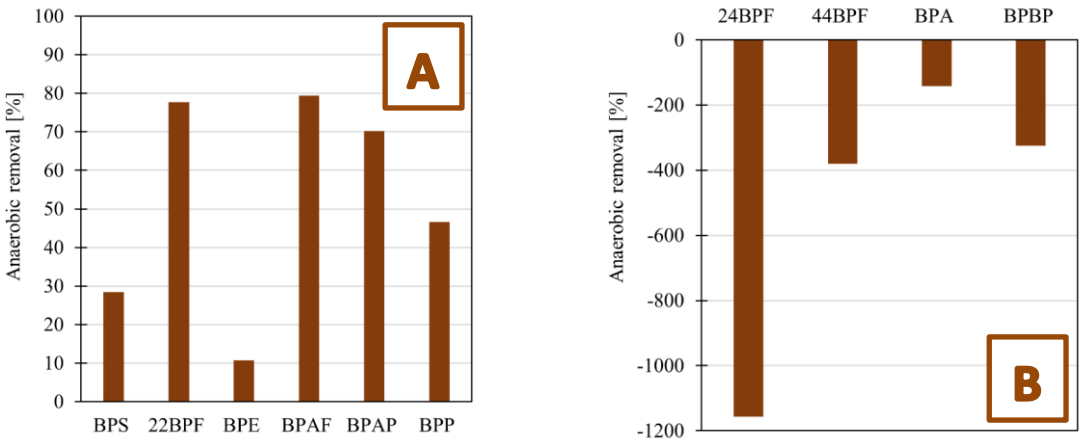

Figure 6. Removal of BPs in anaerobic digesters: A) anaerobic removal (%) for BPS, 22BPF, BPE, BPAF, BPAP, BPP and B) negative anaerobic removal (%) for 24BPF, 44BPF, BPA, BPBP

3. Conclusions

An analytical method for determining 16 BPs was developed and the concentrations of BPs at different points in WWTP were determined. The majority of BPs were removed during the wastewater treatment, while the others remained in the effluent or were adsorbed to anaerobically stabilised sludge. In case of investigated WWTP, each day 2 g of BPs end up in the receiving river through effluent discharge and 6 g are emitted through anaerobically stabilised sludge disposal. Even though the concentrations of BPs in the effluent are low, there are also many other contaminants of emerging concerns present in WW effluents, and since their long-term effects are still very poorly researched, the impacts of the effluent discharges on the environment, river organisms and humans are still to be researched and the inclusion of advanced wastewater treatment techniques, as pre- or post-treatment may be a solution, which would lead to mineralization of organic contaminants to CO_2 and H_2O. Before taking a final decision on the potential of sludge for agricultural or remediation application, the presence of other hazardous contaminants like drugs, heavy metals and their residues has to be evaluated and risk assessment performed. Despite the high costs, currently, the most suitable sludge management option is still incineration.

Funding: This research was supported by the Slovenian Research Agency ARRS, namely Research Program Cycling of Substances in the Environment, Mass Balances, Modelling of Environmental Processes and Risk Assessment P1-0143 (projects N1-0143, L7-1848, J1-9166), Research Program Chemical Engineering P2-0191 and Research Program Systems and Control P2-0001.

Conflicts of Interest: The authors declare no conflict of interest.

References

1. Česen M, Lenarčič K, Mislej V, et. al. The occurrence and source identification of bisphenols compounds in wastewaters. STOTEN. 2018; 616-617: 744-752. DOI: 10.1016/j.scitotenv.2017.10.252
2. Hu Y, Zhu Q, Yan X, Liao C, Jiang G, Occurrence, fate and risk assessment of BPA and its substituents in wastewater treatment plant: A review. Environmental Research. 2019; 178: 108732. DOI: 10.1016/j.envres.2019.108732
3. Kovačič A, Česen M, Laimou-Geraniou M, et. al. Stability, biological treatment and UV photolysis of 18 bisphenols under laboratory conditions. Environmental Research. 2019; 179: 108738. DOI: 10.1016/j.envres.2019.108738
4. Noszczyńska M, Piotrowska-Seget Z, Bisphenols: Application, occurrence, safety, and biodegradation mediated by bacterial communities in wastewater treatment plants and rivers. Chemosphere. 2018; 201: 214-223. DOI: 10.1016/j.chemosphere.2018.02.179

Interdisciplinary Insight on European Spruce (*Picea abies*): Biologically Active Compounds and their Usage

Jeran M[1,2,*], Pečan LI[3], Barrios-Francisco R[4]

1. University of Ljubljana, Faculty of Health Sciences, Laboratory of Clinical Biophysics, Ljubljana, Slovenia
2. University of Ljubljana, Faculty of Electrical Engineering, Laboratory of Physics, Ljubljana, Slovenia
3. University of Ljubljana, Biotechnical Faculty, Department of Biotechnology, Ljubljana, Slovenia
4. Tecnológico Nacional de México/TES de San Felipe del Progreso, División Ingeniería Química, San Felipe del Progreso, Mexico

* Correspondence: Marko Jeran; marko.jeran@fe.uni-lj.si

Abstract:
Plants have the incredible ability, throughout their developmental cycle, to synthesize the active compounds on which today's drugs and therapies are based. They are also able to synthesize compounds that protect them from outside influences (enemies) and release them into individual plant particles to activate them. Many plants are found on European soil, including the European spruce (*Picea abies*). Among many other important active substances, spruce also contains limonene, which, along with α- and β-pinene, is the main group of natural monoterpenes. Limonene, which is mainly found in the peels of citrus fruits, is a useful and sought-after compound in various fields due to its properties. In addition to its use in fragrances, flavors, and beverage additives, it is also used in industry as a solvent and cleaning agent. Due to its ecological potential and a broad spectrum of biological activity, it is classified as an extremely promising active ingredient. Due to limonene's known anti-inflammatory and antiviral activity, it also appears to be of interest in the context of the search for potential agents in the fight against SARS-CoV-2.

Keywords: natural compounds, European spruce (*Picea abies*), natural monoterpenes, total phenols, biologically activity

Citation: Jeran M, Pečan LI, Barrios-Francisco R. Interdisciplinary Insight on European spruce (*Picea abies*): Biologically Active Compounds and their Usage. Proceedings of Socratic Lectures. 2021; 6: 64-70. https://doi.org/10.55295/PSL.2021.D.009

1. European spruce (*Picea abies*)

The European (Norway) spruce (*Picea abies*) belongs to the pine family (*Pinaceae*), which is the most numerous family of conifers, with more than 200 species. Its home is the European mountains of the central and northern regions. It is distributed from southern Scandinavia to the southern parts of the Alps, the Balkans and the Carpathians, where it thrives at altitudes of 600 to 2,000 m above sea level. In Europe it is mostly found in areas that are not optimal for its vitality (Jeran, 2020). Due to human intervention in the environment, it is difficult to determine its natural distribution. Due to its flexibility, it is one of the most numerous tree species in our country. According to the Forestry Administration, the timber stock in Slovenia for 2019 is 30.4%. As elsewhere in Europe, we can find spruce frequently even in lower altitudes due to artificial establishment. Spruce is a monoecious plant, which means that both male and female flowers are produced on the same plant. The male flowers are located on the shoots of the last season, are yellow-brown or yellowred in colour in the middle and upper part of the crowns and reach a length of about 3 cm. The female flowers are in an inflorescence and are bright red. Initially they are erect, as they grow, they become 2-4 cm long and develop into cylindrical, pendulous cones. Unlike the male flowers, which are found in the above-mentioned canopy, the female flowers are only found at the top of the canopy (Jeran et al., 2021).

The spruce is a versatile plant. Its light-coloured, relatively light and soft wood is used mainly in construction, in the furniture and paper industries, and in the manufacture of musical instruments. Many preparations made from spruce wood are also used for medicinal purposes. Of particular note are the essential oils of the needles and the resin in ointments, and the needles and tops are especially useful in the preparation of teas, baths, and vitamin drinks (Jeran, 2020). The active ingredients contained in spruce are said to facilitate the expectoration of mucus in colds, kill bacteria and relieve rheumatism. Ointment made from spruce resin is effective for frostbite and rheumatic pains. From the folk tradition, among the medicinal preparations, the most famous is spruce syrup, prepared by generations to relieve colds and flu in winter. In spring, we harvest the buds, which are up to 2.5 cm long (by then they contain most of the active ingredients), and put them in a glass jar, which we fill in layers with sugar or honey. Then we put the jar in a warm place (e.g., on a sunny windowsill) for about three weeks. After the elapsed time, we mix the contents well and filter (filtrate). Thus ready, store the syrup in a cool place until use (Jeran, 2020).

2. Biologically active compounds in European spruce (*Picea abies*)

The bark of conifers contains large amounts of lipophilic extractives. In spruce, fatty/resin acids, sterols, and triterpenoids are the most abundant extracts in the inner and outer bark. Spruce bark is also known to be a rich source of phenolic extracts, terpenes, resin acids, flavonoids, stilbenes and stilbene glucosides, lignin and holocellulose. Spruce bark is a source of β-sitosterol and methyl dehydroabietate, which have antibacterial and antioxidant properties. Stilbenes from spruce bark extracts are also known for their potent antioxidant properties. Tannins from the bark of conifers are used in the manufacture of foams, in medicine, in cosmetics, and in sewage treatment. In addition, raw or extracted bark can be used as an absorbent, and spruce bark has been suggested as a potential feedstock for the production of ethanol from lignocellulose (Bukhanko et al., 2020).

Needles contains mono- and sesquiterpenes, fatty acids, phenolic compounds, stilbene glucosides, waxes and carbohydrates as well as long-chain alcohols, e. g. nonacosan-10-ol, which has superhydrophobic properties (Bukhanko et al., 2020).

The twigs of spruce contain branches that contain resin acids and lignans. However, the content of lignans in the twigs is much lower than in the branches. This gives it potential for use in the manufacture of surfactants, paints, personal care products, cosmetics, and adhesives, as well as a potential raw material for the manufacture of antioxidants (Bukhanko et al., 2020).

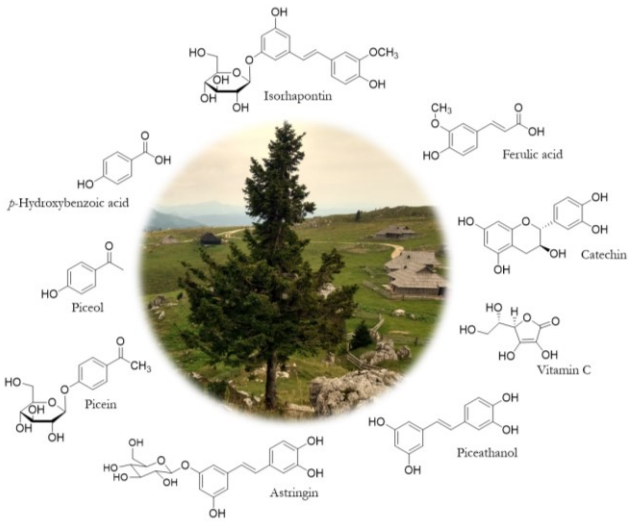

Figure 1. Example of structures of biologically active compounds in European spruce (*middle* part of the photo: European spruce on the Slovenian plateau Velika planina). From (Jeran et al., 2021).

Polyphenols are compounds with one or more hydroxyl groups attached to the benzene ring, which give them the ability to capture free radicals, moreover it gives them a stronger acidic character in comparison to other alcohol groups. This chemical reactivity is responsible for the antioxidant character of polyphenols. Nisca et al. have found a strong correlation between the antioxidant capacity and content of total polyphenols using ultrasound assisted extraction (UAE) and microwave assisted extraction (MAE). Results also suggested that higher polyphenolic content may lead to a stronger antioxidant activity (Nisca et al., 2021).

The bark of woody vascular plants is often considered a forest waste, but it can be an important source of bioactive compounds with a high potential for capitalisation. The large number of publications regarding the analysis of phenolic compounds extracted from the bark of woody vascular plants is testament to their importance and their value. Consequently, biologically active compounds obtained from the bark of woody plants could be exploited on an industrial scale (Tanase et al., 2019).

Several studies that the best results in terms of total phenolic compounds and antioxidant capacity were obtained for ultrasound assisted extraction (UAE) extract. In study conducted by Spinelli et.al (2021) UAE extract exerted the maximum phenolic concentration among the various green techniques adopted (54.97 ± 2.00 mg GAEs/g dray weight). The literature also confirms that UAE applied to various natural matrices significantly increases the phenolic compounds extracted, compared with alternative extraction methods. As a fact, the production of cavitation bubbles promotes better extraction yield and increases the antioxidant activity of these extracts (Spinelli et al., 2021).

We will further focus on the properties of limonene, which, along with α- and β-pinene, the main group of monoterpenes of European spruce (*Picea abies*).

3. Limonene

3.1. Chemical background

Limonene is a liquid, colorless hydrocarbon named after the lemon. It is present in lemon peels and lupins of other citrus fruits in considerable quantities and gives them a characteristic odor. Limonene is an optically active compound and occurs in two enantiomeric forms: the *R*- and *S*- forms. The forms differ in source, odor, and taste (Jeran et al., 2021). The enantiomers have the same chemical and physical properties but differ only in the direction of rotation of the plane of linearly polarized light. The enantiomer in solution rotates the plane of polarized light to the right and the other to the left. For ex-

ample, a chiral molecule that rotates the light to the right is called "right-handed". Some chemical differences between different isomers occur in the presence of other molecules (Barkel, 2012). Despite their physicochemical similarity, they can have different enantiomers that differ significantly in their biological activity. For example, in biochemistry, different enantiomers adapt differently to different enzymes, which explains why they often taste and smell differently and act differently as drugs (Barkel, 2012).

The *R*-(+)-enantiomer of limonene, also known as D-limonene, is the main compound in the essential oils of citrus peels (*Citrus* spp.). It is also widely present in some species of shrubs (*Lippia*) and wormwood (*Artemisia*) (Erasto et al., 2008). The S-limonene form is commonly found in essential oils of the genus Pinus (e.g., pine needles) and the genus Mentha (e.g., meta-spearmint). When both enantiomers of the chiral active ingredient are present in the mixture in equal amounts (in a 1:1 ratio), such a mixture is not optically active and is often referred to in chemistry as a racemic mixture or racemate. The limonene racemate is called dipentene (Jeran et al., 2021).

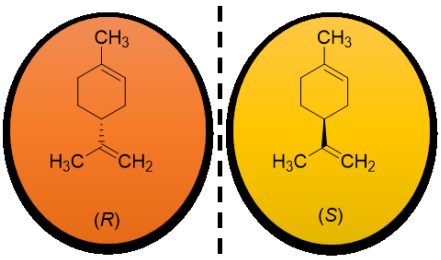

Figure 2. The monocyclic terpene limonene is named 1-methyl-4-(1-methyletenyl)cyclohexene according to IUPAC nomenclature. The figure shows the skeletal form of its enantiomeric forms.

Table 1. Physical properties of limonene. Adapted from: Gupta et al. (2021).

Molecular formula	C10H16
Molecular weight	136.24
State at room temperature	Colorless liquid
Melting point	-73.3 oC
Density	175.5-176 oC
Solubility	Slightly soluble in water at 25 oC: 13.8 mg/L. Moderately soluble in acetone, dimethyl sulfoxide, ethanol, benzene, carbon tetrachloride, diethyl ether, petroleum ether
Storage	Away from light and air. It forms various oxidation products with atmospheric oxygen, such ascarvone, limonen oxyde, carveol and limonene hydroperoxides

Limonene is liquid at room temperature and has proved to be a versatile solvent in the course of the development of its use. Its nonpolar nature shows an affinity for fats, which is why it has been used as an industrial detergent for over thirty years. An important advantage is that it is non-toxic, so it can easily be substituted for toxic and banned solvents such as methyl ethyl ketone (MEK), xylene (dimethylbenzene) and hydrofluorocarbons (CFCs). Its advantages also include biodegradability – it can be broken down relatively quickly to carbon dioxide and water – and the ability to be isolated from renewable sources. It is mainly obtained as a by-product from the processing of citrus peels, from which the lemon is then distilled. Such an isolated lemon is suitable for both technical purposes and for use in food. The essential oil from orange peel obtained by such a process contains 99% by weight of limonene (Burnham, 2008).

Limonene is used in many products as a flavoring and fragrance, for example in perfumes, beverages, detergents and soaps. In the field of synthesis and processing, it is used as a starting material for the production of various natural products and also plays an important role in the production of *p*-cymene (Erasto et al., 2008). The compound *p*-cymene is used as a drug to prevent cough and to loosen phlegm and is also present as a reagent in the synthesis of pesticides and fungicides16. The US Food and Drug Ad-

ministration classifies it in the "GRAS" category, which is generally recognized as safe (Marchese et al., 2017).

3.2. Biological activity of limonene

The widespread use of limonene in soft drinks, cosmetics, and other products has stimulated research into its potential antitumor and antimicrobial properties (Erasto et al., 2008). It is also known as a natural insecticide used to control pests and prevent spoilage of stored products (Erasto et al., 2008). The advantage of limonene over synthetic pesticides is its biodegradability, which is why it is considered "green" or environmentally friendly. Its pharmacological properties, low toxicity and allergenicity open the possibility of its use in various medicinal and cosmetic products. The content of limonene should be stated on if it is above 0.01% on the products that are washed-off (such as shampoos, care balms, etc.) or. 0.001% in products intended for direct application on the body surface (such as varnishes, creams, make-up, etc.) (Erasto et al., 2008).

The chemopreventive properties of limonene have also been studied in various types of cancer (Erasto et al., 2008). Cancer chemoprevention involves various dietary or pharmacological preparations with which we aim to prevent or inhibit the process of tumor development, even before the disease becomes clinically manifest. This requires the effective use of compounds that inhibit specific molecular steps of carcinogenesis at the developmental stage (Jiang, 2018). Consumption of limonene in rodents has been shown to inhibit the development of skin and lung cancer as well as stomach cancer (Erasto et al., 2018 & Abiodun Elegbede et al., 1986).

Nowadays, the biggest problem is the power of microorganisms against various known antimicrobial agents. One of the mechanisms of action is biofilm formation. Agents that inhibit biofilm production (including limonene) are therefore under intense investigation as possible alternative therapeutics (Gupta et al., 2021). Limonene has been shown to be an effective inhibitor of biofilm of *B. cereus*, *E. coli*, *P. putida* and *P. anomala* (Gupta et al., 2021). At a concentration of 400 µg/mL, about 75-95% inhibition of biofilm growth was observed against *S. pyogenes, S. mutans* and *S. mitis* (Kerekes et al., 2013), and the resulting biofilm mass was reduced by up to 90% after 8 hours of incubation in 2000 µL/L for different strains. *S. aureus* (Espina et al., 2018). Further studies with limonene also showed effective biofilm inhibition against *P. aeruginosa*, *C. albicans* and *C. parapsilosis* (Gupta et al., 2021; Pekmezovic et al., 2016). The effect of limonene on *S. mutans* biofilm was also demonstrated in silico studies, making it a suitable candidate for studying these properties (Gupta et al., 2021 & Nosrati et al., 2018).

3.3. Limonene and SARS-CoV-2 virus

Viruses cause many life-threatening diseases. Although many drugs have been developed against viruses in the past, their action has caused many side effects. Therefore, antiviral agents are still being developed and improved. Recent studies on limonene suggest that it may also be of interest in the current epidemic/pandemic (Gupta et al., 2021). In addition to the influenza virus and several other viruses, limonene has been identified as an inhibitor of the coronavirus SARS (Gupta et al., 2021). The SARS virus specifically binds to protein S, an enzyme that converts angiotensin 2 (ACE2). The enzyme ACE2 is found on cell membranes and serves as an entry port for the virus into the host cell (Koren et al., 2021; Kralj-Iglič et al., 2020). In a docking study, it was found that limonene could bind to ACE2 and potentially prevent the virus from entering cells (Abdelli et al., 2021).

4. Conclusions

Recent evidence on spruce suggests that it is a "green" source of various natural organic compounds (such as limonene, borneol) (Jeran et al., 2021) and cellular particles associated with extracellular vesicles (Jeran et al, 2021). The interdisciplinary synthesis of knowledge in the field of natural products shows an extraordinary potential for future applications, because nature offers a large number of active compounds. The model of spruce and the active ingredient limonene also covers the vertical aspect of use – from

industry, education, research to medical applications. Due to the constant development of science, scientists will continue to focus on the mechanism of formation of various active substances in plants and use the knowledge for the benefit of a modern and sustainable society.

Funding: This research was supported by by Slovenian Research Agency through the core foundlings No P3-0388.
Conflicts of Interest: The authors declare no conflict of interest.

References

1. Abdelli I, Hassani F, Bekkel Brikci S, Ghalem S. In silico study the inhibition of angiotensin converting enzyme 2 receptor of COVID-19 by Ammoides verticillata components harvested from Western Algeria. J Biomol Struct Dyn. 2021; 39(9): 3263-3276. DOI: 10.1080/07391102.2020.1763199
2. Abiodun Elegbede J, Elson CE, Tanner MA, Qureshi A, Gould MN. Regression of rat primary mammary tumors following dietary d-limonene. JNCI. 1986; 76(2): 323-325. DOI: 10.1093/jnci/76.2.323
3. Bukhanko N, Attard T, Arshadi M, Eriksson D. Extraction of cones, branches, needles and bark from Norway spruce (Picea abies) by supercritical carbon dioxide and soxhlet extractions techniques. Ind Crop Prod. 2020; 145: 112096. DOI: 10.1016/j.indcrop.2020.112096
4. Burnham PM, Limonene - the industrial degreasing agent found in orange peel (molecule of the month – March 2008). 2008; 1-2. DOI: https://doi.org/10.6084/m9.figshare.5427154
5. Erasto P, Viljoen AM. Limonene - a review: Biosynthetic, ecological and pharmacological relevance. Nat Prod Commun. 2008; 3(7): 1193-1202. DOI:10.1177/1934578X0800300728
6. Espina L, Pagán R, López D, García-Gonzalo D. Individual constituents from essential oils inhibit biofilm mass production by multi-drug resistant Staphylococcus aureus. Molecules. 2015; 20(6): 11357-11372. DOI: https://doi.org/10.3390/molecules200611357
7. Gupta A, Jeyakumar E, Lawrence R. Journey of limonene as an antimicrobial agent. J Pure Appl Microbiol. 2021; 15(3): 1094-1110. DOI: 10.22207/JPAM.15.3.01
8. Jeran M, Barrios-Francisco R, Kralj-Iglič V. Biološko aktivne učinkovine v navadni smreki (Picea abies): Razumevanje kemijskih lastnosti limonena pri njegovi uporabi in vsestranski biološki aktivnosti. Kemija v šoli in družbi. 2021; 1: 1-6. ISSN 2385-989X. Availabe from https://www.kemija.net/clanek/1755
9. Jeran M, Barrios-Francisco R, Sedušak Kljakič A, Remškar H, Non-destructive characterisation of natural ma-terials: quantitative determination of borneol and limonene in European spruce needles (Picea abies) by FTIR spectroscopy. In Kralj-Iglič V, editor. Socratic lectures: 4th International Minisymposium. Ljubljana, Slovenia, University of Ljubljana, Faculty of Health Sciences. 2021; pp. 79-86. ISBN 978-961-7112-02-3. Available from https://www.zf.uni-lj.si/images/stories/datoteke/Zalozba/Sokratska_2021.pdf
10. Jeran M, Božič D, Novak U, Hočevar M, European spruce (Picea abies) as a possible sustainable source of cellu-lar vesicles and biologically active compounds. In Kralj-Iglič V, editor. Socratic lectures: 5th International Min-isymposium. Ljubljana, Slovenia, University of Ljubljana, Faculty of Health Sciences. 2021; pp. 104-113. ISBN 978-961-7112-05-4. Available from https://www.zf.uni-lj.si/images/stories/datoteke/Zalozba/Sokratska_5.pdf
11. Jeran M. Navadna smreka (Picea abies) kot vir aktivnih učinkovin. Trdoživ: Bilten slovenskih terenskih biolo-gov in ljubiteljev narave. 2020; 9(2): 22-24. ISSN 2232-5999. Available from: https://issuu.com/trdoziv/docs/trdoziv18_web_v01
12. Jiang X, Liu Y, Ma L, Ji R, et al. Chemopreventive activity of sulforaphane. Drug Des Devel Ther. 2018; 12: 2905-2913. DOI: 10.2147/DDDT.S100534
13. Kerekes E-B, Deák É, Takó M, Tserennadmid R, et al. Anti-biofilm forming and anti-quorum sensing activity of selected essential oils and their main components on foodrelated micro-organisms. J Appl Microbiol. 2013; 115(4): 933-942. DOI: 10.1111/jam.12289
14. Koren J, Scott D, Jeran M, Renin-angiotensin system inhibitors and their implications for COVID-19 treatment. In Kralj-Iglič V, editor. Socratic lectures: 5th International Minisymposium. Ljubljana, Slovenia, University of Ljubljana, Faculty of Health Sciences. 2021; pp. 115-123. ISBN 978-961-7112-05-4. Available from https://www.zf.uni-lj.si/images/stories/datoteke/Zalozba/Sokratska_5.pdf
15. Kralj-Iglič V, Dahmane R, Griessler Bulc T, Trebše P. From extracellular vesicles to global environment: a cos-mopolite Sars-Cov-2 virus. Int J Clin Stud Med Case Reports. 2020; 4(1): 1-23. DOI: 10.46998/IJCMCR.2020.04.000079
16. Marchese A, Arciola CR, Barbieri R, Silva AS, et al. Update on monoterpenes as antimicrobial agents: A partic-ular focus on p-cymene. Materials. 2017; 10(8): 947. DOI: https://doi.org/10.3390/ma10080947

17. Nisca A, Ștefănescu R, Stegăruș DI, Mare AD. Phytochemical profile and biological effects of spruce (Picea abies) bark subjected to ultrasound assisted and microwave-assisted extractions. Plants. 2021; 10(5): 870. DOI: https://doi.org/10.3390/plants10050870
18. Nosrati M, Behbahani M, Mohabatkar H, Shakeran Z. Antibacterial and antibiofilm activities of Prangos acaulis Bornm. extract against Streptococcus mutans: an in silico and in vitro study. J Herbmed Pharmacol. 2018; 7(3): 176-184. DOI: 10.15171/jhp.2018.29
19. Pekmezovic M, Aleksic I, Barac A, Arsic-Arsenijevic V. Prevention of polymicrobial biofilms composed of Pseudomonas aeruginosa and pathogenic fungi by essential oils from selected Citrus species. FEMS Immunology & Medical Microbiology. 2016; 74(8): ftw102. DOI: 10.1093/femspd/ftw102
20. Spinelli S, Costa C, Conte A, La Porta N, et al. Bioactive compounds from Norway spruce bark: Comparison among sustainable extraction techniques for potential food applications. Foods. 2019; 8(11): 524. DOI: https://doi.org/10.3390/foods8110524
21. Tanase C, Coșarcă S, Muntean D-L. A critical review of phenolic compounds extracted from the bark of woody vascular plants and their potential biological activity. Molecules. 2019; 24(6): 1182. DOI: https://doi.org/10.3390/molecules24061182
22. van Brakel J, Substances: The ontology of chemistry. In Woody AI, Findlay HendryR, Needham P, editors. Phi-losophy of chemistry. North Holland, The Nederlands, Elsevier. 2012; pp. 191-229. DOI: 10.1016/B978-0-444-51675-6.50018-9

Scientific contribution/Review

Digital Physiotheraphy and COVID-19

Amon M[1]*, Kresal F[1],

1. Institution of Higher Education FIZIOTERAPEVTIKA, Ljubljana, Slovenia
* Correspondence: Mojca Amon; amon.mojca@gmail.com

Abstract:
During the burning period of the coronavirus disease (COVID-19) pandemic, the need to provide remote health services has already increased. Today, the indefinitely defined state of long COVID-19 combines a complex of consequences after COVID-19, which is currently considered a long-term pathogenic mechanism after overcoming the disease, but it may not be wrong to predict that the consequences will increase the importance of physical activity and malnutrition of the health system, only remotely. Remote rehabilitation or telerehabilitation is an example of an emergency solution such as the COVID-19 pandemic. The results of research indicate the success of telerehabilitation of older adults of various diagnoses in tracking functional outcomes and satisfaction.

Keywords: Telemedicine; Telerehabilitatation; Virtual physiotherapy; Telephysiotherapy; Exercise; Health prevention

Citation: Amon M, Kresal F. Digital physiotherapy and COVID-19. Proceedings of Socratic Lectures. 2021; 6: 72-75. https://doi.org/10.55295/PSL.2021.D.010

Publisher's Note: UL ZF stays neutral with regard to jurisdictional claims in published maps and institutional affiliations.

1. Introduction

Modern hybrid approaches to a combination of face-to-face and remote meetings (telephone, home visits, telerehabilitation visits) have shown positive results in terms of functional capacity, depression and overload reduction (Oh-Park et al., 2021). The results of individuals after humerus fracture, complete knee arthroplasty and after heart attack were evaluated as positive in telemedicine rehabilitatation.

There is no direct evidence that physical activity can prevent or cure COVID-19, but promoting an active lifestyle is a key intervention to prevent health restrictions and the effects of social exclusion, especially in older adults and other at-risk individuals such as those living with chronic diseases. related to aging and lifestyle.

Since most COVID-19 patients are mostly associated with an associated disease, it is important that physical rehabilitation (physiotherapeutic kinesiotherapy) is performed by professionals such as physiotherapists (health workers).

2. Methods

The search strategy and the selection of the literature were carried out with the help of the PubMed, so that the MEDLINE database with the following combination of key-words was basically used: telemedicine; virtual reality; elderly; COVID-19. Although the search did not follow the guidelines of the systematic review article, the final database included articles younger than 10 years, telerehabilitation, which combined elements of the health impact of therapeutically oriented physical activity, and compared results across different physiological systems.

3. Results

3.1 Physical inactivity and muscle dysfunction

Indirect physical inactivity and its consequences, such as accumulation of adipose tissue and muscle dysfunction, can affect the flexibility of immunity. Given the recent emergence of COVID-19, future studies should examine whether physical activity is a protective factor to reduce the risk of complications caused by COVID-19 (Damiot et al., 2020).

3.2 Fragilty prevention

Fragility is a geriatric syndrome that affects several domains of an individual's functioning. Various problems contribute to the development of fragility syndrome. Impaired nutritional status is an important determinant of fragility. Recent evidence on the link between nutritional status and fragility syndrome in older adults confirms the importance of both quantitative (energy intake) and qualitative (nutritional quality) dietary factors in the development of fragility syndrome in older adults (Lorenzo-Lopez et al., 2017). However, further research is needed on this topic to elucidate the mechanism of the potential role of diet in preventing, postponing, or even reversing fragility syndrome.

3.3 Ageing control

The aging process may be accompanied by an increased risk of functional limitations, disability and social disabilities, social isolation and dependence on the help of others. Strengthening health status with increasing longevity is essential and also a decisive factor in maintaining an individual's independence.

It is desirable that future proposals for health measures will focus on solutions to strengthen the physical capacity of the population, including neurocognitive stimulation (Kara et al., 2020), which can provide an example of long-term physiotherapy support and intergenerational integration through rehabilitation offer to maintain physical fitness and active lifestyle.

3.4 Immune function control

Over the years, the immune system changes and this affects the acquired and innate response of the immune system. Infections, cancers, and autoimmune diseases are more common in older adults, and a number of factors are responsible for this phenomenon (Fuentes et al., 2017). Age-related changes and the weakening of the innate and acquired immune systems play the greatest role.

When the immune system is weakened, there are changes in the immune response (Dugan et al., 2020), which can be increased, weakened or uncontrolled and leads to poorer outcomes in bacterial and viral infections or vaccine response. Immune system involvement is also described as restructuring of the immune system due to oxidative stress and is the result of an imbalance between inflammatory and anti-inflammatory mechanisms t.i. age-related inflammation.

Stable health status of older adults is not only the result of inflammatory mechanisms, but also the effectiveness of the entire system acquired over a lifetime. Combined with hormonal changes, nutritional deficiencies, and physical inactivity, the condition can lead to fragility or sarcopenia. The state of the immune system may play a central role in regulating the mechanisms of aging and the occurrence of age-related diseases (Oh et al., 2019). The immune system is also associated with the state of the endocrine, digestive, renal, respiratory-cardiovascular and neuromuscular and skeletal systems.

4. Discussion

An effective immune system typically adapts to changes in the environment (Nicholson, 2016). Chen et al. (2021) emphasize the need for research monitoring of older adults after Covid-19 vaccination for future understanding of the pathogenesis of the disease and its consequences (long Covid) and the development of appropriate measures. Partial or full social distance across much of the world has been introduced to control Covid-19 transmission.

Social isolation can lead to a decline in physical activity, which could lead to immune system dysfunction, increasing susceptibility to infections and exacerbating the pathophysiology of diseases common among older adults or vulnerable groups, including cardiovascular disease, cancer, and inflammatory disorders.

Older adults and people living with different comorbidities are at higher risk for complications during Covid-19 (Damiot et al., 2020). On the other hand, the literature indisputably describes in detail the many benefits of physical activity during the period of growth and adolescence, as the movement has exceptional educational and developmental potential (Škof et al., 2016). Researchers report the negative impact of physical inactivity on immune function, and we are showing evidence that regular physical activity can be an effective strategy to prevent some of the detrimental effects of social exclusion. Moreover, there is consensus that the way to reduce the rate of contamination and spread of SARS-CoV-2 via human-to-human transmission is social distancing. However, the practice of moderate-intensity exercise at home is recommended. Low-to-moderate exerci-se-induced immunomodulation might be an important tool to improve immune responses against the progression of Covid-19 infection (Leandro et al., 2020).

Additionally, malnutrition is common in the elderly and is a burden responsible for negative health-related outcomes. Nutritional status, which includes nutrition and hydration control, has been largely ignored in routine clinical physiotherapy practice since normal times. Patients at high risk for adverse clinical outcomes of COVID-19 infection are at risk of malnutrition in older adults and multimorbid individuals (Barazzoni et al., 2020).

Attention to this critical aspect for the health of the elderly is dramatically ignored in the acute care units overwhelmed by the COVID-19 emergency today, despite evidence of how malnutrition negatively affects patients 'prognosis and recovery. In addition, sarcopenia is one of the most proven conditions for successful rehabilitation of the elderly. It is defined as a loss of muscle mass and strength that leads to impaired performance

(Cruz-Jentoft et al., 2014). Sarcopenia is closely associated with an impoverished diet and has been indicated as one of its clinical manifestations (Cederholm et al., 2019).

5. Conclusion

The biological benefits of regular physical activity are undeniable. Among the more interesting adaptive consequences of physical activity is the mechanism of exercise-induced immunomodulation, which can become a means of precautionary action as well as clinical treatment of COVID-19. The mechanism of exercise-induced immunomodulation has been known for more than 30 years and is presented in approximately 5,000 professional original and review articles available in Medline and the PubMed database. Exercise-induced immunomodulation depends on the interaction of external exercise factors such as exercise type, duration, and frequency of exercise. In the future, further studies of distance physical rehabilitation will be needed, especially in the elderly adult population.

Potential benefits of telerehabilitation in geriatrics represent improved accessibility of health services for adults with transport limitations; avoidable risks of communicable disease transmission (COVID-19 case), avoidable inconveniences, loss of time and transport costs. It is important to be aware of the disadvantages of telerehabilitation in geriatrics, which may relate to the requirement for a certain level of technological skill, the requirement for assistance to individuals with hearing, vision or cognitive impairments, the requirement for increased responsibility for reporting health and monitoring responses. Last but not least, the disadvantage of alternative remote access to health services in the form of telerehabilitation is also the absence of human contact and at the same time the patient's motivation at a distance can be limited.

Conflicts of Interest: The authors declare no conflict of interest.

References

1. Barazzoni R, Bischoff SC, Breda J, Wickramasinghe K, et al. ESPEN expert statements and practical guidance for nutritional management of individuals with SARS-CoV-2 infection. Clin Nutr. 2020; 39: 1631-1638. DOI: 10.1016/j.clnu.2020.03.022.
2. Cederholm T, Jensen GL, Correia M I T D, Gonzalez M C, et al. GLIM criteria for the diagnosis of malnutrition - A consensus report from the global clinical nutrition community. Clin Nutr. 2019; 38:1-9. DOI: 10.1016/j.clnu.2018.08.002
3. Chen C, Amelia A, Ashdown GW, Mueller I, et al. Risk surveillance and mitigation: autoantibodies as triggers and inhibitors of severe reactions to SARS-CoV-2 infection. Mol Med. 2021; 27:160. DOI: 10.1186/s10020-021-00422-z.
4. Cruz-Jentoft AJ, Bahat G, Bauer J, Boirie Y, et al. Sarcopenia: revised European consensus on definition and diagnosis. Age Ageing. 2019; 48: 16–31. DOI: 10.1093/ageing/afy169
5. Damiot A, Pinto AJ, Turner JE, Gualano B. Immunological Implications of Physical Inactivity among Older Adults during the COVID-19 Pandemic. Gerontology. 2020; 66:431-438. DOI: 10.1159/000509216
6. Dugan HL, Henry C, Wilson PC. Aging and influenza vaccine-induced immunity. Cell Immunol. 2020; 348:103998. DOI: 10.1016/j.cellimm.2019.103998
7. Fuentes E, Fuentes M, Alarcón M, Palomo I. Immune System Dysfunction in the Elderly.An Acad Bras Cienc. 2017; 89:285-299. DOI: 10.1590/0001-3765201720160487
8. Kara M, Özçakar L, Kaymak B, Ata AM, Frontera WJ. A "Neuromuscular Look" to sarcopenia: Is it a movement disorder? J Rehabil Med. 2020; 52: 52: jrm00042. https://doi.org/10.2340/16501977-2672
9. Leandro CG, Ferreira E Silva WT, Lima-Silva AE. Covid-19 and Exercise-Induced Immunomodulation. Neuroimmuno-modulation. 2020; 27:75-78. DOI: 10.1159/000508951
10. Lorenzo-López L, Maseda A , de Labra C, Regueiro-Folgueira L , Rodríguez-Villamil JL. Nutritional determinants of frailty in older adults: A systematic review BMC Geriatr. 2017; 17:108. DOI: 10.1186/s12877-017-0496-2.
11. Nicholson LB. The immune system. Essays Biochem. 2016; 60: 275-301. DOI: 10.1042/EBC20160017.
12. Oh SJ, Lee JK, Shin OS. Aging and the immune system: the impact of immunosenescence on viral infection, immunity and vaccine immunogenicity. Immune Netw. 2019; 19: e37. DOI: 10.4110/in.2019.19.e37
13. Oh-Park M, Lew HL., Raghaven P. Telerehabilitation for geriatrics. Phys Med Rehabil Clin N Am. 2021; 32: 291-305. DOI: 10.1016/j.pmr.2021.01.003
14. Škof B, Bačanac L, Bratina N, Stepančič D, et al. Šport po meri otrok in mladostnikov : pedagoški, didaktični, psiho-socialni, biološki in zdravstveni vidiki športne vadbe mladih. Ljubljana: Fakulteta za šport, Inštitut za kineziologijo, 2016.

Scientific contribution/Original research

Air Pollution of Particulate Matter and its Effect on Red Blood Cell Membranes

Orel M[1], Berglez K[1], Skube U[2], Bele M[3], Božič D[1,4] Kroflič A[2,*], Jeran M[1,4,*]

1. University of Ljubljana, Faculty of Health Sciences, Laboratory Clinical Biophysics, Ljubljana, Slovenia
2. National Institute of Chemistry, Department of Analytical Chemistry, Ljubljana, Slovenia
3. National Institute of Chemistry, Department of Materials Chemistry, Ljubljana, Slovenia
4. University of Ljubljana, Faculty of Electrical Engineering, Laboratory of Physics, Ljubljana, Slovenia

* Correspondence: Marko Jeran; marko.jeran@fe.uni-lj.si & Ana Kroflič; ana.kroflic@ki.si

Abstract: Particulate matter (PM) is classified as one of the most dangerous air pollutants which cause numerous adverse health effects. Prolonged exposure to high PM concentrations can lead to serious health complications and severe chronic conditions. Our research work is focused on the concentration of PM particles in ambient air. We studied how the concentration changes with different seasons (summer and autumn). The results of our experimental work show that the concentration of PM in the air increased during the colder period of the year. In autumn, the average daily mass concentration was determined at 0.85 μg/m^3, which means it was over the daily limit set by the WHO. These results indicate that the level of air pollution has a detrimental impact on human health in Ljubljana, the capital city of Slovenia. Due to strong impacts of PM particles on our body, we further studied the impact of PM_{10} particles on human blood erythrocytes, with the aim of interdisciplinary synthesis of knowledge from the scientific fields like environmental protection and medicine. The results of *in vitro* studies show that a prolonged exposure to increasing concentration of PM_{10} particles causes a decrease in erythrocyte population. We also observed changes in membrane shapes when erythrocytes were exposed to PM particles for a longer time. We also observed the transition from echinocyte to stomatocyte cell shape with help of a scanning electron microscope (SEM). The results of this research can be used as a basis for more extensive research on the systemic impact of inhaled PM particles on the human body.

Keywords: PM particles, air pollution, cell response, erythrocytes, erythrocyte membranes, medicine

Citation: Orel M, Berglez K, Skube U, Bele M, Božič D, Kroflič A, Jeran M. Air Pollution of Particulate Matter (PM) and its Effect on Red Blood Cell Membranes. Proceedings of Socratic Lectures. 2021; 6: 77-86. https://doi.org/10.55295/PSL.2021.D.011

1. Introduction

1.1. Particulate matter (PM)

Particulate matter or PM is a mixture of solid particles and liquid droplets that can be found floating in the Earth's atmosphere. PM particles are one of the main air pollutants and are divided into different groups according to their size. The most common and the most dangerous are particles named $PM_{2.5}$ and PM_{10}. The numbers next to the abbreviation indicate the largest aerodynamic diameter of the particles in a particular group (Lesjak, 2016). PM groups are composed mainly of inorganic ions, but they can also contain organic and inorganic carbon and traces of toxic metals (Siwek et al., 2016). Carbon represents a high percentage of atmospheric particles, especially in urban areas. It occurs in various forms, which can be broadly divided into three groups: organic carbon, elemental or black carbon and carbonates (CO_3^{2-}). Carbon in all his forms plays and important role in terms of its impact on health, chemical processes in the atmosphere, visibility, and effects on climate change (Siwek et al., 2016).

1.2. Main sources of pollution

PM can originate both from natural and anthropogenic sources. Natural sources of air pollution with PM particles include desert dust, volcanic eruptions, forest fires and marine aerosols, while anthropogenic sources include combustion emissions of fuels in thermal power stations, industrial emissions, emissions from heating and traffic (Bilban, 2014). The largest anthropogenic sources of PM particles are household combustion and emissions of the service sector. The woody biomass is the largest source of organic particles in atmospheric aerosol, which makes the use of small combustion facilities particularly problematic. In addition to heating, traffic is also one of the biggest producers of particulate emissions in urban areas. The situation gets even more severe during the winter time, when the phenomenon of temperature inversion restricts the passage of polluted air into the higher layers of the atmosphere and causes the highest level of air pollution (Agencija Republike Slovenije za okolje, 2019).

1.3. Effects of PM particles on human health

Ambient air pollution is the major cause of premature death in Europe. Moreover, PM pollution importantly increases the risk for the development of cardiovascular and respiratory diseases, and lung cancer. Exposure to polluted air can cause reduced lung function, respiratory infections or asthma in children and adults, while the exposure of pregnant women to particulate emissions can affect fertility, the course of pregnancy, and the development of foetus itself. The results of various studies have shown that polluted air can affect the progression of type 2 diabetes, it can as well cause obesity, premature aging, and onset of Alzheimer's disease and dementia (European Environment Agency, 2019).

As $PM_{2.5}$ particles are much smaller in diameter than PM_{10} particles, when inhaled, it is easier for them to penetrate deep into the body all the way to pulmonary alveoli. After absorption into the bloodstream, they cause narrowing of the blood vessels and formation of cloths, which can lead to heart failure or hearth attack. Some of the studies have shown that $PM_{2.5}$ particles reduce cognitive abilities due to faster brain aging and disruption of communication between different parts of the brain (European Environment Agency, 2019).

1.4. Interaction with biological material

The effects of PM particles on human health depend on the size and shape of the particles, as well as their chemical composition. The most common way of entering the body is through the airways of respiratory tract, from where the smallest particles can reach just about any part of the lungs. After they enter the lungs and interact with lung

cells, the metal part of the particles oxidizes, which causes damage to the DNA structures and increases the risk of developing cancer and respiratory diseases, like bronchitis (European Environment Agency, 2019). Studies have shown that exposure to nanoparticles raises the risk of pulmonary inflammation, which can be later transmitted to other organs (liver, heart, spleen, and brain) through the circulatory system (Bilban, 2019). Some pathophysiological changes associated with cardiovascular diseases, like changes in heart rate, high blood pressure, and arrhythmia, were also observed. It was proven that if we increase the concentration of 250 nm particles for 10 μg/m^3, there will be an 8–18% increase in mortality from malignant cardiac rhythm disturbances or cardiac arrest (Bilban, 2019).

1.5. Cell membrane

The cell membrane, also called the plasma membrane, is one of the main parts of any cell. Its main task is to protect the cell and regulate the transport of materials entering and exiting the cell. It consists of phospholipid bilayer which provides elasticity and fluidity of the cell. The amphiphilic character of phospholipid molecules allows membrane lipids to build a stabile bilayer in an aquatic environment (Pečavar Nežmah, 2018). In addition to phospholipids, the membrane also contains lipids, which belong to the group of glycolipids and cholesterols. Glycolipids are located on the outer part of the membrane – to protect the cell, while cholesterols are important primarily because they increase impermeability of the membrane to certain substances, reduce the fluidity of the outer membrane when temperature is high and prevent the membrane from freezing or decreasing its fluidity when temperature is low (Pajnič, 2019). Apart from lipids, there are also membrane proteins which are an important building blocks of every cell membrane. The proteins bind with sugar to form glycoproteins, which are responsible for maintaining or changing the shape and structure of a cell, they impact intercellular communication and active/passive transport. They also act like receptors for hormones and other molecules (Pajnič, 2019).

1.6. Blood and its components

Blood is a fluid that is constantly circulating through our body and delivers essential substances like oxygen and nutrients to body's cells. It is made up of blood serum (blood plasma and fibrinogen) and blood cells. We know three different forms of blood cells: red blood cells (erythrocytes), white blood cells (leukocytes) and platelets (Hoffman, 2014). Red blood cells carry oxygen to all cells in the body. White blood cells play an important role in defending the body against infections and building resistance with help of antibodies. Platelets and other clotting factors help form clots to stop bleeding (Blood Transfusion Centre of Slovenia, 2021).

1.7. Red blood cells or erythrocytes

Red blood cells or erythrocytes are the cells that supply our body with oxygen. The size range of those flattened cells is between 7 and 8 μm (American Society of Haematology, 2021). Almost 1/3 of cell's volume represents haemoglobin, a protein which is crucial for the transport of respiratory gases (Orel and Berglez, 2021). Special properties of erythrocyte membranes are reflected in the shape of the whole cell, as erythrocytes do not have an internal cytoskeleton to determine their shape (Lim et al., 2002). Instead, red blood cells have a protein network attached to the inside of the cell membrane, known as the membrane skeleton. Since the skeleton fits everywhere on the phospholipid bilayer, it can be considered as the third membrane layer. Both, phospholipid bilayer and cytoskeleton contribute to membrane elasticity and fluidity that affect deformation of erythrocytes in a bloodstream; the cells easily adapt to changed conditions in the surrounding solution because of the small elastic modulus of their membrane (Lim et al., 2002). Although the diameter of erythrocytes is larger than the diameter of capillaries in the microcirculatory system (Lim et al., 2002), sufficient elasticity and appropriate osmotic

balance still allow them to pass smoothly through the capillary system. The elastic structure, which allows erythrocytes to optimally adapt to the narrow capillaries, is their key feature. It is important that the erythrocyte cell has enough of its membrane available (this is determined by the osmotic balance); if the membrane is overstretched, it easily ruptures under excessive load, which causes haemolysis (Mohandas et al., 2008).

2. Methods

During our research, we used several different research methods. One of them was microscopy – we used both inverted light microscope for observing cells in an aqueous medium and scanning electron microscope (SEM) to observe the surface of solid samples under a beam of electrons. Using this technique, we determined morphology and elemental composition of the studied samples.

For our further research, we used a Particulate Matter (PMx) Sampler, an instrument that allows us to measure mass concentration of PM particles in the air. Using a special filter it collects a particular fraction of particles from the outdoor air, which is later weighed and translated into mass concentration.

We also used a scanning mobility particle sizer (SPMS) spectrometer, a measuring device that measures the size of nanoparticles in the atmosphere in real time.

In the end we used the technique of flow cytometry to measure and analyse properties of individual cells.

2.1. Particle measurement

Samples were collected in the premises of the National Institute of Chemistry in Ljubljana and the composition of air was monitored every day from 9th August 2020 to 15th August 2020 and from 22nd November 2020 to 28th November 2020. Each filter was weighed separately before and after the sampling, to accurately determine the difference in mass. By doing this, we determined the mass of collected PM particles during the 24 hours of exposure. Prior to use, the filters were pre-baked at 450 °C for 4 hours to remove potential organic contaminants.

We weighted the filters in a special air-conditioned room, where the working conditions are constantly monitored (20 °C, 45% RH). We used a scale that was specifically designed to weigh filters. We considered the average filter mass and all potential errors that could occur.

The weighed filters were then placed into a tube, which was inserted into the PM sampler, and we set a sampling programme. Each filter was sampled for 24 hours at an air flow of 2.3 m^3/h. At the end of the sampling procedure, the filters were removed from the sampler and weighed again according to the procedure mentioned above.

In parallel with the PM sampling, we draw the outdoor air into an SMPS Spectrometer, where it was analysed for PM size distribution. In the end, we used SEM to show the binding of PM particles to the filter fibres.

2.1. Scanning electron microscopy (SEM)

SEM imaging of ambient PM deposited on a quartz fiber filter was carried out using a Zeiss Supra 35 VP (Carl Zeiss, Oberkochen, Germany) microscope. The operating voltage was at 1 kV.

2.2. Light microscopy

Blood samples, PM_{10} particle suspensions, and their mixtures were examined with a Nikon EM CCD inverted light microscope (Eclipse TE2000-S, Tokyo, Japan; coupled with a digital camera system: spot boost, Visitron Systems) at 100× magnification using an immersion oil. 200 μL Of diluted blood, particle suspension, or a mixture of PM_{10} particles with blood were pipetted into experimental perfusion chambers (26 mm × 43 mm, CoverWell™, PC4L-0.5, Grace Bio-Labs) for efficient analysis and analytical image acquisition under the microscope.

2.3. Effect of PM particles on erythrocyte membranes

We used a certified reference material, fine dust called ERM–CZ100 PM_{10}-like as a surrogate for ambient PM_{10} particles. For the treatment, we prepared its 50, 100 and 200 µg/mL suspensions in sterile conditions (laminar flow) with use of sterile deionized water. For this purpose, we used a stock suspension of PM_{10} particles with a concentration of 20 mg/mL, which was then added to the working solution of blood or the working buffer solution in appropriately low doses.

To nicely observe the distribution of particles under the microscope, we used samples with approximately 1.0×10^6 cells (events)/µL in their erythrocyte region. On the basis of previous experience, we pipetted 50.0 µL of freshly drawn blood from an adult male into 20.0 mL of phosphate-citrate buffer, the mixture was homogenised, and the cell concentration was confirmed under the microscope.

Before treatment and after 1, 8, and 24 hours, the prepared samples were quantitatively evaluated by flow cytometry to determine the concentration of erythrocytes. After 1 hour of treatment, control samples were first analysed and detection regions were determined: PM particle population, erythrocyte region, and spherocyte region (**Figure 1**).

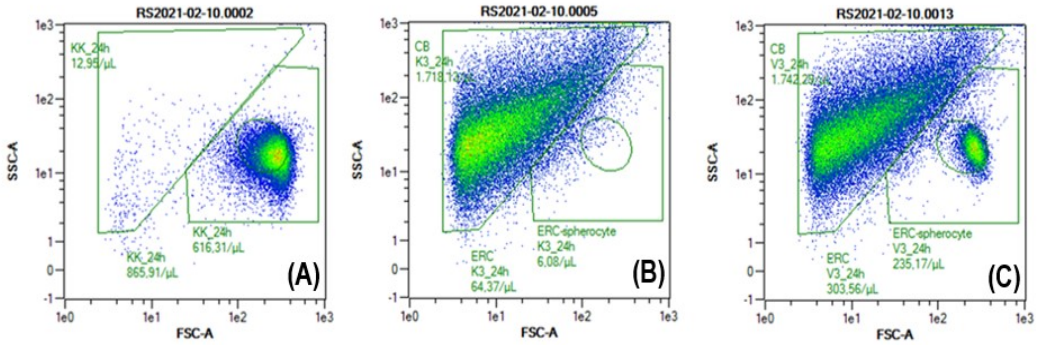

Figure 1. Example of scatter plots after 24 hours: (**A**) diluted blood, (**B**) PM_{10} particles with a concentration of 200 µg/mL, and (**C**) a treated blood sample with a PM_{10} particles concentration of 200 µg/mL. The triangular shape of the region in the upper left corner represents the scattering region of PM_{10} particles. The region resembling the shape of a rectangle covers the erythrocyte (ERC) region and the region in the central part (circle, ERC-spherocyte) covers the spherocyte forms of the erythrocytes.

3. Results

3.1. Results of air sampling with PM particle sampler

Figure 2 shows mass concentrations of PM particles in summer and autumn 2020. The green straight line represents the maximum permissible mass concentration of PM particles in ambient air as defined by WHO, which is not yet considered dangerous to human health. Measurements show that mass concentrations of particles are mostly lower in summer than in autumn. We can attribute this to domestic heating and increased traffic emissions during the transition to the colder part of the year. Still, summer results are expected to be influenced by the local $PM_{2.5}$ emissions as a consequence of a laboratory cleaning after a fire.

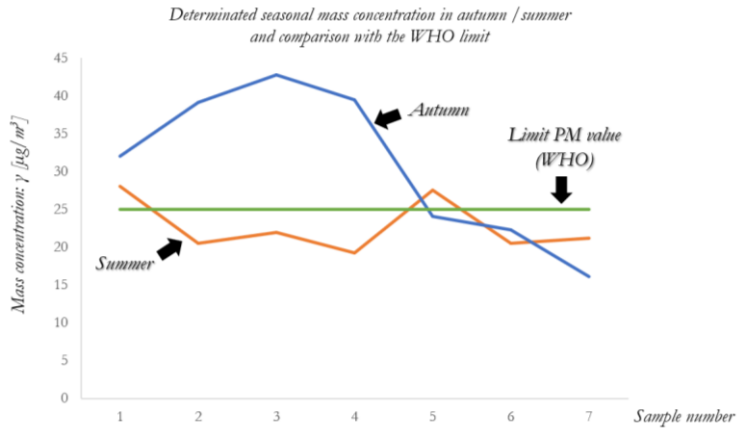

Figure 2. The mass concentration of PM particles in summer and autumn.

Figure 3 shows a SEM image of PM particles collected on a quartz fiber filter in autumn 2020. The fibers in the image represent the filter. A large soot aggregate (white arrow) can be seen in the center of the image. Smaller accumulations of other PM particles (red arrows) can be also seen all around the sample.

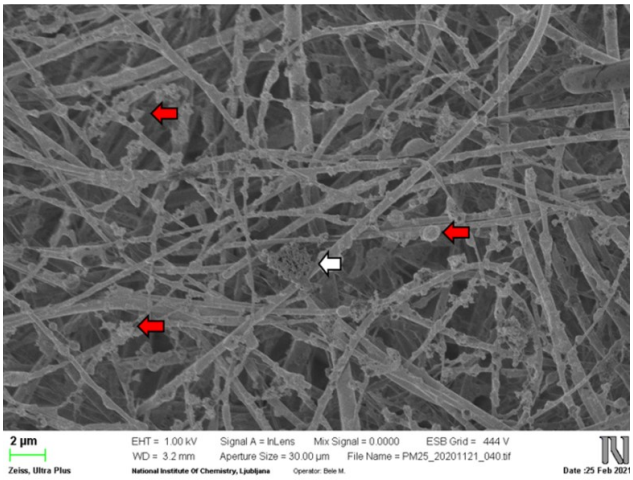

Figure 3. SEM image of a sample collected in autumn 2020.

3.2. Results of erytrhrocyte population measurements (flow cytometry)

Figure 4 shows variation over time of the population (cell number) in the negative control (blood) and the samples treated with PM_{10} particles (c = 50, 100 and 200 µg/mL). After 24-hours exposure and at the highest concentration, the highest impact on of the erythrocyte particles is detected. On the other hand, the lowest impact on erythrocytes is observed at the lowest concentration of PM particles after only one hour of exposure. in general we found out that the number of erythrocytes in the samples decreases with increasing particle concentration and longer exposure to the particles.

The variations in the spherocyte population after 1 and 8 hours of exposure in 50 and 100 µg/mL samples corresponds to the trend of the control sample and cannot be attributed to the treatment. The change in spherocyte population is most pronounced after 24 hours. Variations of the population are mostly proportional to the basic erythrocyte region.

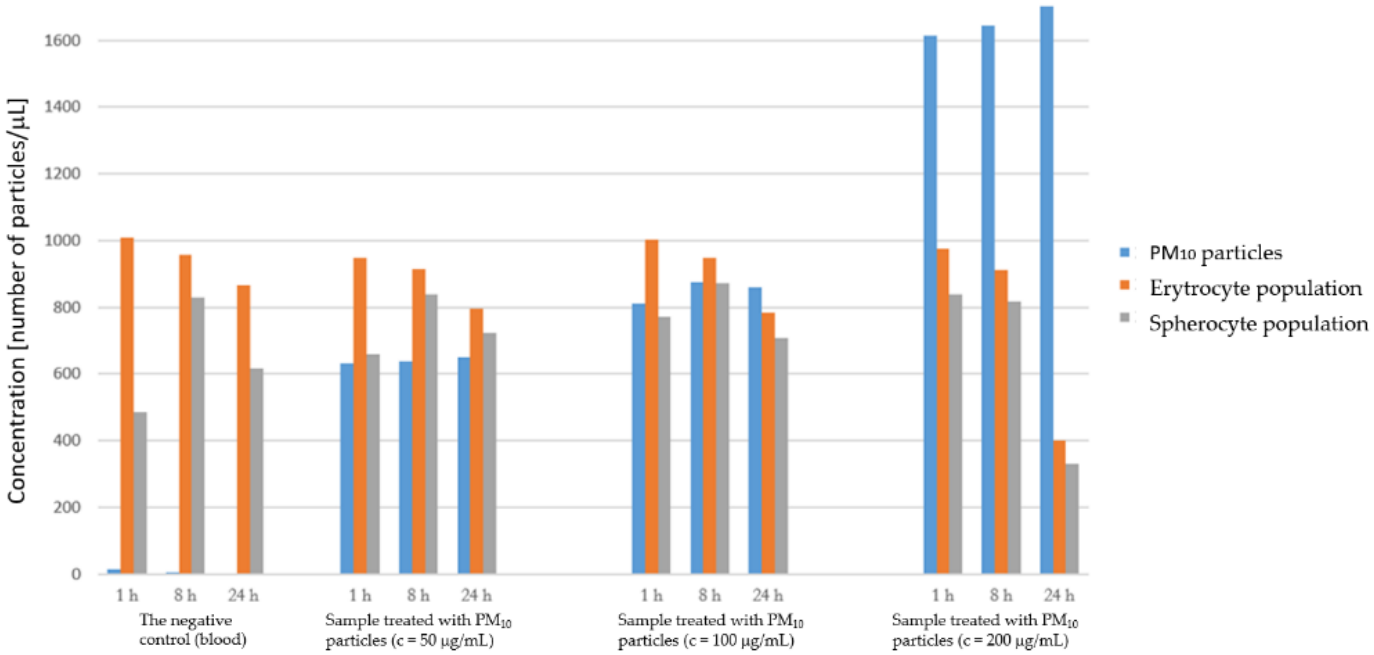

Figure 4. PM particle impact on erytrocyte and spherocyte population in samples (flow cytometry).

3.3. Results of cell microscopy (inverted light microscope)

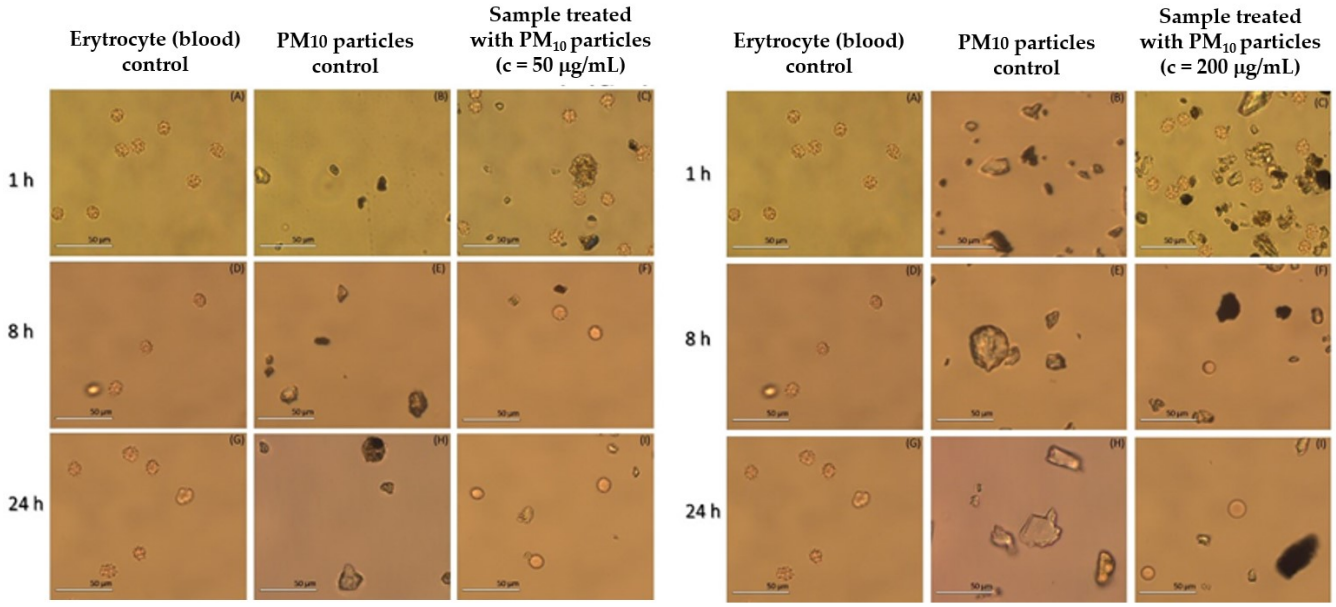

Figure 5. The comparison of the sample with the lowest and the highest concentration of PM particles.

Figure 5 shows the comparison of the samples with the lowest and the highest concentration of PM particles. In both cases, there is only an echinocyte form observed at the beginning of the treatment. However, after several hours of exposure, erythrocytes are transformed from the echinocyte to a stomatocyte form. At higher concentrations of PM particles, this change in shape is observed much earlier. Moreover, it can also be seen that after 24 hours of exposure the membranes in the sample with the highest concentration become very stretched, nearly rupturing.

After the 24-hour exposure of erythrocytes to PM_{10} particles, at a concentration of 200 µg/mL we detected extracellular vesicles on the erythrocyte membrane. Extracellular vesicles are membrane-enclosed fragments of a cell membrane that are released by all types of cells into their environment, both in vitro and in vivo. In medicine, vesicles are considered as biomarkers of various diseases.

The presence of PM_{10} particle was probably perceived by erythrocyte cells as a foreign body, which consequently triggered the synthesis of vesicles. The reason for the formation of extracellular vesicles presumably depends on the damage added particles caused on the erythrocyte membrane, causing smaller fragments to be released into the surrounding solution, which resulted in the appearance of vesicles.

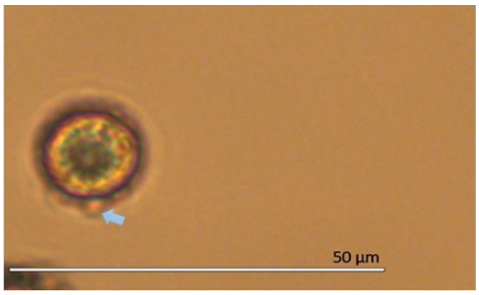

Figure 6. Example of the extracellular vesicle on the erythrocyte membrane.

4. Discussion

4.1. Concentrations of PM particles in the air

The purpose of our research was to determine when the concentration of PM particles in the atmosphere is the highest and consequently which period of the year is most harmful to human health. Ambient PM concentration was measured at the same monitoring station during different seasons. The average mass concentration of PM particles was 22.71 µg/m^3 in summer and 30.85 µg/m^3 in autumn. From the results we gathered, we can conclude that in autumn the concentration of PM particles is higher than that in summer, which is the consequence of household heating and increased traffic emissions in autumn months. One of the largest anthropogenic sources of PM particles in Slovenia are household combustion and emissions of the service sector. The use of small combustion installations, which use wood biomass as a fuel, is particularly problematic and is very common in not so cold autumn days. In addition to heating, traffic and road dust resuspension make a significant contribution to particulate emissions, especially in Ljubljana, where traffic density is the highest in the country. Another reason for higher levels of air pollution is also the phenomenon of temperature inversion, which is especially characteristic for Ljubljana basin. During the summer, the concentration of PM particles in the air was significantly lower, which makes sense since there is no household heating and no temperature inversion in the lowlands. The PM particles in the air originated from traffic emissions, as the PM sampler was placed in the area where traffic is relatively dense. Besides, the obtained results were likely influenced by the already mentioned local origin of $PM_{2.5}$ particles from cleaning of a laboratory after a fire.

A detailed examination of particle sizes showed that smaller particles were more numerous, while bigger particles represented a bigger mass (data not shown). Smaller particles are more dangerous to human health, since they can penetrate deeper into the body through the airways of respiratory tract. Nanoparticles that penetrate all the way to the end of the airways are retained in the alveoli, and their accumulation can consequently lead to a decrease in lung capacity. One of the things we must not forget is that PM particles are soluble in water, which allows water-soluble substances to be transported in the body after the absorption in lung cells, and some of them can be harmful to human health (for example PAHs, which are considered toxic and carcinogenic).

The average daily mass concentration of $PM_{2.5}$ particles only exceeded the daily limit set by WHO in the autumn, so we can conclude that human health is more endangered in colder months of the year. On the other hand, all the measurements exceeded the annual recommended concentration set by WHO, which is at 10 μg/mL.

4.2. Effects of PM particles in erythrocite membranes

The main goal of our research was to study the influence of PM_{10} particles on membranes of erythrocytes in human blood. Erythrocytes were exposed to three different concentrations of PM_{10} particles (50, 100 and μg/mL) and later analysed at 3 different intervals (after, 1h, 8h and 24h). The aim was to determine which of the concentrations will cause the greatest impact on erythrocyte membranes and consequently on their population in the sample suspension. We found out that PM_{10} particles form agglomerates in PBS buffer, which later interact with erythrocytes. Using an inverted microscope, we observed that if the agglomerate adheres to the membrane on a large part of its surface, erythrocyte damage can occur. Changes in erythrocyte membranes were observed at all three concentrations. After a few hours of exposure, erythrocytes changed from echinocyte to stomatocyte form. The difference is most noticeable in the sample of erythrocytes which was exposed to particles with a concentration of 200 μg/mL, where the change in membrane shape and agglomerate formation is observed after only 1 hour of exposure. The formation of extracellular vesicles, the biomarkers of different diseases, was also observed in the sample of erythrocytes with a particle concentration of 200 μg/mL.

We can conclude that the biggest concentration of PM_{10} particle is the one that has the most pronounced negative effects on erythrocytes. However, the results of flow cytometry show that after a certain time of exposure to PM particles, there is a decrease in erythrocyte population independent on the particle concentration. Moreover, membrane ruptures are also more common when the concentration of particles is the highest. If we compare the effects of PM particles with the effect of black carbon nanoparticles on blood cells, we can conclude that erythrocytes change their shape in both cases after a few hours of exposure. However, when exposed to black carbon nanomaterial, erythrocytes coalesced into bigger agglomerates, whereas no obvious sticking occurred in our case. The reason probably lies in different reaction surfaces of the materials, in particle sizes and chemical nature.

Funding: This research was supported by European Union's Horizon 2020 research and innovation program under grant agreement No 801338 (Ves4Us), and by Slovenian Research Agency through the core foundlings No P3-0388, P1-0034, and projects No L3-2621 and J1-1707.

Institutional Review Board Statement: The study was conducted according to the guidelines of the Declaration of Helsinki, blood was donated voluntarily by the authors of the study.

Conflicts of Interest: The authors declare no conflict of interest.

References

1. Agencija Republike Slovenije za okolje (2009), Meritve Delcev PM10 na merilnem mestu Hrastnik. Updated 2009. Accessed 26. 02.2020. Avaliable from https://www.arso.gov.si/zrak/kakovost%20zraka/poro%C4%8Dila%20in%20publikacije/PM10_Hrastnik.pdf
2. Agencija Republike Slovenije za okolje (2019), Kakovost zraka v Sloveniji v letu 2018. Updated 2019. Accessed 26.02.2020. Avaliable from http://www.arso.gov.si/zrak/kakovost%20zraka/poro%C4%8Dila%20in%20publikacije/Letno_Porocilo_2018.pdf
3. American Society of Hematology (2021), Blood Basics. Updated 2021. Accessed 2.1.2021. Avaliable from https://www.hematology.org/education/patients/blood-basics?
4. Bilban M. Nanodelci. Delo in varnost. 2013; 58(4): 42-54. Available from https://www.dlib.si/stream/URN:NBN:SI:DOC-71DEG451/ca2a936a-ba21-4d21-8cfd-c39f6921704e/PDF
5. Bilban M. Onesnaževala zraka. Delo in varnost. 2014; 59(4): 16-19. Available from http://www.dlib.si/stream/URN:NBN:SI:DOC-JZ9QA2GF/b9d39915-55c9-40c1-9f75-3a3ea6c5412f/PDF
6. Blood Transfusion Centre Slovenia (2021), Kri in krvne skupine. Accessed 03.01.2021. Available from http://www.ztm.si/krvodajalstvo/kri-in-krvne-skupine/

7. Carrington D. Air pollution nanoparticles linked to brain cancer for first time. The Guardian. Updated 2019. Accessed 22.02.2021. Avaliable from https://www.theguardian.com/environment/2019/nov/13/air-pollution-particles-linked-to-brain-cancer-in-new-research
8. Carrington D. Air pollution particles in young brains linked to Alzheimer's damage. The Guardian. Updated 2020. Accessed 22.02.2021. Avaliable from https://www.theguardian.com/environment/2020/oct/06/air-pollution-particles-in-young-brains-linked-to-alzheimers-damage
9. European Environment Agency (2019), Air Quality in Europe - 2019 Report. ISSN: 1977-8449. Available from https://www.eea.europa.eu/publications/air-quality-in-europe-2019
10. Hoffman M. Picture of Blood. WebMD. Published 2014. Dostopno 02.01.2021. Available from https://www.webmd.com/heart/anatomy-picture-of-blood
11. Lesjak T. Ognjemeti in njihov vpliv na prisotnost trdnih delcev v zraku. Bachelor Degree (University of Ljubljana, Faculty of Chemistry and Chemicl Technology, Slovenia). Updated 2016. Accessed 05.02.2021. Available from http://fundacija-avgustakuharja.si/wp-content/uploads/2020/10/2016-diploma-Tadej-Lesjak.pdf
12. Lim HWG, Wortis M, Mukhopadhyay R. Stomatocyte–discocyte–echinocyte sequence of the human red blood cell: Evidence for the bilayer–couple hypothesis from membrane mechanics. PNAS. 2002; 99: 16766–16769. DOI: https://doi.org/10.1073/pnas.202617299
13. Ministry for the Environment (2009), Good Practice Guide for Air Quality Monitoring and Data Management 2009. Updated 2009. Accessed 16. 12. 2020. Available from: https://environment.govt.nz/publications/good-practice-guide-for-air-quality-monitoring-and-data-management-2009/
14. Mohandas N, Gallangher PG. Red cell membrane: past, present, and future. Blood. 2008; 112(10): 3939–3948. DOI: 10.1182/blood-2008-07-161166
15. Pečavar Nežmah P. Priprava vodotopne fluorescenčne učinkovine za označevanje normalnih in rakavih celic urotelija sečnega mehurja in vitro (Engl. Synthesis of a water-soluble fluorescent dye for labelling normal and cancerous urothelial cells of the urinary bladder in vitro). Research work. University of Ljubljana, Slovenia. 2018.
16. Pajnič M .Vpliv nanomateriala črnega ogljika na membrane krvnih celic (Engl. Effect of carbon black nanomaterial on blood cell membranes). Doctoral Dissertation (University of Ljubljana, Biotechnical Faculty, Slovenia). Updated 2019. Accesed 18.02.2020. Avaliable from https://repozitorij.uni-lj.si/IzpisGradiva.php?id=112665&lang=slv&prip=dkum:8729640:d3
17. Orel M, Berglez K. Onesnaževanje zraka z lebdečimi (PM) delci ter proučevanje njihovega vpliva na membrane celic (Engl. Air pollution with particulate matter (PM) particles and the study of their impact on cell membranes). Research work. University of Ljubljana (Slovenia), and National Institute of Chemistry, Ljubljana (Slovenia). 2018.
18. Siwek K, Osowski S. Data mining methods for prediction of air pollution. Int J Math Comput Sci. 2016; 26(2): 467-478. DOI: 10.1515/amcs-2016-0033
19. World Health Organization (2018). Ambient (outdoor) air pollution. Updated 2018. Accessed 20.02.2021. Avaliable from https://www.who.int/news-room/fact-sheets/detail/ambient-(outdoor)-air-quality-and-health

Scientific contribution/Review

An Insight into Special Purpose Acquisition Companies Within the United States' Healthcare Sector in 2021

Smerkolj N[1], Jeran M[2,3,*]

1. University of Ljubljana, School of Economics and Business, Slovenia
2. University of Ljubljana, Faculty of Health Sciences, Laboratory of Clinical Biophysics, Slovenia
3. University of Ljubljana, Faculty of Electrical Engineering, Laboratory of Physics, Slovenia

* Correspondence: Marko Jeran; marko.jeran@fe.uni-lj.si

Abstract: Special purpose acquisition companies (SPAC) have become an increasingly popular way for private companies to go public due to their flexibility and ease in regulatory procedures. SPAC is in essence a blank check company with no business operations and assets (apart from cash and cash equivalents after the initial public offering (IPO)) that is formed with a purpose of acquiring a certain private company or companies. SPAC's initial public offering proceeds in the United States in 2021 have surpassed those of 2020 and have just passed 160 billion dollars. Merger
activity of SPACs and target companies has been especially intense in sectors of technology and healthcare. This scientific contribution analyzes IPO proceedings and total enterprise values (TEV) data for SPACs in the healthcare sector in the US and portrays a comparison with the technology sector.

Keywords: Special purpose acquisition company, initial public offering, merger, healthcare sector

Citation: Smerkolj N, Jeran M. An insight into special purpose acquisition companies within the United States' healthcare sector in 2021. Proceedings of Socratic Lectures. 2021; 6: 88-92. https://doi.org/10.55295/PSL.2021.D.012

1. Introduction and theoretic overview

Special purpose acquisition companies (SPAC) have become a popular and preferred vehicle for taking private companies public with 83.4 billion dollars raised in 2020 and 151.6 billion dollars raised in the first nine months of 2021 in the United States (SPAC Research Database, 2021). Sectors of technology and healthcare accounted for almost 80 % of all initial public offering proceedings (IPOs) in the United States in 2020, thus it is to no surprise that 60 % of completed SPAC mergers in 2020 were in information technology, healthcare and consumer discretionary sectors (The Goldman Sachs Group, Inc., 2021). European initial public offerings of SPACs are substantially lower than those overseas with only four IPOs (compared to 248 in the US) and 496 million dollars raised in 2020 (Heredia et al., 2021). European SPACs deals have shown rapid growth in 2021, however, the importance of SPACs in Europe remains lower than that in the United States.

Special purpose acquisition company is a publicly-traded blank-check company without any business activity – its main goal is to raise capital through an IPO for a future acquisition[1] of an operating private company (Hale, 2006). A so-called sponsor creates a SPAC, which is taken public by underwriters (investment banks) – during the phase of an initial public offering, a SPAC sells units made of a common share and a fraction warrant for a fixed price of 10 dollars. Important aspects of SPACs are two rights that are bound to each common share purchased by investors – the right to redeem and the right to vote. The first right allows investors to redeem their shares and gather 10 dollars for each share plus the accrued interest if they don't want to participate in the merger with a selected private company, and the second right allows investors to vote on the merger with a proposed private company (The Goldman Sachs Group Inc., 2021). Another peculiarity of SPACs is the previously mentioned warrant, which gives an investor a right to purchase a fraction of a common share at an exercise price of 11.50 dollars per share. SPAC can use the received capital from IPO only to acquire a targeted company, to contribute to the capital of a newly formed company via merger, to repay investors if SPAC doesn't complete a merger or to fulfil investors' right to redeem (Klausner et al., 2020). SPAC has two years to complete an acquisition or merger, otherwise, it has to repay the initial investment to the investors (Jenkinson et al., 2011). Once the initial public offering phase has been completed, the management team of SPAC starts searching for a target company. In many instances, the target company is not known in advance, which increases the risk associated with investment during the IPO phase. Sponsor and target company agree to a letter of intent and new investors are brought in with the so-called PIPE (private investment in public equity) phase (Klausner et al., 2020). Shareholders vote on a potential merger and if a merger is approved, SPAC becomes an operating company and will usually change its name and ticker.

Special purpose acquisition companies as a vehicle of taking private companies public aren't a new thing, they have been present since the nineties. Last year, SPACs have seen a huge surge both in the number of IPOs (a 320% increase compared to 2019) and in total proceeds (a 513 % increase compared to 2019). Analysts predict that this surge partially corresponds to the disruption caused by COVID-19. When many companies were faced with the problem of irregular cash flows, public companies had easier access to debt and equity markets (The Goldman Sachs Group Inc., 2021). Additionally, investors seeking investments in businesses with higher growth potential turned to early-stage businesses (in industries such as nanotechnology, green technology and gambling) that used SPACs as their way to the public market. **Figure 1** shows the number of initial public offerings of SPACs and yearly accumulative proceedings in the United States.

[1] Although the name suggests the acquisition of a company it is often merely a merger of SPAC and target company. This issue and the problem of dilution of ownership is discussed and analyzed in-depth by Klausner and Ohlrogge (2020). In this article, we will take acquisition and merger as being synonymous, although there are important theoretic differences.

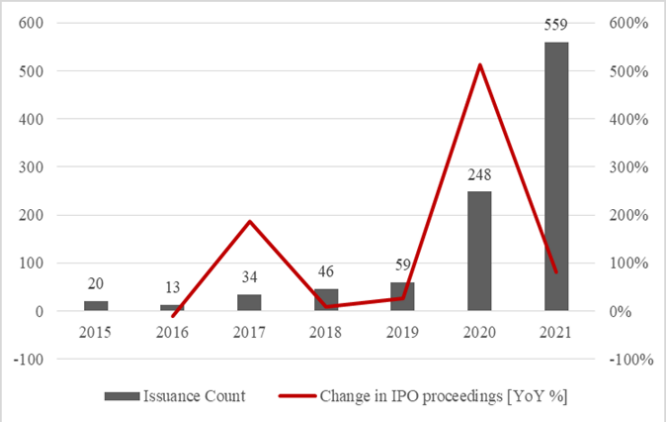

Figure 1. Special purpose acquisition companies' (SPACs) initial public offerings (IPOs) in the United States. The left vertical axis shows the total number of IPOs of SPACs in a given year (labelled issuance count), the right vertical axis shows the percentage change in IPO proceedings in billions of USD in a given year. The authors' calculation is based on historical data available at the SPAC Insider Statistics database.

2. Methods

Quantitative data has been gathered from publicly available databases (such as SPAC Research and SPAC Insider) that consolidate information from companies' legally binding reports and filings to the Securities and Exchange Commission (SEC). Information gathered include but are not limited to a number of SPACs' IPOs, IPO proceedings (individual and total), the value of merger transactions (individual and total) and total enterprise value after the merger (individual and total). Authors have used various tools for quantitative analysis and descriptive statistics, which can be seen in **Table 1**. Table and graphs were generated in a Microsoft Excel environment.

Table 1. Descriptive stastistics data on SPACs in the healthcare sector in the US (Jan-Nov 2021). The authors' calculation is based on data available at the SPAC Insider Statistics database.

	Pre-mergers; IPO proceeds (M$)	Active mergers; total enterprise value (M$)	Completed mergers; total enterprise value (M$)
Mean	208.9	2899.7	1752.5
Standard error	16.8	1869.6	400.4
Median	200.0	660.0	1084.5
Mode	230.0	no mode	184.0
Standard deviation	126.6	7708.6	2532.1
Range	805.0	32472.0	15080.0
Minimum	57.5	128.0	84.0
Maximum	862.5	32600.0	15164.0
Count	57	17	40

3. Results and Discussion

As previously mentioned, 60% of completed SPAC mergers in the United States in 2020 were in sectors of information technology, healthcare and consumer discretionary. In the following paragraph, we focus on the developments of SPAC activity within the healthcare sector and present statistics on closed mergers, active merger transactions and completed initial public.

There have been 40 completed mergers in the first eleven months of 2021 in the healthcare sector with an average total enterprise value after the merger of 1.75 billion dollars and a median of 1.08 billion dollars. Total enterprise values vary from 84 million to

15.2 billion dollars with a standard deviation of 2.5 billion dollars. There have also been 57 successful IPOs of SPACs that are currently searching for a target company, accumulative proceedings equal to 11.9 billion dollars. Average proceedings equal 208.9 million dollars, while median proceedings equal 200 million dollars. As of the beginning of December, 17 SPACs are in the process of merging with a target company, meaning that the target has been selected by the management team and confirmed by the shareholders of SPAC, but the merger has not been completed yet. Such remains also the biggest deal in the healthcare sector in 2021 with a total enterprise value of more than 32 billion dollars. Additional statistics about previously mentioned phases are presented in Figure 2.

Another sector that has seen rising numbers of SPACs is technology.
There have been 107 initial public offerings of SPACs that are looking for targets in the technology sector, which is 50 more than in the healthcare sector. Total proceedings of these IPOs equal 27.7 billion dollars compared to 11.9 billion dollars raised by the SPACs searching for targets in the healthcare sector. Average and median proceedings of IPO are also higher in the technology sector, 259 million and 230 million, respectively. The range of these proceedings is larger for the healthcare sector as is the standard deviation. Visual representation of the spread of SPAC IPO proceedings in the two sectors is provided in **Figure 3A**.

There have been 28 completed mergers (joint total enterprise value of 54.9 billion dollars) in the technology sector compared to 40 (joint total enterprise value of 70.1 billion dollars) in the healthcare sector. Completed mergers in the technology sector had higher average total enterprise value after the merger (1.96 billion dollars), higher median total enterprise value after the merger (1.22 billion dollars) and lower standard deviation (2.1 billion dollars). Visual representation of the spread of total enterprise values for completed mergers is presented in **Figure 3B**.

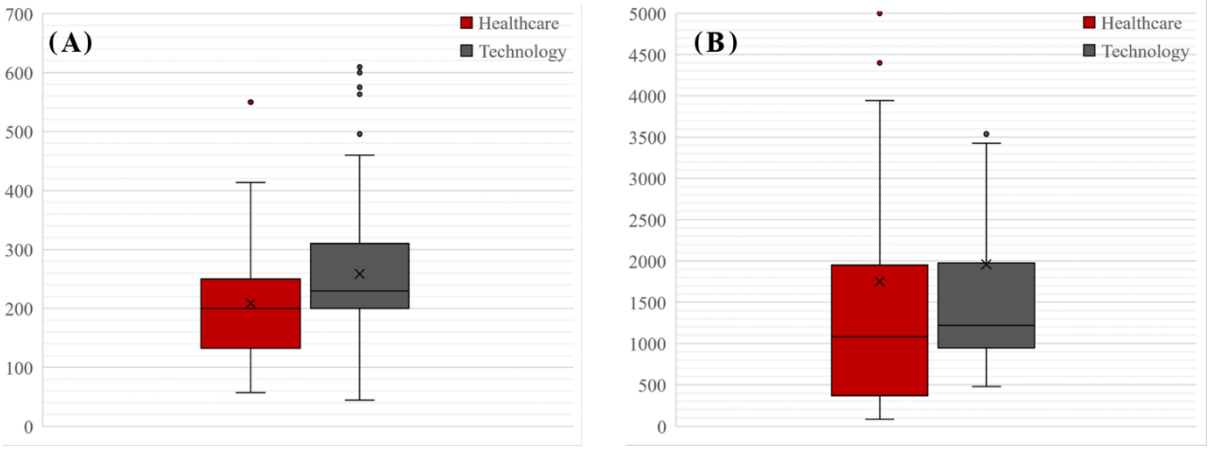

Figure 3. (A): Comparison of IPO proceedings of SPACs searching for a target in the selected sectors in 2021 (ordinate axis showing proceedings in M$). One outlier for the healthcare sector is not shown on the boxplot. The authors' calculations are based on data available at the SPAC Insider Statistics database. **B:** Comparison of total enterprise values after the merger for the selected sectors in 2021 (ordinate axis showing total enterprise value in M$). Two outliers for the technology sector and one outlier for the healthcare sector are not shown on the boxplot. The authors' calculations are based on data available at the SPAC Insider Statistics database.

4. Conclusions

SPACs have gained much popularity in the past two years, however, due to increased threats of regulatory actions, the excitement is decreasing (The Economist, 2021). Although the Securities and Exchange Commission (abbreviated SEC) did not take much interest in SPACs from the beginning, it changed its stance in July 2021 with a charge for misleading disclosures ahead of a merger (Securities and Exchange Commission, 2021). With this charge, SEC showed that it demands the same level of transparency and

pre-transaction due diligence for SPACs as it does for traditional IPO deals and mergers (Brown Brothers Harriman, 2021). Similarly to American counterpart, European regulator European Securities and Markets Authority (ESMA) announced the requirement of adequate reviews of SPACs in addition to mandatory disclosure for retail investors with an explanation of potential risk factors, such as share dilution and funding structure (European Securities and Markets Authority, 2021). What the future holds for SPACs is uncertain, but if their growth continues, regulators will inevitably enforce stricter protocols of oversight.

Conflicts of Interest: The authors declare no conflict of interest.

References

1. Brown Brothers Harriman (2021), SPACs: Fad or future?. Accessed 17.12.2021. Available from: https://www.bbh.com/us/en/insights/blog/on-the-regs/spacs--fad-or-future-.html
2. European Securities and Markets Authority (2021), SPACs: prospectus disclosure and investor protection considerations. Accessed 22.12.2021. Available from: https://www.esma.europa.eu/sites/default/files/library/esma32-384-5209_esma_public_statement_spacs.pdf
3. Hale L. SPAC: A financing pool with something for everyone. J Corp Account Finance. 2006; 18(2): 67-74
4. DOI: 10.1002/jcaf.20278
5. Heredia T, Fernandez-Galiano J, Garcia M. The SPACs boom. Deloitte insights. 2021. Available from: https://www2.deloitte.com/xe/en/insights/industry/financial-services/spacs-in-europe.html
6. Jenkinson T, Sousa M. Why SPAC investors should listen to the market. SSRN Electronic J. 2009. DOI: 10.2139/ssrn.1341771
7. Klausner M, Ohlrogge, M. A sober look at SPACs. SSRN Electronic J. 2020. DOI: 10.2139/ssrn.3720919
8. Securities and Exchange Commission (2021), SEC Charges SPAC, sponsor, merger target, and CEOs for misleading disclosure ahead of proposed business combination. Accessed 23.12.2021. Available from: https://www.sec.gov/news/press-release/2021-124
9. SPAC Insider (2021), SPAC IPO Transactions statistics. Accessed 28 November 2021. Available from: https://spacinsider.com/stats/
10. SPAC Research (2021), Special purpose acquisition company. Accessed 17.12.2021. Available from https://www.spacresearch.com/
11. The Economist (2021), Have SPACs been cleaned up?. Accessed 24.12.2021. Available from: https://www.economist.com/finance-and-economics/2021/12/04/have-spacs-been-cleaned-up
12. The Goldman Sachs Group, Inc. (2021), The IPO SPAC-tackle. Accessed 15.12.2021. Available from https://www.goldmansachs.com/insights/pages/top-of-mind/the-ipo-spac-tacle/report.pdf

Scientific contribution/Review

The role of Extracellular Vesicles in Alopecia and its Treatment

Tehovnik J[1,*]

1. University of Ljubljana, Faculty of Medicine, Ljubljana, Slovenia
* Correspondence: Jan Tehovnik; jan.tehovnik5@gmail.com

Abstract:
Extracellular vesicles are cell-derived membranous bodies that function as intercellular communicators, carrying proteins, lipids, DNA and RNA molecules. Many therapeutic approaches have focused on using extracellular vesicles, due to smaller risk compared to invasive cell-based therapies. Hair follicles are skin appendices that are composed of epidermal and mesenchymal component, with the former including a major reservoir of epithelial stem cells. Hair follicles continuously cycle, undergoing consecutive phases of resting, growing, and regression. Many molecules carried by extracellular vesicles are involved in the control of the hair follicle cycle and stem cell function. Thus, investigating the role of extracellular vesicles as signaling bodies potentially involved in hair cycling may be an important step in the attempt to design future alopecia treatment strategies.

Keywords: Alopecia; Hair growth; Hair regeneration; Hair follicle morphogenesis; Stem cell extracellular vesicles; Telogen to anagen transition

Citation: Tehovnik J. The role of extracellular vesicles in alopecia and its treatment. Proceedings of Socratic Lectures. 2021; 6: 94-97. https://doi.org/10.55295/PSL.2021.D.013

1. Alopecia

Hair loss (alopecia) is a common problem in adults. Alopecia mostly affects males in their 20s, starts on the forehead and continues spreading towards the back of the scalp. Alopecia often represents a negative psychological effect on affected individuals. The most important factor in the development of alopecia is genetics, in addition, the phenomenon is also influenced by hormonal changes, vitamin deficiency and medication (the most common being chemotherapy) (Phillips et al., 2017). Alopecia can also be iatrogenic in which the reason is unknown. Modern medicine allows us to slow down alopecia, especially with drugs such as finasteride and minoxidil. Finasteride is a drug that inhibits testosterone 5-alpha reductase and is used to treat hair loss, as well as prostate hypertrophy (Phillips et al., 2017). Minoxidil is used as an antihypertensive and is used topically to treat hair loss, as it activates the beta-catenin pathway, which in turn leads to faster regeneration of hair follicles (Phillips et al., 2017). Both drugs have proven to be effective, but are only intended to improve hair loss in the short term. In addition, discontinuation of therapy can result in rapid hair loss (Phillips et al., 2017). Therapeutically, there are also various surgical procedures in which hair is aesthetically transplanted from more densely overgrown areas (Phillips et al., 2017; Khanna, 2008). It is usually an autologous transplant. The disadvantage of transplantation is the limited number of hair follicles (Khanna, 2008), and transplantation requires aggressive drug therapy (for example corticosteroids), so we are looking for new ways to treat hair loss.

Hair grows in three stages (Murphrey et al., 2021). The hair cycle begins with the anagen phase - the growth phase of the hair follicle. It is the proliferation of follicle epithelial cells in the hair follicle, which then differentiate and form hair in the follicular root cells (Murphrey et al., 2021). The next phase is the catagen phase, in which the supply of nutrients to the hair follicle from the bloodstream is interrupted (Murphrey et al., 2021). The cycle ends with the telogen phase, in which the hair follicle falls out (Murphrey et al., 2021). The dermal papilla cells located in the papilla of normal human hair follicles play a crucial role in the dermal–epidermal interactions that control hair production and events of the hair growth cycle (Murphrey et al., 2021). Dermal papilla cells manage hair follicle cycling through interacting between endothelial cells, stem cells and stem cells of the hair follicle (3). A defect in any one of the cells can lead to hair loss. Thus, restoration of these cells for better interaction is considered a potential therapeutic strategy for treating hair loss.

2. Extracellular vesicles

Extracellular vesicles are membrane nanovesicles measuring 30-1000 nanometres in diameter, which are secreted by most body cells into extracellular fluid (Doyle and Wang, 2019). They contain proteins, lipids and nucleic acids. Extracellular vesicles are composed of exosomes and microvesicles (Doyle and Wang, 2019). Exosomes are synthesized intracellularly, and form vesicle-containing endosomes. They are called multivesicular bodies. These fuse with the plasma membrane and excrete their contents into the extracellular. Cells can communicate on short and further distance via extracellular vesicles. Studies have shown that exosomes play a key role in intercellular signalling, which is important in a variety of physiological and pathological processes (Doyle and Wang, 2019).

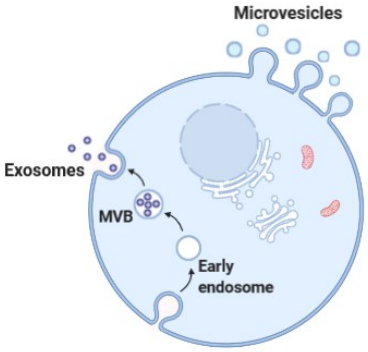

Figure 1. Extracellular vesicles - exosomes and microvesicles.

3. Potential pathways of extracellular vesicles derived treatment in hair cycle

Wingless and Int-1 (Wnt) factors are the most important regulators of hair follicle morphogenesis and hair growth. Namely, epidermal Wnt ligands play a main role in wound-induced de novo hair formation in adult skin (Carrasco et al., 2019). Consequently, they have been pointed out as potential targets for the treatment of hair-related syndromes like alopecia. Active Wnt factors have been identified as exosome-secreted molecules which can be contained in the interior compartment of these vesicles as well as transported exteriorly (Carrasco et al., 2019). Several studies have demonstrated that Wnt signaling in recipient cells can be mediated by the transition of the proteomic contents of extracellular vesicles (Carrasco et al., 2019). Additionally, Wnt signalling has been found to be activated in target cells by extracellular vesicles containing both β-catenin, the major effector protein of the Wnt pathway (Carrasco et al., 2019). For instance, Wnt4 enhances Wnt/β-catenin signaling and promotes angiogenesis. In agreement with these observations, an upregulation in the expression of Wnt3a and Wnt5a has been found in mouse skin treated with intradermically-injected extracellular vesicles obtained from mesenchymal stem cells (Carrasco et al., 2019; Rajendran et al., 2017)

MicroRNAs (miRNAs) are small noncoding RNA molecules which are capable of altering gene expression post transcriptionally and are typically transported in extracellular vesicles. These molecules have been implicated in the control of hair follicle development through the modulation of Wnt signaling, but the mechanism is not entirely understood (Carrasco et al., 2019).

An interesting area are mesenchymal stem cells in the field of cell regeneration, due to the great potential for self-renewal and the possibility of differentiation. The extracellular vesicles of mesenchymal cells have a proven anticancer effect and can also promote angiogenesis, which would be particularly useful in patients with ischemic disease (Rajendran et al., 2017). Thus, they could be used for ischemic tissue regeneration after cerebral / cardiac infarction. Many studies have shown that cytokines and dermal papilla growth factors play a role in regulating hair growth (Rajendran et al., 2017). The cells of the dermal papilla have the ability to release growth factors into the environment, which in turn signals the epithelial cells to divide, the end result of which is the growth of hair and the acceleration of hair regrowth (Rajendran et al., 2017). According to research, after treatment of these cells with extracellular vesicles of mesenchymal cells, the expression of VEGF and IGF-1 increased (Rajendran et al., 2017). VEGF has been shown to promote hair growth, increase follicle size and increase the thickness of the hair itself (Rajendran et al., 2017). IGF-1 is secreted by the cells of the dermis, as well as the cells of dermal papillae of the hair follicle, and when stimulated, hair growth is accelerated. Lastly, intradermically injected mesenchymal stem cells extracellular vesicles have been shown to favor telogen to anagen transition in a mouse model (Carrasco et al., 2019; Rajendran et al., 2017).

3. The role of macrophages' extracellular vesicles in hair growth and regeneration

A recent study identified the involvement of perifollicular macrophages in the activation of skin epithelial stem cells, as an additional signal that regulates hair follicle growth (Rajendran et al., 2020). Another study showed that macrophages induce hair follicle growth through tumour necrosis factor (TNF)-induced AKT/β-catenin signaling in Leucine-rich G-protein-coupled receptor 5 hair follicle stem cells (Rajendran et al., 2020). Human perifollicular macrophages maintain the anagen stage (making the hair follicle stronger) in humans by activating dermal papilla cells by secreting Wnt proteins (Rajendran et al., 2020). It was shown that macrophages' extracellular vesicles promote proliferation and the activation of the Wnt/β-catenin signaling pathway in dermal papilla cells (Doyle and Wang, 2019, Rajendran et al., 2020). The macrophages' extracellular vesicles enhanced the hair-inductive properties of dermal papilla cells by increasing the levels of hair-inductive proteins and survival/proliferation markers (Rajendran et al., 2020). Further experiments revealed that macrophages' extracellular vesicles promote hair growth through stimulation of vascular endothelial growth factor (VEGF) and keratinocyte growth factor (KGF) in dermal papilla cells (Rajendran et al., 2020). Macrophages' extracellular vesicles accelerate hair growth by increasing the number of hair follicle s and dermis thickness. The extracellular vesicles derived from macrophage could be excellent candidates for stimulating hair growth in humans, since their isolation from the same patients is relatively simple and less invasive than isolation of mesenchymal stem cells from the adipose tissue or bone marrow.

4. Conclusions

The emergent role of extracellular vesicles in hair follicle cycle dynamics is likely to become a high-impact tool in cosmetic medicine. For patients suffering from alopecia, extracellular vesicles isolated from autologous mesenchymal stem cells may represent a solution in the future. Nevertheless, many investigations should be done before the clinical use of extracellular vesicles, namely the most suitable cell type for isolation of extracellular vesicles (despite the fact that mesenchymal stem cells represent a very good prototype), the optimal concentration and mode of entry (intradermal or topical), the mode of treatment itself, the frequency of dosing and the duration of treatment.

Conflicts of Interest: The author declares no conflict of interest.

References

1. Carrasco E, Soto-Heredero G, Mittelbrunn M. The role of extracellular vesicles in cutaneous remodeling and hair follicle dynamics. Int. J. Mol. Sci. 2019; 20:2758. DOI: 10.3390/ijms20112758
2. Doyle LM, Wang MZ. Overview of extracellular vesicles, their origin, composition, purpose, and methods for exosome isolation and analysis. Cells. 2019; 8:727. DOI:10.3390/cells8070727
3. Khanna M. Hair transplantation surgery. Indian J Plast Surg. 2008; 41(Suppl):S56-S63.
4. Murphrey MB, Agarwal S, Zito PM. Anatomy, Hair. [Updated 2021 Aug 11]. In: StatPearls [Internet]. Treasure Island (FL): StatPearls Publishing; 2021. Available from: https://www.ncbi.nlm.nih.gov/books/NBK513312/
5. Phillips TG, Slomiany WP, Allison R. Hair loss: common causes and treatment. Am Fam Physician. 2017; 96:371-378. PMID:28925637.
6. Rajendran RL, Gangadaran P, Bak SS, et al. Extracellular vesicles derived from MSCs activates dermal papilla cell in vitro and promotes hair follicle conversion from telogen to anagen in mice. Sci Rep. 2017; 7:15560. DOI: 10.1038/s41598-017-15505-3
7. Rajendran RL, Gangadaran P, Seo CH, Kwack MH, et al. Macrophage-derived extracellular vesicle promotes hair growth. Cells. 2020; 9:856. DOI: 10.3390/cells9040856

Scientific contribution/Original research

Open Science: Development of Open Platform for Giant Unilamelar Phospholipid Vesicles Electroformation

Gazvoda de Reggi M[1], Malavašič U[1], Jeran M[1,2], Penič S[1,*]

1. University of Ljubljana, Faculty of Electrical Engineering Laboratory of Physics, Tržaška cesta 25, SI-1000 Ljubljana
2. University of Ljubljana, Faculty of Health Sciences, Laboratory of Clinical Biophysics, Zdravstvena pot 5, SI-1000 Ljubljana

* Correspondence: Samo Penič; samo.penic@fe.uni-lj.si

Abstract:
Open Science is, by definition, the transparent and accessible knowledge that is shared and developed through collaborative networks. It allows for broader availability of research data and speeds up the process of obtaining new knowledge. Open-source software has publicly available source code that anyone can inspect, modify, and enhance. This work focuses on the importance of Open Science practice and illustrates that on an example of cell membrane research. Cell membranes are vital components of the cell as their structure and properties influence many important cellular functions. Due to their complicated composition, researchers use simpler structures that resemble the membrane, called unilamellar vesicles, especially giant unilamellar vesicles, due to their size. There are many methods for acquiring the vesicles using their main building blocks – phospholipids, electroformation being the most commonly used. In this work, an open-source sinusoidal voltage source designed for electroforming giant unilamellar vesicles will be presented as an alternative to expensive and impractical function generators. The device has been successfully used to produce vesicles from the phospholipid POPC (1-palmitoyl-2-oleoyl-*sn*-glycero-3-phosphocholine) and a mixture of POPC and cholesterol (4/1).

Keywords: Open Science, Open Source, Arduino AC voltage source, Giant unilamellar phospholipid vesicles (GUVs), Cell membranes, Electroformation.

Citation: Marin Gazvoda de Reggi, Urban Malavašič, Marko Jeran, Samo Penič. Open science: development of open platform for giant unilamelar vesicles electroformation. Proceedings of Socratic Lectures. 2021; 6: 99-113. https://doi.org/10.55295/PSL.2021.D.014

1. Introduction

1.1. Open science

Open Science is, by definition, the transparent and accessible knowledge that is shared and developed through collaborative networks. There are six fundamental principles of open science, which include open methodology, open source, open data, open access, open peer review and open educational resources. Open science practice has many advantages. It allows for broader availability of research data and it also has the potential for speeding up the process of obtaining new knowledge (Vicente-Saez and Martinez-Fuentes, 2018).

1.2. *Open-source hardware and software*

The term open source refers to something that is freely available for modification and redistribution because its design is publicly accessible. It most commonly represents open-source software with source code that anyone can inspect, modify, and enhance. Open-source technology not only benefits computer programmers but practically everyone –Linux kernel is one such example as its variations can be found on a wide range of devices ranging from smallest wearables, smart household appliances, personal computers to giant servers and supercomputers (Opensource.com, 2021).

In a similar manner, open-source hardware adopts the open-source principles by making design specifications of a physical object (which include schematics, blueprints, logic designs) publicly available so that they can be studied, modified, created, and distributed by anyone. Preferably its components should be easy for anyone to obtain which reduces common barriers to the design and manufacture of physical goods. Arduino and Raspberry Pi are among the most renowned examples (Opensource.com, 2021).

1.3. Scientific Computing

Scientists are frequently presented with various tasks which include computation and managing large amounts of data. Instead of doing repetitive action by hand, scientists utilize the help of computers and typically develop their own software for such purposes, as it requires significant domain-specific knowledge. The resulting software is often buggy and difficult to maintain since most are self-taught. In order to improve the quality of code, the subsequent practices are to be followed: improving the human readability of code (distinctive and consistent naming, formatting), automating workflows and repetitive tasks, making incremental changes (as well as using a version control system), reusing and modularizing code instead of rewriting it, planning for mistakes and optimizing it only after it works correctly, collaborating and documenting (Wilson et al., 2014).

1.4. Cells and their membranes

We chose the preparation of cell membrane substitutes in a laboratory as an example of what can be achieved by following the principles of open science and open-source software and hardware as well as best practices for scientific computing (Gazvoda de Reggi et al., 2021).

Cells are the main building blocks of all living organisms. Their exterior and interior are separated by a thin layer called the cell membrane, through which substances pass into and out of the cell. The cell membrane is primarily composed of phospholipid molecules organized into a bilayer (Cevc and Marsh, 1987). It also consists of various inclusions, such as different types of proteins, cholesterol and other biologically important building blocks that define cell's function (**Figure 1**).

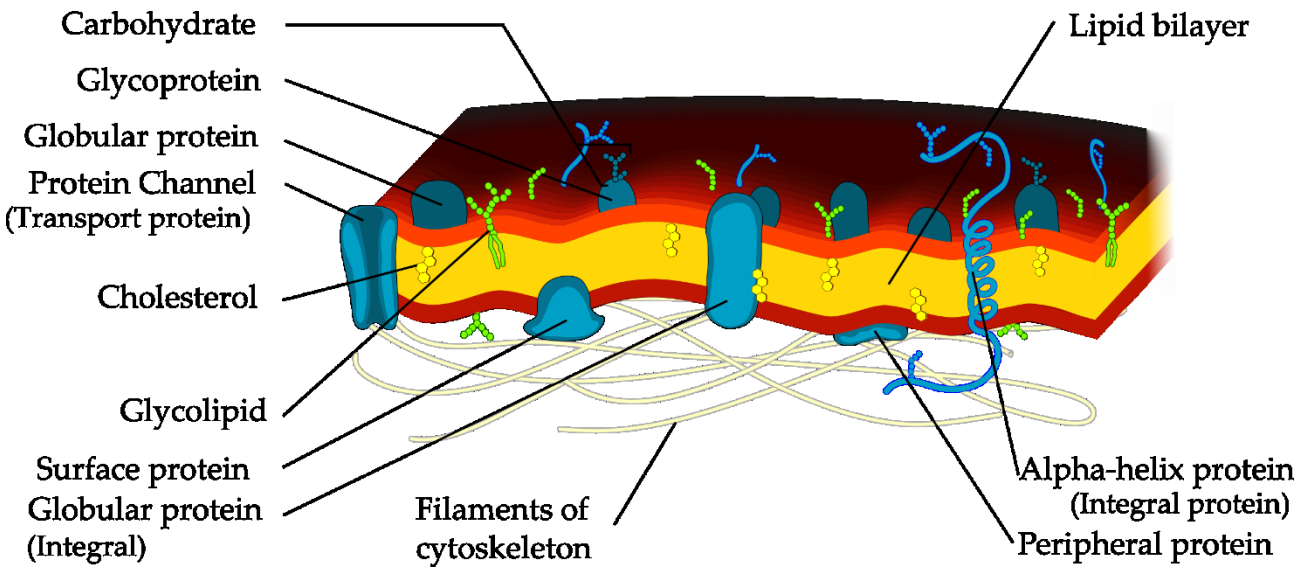

Figure 1. The cell membrane is a complex structure whose basic building block is a phospholipid bilayer. The two red-colored layers are composed of many polar phospholipid heads, while the yellow-colored area represents the non-polar tails of the phospholipid molecules (Wikipedia Contributors, 2021).

The most important functions of a membrane are to protect the inside of the cell from external influences and to regulate the transport of substances in and out of the cell. The structure of the membrane thus determines the specific functions of the cell. In the interior of the cell, we also find membranes with a similar structure, which act as dividers between two subcellular compartments (e.g., membranes surrounding intracellular organelles) (Coskun and Simons, 2011).

The study of cell membrane properties in a living cell model is challenging because membrane properties and functions are determined by multiple cellular mechanisms and a complex biological structure. As a result, simplified cell models are often used in research. Liposomes ranging in size from 1–200 μm are also called giant unilamellar vesicles (GUVs) and are commonly used cell substitute. They consist of a bilayer of phospholipids which start to form lipid vesicles as a result of hydrophobic interactions in aqueous solution (Seifert, 1997; Safran, 1999; Nagle, 2013; Dimova, 2014). Due to their appropriate size, they can be directly observed under a light phase-contrast microscope. Typically, researchers isolate a vesicle or a small group, expose it to a change in its microenvironment and observe the differences over an extended period of time (Zupanc and Drobne, 2011; Stein et al., 2017; Penič et al., 2020).

1.5. *Preparation of phospholipid vesicles*

Several approaches are used to prepare giant unilamellar phospholipid vesicles, such as lipid film hydration, electroformation, lipid emulsification, microfluidic methods (hydrodynamic flow directing) and others (Pereno et al., 2017). A more detailed review of vesicle preparation methods is described in (Walde et al., 2010).

Electroformation is the most commonly used process for preparing vesicles from phospholipid components in the laboratory as it is fast (1–3 hours on average) and efficient. The method was first reported in 1986 (Angelova and Dimitrov, 1986). The proposed electroformation process is carried out by applying a lipid solution to a platinum electrode. When the solvent evaporates, a lipid film forms on the electrodes. The electrodes are transferred into an aqueous solution of sugar or salt and the alternating electrical field between the electrodes stimulates and accelerates the lipid vesicle formation process.

1.6. *Voltage source for electroformation*

A function generator is most commonly used as a sine wave AC voltage source. The electroformation of vesicles takes place in a weak electrical field (< 100 V/m), which, given the small distance between the electrodes, can be obtained at low voltages (1–5 V) and harmonically alternates with frequencies in the range of 1–10 Hz, allowing simpler, cheaper and smaller devices to be used for the process. That is why we chose to substitute the function generator with an affordable open-source AC voltage source alternative as a great example of applying Open Science principles.

We used a microcontroller and a filtered PWM (pulse-width modulated) digital output. This allows for the complete electroforming protocol to be stored in the memory of the microcontroller and triggered at the push of a button and thus eliminating repetitive action of needing to configure the source.

An important part of this research involves the prototyping of the AC generator and the evaluation of the device's performance. The circuit was built around the open-source Arduino microcontroller system. The circuit and the source code have been released under the MIT open-source license to promote wider adoption. In order to make the final product small and thus portable, easy to use and fully powered via the USB, we used only readily available and low-cost electronic components. The documentation for making the AC source for electroformation is available on GitHub (https://github.com/umalavasic/electroformation).

2. GUV electroformation protocol

The protocol for the preparation of giant unilamellar vesicles is determined in advance to achieve reproducibility of the experimental results. In this section we will focus only on the part of the protocol that is directly related to the source of the electrical voltage between the electrodes, irrespective of the choice of lipids, solutions, type of electrodes and other factors.

The standard electroformation protocol consists of three steps. In the first phase, the amplitude of the electrical field strength between the electrodes is gradually increased to a maximum value (typically E_{max} < 100 V/m). This phase is followed by an optional vesicle swelling phase, where the field amplitude is maintained at the maximum value for a certain time interval. This is followed by a final phase where we typically reduce the frequency and stimulate the phospholipid bilayer to assemble into spherical vesicles (Méléard et al., 2009). The shape of the electrodes, and particularly their distance from each other, are important factors in determining the voltage of the generator in order to achieve the correct electrical field strength in the solution. Voltage between the electrodes, frequency and duration of each phase can have an overall effect on the size and mechanical properties of the formed vesicles (Drabik et al., 2018).

The operating protocol can also be modified accordingly by adding or substituting different reagents, such as using a salt solution instead of sugar (Méléard et al., 2009). In applied research, the first two operational phases are usually combined into one (Santhosh et al., 2020).

In routine laboratory experiments, the electroformation process is most often carried out in aqueous glucose solutions. Our work follows the key steps described by Stein et al. (Stein et al., 2017). The two platinum wire electrodes with a diameter of ≈ 2 mm are spaced 5 mm apart. The operating parameters of the vesicle electroformation system are also given in **Figure 2**.

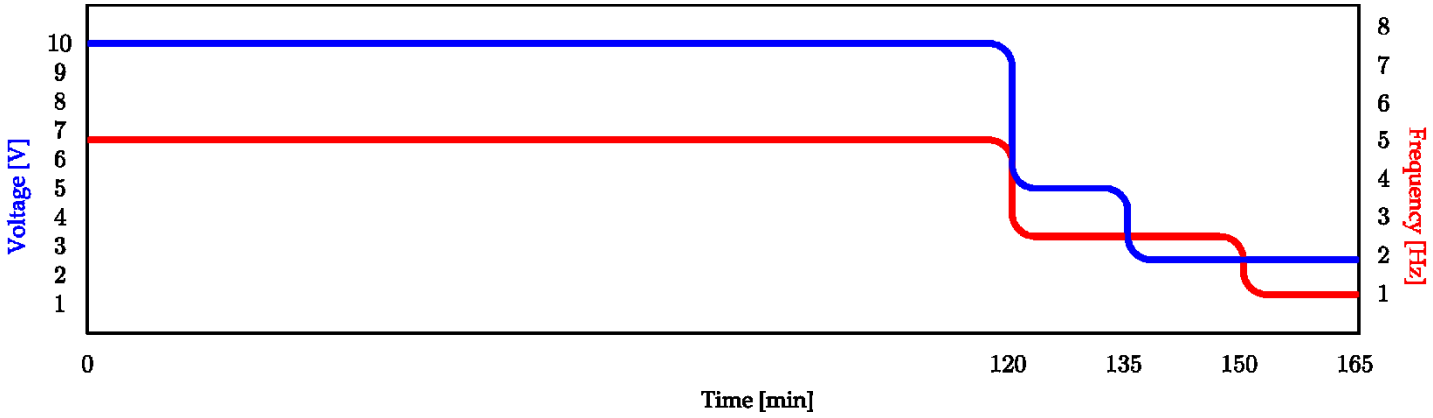

Figure 2. Typical electroformation protocol parameters. Red line describes time variance of frequency, and blue line the voltage of sinusoidal signal.

A gradual decrease in the frequency and voltage of the electrical field causes the swollen lipid vesicles to slowly detach from the surface of the electrodes and remain free floating in solution.

3. Generator circuit description

Using the Arduino Uno microcontroller platform, we generated a PWM signal with a frequency of 31,4 kHz. The duty cycle was determined based on a pre-calculated table of sine values. The signal was filtered with a first-order low-pass filter that attenuated frequencies above 150 Hz to obtain the desired sinusoidal signal. The signal manipulation circuit is shown in **Figure 3**.

The output of the low-pass filter is connected to the non-inverting input of the operational amplifier, which has been set to a gain of a factor of 2. The operational amplifier used is a Texas Instruments LM358, which has two units in a DIP-8 housing. The second unit was used as an inverting operational amplifier. Potentiometer RV1 was used to set the gain to a factor of 2,5 while potentiometer RV2 was used to set the offset voltage of the operational amplifier to prevent it from being saturated by the signal.

Due to the single power supply of the operational amplifier, the electrodes were connected differentially between the outputs of the two operational amplifiers.

The calibration was performed using an oscilloscope. First, we set the gain with potentiometer RV1 so that when the maximum amplitude of the microcontroller output was set, we got a peak voltage of 10 V_{pp} between the output terminals, followed by cancellation of the DC component of the voltage with potentiometer RV2.

The operational amplifier was powered with a voltage of 15 V, which was obtained from the supply voltage of the Arduino microcontroller system using a boost converter. We used a module based on the SX1308 converter from Sunrom.

The maximum achievable frequency at the output is limited to about 150 Hz and the voltage to 10 V_{pp}. The current capacity of the output is limited by the characteristic of the selected operational amplifier which is ≈ 40 mA. This does not pose a practical problem for a high-ohm load represented by a vial with electrodes and solution.

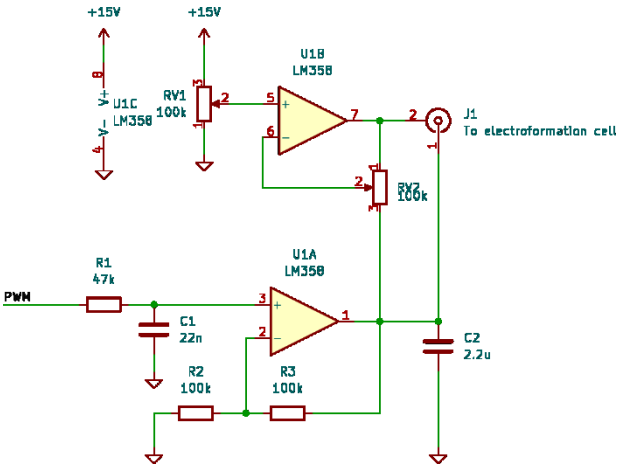

(a)

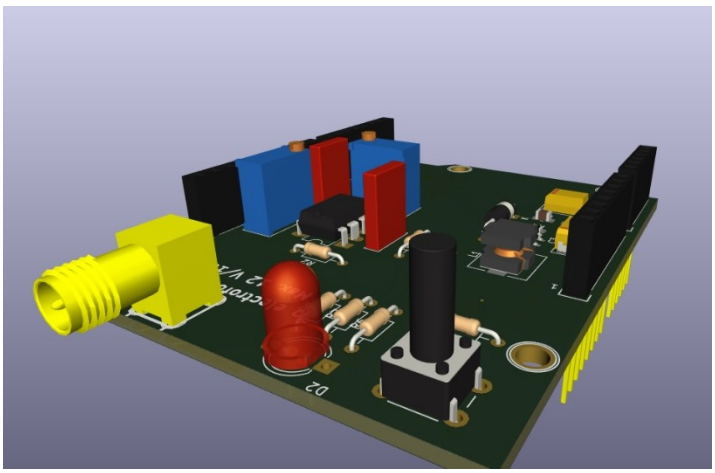

(b)

Figure 3. Circuit diagram (a) and a 3D graphic showing the board (b).

4. Code execution flow

The parameters for the execution of the vesicle preparation protocol (**Figure 4**) are stored on the device in an electrically erasable programmable read-only memory (EEPROM). After switching on the device, the colored LED lights up and turns light blue.

Pressing the button starts the stored protocol and the LED turns purple. When the protocol is finished, the LED turns green. The protocol execution can be aborted during operation by pressing the button and the LED will turn red. A flow chart of the device operation is presented in Figure 4a.

The last used protocol is persistently stored in the device's memory and can be edited by connecting the device via USB to a computer and using an application developed in Python. The device receives the new instruction for protocol execution via the serial port at a baud rate of 115 200 Bd. The instruction consists of comma-separated electric field parameters, with the individual steps separated by semicolons. The beginning and the end of the instruction are delimited by the characters "<" and ">". When accepted by the device, the old protocol is overwritten by the new one and the LED turns dark blue. A schematic of the implementation of the electroformation protocol is shown in Figure 4b.

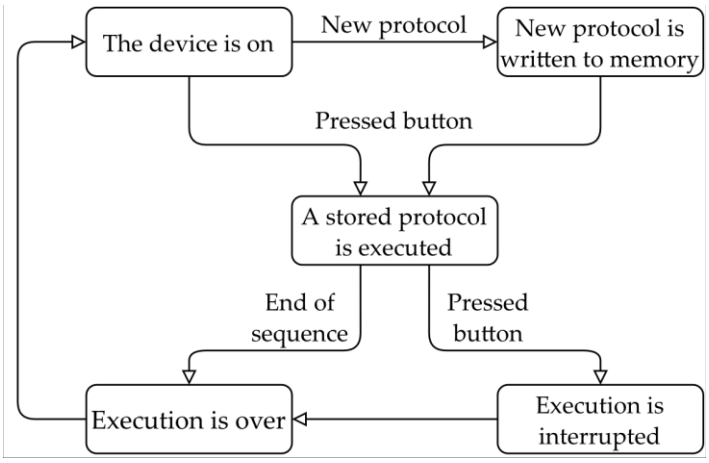

(a)

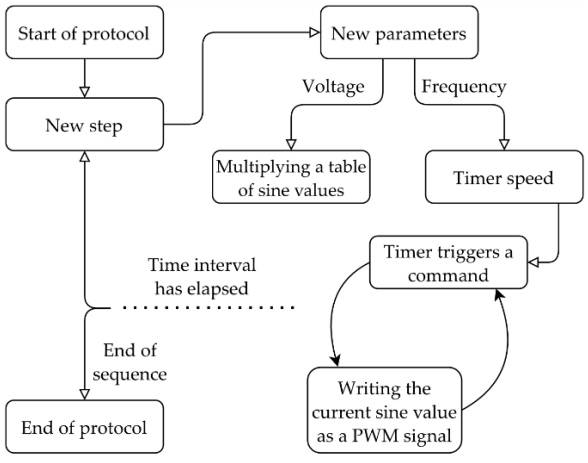

(b)

Figure 4. Flow chart of the device's operation (a) and of the electroformation protocol (b).

5. Results and conclusion

The harmonic voltage source was tested in the laboratory, following the preparation instructions of reference (Stein et al., 2017). Giant phospholipid vesicles were first prepared by electroformation from the synthetic lipid POPC (1-palmitoyl-2-oleoyl-*sn*- glycero-3-phosphocholine), and then from its mixture with cholesterol (both from Avanti Polar Lipids). On each platinum wire electrode, 20 μL of the above lipid diluted in a 2:1 mixture of chloroform and methanol to a concentration of 1 mg/mL was applied by drop creep to the electrodes and dried in a desiccator for 45 min at constant vacuum. After drying, the electrodes were placed in a 2 mL plastic vial containing 1,8 mL of 0,3 M sucrose solution.

The electrodes were connected to the terminals of the harmonic voltage source and the procedure was started according to the protocol described in Section 2. After a total of 165 min, the electrodes were disconnected and the contents of the vial were carefully transferred into 3,60 mL of 0,3 M glucose solution (the volume ratio of sucrose to glucose in the final mixture was 1:2). 200 μL of the suspension was pipetted into experimental chambers (manufactured by Grace Bio-Labs) which allow quantitative field analysis and uniform image capture under the microscope. The chambers were placed under the microscope and left for 30 minutes to allow the contents to settle to the bottom. A light microscope (Nikon Eclipse TE2000-S) was used to examine the samples using immersion oil at 100x magnification.

Samples of giant phospholipid vesicles from both formations were captured with a microscope camera (model UI-3280CP from IDS Imaging). Figure 5a shows a vesicle whose membrane consists only of POPC phospholipid without added cholesterol, while Figure 5b shows a set of vesicles whose membranes contain a mixture of the two. The addition of cholesterol also results in a slightly thicker membrane, which is nicely highlighted by microscopy.

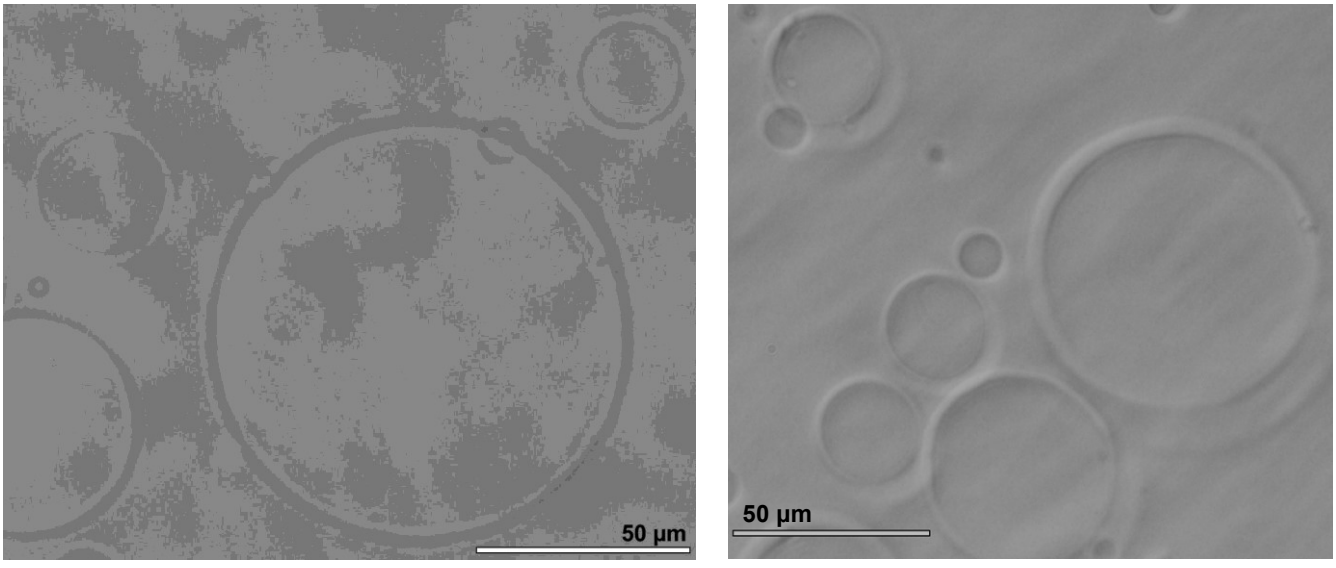

(a) (b)

Figure 5. A 100x magnification image of giant phospholipid vesicles. The images show membranes with POPC phospholipid (a) and its 1:4 mixture with cholesterol (b).

The amounts of vesicles formed in both formation cases were comparable to those obtained using a commercial function generator. The electroforming process does not require an exact sinusoidal waveform, so the signal construction using PWM modulation

is sufficient. The protocols reported in the literature even mention other signal waveforms. In his review article, Méléard mentions the use of an alternating source of either rectangular or sinusoidal form (Méléard et al., 2009), and under specific conditions certain authors (Breton et al., 2015) use protocols that combine both signals – sinusoidal and rectangular.

The presented sinusoidal voltage generator of adjustable amplitude and frequency represents a portable and inexpensive solution for the electroformation of giant unilamellar vesicles. An additional advantage is the complete automation of the electroformation process and the ease of use of the generator, since the protocol steps are stored in memory and executed automatically in sequence, so that the device does not need to be reconfigured during the execution of the protocol. The generator does not need any additional power supply, as it can be operated using the USB output of the computer. An additional benefit of the connection to the computer is the possibility to implement communication with the computer and to be informed via the Internet connection about the current status of the protocol execution. In order to make the generator available to a wider community, we have released the design and the software code under the MIT open-source license.

We conclude that our research stands as an example of importance in practice of Open Science. By publishing source code and documenting the design openly and freely we simplify the work of other researchers and provide them with an affordable and open-source replacement for an expensive device. That not only makes their job easier but also, through collaboration, improves code quality as potential bugs can be identified earlier in the process. The code can also be modified to be applied for other projects that require voltage generation with similar parameters.

Funding: This research was supported by European Union's Horizon 2020 research and innovation program under grant agreement No 801338 (Ves4Us), and by Slovenian Research Agency through the core foundlings No P3-0388 & P2-0244, and project No L3-2621.

Conflicts of Interest: The authors declare no conflict of interest.

References

1. Angelova MI, Dimitrov DS. Liposome electroformation. Faraday discussions of the Chemical Society. 1986; 81: 303–311. DOI:10.1039/dc9868100303
2. Breton M, Amirkavei M, Mir LM. Optimization of the electroformation of giant unilamellar vesicles (GUVs) with unsaturated phospholipids. The journal of membrane biology. 2015; 248: 827–835. DOI: 10.1007/s00232-015-9828-3
3. Cevc G, Marsh D. Phospholipid bilayers: physical principles and models. Wiley. 1987.
4. Coskun Ü, Simons K. Cell membranes: the lipid perspective. Structure. 2011; 19: 1543–1548. DOI: 10.1016/j.str.2011.10.010
5. Dimova R. Recent developments in the field of bending rigidity measurements on membranes. Adv. Coll. Interf. Sci. 2014; 208: 225–234. DOI: 10.1016/j.cis.2014.03.003
6. Drabik D, Doskocz J, Przybyło M. Effects of electroformation protocol parameters on quality of homogeneous GUV populations. Chemistry and physics of lipids. 2018; 212: 88–95. DOI: 10.1016/j.chemphyslip.2018.01.001
7. Gazvoda de Reggi M, Malavašič U, Jeran M, et al. Generator izmenične napetosti za elektroformacijo orjaških fosfolipidnih veziklov. In: Žemva A, Trost A, editors. Zbornik tridesete mednarodne Elektrotehniške in računalniške konference. ERK Portorož, Društvo Slovenska sekcija IEEE. 2021; pp. 419-422.
8. Méléard P, Bagatolli LA, Pott T. Giant unilamellar vesicle electroformation: From lipid mixtures to native membranes under physiological conditions. Methods in enzymology. 2009; 465: 161–176. DOI: 10.1016/S0076-6879(09)65009-6
9. Nagle JF. Introductory Lecture: Basic quantities in model biomembranes. Faraday Discuss. 2013; 161: 11–29. DOI: 10.1039/C2FD20121F.
10. Penič S, Mesarec L, Fošnarič M, et al. Budding and fission of membrane vesicles: A mini review. Frontiers in Physics. 2020; 8: 342. DOI: 10.3389/fphy.2020.00342
11. Pereno V, Carugo D, Bau L, et al. Electroformation of Giant Unilamellar Vesicles on Stainless Steel Electrodes. ACS Omega. 2017; 2: 994–1002. DOI: 10.1021/acsomega.6b00395
12. Safran SA. Curvature elasticity of thin films. Adv. Phys. 1999; 48: 395–448. DOI: 10.1080/000187399243428.
13. Santhosh P, Genova J, Iglic A, et al. Influence of cholesterol on bilayer fluidity and size distribution of liposomes. Comptes rendus de l'Académie bulgare des Sciences. 2020; 73. DOI:10.7546/crabs.2020.07.07

14. Seifert U. Configurations of fluid membranes and vesicles. Adv. Phys. 1997; 46: 13–137. DOI: 10.1080/00018739700101488.
15. Stein H, Spindler S, Bonakdar N, et al. Production of isolated giant unilamellar vesicles under high salt concentrations. Frontiers in physiology. 2017; 8: 63. DOI: 10.3389/fphys.2017.00063
16. Vicente-Saez R, Martinez-Fuentes C. Open Science now: A systematic literature review for an integrated definition. Journal of Business Research. 2018; 88: 428–436. DOI: https://doi.org/10.1016/j.jbusres.2017.12.043.
17. Walde P, Cosentino K, Engel H, et al. Giant vesicles: preparations and applications. ChemBioChem. 2010; 11: 848–865. DOI: 10.1002/cbic.201000010
18. Wikipedia contributors. Celična membrana – Wikipedia, The Free Encyclopedia. Accessed 20 July 2021 Available from https://sl.wikipedia.org/wiki/Celična_membrana.
19. Wilson G, Aruliah DA, Brown CT, et al. Best practices for scientific computing. PLoS Biol. 2014; 12: e1001745. DOI: 10.1371/journal.pbio.1001745.
20. Zupanc J, Drobne D. Populacije orjaških lipidnih veziklov kot model za studij bio-nano interakcij/Giant Lipid Vesicle Populations as a Model for Bio-nano Interaction Studies. Informatica Medica Slovenica. 2011; 16: 1-12.
21. What is open source? Opensource.com. Accessed 31 December 2021a Available from https://opensource.com/resources/what-open-source.
22. What is open hardware? Opensource.com. Accessed 31 December 2021b Available from https://opensource.com/resources/what-open-hardware.

Appendix A: Firmware for Arduino

```
// WAVEFORM
#define WAVEFORM_PIN              11            // Don't change unless you also adjust timers and PWM
                                                // frequency accordingly
#define SIGNAL_VOLTAGE_AMPLITUDE  5             // [V]
#define PROTOCOL_MAX_STAGES       10            // Currently set to accept 10 stages in single protocol

// BUTTON
#define BUTTON_IS_USED            true
#define BUTTON_PIN                2
#define BUTTON_PIN_MODE           INPUT_PULLUP  // change to INPUT when using external resistors

// RGB LED
#define RGB_LED_IS_USED           true
#define RED_LIGHT_PIN             3
#define GREEN_LIGHT_PIN           6
#define BLUE_LIGHT_PIN            5

// TIMER
#define USE_TIMER_1               true
#include <TimerInterrupt.h>
#include <ISR_Timer.h>

// EEPROM
#include <EEPROM.h>

// MARK: - Signal Generation
const byte sineWave[] = {
  128, 131, 134, 137, 140, 143, 146, 149, 152, 155, 158, 162, 165, 167, 170, 173, 176, 179, 182, 185, 188,
         190, 193, 196, 198, 201, 203, 206, 208, 211, 213, 215, 218, 220, 222, 224, 226, 228, 230, 232, 234,
         235, 237, 238, 240, 241, 243, 244, 245, 246, 248, 249, 250, 250, 251, 252, 253, 253, 254, 254, 254,
         255, 255, 255, 255, 255, 255, 255, 254, 254, 254, 253, 253, 252, 251, 250, 250, 249, 248, 246, 245,
         244, 243, 241, 240, 238, 237, 235, 234, 232, 230, 228, 226, 224, 222, 220, 218, 215, 213, 211, 208,
         206, 203, 201, 198, 196, 193, 190, 188, 185, 182, 179, 176, 173, 170, 167, 165, 162, 158, 155, 152,
         149, 146, 143, 140, 137, 134, 131, 128, 124, 121, 118, 115, 112, 109, 106, 103, 100, 97, 93, 90, 88,
         85, 82, 79, 76, 73, 70, 67, 65, 62, 59, 57, 54, 52, 49, 47, 44, 42, 40, 37, 35, 33, 31, 29, 27, 25,
         23, 21, 20, 18, 17, 15, 14, 12, 11, 10, 9, 7, 6, 5, 5, 4, 3, 2, 2, 1, 1, 1, 0, 0, 0, 0, 0, 0, 0, 1,
         1, 1, 2, 2, 3, 4, 5, 5, 6, 7, 9, 10, 11, 12, 14, 15, 17, 18, 20, 21, 23, 25, 27, 29, 31, 33, 35, 37,
         40, 42, 44, 47, 49, 52, 54, 57, 59, 62, 65, 67, 70, 73, 76, 79, 82, 85, 88, 90, 93, 97, 100, 103,
         106, 109, 112, 115, 118, 121, 124
  // https://www.daycounter.com/Calculators/Sine-Generator-Calculator.phtml
};
```

```
const unsigned waveformResolution = sizeof(sineWave) / sizeof(sineWave[0]); // = 256
byte waveform[waveformResolution];
unsigned waveformPosition;

// MARK: - Protocol
struct Protocol {
  unsigned long duration; // [s]
  float frequency;        // [Hz], 0.0 < float frequency
  float amplitude;        // [V],  0.0 < float amplitude < SIGNAL_VOLTAGE_AMPLITUDE
};
Protocol protocol[PROTOCOL_MAX_STAGES];
byte protocolStages;
bool protocolInProgress = false;

// MARK: - Serial Communication
const unsigned messageSize = 512; // Maximum amount of characters in one serial port message
char receivedMessage[messageSize];
bool receivedProtocol = false;

// MARK: - Button
byte buttonState = HIGH, lastButtonState = HIGH;
unsigned long lastDebounceTime, debounceDelay = 50; // debounce time; increase if the output flickers

// MARK: - RGB LED
struct Color {
  byte red, green, blue;
};

const struct Colors {
  Color red = {255, 0, 0};
  Color green = {0, 255, 0};
  Color blue = {0, 0, 255};
  Color cyan = {0, 255, 255};
  Color magenta = {255, 0, 255};
  Color yellow = {255, 75, 0};
  Color white = {255, 255, 255};
} colors;

// MARK: - Life Cycle
void setup() {
  setupPWM();
  setupTimer();
  setupSerial();
  setupButton();
  setupLED();

  loadProtocol();
  exportProtocol();

  setRGBColor(colors.cyan);
}

void loop() {
  if (!protocolInProgress) {
    receiveProtocol();
    if (receivedProtocol) {
      receivedProtocolMessage();
      receivedProtocol = false;
    }
  }

  if (BUTTON_IS_USED) {
    handleButton();
  }
}

// MARK: - Setup Functions
```

```
void setupPWM() {
  pinMode(WAVEFORM_PIN, OUTPUT);
  // Set Pin 11 (WAVEFORM_PIN) PWM frequency to 31372.55 Hz, instead of default 490.20 Hz.
  TCCR2B = TCCR2B & B11111000 | B00000001;
}

void setupTimer() {
  ITimer1.init();
}

void setupSerial() {
  Serial.begin(115200);
  Serial.print("READY");
}

// MARK: - RGB LED
void setupLED() {
  if (RGB_LED_IS_USED) {
    pinMode(RED_LIGHT_PIN, OUTPUT);
    pinMode(GREEN_LIGHT_PIN, OUTPUT);
    pinMode(BLUE_LIGHT_PIN, OUTPUT);
  }
}

void setRGBColor(Color color) {
  if (RGB_LED_IS_USED) {
    analogWrite(RED_LIGHT_PIN, color.red);
    analogWrite(GREEN_LIGHT_PIN, color.green);
    analogWrite(BLUE_LIGHT_PIN, color.blue);
  }
}

// MARK: - Button
void setupButton() {
  if (BUTTON_IS_USED) {
    pinMode(BUTTON_PIN, BUTTON_PIN_MODE);
  }
}

void handleButton() {
  int reading = digitalRead(BUTTON_PIN);
  if (reading != lastButtonState) {
    lastDebounceTime = millis();
  }
  if ((millis() - lastDebounceTime) > debounceDelay) {
    byte state = buttonState;
    buttonState = reading;
    if (reading != state && reading == HIGH) {
      buttonPressed();
    }
  }
  lastButtonState = reading;
}

void buttonPressed() {
  Serial.println("Button pressed");
  if (protocolInProgress) {
    cancelProtocol();
  } else {
    runProtocol();
  }
}

// MARK: - Serial Communication Functions
void receiveProtocol() {
  static bool receiving = false;
  static unsigned index;
```

```
  char startMarker = '<', endMarker = '>', receivedByte;
  while (Serial.available() > 0 && !receivedProtocol) {
    receivedByte = Serial.read();

    if (receiving) {
      if (receivedByte != endMarker) {
        receivedMessage[index] = receivedByte;
        index++;
        if (index >= messageSize) {
          index = messageSize - 1;
        }
      } else {
        receivedMessage[index] = '\0';
        receiving = false;
        index = 0;
        receivedProtocol = true;
      }
    } else if (receivedByte == startMarker) {
      receiving = true;
    }
  }
}

void receivedProtocolMessage() {
  parseProtocol();
  exportProtocol();
  saveProtocol();
  setRGBColor(colors.blue);
  if (!BUTTON_IS_USED) {
    runProtocol();
  }
}

void parseProtocol() {
  char * token = receivedMessage;
  unsigned int stages = 0;
  for (int i = 0; token; i++) {
    token = (i == 0) ? strtok(receivedMessage, ",") : strtok(NULL, ",");
    if (!token) {
      // When the token == NULL, we've reached the end of data.
      continue;
    }
    unsigned long duration = atol(token);
    token = strtok(NULL, ",");
    float frequency = atof(token);
    token = strtok(NULL, ";");
    float amplitude = atof(token);

    protocol[i] = { duration, frequency, amplitude };
    stages++;
  }
  protocolStages = stages;
}

void exportProtocol() {
  Serial.print("<");
  for (int i = 0; i < protocolStages; i++) {
    unsigned long duration = protocol[i].duration;
    float frequency = protocol[i].frequency;
    float amplitude = protocol[i].amplitude;

    if (i != 0) {
      Serial.print(";");
    }
    Serial.print(duration);
    Serial.print(",");
    Serial.print(frequency);
```

```
    Serial.print(",");
    Serial.print(amplitude);
  }
  Serial.print(">");
}

// MARK: - EEPROM Functions
void saveProtocol() {
  EEPROM.write(0, protocolStages); // Save number of stages to address 0

  for (int i = 0; i < protocolStages; i++) {
    Protocol stage = protocol[i];

    unsigned long duration = stage.duration;
    float frequency = stage.frequency;
    float amplitude = stage.amplitude;

    int durationAddress = (sizeof(duration) + sizeof(frequency) + sizeof(amplitude)) * i + 1;
    int frequencyAddress = durationAddress + sizeof(duration);
    int amplitudeAddress = frequencyAddress + sizeof(frequency);

    writeUnsignedLong(duration, durationAddress);
    writeFloat(frequency, frequencyAddress);
    writeFloat(amplitude, amplitudeAddress);
  }
}

void loadProtocol() {
  protocolStages = EEPROM.read(0);

  for (int i = 0; i < protocolStages; i++) {
    unsigned long duration;
    float frequency;
    float amplitude;

    int durationAddress = (sizeof(duration) + sizeof(frequency) + sizeof(amplitude)) * i + 1;
    int frequencyAddress = durationAddress + sizeof(duration);
    int amplitudeAddress = frequencyAddress + sizeof(frequency);

    duration = readUnsignedLong(durationAddress);
    frequency = readFloat(frequencyAddress);
    amplitude = readFloat(amplitudeAddress);

    protocol[i] = { duration, frequency, amplitude };
  }
}

void writeUnsignedLong(unsigned long value, int startAddress) {
  byte* bytes = (byte*) &value;
  for (int i = 0; i < sizeof(unsigned long); i++) {
    EEPROM.write(startAddress + i, bytes[i]);
  }
}

unsigned long readUnsignedLong(int startAddress) {
  const byte valueSize = sizeof(unsigned long);
  union {
    byte bytes[valueSize];
    unsigned long value;
  } valueUnion;
  for (int i = 0; i < valueSize; i++) {
    valueUnion.bytes[i] = EEPROM.read(startAddress + i);
  }
  return valueUnion.value;
}

void writeFloat(float value, int startAddress) {
```

```
  byte* bytes = (byte*) &value;
  for (int i = 0; i < sizeof(float); i++) {
    EEPROM.write(startAddress + i, bytes[i]);
  }
}

float readFloat(int startAddress) {
  const byte valueSize = sizeof(float);
  union {
    byte bytes[valueSize];
    float value;
  } valueUnion;
  for (int i = 0; i < valueSize; i++) {
    valueUnion.bytes[i] = EEPROM.read(startAddress + i);
  }
  return valueUnion.value;
}

// MARK: - Protocol Execution
void runProtocol() {
  protocolInProgress = true;
  setRGBColor(colors.magenta);
  for (int i = 0; i < protocolStages; i++) {
    if (!protocolInProgress) {
      return; // Protocol has been canceled.
    }
    Protocol stage = protocol[i];
    runStage(stage);
  }
  protocolFinished(true);
}

void runStage(Protocol stage) {
  unsigned long duration = stage.duration;
  float frequency = stage.frequency;
  float amplitude = stage.amplitude;

  // 1. Populate 'waveform' array with sine wave values modulated with amplitude.
  float scaler = amplitude / SIGNAL_VOLTAGE_AMPLITUDE;
  for (int i = 0; i < waveformResolution; i++) {
    waveform[i] = byte(round(sineWave[i] * scaler));
  }

  // 2. Start the timer interrupt process.
  float timerFrequency = frequency * 2 * waveformResolution;
  ITimer1.attachInterrupt(timerFrequency, tick);

  // 3. Wait for the duration of the sequence, then stop the timer interrupt process.
  unsigned long startTime = millis(), currentTime = millis();
  while (currentTime - startTime < duration * 1000) {
    if (BUTTON_IS_USED) {
      handleButton();
    }
    currentTime = millis();
  }

  ITimer1.disableTimer();
}

void tick() {
  byte instantaneousValue = waveform[waveformPosition];
  analogWrite(WAVEFORM_PIN, instantaneousValue);
  waveformPosition = (waveformPosition + 1) % waveformResolution;
  // Serial.println(instantaneousValue); -- to check sinewave using serial plotter
}

void cancelProtocol() {
```

```
  ITimer1.disableTimer();
  waveformPosition = 0;
  protocolFinished(false);
}

void protocolFinished(bool finished) {
  protocolInProgress = false;
  if (finished) {
    setRGBColor(colors.green);
  }
  else {
    setRGBColor(colors.red);
  }
  analogWrite(WAVEFORM_PIN, 0);
}
```

Scientific contribution/Original research

Experimental measurement of bending stiffness of phospho-lipid vesicles by non-invasive method

Penič S[1,*], Kralj-Iglič V[2], Iglič A[1]

1. Laboratory of Physics, Faculty of Electrical Engineering, University of Ljubljana, Ljubljana, Slovenia
2. Laboratory of Clinical Biophysics, Faculty of Health Sciences, University of Ljubljana, Ljubljana, Slovenia
* Correspondence: Samo Penič; samo.penic@fe.uni-lj.si

Abstract:

Biological membranes, thin barriers between compartments, can fluctuate due to their interacting mechanical properties. They behave as two-dimensional liquids and are so soft that collision of molecules in the surrounding media can cause undulations of the shape. Flickering of red blood cells was already recorded in the late 19th century by Browicz using the light microscope. Today improved contrast images can be recorded directly on computer with phase-contrast microscopy with attached cameras allowing non-invasive spectral analysis of those thermal fluctuations of biological membranes. The measurement setup must provide means for sharp and focused image acquisition for subsequent numerical determination of elasticity parameters (bending stiffness of bending elasticity). Microscope cameras have rather long integration times, resulting in blurry images, since high speed motion of the membrane is lost due to long opening of the shutter. The adaptation of phase-contrast microscope with stroboscopic illumination will be presented to achieve better resolution of acquired images, allowing higher spectral nodes to be used in the analysis of bending stiffness. Other methods of determining bending stiffness will be briefly presented to provide an overview of experimental determination of mechanical properties of phospholipid membranes.

Keywords: Phospholipid bilayer properties; Vesicle characterization; Thermal fluctuations; Phase contrast microscopy; Monte Carlo simulations

Citation: Penič S, Kralj-Iglič V, Iglič A. Experimental measurement of bending stiffness of phospho-lipid vesicles by non-invasive method. Proceedings of Socratic Lectures. 2021; 6: 115-123. https://doi.org/10.55295/PSL.2021.D.015

1. Introduction

Biological cells are the building blocks of all life. They are very diverse in its capabilities and shape, however the basic structural elements are the same as well as its chemical compositions (Boal 2012, Phillips 2013). Cell membranes enclose the cell and its compartments, while networks of filaments, if present, help to maintain the shape of the cell. The mechanical properties of the cell elements can be much different from those of objects familiar in everyday life. In this article, we will present methods of determining the bending stiffness measurements of a lipid bilayer, that is a main building block of the cell membrane. Lipid bilayer consists of lipid molecules (**Figure 1**) and it is very soft. It shows very small resistance to bending, so that even thermal fluctuations at room temperature can generate gentle undulations of the membrane. To simplify the cell membrane and to analyse only the bilayer, the measurement can be done on synthetically produced giant unilamellar vesicles (GUVs). The influence of other constituents on mechanical properties can then be controllably investigated. The diameter of GUVs is in order of few microns to 200 μm. GUVs thus present ideal structures for investigation under optical microscope.

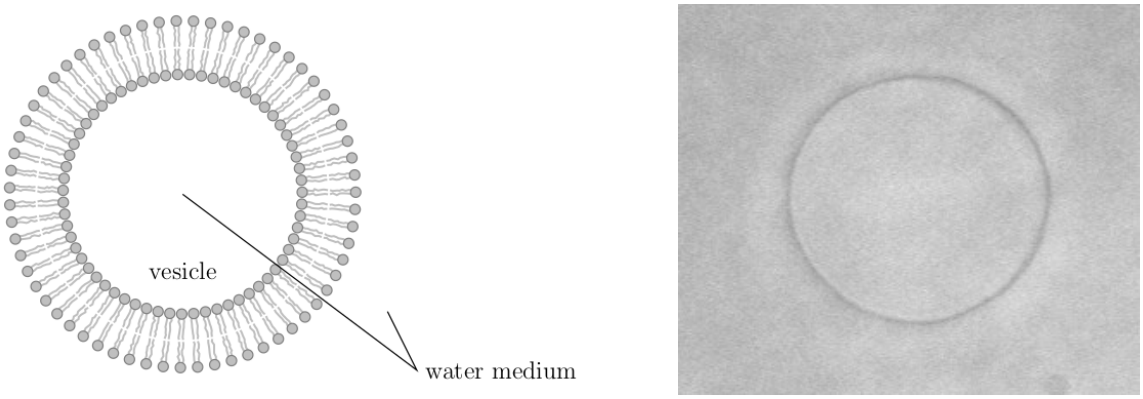

Figure 1. On the left panel, there is a schematic representation of phospholipid bilayer forming a vesicle (membrane). The right panel shows an image acquired by the digital camera attached to the viewport of phase contrast optical microscope. Phase contrast microscopy greatly emphasizes the membrane.

The study of physical properties of the cell membranes is highly important for better understanding of the working of the cell. Many studies deals with basic properties of the phospholipid membranes including the measurement of bending stiffness and the external influences or structural changes to the stiffness of the membrane (as it was for example reported in Mohandas et al. (1983), Evans and Leung (1984), Song and Waugh (1993), Zhou and Raphael (2005).

The methods for measuring the bilayer bending stiffness belong to two groups. Microscopic methods provide structural data at the molecular level, yet numerical modelling or molecular dynamics simulations are required to relate these data to macroscopic properties. Macroscopic methods offer more direct measurements on membrane response to external perturbations, but contact methods which are a common subgroup of macroscopic methods are mostly invasive, which may drive the specimen out of its natural state (Lee et al. 2001). In the following section, some of the most frequently used methods will be described, where the main focus will be on spectral analysis of thermal shape fluctuations.

Optical macroscopic methods, such as spectral analysis of shape fluctuations do not impose external influence on the measured specimen. However, using purely optical macroscopic methods, the measurement precision is limited with optical imaging resolution, therefore many research is focused mainly on GUVs (Menger and Keiper, 1998). Furthermore, the properties of imaging sensor decrease the sharpness of the image due to fast movement of the membrane and due to a relatively long time during which the camera has its shutter open and collects light. Therefore, using fast cameras can be beneficial to improving the sharpness of the acquired image. Another approach with stroboscopic illumination was proposed by Genova et al. (2009). In this contribution, the procedure of adapting phase-contrast microscope for stroboscopic illumination will be presented from the engineering point of view.

2. Brief overview of the methods

Numerous methods are available to determine bending stiffness of the membrane, with their virtues and drawbacks. Taking into the account the temporal and dimensional resolution of the method, one may find that some method may be more suitable for a particular kind of membranes, but the other may be better for the others. A major drawback of some methods is that they deform the measured specimen thus changing its mechanical or other properties that may be relevant to the study. For example, fluid flow imposes mechanical loading to the membrane that can then change the structure of actin cytoskeleton of the cell (Cucina et al., 1995, Pavalko et al., 1998). Furthermore, localized mechanical stress on the membrane can be transmitted over the whole cell by means of cytoskeleton propagation (Maniotis et al., 1997). Here, the various commonly used methods will be briefly presented, however, the list of methods is far from being complete.

Atomic force microscopy (AFM) is used for characterization of materials and can be used as a method to determine bending stiffness of the phospholipid membranes (Jaasma et al., 2006, Lin et al., 2007). Observation of the deflection of the AFM cantilever beam is used to determine the "softness" of the material. The mathematical models that connect deformation and the Young's modulus and bending stiffness is based on Hertz indentation model (Lin et al., 2007). AFM method is fast (in order of milliseconds) and can be used for cells and vesicles with small radii down to 1 nm (Morshed et al. 2020). The method does not impose a large deforming force on the vesicle, however, the sample must be immobilized on substrate for AFM probing.

On same time and dimension scale, optical tweezers and magnetic tweezers are used. Optical tweezers (or optical trapping) use highly focused laser beam to trap and manipulate microscopic neutral dielectric particles. When particles are small compared with the laser wavelength, they behave as dipoles subjected to gradient forces due to photon scattering that is the consequence of different dielectric properties of materials. The scattering force is proportional to the intensity of the light and acts in the direction of incident light propagation (Nussenzveig 2018). The magnetic tweezers do not exert the heating stress due to strong light sources to the sample, but the sample should be treated with small ferromagnetic particles of iron oxide. The particles are usually in the micrometer range and coated with fibronectin to be able to attach to the integrin receptor on the cell (Morshed et al., 2020). The cell with ferromagnetic attachments is then exposed to external magnetic field which acts on the attachments with magnetic force. The magnetic force is then linked to bending stiffness (Fabry et al. 1999).

Electrodeformation is a method that can be used on cell membranes or vesicles on a larger scale, usually in the micrometer range (Jubery et al. 2014). Electric fields provide an alternative way of micromanipulation of vesicles. Compared to previously described micromanipulation methods, the electric field deformation is usually much cheaper while minimizing the risk of contamination the samples as for example in AFM. The most

straightforward approach is to use direct current or DC pulses. When an electric pulse is applied to a vesicle, the vesicle deforms in relation to its mechanical properties. At the end of the pulse, the vesicle returns back to its initial shape. In the absence of excess area, relaxation depends on the properties of the membrane - stretching, viscosity and bending rigidity (Piontek et al. 2021).

Micropipetting is the last method in the brief presentation of methods used in determination of the bending stiffness of the vesicle membranes. With this method we are limited by the optical resolution of the microscope and by the ability of the operator to perform the procedure. The membrane is sucked into the glass cylinder of known inner diameter with predetermined pressure. From the length and radius of the membrane sucked into the pipette tube, the bending stiffness is calculated (Shao and Hochmuth 1996). This method is the simplest in terms of the required apparatus, but it deforms the specimen by a large extent.

In contrast to the forced mechanical deformation, the method based on thermal fluctuations is non-invasive. The method of thermal fluctuation that described in detail in the continuation, has a distinct advantage of not loading the measured specimen and thus preserves its original properties.

2.1. Method of thermal fluctuations

The flickering of the red blood cells, which is a consequence of the fluctuations of their membrane was observed already in 1890 by means of the bright-field optical microscope (Browicz, 1890). Thermal fluctuations of bilayer membranes of vesicles occur due to Brownian motion of the water molecules, colliding with the membrane of the vesicle, causing a localized displacement. As stated in (Schneider et al., 1984), the magnitude of the bending stiffness could be theoretically deduced by measuring the shape of the vesicle as a function of the excess of the hydrostatic pressure of water exterior over the vesicle interior, however the pressure excess is too small to measure (Schneider et al., 1984). Due to small curvature modulus, there are many thermally accessible shapes having the same area and volume that are within kT (where $k = 1.38 \cdot 10^{-23}\ \mathrm{m^2 kg\, s^{-2} K^{-1}}$ is the Boltzmann constant and T the absolute temperature) of the equilibrium configuration of the flaccid vesicle. For this reasons, the shapes of a thin-walled unilamellar vesicle are observed to fluctuate.

The basic principles of spectral analysis of shape fluctuations are described in (Méléard et al., 1998). The sample vesicle equatorial cross section is focused under the microscope. For measurement of thermal fluctuations of phospholipid bilayer, the phase contrast or fluorescent microscopy is commonly used, as they emphasize the membrane outline. The series of still images taken from the experiment is analysed, to numerically evaluate the shape of the vesicle membrane (Genova et al., 2006, Fošnarič et al., 2013, Penič et al., 2015). The shapes are then developed into series of spherical harmonics functions and analzyed by a method proposed by Milner and Safran (1987). The time average of coefficients of spherical harmonics up to maximal possible mode are used to determine (K_c)

$$\langle U_l^m(t)^2 \rangle = \frac{k_B T}{K_c} \frac{1}{(l-1)(l+2)(\bar{\sigma} + l(l+1))}.$$

Besides the bending stiffness, this equation has a free parameter $\bar{\sigma}$ which corresponds to the average stretching energy of the vesicle and is estimated to be near zero for perfectly fluid membranes.

The fluctuation of the synthetically prepared GUVs is therefore measured by means of merely observing the behaviour of the phospholipid bilayer in its environment without any interaction with the vesicle itself. The measurement is fairly slow in comparison

with other methods presented in this work, as the measurement of a single vesicle takes 2-5 minutes. The reason for slow measurement process lays in the fact that the lowest modes of fluctuations are slow to dissipate. For analysis we require a series of independent shapes, thus we are required to take a still image every second in average.

3. Results

3.1. Optical phase-contrast microscope adaptation

Optical phase-contrast microscope is frequently used as research tool for observing thin phospholipid layers due to contrast enhancement of two optically different media (e.g. water and phospholipid mixture). The optical path of the microscope can be switched between ocular and camera output ports. By attaching CCD or newer CMOS camera sensor to the camera port, image can be acquired electronically and transported to computer as video signal or via common USB computer port.

The microscope modification for stroboscopic illumination was already implemented and described in (Genova et al., 2009, Genova and Pavlič, 2012). According to the distributor of Nikon microscopes, there is no light source splitter available for Nikon Eclipse TE2000-S phase-contrast microscope (that is used for research in our laboratory) on the market. The adaptation of the microscope to accept two light sources was done by means of additional aluminium wall chamber with retractable mirror to enable the additional light source port.

With the retractable mirror the experimenter can choose between the "constant intensity" halogen lamp light source or pulsing, stroboscopic flash light for sharper image registration for measurement of bending stiffness. The mirror is fixed on a hinge that can rotate about its axis and is controlled by a handle on top of the splitter fixture. The existing halogen lamp is fixed on the back of the chamber and the stroboscope light source is attached at the side with rubber spacers to reduce mechanical movement (shaking) of the microscope due to the flash tube discharge.

High intensity flash illumination, combined with CCD camera is cheap replacement for high sensitivity, high-speed camera, to register sharp images of vesicles. Most of the integration time of the camera the sample with the vesicle is in darkness, only a short burst of strong light is made during that time by the flash lamp. This produces sharp images of the vesicle in each frame and results in decreased error of determination of bending stiffness (Genova et al. 2006).

The Hamamatsu L7684 is a xenon flash lamp for industrial applications. It generates output power of 60 W in spectral range 240 nm to 2000 nm. It has a built-in reflective mirror, which focus all light made by arc of size 3 mm towards the borosilicate glass opening in the aluminium case. It can be triggered with voltages from 5-10 kV and can be operated under maximal repetition rate of 60 Hz. To achieve full power flashes an additional capacitor box Hamamatsu E7289 is connected to the xenon Flash Lamp power supply Hamamatsu C6096. High energy flashes also results in some energy losses in the lamp, therefore the cooling jacket Hamamatsu E6611 with the brushless DC motor fan is needed to keep the lamp at the operating temperature. The cooling jacket provides at the same time the socket into which the xenon flash lamp is inserted. It provides mechanical stability and allows mounting to the adapted light chamber of the microscope.

The controller that synchronizes camera with the flash light has been made using the microcontroller ATmega16, produced by Microchip. The choice of the microcontroller is not critical, as the signals timings are well below kHz range. The schematics of microcontroller and with main parts of the trigger system is shown in **Figure 2**. The microcontroller clock is generated with the 7,3728 MHz quartz crystal, allowing synchronization with standard UART speed. The connection with the computer for controlling the operation of the controller is made through serial connection with the FT232 adapter to enable USB connection. The speed of communication is 9600 baud 8N1.

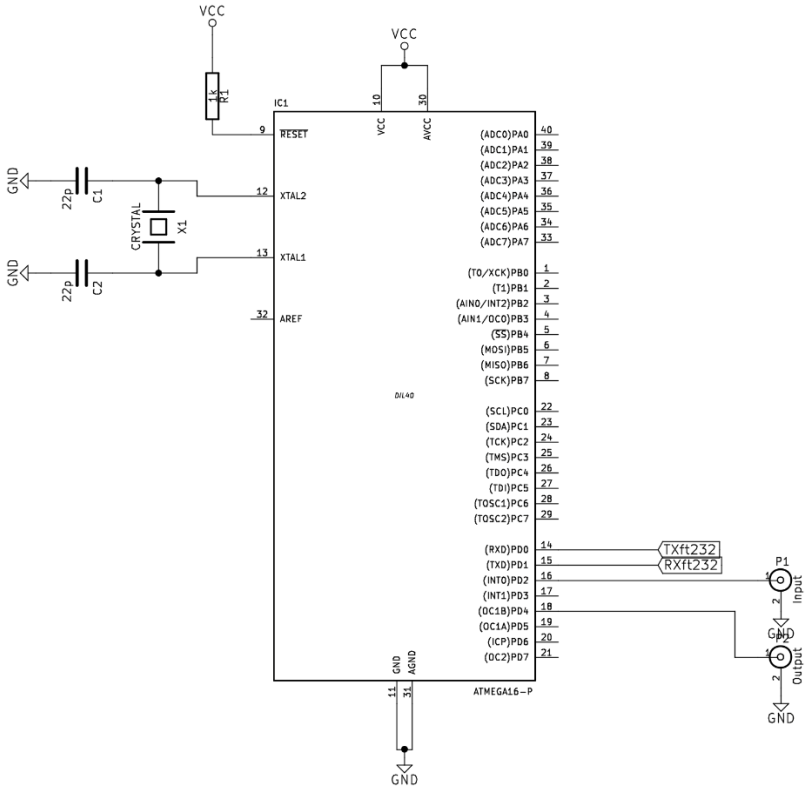

Figure 2. The electric schematics of the flash light controller using ATmega16 microcontroller. Only the most important connections are shown. At the bottom right there are input and output connections, where input presents trigger information from camera and output is trigger command signal to flash light source. The TX and RX pins are connected through RS232 to USB adapter to computer. Top left corner shows just components that are absolutely required for microcontroller to operate. By uploading the firmware to the microcontroller, the functionality can be altered, which adds to the flexibility of this design.

When the controller is switched on, the trigger is armed and waits for the camera sync pulses that generates lamp pulses for flash discharge. There is a possibility to turn on or off the trigger by sending single letter commands. This improves the automation of the measurement process. The microcontroller control of the triggering is flexible also because it is possible to programmatically set the time of the flash discharge within the integration frame of the camera if that is necessary, due to the possible camera integration start time jitter. The controller is connected to the computer via USB cable form which it also draws power.

The stroboscopic light was attached to microscope light port. There was mechanical adaptation of the microscope light port to gain additional light plug with mirror selector. The blueprint for the light mixing chamber is presented in **Figure 3**. On top of the chamber, stroboscopic light was mounted via 3D printed adaptor from white ABS plastics with shake reducing rubber spacer (see left panel of Figure 4 for exploded view of the final apparatus). The original halogen light source was mounted at the back of the mixing chamber. The final arrangement is shown on the photo in right panel of **Figure 4**. The detailed procedure of manufacturing the adaptor and light mixing chamber with two light ports is described in (Klanjšček and Penič, 2021).

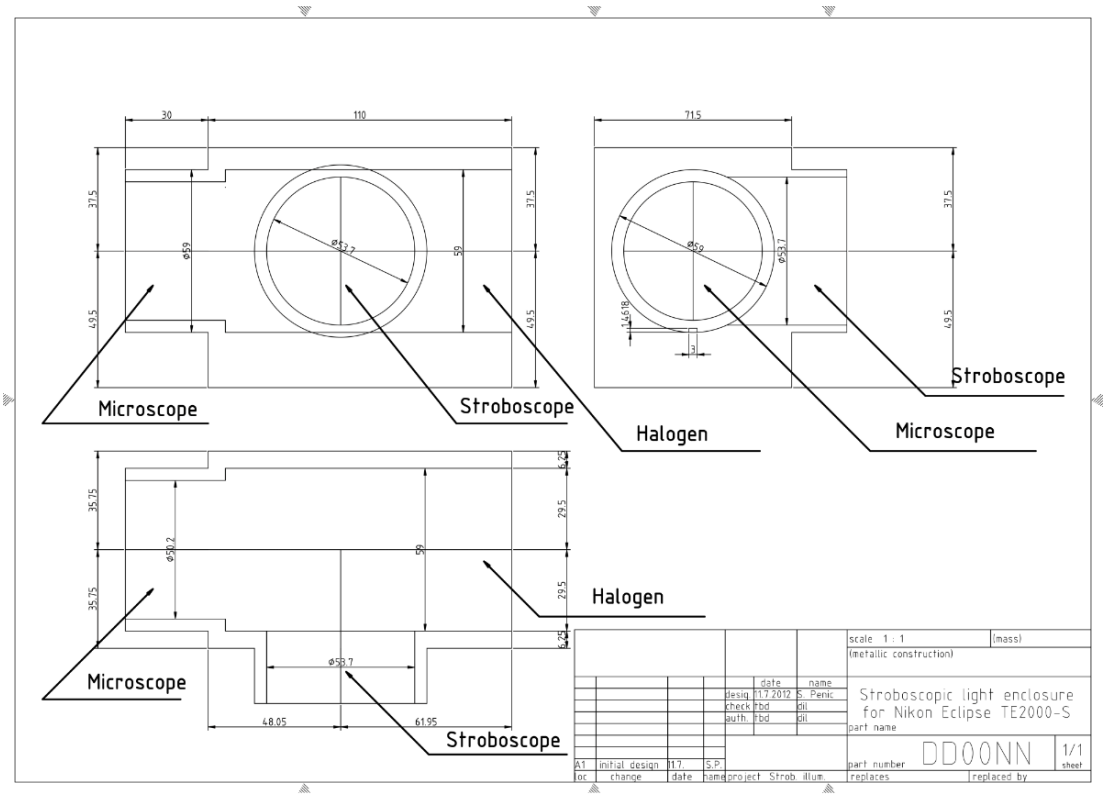

Figure 3. The blueprint for aluminium casing of light mixer with two input light ports and one output light conduit port.

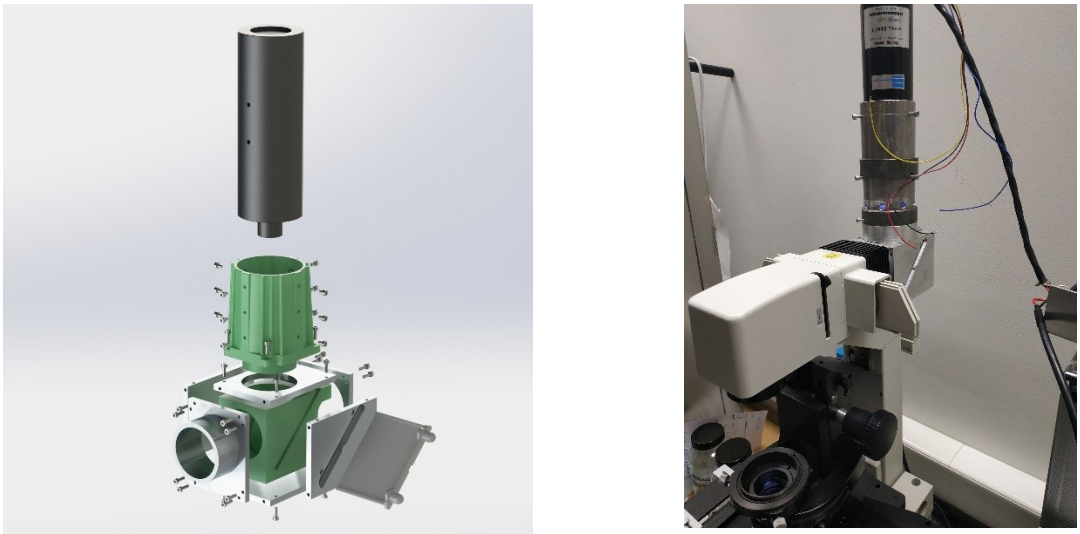

Figure 4. On the left panel, the exploded view of the microscope adaptation is shown. Metal parts are bolted together, the green part is a 3D printed plastic insert for the mirror assembly and stroboscope holder, which is represented in this figure in black color. Mirror tray is fully retraceable, allowing the selection of top light source or direct source from the back of the microscope. The right panel shows a photograph of mounted prototype to the microscope.

3. Conclusion

There are many different approaches to measuring bending stiffness. They vary in precision, the spatial and temporal precision of the method and amount of invasiveness to the measured specimen. A closer look of the thermal fluctuation measurement method was presented. The precision of the results depends on the image clarity, focus and blur.

The method of increasing the precision of the measurement was proposed, based on the experiences from authors in the literature and experiences gained by implementing the electro-mechanical system for the specific microscope in the laboratory.

The phase-contrast microscope was upgraded with flash light to enable registration of sharp images of vesicles for experimental determination of the bending stiffness of the giant unilamellar phospholipid vesicles. The mechanical modifications for attaching the additional light source to the microscope without the secondary light port was made and the electronics with corresponding software for controlling the flash discharge in sync with camera was devised. With modified light source, the analysis of fluctuaction modes is increased, resulting in more precise calculations of bending stiffness. The integration time of the camera is specified to be around 3 ms and can deviate from this value, depending on the frames-per-second settings. Stroboscopic pulse lasts around 2 μs and is therefore three orders of magnitude shorter. This does not necessary imply the highest recorded frequency will be three orders of magnitude higher, since this high frequency fluctuation modes tend to be lower in amplitude than low frequency ones and they depend on the stiffness of the vesicle and the type of the solution where the vesicles are in.

Conflicts of Interest: The authors declare no conflict of interest.

References

1. Boal DH. Mechanics of the cell. 2nd ed ed. Cambridge ; New York, Cambridge University Press. 2012.
2. Browicz T. Further observation of motion phenomena on red blood cells in pathological states. Zbl. med. Wissen. 1890; 28: 625–627.
3. Cucina A, Sterpetti AV, Pupelis G, et al. Shear stress induces changes in the morphology and cytoskeleton organisation of arterial endothelial cells. Eur J Vasc Endovascu Surg. 1995; 9: 86–92. DOI: 10.1016/S1078-5884(05)80230-8.
4. Evans E, Leung A. Adhesivity and rigidity of erythrocyte membrane in relation to wheat germ agglutinin binding. J Cell Biol. 1984; 98: 1201–1208. https://doi.org/10.1083/jcb.98.4.1201
5. Fabry B, Maksym GN, Hubmayr RD, et al. Implications of heterogeneous bead behavior on cell mechanical properties measured with magnetic twisting cytometry. Journal of Magnetism and Magnetic Materials. 1999; 194: 120–125. DOI: 10.1016/S0304-8853(98)00564-2.
6. Fošnarič M, Penič S, Iglič A, Bivas I. Thermal Fluctuations of Phospholipid Vesicles Studied by Monte Carlo Simulations. In: Iglič A, Genova J, editors. Advances in Planar Lipid Bilayers and Liposomes. 2013; 17: 331–357. DOI: 10.1016/B978-0-12-411516-3.00012-7
7. Genova J, Pavlič J. Realization of Marin Mitov's idea for the stroboscopic illumination used in optical microscopy. Bulgarian Journal of Physics. 2012; 39: 65–71.
8. Genova J, Zheliaskova A, Mitov MD. The influence of sucrose on the elasticity of SOPC lipid membrane studied by the analysis of thermally induced shape fluctuations. Colloids adn Surfaces A. 2006; 282–283: 420–422. DOI: 10.1016/j.colsurfa.2005.11.065
9. Genova J, Zheliaskova A, Vitkova V, Mitov MD. Stroboscopic illumination study of the dynamics of fluctuating vesicles. Journal of optoelectronics and advanced materials. 2009; 11: 1222–1225.
10. Jaasma MJ, Jackson WM, Keaveny TM. Measurement and Characterization of Whole-Cell Mechanical Behavior. Ann Biomed Eng. 2006; 34: 748–758. DOI: 10.1007/s10439-006-9081-0.
11. Jubery TZ, Srivastava SK, Dutta P. Dielectrophoretic separation of bioparticles in microdevices: A review: Microfluidics and Miniaturization. Electrophoresis. 2014; 35: 691–713. DOI: 10.1002/elps.201300424.
12. Klanjšček N, Penič S. Stroboskopski sistem za zajem slik fosfolipidnih veziklov za določanje mehanskih lastnosti. Proceedings of the 30th International Electrotechnical and Computer Science Conference ERK 2021 30: 423–426.
13. Lee C-H, Lin W-C, Wang J. All-optical measurements of the bending rigidity of lipid-vesicle membranes across structural phase transitions. Physical Review E. 2001; 64: 020901. DOI: 10.1103/PhysRevE.64.020901
14. Lin DC, Dimitriadis EK, Horkay F. Robust Strategies for Automated AFM Force Curve Analysis—I. Non-adhesive Indentation of Soft, Inhomogeneous Materials. J Biomech Eng. 2007; 129: 430–440. DOI: 10.1115/1.2720924.
15. Maniotis AJ, Chen CS, Ingber DE. Demonstration of mechanical connections between integrins, cytoskeletal filaments, and nucleoplasm that stabilize nuclear structure. Proceedings of the National Academy of Sciences. 1997; 94: 849–854. DOI: 10.1073/pnas.94.3.849.

16. Méléard P, Gerbeaud C, Bardusco P, et al. Mechanical properties of model membranes studied from shape transformations of giant vesicles. Biochimie. 1998; 80: 401–413. DOI: 10.1016/S0300-9084(00)80008-5.
17. Menger FM, Keiper JS. Chemistry and physics of giant vesicles as biomembrane models. Curr Opin Chem Biol. 1998; 2: 726–732. DOI: 10.1016/S1367-5931(98)80110-5.
18. Milner ST, Safran SA. Dynamical fluctuations of droplet microemulsions and vesicles. Physical Review A. 1987; 36: 4371–4379. DOI: 10.1103/PhysRevA.36.4371.
19. Mohandas N, Chasis JA, Shohet SB. The influence of membrane skeleton on red cell deformability, membrane material properties, and shape. Semin Hematology. 1983; 20: 225–242.
20. Morshed A, Karawdeniya BI, Bandara YMNDY, et al. Mechanical characterization of vesicles and cells: A review. Electrophoresis. 2020; 41: 449–470. DOI: 10.1002/elps.201900362.
21. Nussenzveig HM. Cell membrane biophysics with optical tweezers. Eur Biophys J. 2018; 47: 499–514. DOI: 10.1007/s00249-017-1268-9.
22. Pavalko FM, Chen NX, Turner CH, et al. Fluid shear-induced mechanical signaling in MC3T3-E1 osteoblasts requires cytoskeleton-integrin interactions. American Journal of Physiology-Cell Physiology. 1998; 275:1591–1601. DOI: 10.1152/ajpcell.1998.275.6.C1591.
23. Penič S, Iglič A, Bivas I, et al. Bending elasticity of vesicle membranes studied by Monte Carlo simulations of vesicle thermal shape fluctuations. Soft matter. 2015; 11: 5004–5009. DOI:10.1039/C5SM00431D
24. Phillips R. Physical biology of the cell. Second edition ed. London : New York, NY, Garland Science. 2013.
25. Piontek MC, Lira RB, Roos WH. Active probing of the mechanical properties of biological and synthetic vesicles. Biochim Biophys Acta Gen Subj. 2021; 1865: 129486. DOI: 10.1016/j.bbagen.2019.129486.
26. Schneider MB, Jenkins JT, Webb WW. Thermal fluctuations of large quasi-spherical bimolecular phospholipid vesicles. J. Phys.France 1984; 45: 1457–1472. DOI: 10.1051/jphys:019840045090145700.
27. Shao JY, Hochmuth RM. Micropipette suction for measuring piconewton forces of adhesion and tether formation from neutrophil membranes. Biophys J. 1996; 71: 2892–2901. DOI: 10.1016/S0006-3495(96)79486-9.
28. Song J, Waugh RE. Bending rigidity of SOPC membranes containing cholesterol. Biophys J. 1993; 64: 1967-1970. DOI: 10.1016/S0006-3495(93)81566-2
29. Zhou Y, Raphael RM. Effect of salicylate on the elasticity, bending stiffness, and strength of SOPC membranes. Biophys J. 2005; 89: 1789–1801. DOI: 10.1529/biophysj.104.054510

Scientific contribution/Original research

Nonspecific Influence of Surfactin on Lipid Membranes is Temperature Dependent

Drab M[1,*], Pandur Ž[2], Penič S[3], Iglič A[1,4], Kralj-Iglič V[5], Stopar D[2]

1. University of Ljubljana, Faculty of Electrical Engineering, Laboratory of Physics, Ljubljana, Slovenia
2. University of Ljubljana, Biotechnical Faculty, Department of Food Science and Technology, Ljubljana, Slovenia
3. University of Ljubljana, Faculty of Electrical Engineering, Laboratory of Bioelectromagnetics, Ljubljana, Slovenia
4. University of Ljubljana, Faculty of Medicine, Laboratory of Clinical Biophysics, Ljubljana, Slovenia
5. University of Ljubljana, Faculty of Health Sciences, Laboratory of Clinical Biophysics, Ljubljana, Slovenia

* Correspondence: Mitja Drab mitja.drab@fe.uni-lj.si

Abstract:
Surfactin is a lipopeptide produced by bacillus subtilis, and is a membrane fusion inhibitor that has a strong anti-viral effect. Surfactin has shown to solubilize cell and model membranes with a detergent-like mechanism that is highly unspecific. Unlike typical detergents its peptide headgroup is partially hydrophobic, resulting in a deeper insertion into the hydrophobic tail region of model membranes, which may be the reason for its high activity and specific, chain-tilting effects on membrane order. In this work we exposed dipalmytoyl-oleoylphosphatidylcholine (DOPC) giant unilamellar vesicles (GUVs) to different concentrations of Surfactin and found that at room temperatures, the membranes are stabilized with a network of pores resembling crater-like structures in optic and fluorescent microscopy images. At higher temperatures (60 °C), the pores disappeared and the vesicles were smooth like the control groups. We used a three-dimensional Monte Carlo scheme emulating the permeabilization process and found that simulations are a good predictor of experiments is we take into account the temperature-dependent spontaneous curvature of Surfactin. This is in line with previous experiments that show Surfactin disorders the acyl chains, rendering microdomain complexes on the membrane less negatively curved at an increased temperature.

Keywords: Giant phospholipid vesicles; Giant unilamellar vesicles; Surfactin; Lipid membrane; Monte Carlo simulation of vesicle shape; Membrane pore

Citation: Drab M, Pandur Ž, Penič S, Iglič A, Kralj -Iglič V, Stopar D. Nonspecific influence of surfactin on lipid membranes is temperature dependent. Proceedings of Socratic Lectures. 2021; 6: 125-129. https://doi.org/10.55295/PSL.2021.D.016

1. Introduction

Surfactin is a cyclic molecule with the characteristics of a wedge lipid: two acidic amino acid residues form a larger hydrophilic head, while the long chain fatty acid forms a smaller hydrophobic tail (Yuan et al., 2018). Surfactin has shown to solubilize cell and model membranes with a detergent-like mechanism that is highly unspecific. Unlike typical detergents its peptide headgroup is partially hydrophobic, resulting in a deeper insertion into the hydrophobic tail region of model membranes, which may be the reason for its high activity and and specific, chain-tilting effects on membrane order. Solid-state NMR studies of the structural effects exerted by surfactin show that only surfactin promotes a tilt of the acyl chains, behavior that is not observed in detergents (Heerklotz et al., 2004). However, the simple pizza-slice logic of a wedge-shaped Surfactin does not apply in reality. Since Surfactin promotes the tilting of the acyl chains of nearby lipids, a surfactin-lipid nanodomain can have net negative curvature. In this paper, this hypothesis is tested with optic and fluorescence microscopy and via a 3D Monte Carlo simulation.

2. Experimental observation

Giant DOPC unilamellar lipid vesicles were prepared as described by Moscho et al. (1996). Giant DOPC lipid vesicles were exposed to Surfactin under the microscope and monitored online to capture the early lipid vesicle dynamics. In the experiments, the concentration of GUV were between 106 and 107 vesicles/mL. All experiments were made under ambient conditions (room temperature, ambient air pressure) and higher temperatures (60 °C). The binary solutions were prepared with 9 μL of vesicle solution pipetted onto #1,5 microscope cover glass to form hemispheric drop, after positioning and focusing the solution on the microscope, approximately 1 μL of appropriate Surfactin solution final concentrations of Surfactin were approx. 0,2 mM. Image acquisition started right after the start of addition of surfactin. Dynamics of lipid solubilization with surfactin was visualized with laser microscope fluorescence microscope Zeiss Axio Observer Z1 equipped with confocal unit LSM 800 (**Figure 1**).

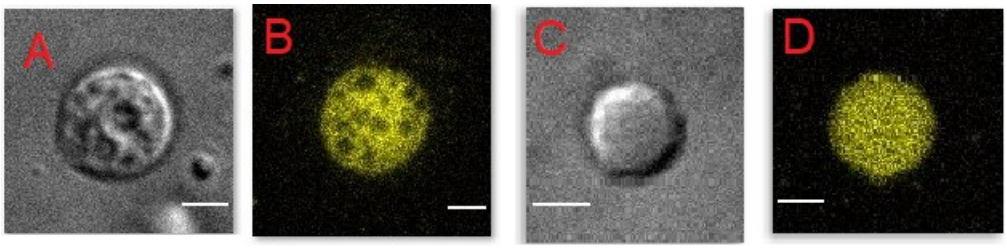

Figure 1. Surfactin and GUV microscopy results taken at room temperature (A, B) and at 60 °C (C, D). The vesicles are stable for many minutes and display no violent dynamics like in the case of detergent Triton X-100. The bar represents 5 μm. From (Drab et al., 2021).

3. Monte Carlo simulation results

The membrane is represented by a set of N vertices that are linked by tethers of variable length l to form a closed, dynamically triangulated, self-avoiding two-dimensional network (as described in (Gompper and Kroll, 1996; 2004; Fošnarič et al., 2019)). The microstates of the membrane are sampled according to the Metropolis algorithm. The probability of accepting the change of the microstate due to vertex move or bond flip is $\min[1, \exp(-\Delta E/kT)]$, where ΔE is the energy change, k is the Boltzmann constant and T is absolute temperature. The energy for a given microstate is specified by the standard Helfrich equation (Helfirch, 1973):

$$W_b = \frac{\kappa}{2}\int_A (c_1 + c_2 - c_0)^2 dA, \quad (1)$$

where the integral runs over the whole area of the membrane with bending stiffness κ, c_1 and c_2 are principal curvatures and c_0 the spontaneous curvature of the surfactin inclusions. The surfactin inclusions on the membrane are therefore modeled as patches of the membrane with given spontaneous curvature c_0. The patches occupied by the surfactins we set $c_0 < 0$ and elsewhere we assume a symmetric membrane $c_0 = 0$.

Additionally, to account for associative nature of membrane inclusions, a step potential between neighboring curved inclusions is taken into account by an additional energy term:

$$W_d = -w \sum_{i<j} \mathcal{H}(r_0 - r_{ij}), \tag{2}$$

where w is a direct interaction constant, the sum runs over all surfactin-surfactin pairs, r_{ij} are their mutual in-plane distances, $\mathcal{H}(r)$ is the Heaviside step function and r_0 is the range of the direct interaction. We consider here attractive interactions $w > 0$ that induce phase-separation of the lipid bilayer.

In this work we set N_d of the total $N = 1447$ vertices to represent surfactin domains (curved inclusions), which have spontaneous curvature c_0 that can be described well by the discrete mesh. All other vertices represent symmetric membrane and have zero spontaneous curvature. The positive sign of c_0 for curved inclusions indicates a tendency to curve the membrane outwards. The density of curved inclusions on the membrane is given by a fraction:

$$\rho = \frac{N_d}{N}. \tag{3}$$

We presume that surfactin has a temperature-dependent spontaneous curvature. We approximate this function by setting

$$c_0 = \frac{1}{2}\left(\frac{T}{T_0}\right) - 1. \tag{4}$$

In each such step, the total energy $W = W_b + W_d$ is numerically minimized. We can also define the mean cluster size of nanodomains with the equation:

$$\langle N_{vc} \rangle = \langle \frac{\sum N_{vc}^i N_{cl}^i}{N_{cl}^i} \rangle. \tag{5}$$

Here, the angle brackets denote the canonical ensemble average. At any given time during the simulation, N_{vc} is the mean cluster size and the sums run over all clusters of vertices representing proteins. In the sums N_{vc}^i is the number of vertices in cluster i and N_{cl}^i is the number of clusters of size N_{vc}^i. The cluster increase in size with increasing density of surfactin inclusions.

Simulation results shown in **Figure 2** reveal that the phase space of solutions in the (ρ,(T/T_0)) plane results in smooth vesicles, while at lower temperatures, a transition towards buds is seen (marked by the S-E transition line). At lower temperatures, more of these buds are seen (E(4) means that 4 buds are seen in the simulation). Some of these simulated shapes are shown in **Figure 3**.

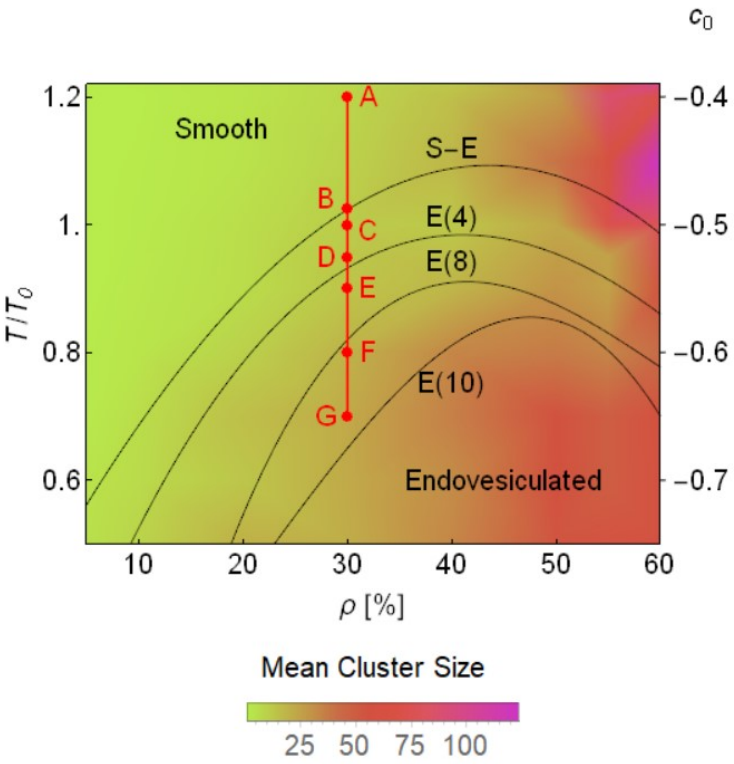

Figure 2. A phase diagram of the simulations in the (ρ,(T/T_0)) plane. Note that increasing temperature corresponds to less negative net spontaneous curvature of the nanodomains. The lines denote regions where inward curving buds are observed that correspond to crater like shapes in microscopic images. The cross-sections of the final micorstates of the vesicles shown in the slice of the phase diagram denoted by the red line are seen in **Figure 3**. The color scheme represents the mean cluster size given by Eq.(4).

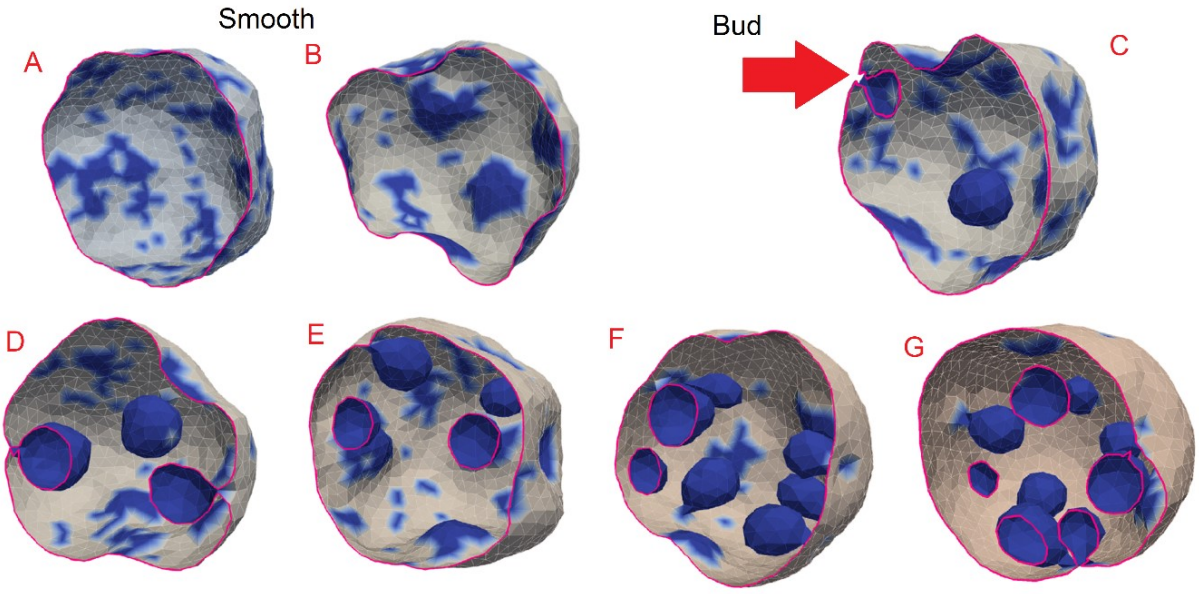

Figure 3. Cross sections of final microstates of vesicles for points shown in **Figure 2**. The patches of flat membrane with no spontaneous curvature are shown gray, while the blue areas correspond to negative spontaneous curvature c_0 where curved inclusions are present.

4. Discussion

Solubilization mechanisms of Surfactin are not completely understood and their use remains empirical even for systems of liposomes. The structural changes of liposomes induced by detergent solutions are known experimentally for some time and reveal that liposomes take various types of solubilization pathways depending on the types of lipids and detergents (Arnulphi et al., 2007; Tomita et al., 2011). In the present work, a possible mechanism of membrane structural changes seen in experiments with DOPC liposomes and Surfactin is presented within a simple Monte Carlo model of curved inclusions that can move over the membrane laterally and induce local curvature changes due to their molecular shape. This leads to a temperature dependent shapes seen in experiments before total solubilization and micellization of liposomes takes place. This is due to the unspecific surfactin mechanism that tilts the acyl chains at higher temperatures, rendering the net spontaneous curvature of the nanodomains less negative.

5. Conclusions

In this work the interaction between DOPC GUVs and Surfactin was studied with an emphasis on the processes prior to solubilization. An interesting temperature dependence of pore foramtions was observed at room temperature and 60 °C. A possible mechanism for such a process was proposed that is based on the geometrical and associative properties of the surfactin molecules that are adsorbed and laterally diffuse across the lipid vesicle. A 3D Monte Carlo numerical simulations were used to study the phase space of stable shapes and their spontaneous curvature dependence on temperature explored. It was found that at lower temperatures, the nanodomains form to construct a highly ordered membrane with buds that curve inward, while at higher temperatures, the more fluid membrane results in a less net negative curvature, rendering the shapes smoother. The results are in line with the existing literature and shed a new light on the mechanical and dynamical aspects of the early stages of the solubilization process.In his view the problem is ill-posed. He was asked to sing the love as if it were a single thing, then there are several types of love. We must look what kind of love is worthy of praise.

Funding: Authors acknowledge support of ARRS, grants P2-0232, P3-0388, P4-0116, L3-2621, J3-0388.
Conflicts of Interest: The authors declare no conflict of interest.

References

1. Arnulphi C, Sot J, Garcia-Pacios M, Arrondo JLR, et al. Triton X-100 partitioning into sphingomyelin bilayers at subsolubilizing detergent concentrations: effect of lipid phase and a comparison with dipalmitoylphosphatidylcholine. Biophys J. 2007; 93: 3504-3514. DOI: 10.1529/biophysj.107.104463
2. Drab M, Pandur Z, Penic S, et al. A Monte Carlo study of giant vesicle morphologies in nonequilibrium environments. Biophys J. 2021; 120: 4418-4428. DOI: 10.1016/j.bpj.2021.09.005
3. Fošnarič M, Penič S, Iglič A, Kralj Iglič V, et al. Theoretical study of vesicle shapes driven by coupling curved proteins and active cytoskeletal forces. Soft Matter. 2019; 15: 5319-5330. DOI:10.1039/C8SM02356E
4. Gompper G, Kroll DM. Random surface discretizations and the renormalization of the bending rigidity. J. Phys. I France. 1996; 1305-1320. DOI: 10.1051/jp1:1996246
5. Gompper G, Kroll D. Triangulated-surface models of fluctuating membranes. Statistical mechanics of membranes and surfaces. 2004; World Scientific. 359-426. DOI: 10.1142/9789812565518_0012
6. Heerklotz H, Wieprecht T, Seelig J. Membrane perturbation by the lipopeptide surfactin and detergents as studied by deuterium NMR. J. Phys. Chem. B. 2004; 108: 4909-4915. https://doi.org/10.1021/jp0371938
7. Helfrich W. Elastic properties of lipid bilayers: theory and possible experiments. Z Naturforsch C. 1973; 28: 693-703. DOI: 10.1515/znc-1973-11-1209
8. Moscho A, Orwar O, Chiu DT, et al. Rapid preparation of giant unilamellar vesicles. Proc Natl Acad Sci USA. 1996; 93: 11443-11447. DOI: 10.1073/pnas.93.21.11443
9. Tomita T, Sugawara T, Wakamoto Y. Multitude of morphological dynamics of giant multilamellar vesicles in regulated nonequilibrium environments. Langmuir. 2011; 27: 10106-10112. DOI: 10.1021/la2018456
10. Yuan L, Zhang S, Wang Y, et al. Surfactin inhibits membrane fusion during invasion of epithelial cells by enveloped viruses. J Virol. 2018; 92 : 00809-18. DOI: 10.1128/JVI.00809-18

Scientific contribution/Review

The Big Bang Theory

Mesarec L[1]*

1. Laboratory of Biophysics, Faculty of Electrical Engineering, University of Ljubljana, 1000 Ljubljana, Slovenia
* Correspondence: Luka Mesarec; luka.mesarec@fe.uni-lj.si

Abstract:
In this contribution, the Big Bang theory is presented to describe the evolution of our universe. The Big Bang theory states that the universe started in a point with an infinite energy density about 14 billion years ago and has been expanding ever since. Crucial for this theory is the Hubble's discovery that observed galaxies are moving away from us. The evolution of our universe has mostly been governed by the forces of gravitation; therefore, Newton's law of gravity is used to derive the equations that describe how the size of our universe is changing with time. From these equations, it is possible to estimate the age of our universe. In this contribution we present the model of the universe and derivation of the estimation of the universe age.

Keywords: The Big Bang; Universe; Gravity; Hubble's constant; Age of the universe

Citation: Mesarec L The Big Bang Theory. Proceedings of Socratic Lectures. 2021; 6: 131-136. https://doi.org/10.55295/PSL.2021.D.017

1. Introduction

The Big Bang theory describes the evolution of the universe. The essence of the theory is that the universe started in a point with an infinite energy density and has been expanding ever since (Peebles et al., 1994). Consequently, the galaxies today are moving away from each other, which can be observed by measuring the amount of red shift in the light emitted by a galaxy. We will use Hubble's discovery that the galaxies, which are further away from us, are actually moving away from us faster. With the aid of the Newton's law of gravitation, we will derive the equations which govern the evolution of the universe and estimate the age of the universe.

2. Methods

Edwin Powell Hubble discovered that almost all galaxies in the universe are moving away from us. This was a revolutionary discovery since theories before that assumed a static universe. Furthermore, by measuring the red shift in the light emitted by galaxies, he discovered an even more important fact: the galaxies that are further away from us are moving away from us faster (Osterbrock et al., 1993). Hubble's law states that the velocity with which a certain galaxy is moving away from us is proportional to the distance to that galaxy (**Figure 1**). Note that some neighbouring galaxies could be approaching each other because of gravitational forces.

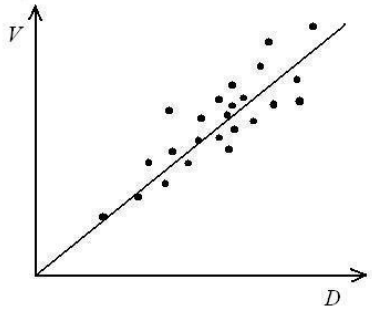

Figure 1. The velocity (V) of the galaxies that are moving away from us as a function of the distance (D) of those galaxies relative to us (Liddle, 2003).

We can visualise space as an elastic band which is expanding. If both ends of the elastic band are moving away from each other with a constant velocity then any two points on the elastic band are also moving away from each other. Larger the distance between the two points on the elastic, higher the relative velocity between them. The observer can be placed on any point on the elastic band and they will see all the other points moving away from them. We use a simple 1D model, where galaxies are homogeneously distributed along the x-axis (**Figure 2**). Coordinate x is in this formulation used to number the galaxies. The distance between the neighbouring galaxies is denoted by the scale factor $a(t)$, which is a function of time because the universe in not static.

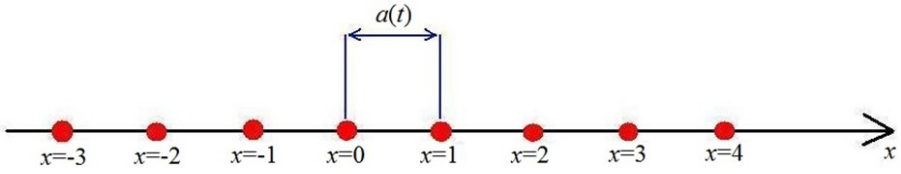

Figure 2. Galaxies that are moving away from each other are homogeneously distributed along the x-axis.

The distance between any two galaxies in these coordinates can be written as:

$$D = a(t)\Delta x. \tag{1}$$

The relative velocity between any two galaxies is therefore:

$$V = \dot{a}(t)\Delta x = \frac{\dot{a}(t)}{a(t)}a(t)\Delta x = \frac{\dot{a}(t)}{a(t)}D, \tag{2}$$

where the dot denotes the derivative with respect to time. Hubble's constant is introduced as:

$$H = \frac{\dot{a}(t)}{a(t)}\ . \tag{3}$$

Hubble's constant is a constant in space, which means that it is the same throughout the universe at a certain time. Nevertheless, it is changing with time when the universe is expanding because the scale factor $a(t)$ changing with time. By inserting Eq. (3) into Eq. (2) we obtain:

$$V = HD. \tag{4}$$

The velocity of a certain galaxy moving away from us is therefore proportional the distance to that galaxy, which is also an experimental fact presented in **Figure 1**, where Hubble's constant H is the slope of the line presented in the graph.

To study the evolution of the universe, we will use Newton's gravitational law. Newton's cosmology assumes that gravitation is the only force that governs the universe. This is actually not correct because today the evolution of the Universe in mostly dictated by the dark energy, while right after the Big Bang, radiation was the most important (Liddle, 2003). Nevertheless, classic gravitation is sufficient to describe the most of the universe's evolution so far. We will assume that universe is homogeneous and isotropic. We will write equations relative to the virtual origin in $x = 0$ as presented in **Figure 3**.

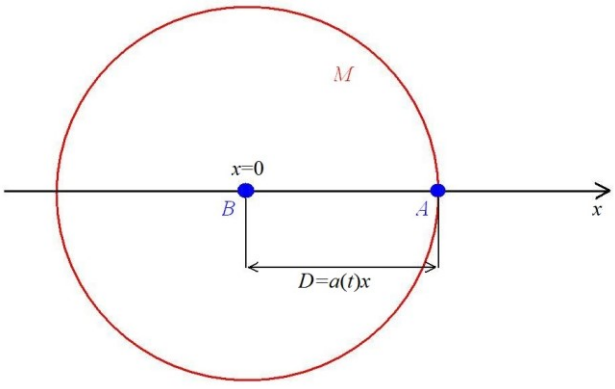

Figure 3. Coordinates that are used to derive the time dependence of the scale factor $a(t)$. Red circle represents a spherical shell with the radius D, which contains homogeneously distributed galaxies. M is the mass of all galaxies inside the shell.

First, we write the energy of the galaxy located at the point A as this galaxy is moving away from the origin at the point B (**Figure 3**). From the Newton's shell theorem, we know that the mass inside the shell with the radius D is acting on the galaxy located at the

point *A* as it would all be concentrated in the centre of the shell at the point *B*. Furthermore, all the mass outside of the shell has no gravitational effect on the galaxy located at the point *A*. Total energy of the galaxy at the point *A*, which is moving away from the origin, is written as a sum of kinetic and potential energy:

$$\frac{1}{2}mV^2 - \frac{MmG}{D} = E, \tag{5}$$

where *m* is the mass of that galaxy and *V* its velocity. *M* is the mass of all galaxies inside the shell and *G* is gravitational constant. Total energy of the galaxy *E* is conserved with time. By inserting Eqs. (1) and (2) into Eq. (5) we get:

$$x^2\dot{a}(t)^2 - \frac{2MG}{xa(t)} = \frac{2E}{m}\ . \tag{6}$$

Note that Δx from Eqs. (1) and (2) was replaced with x since the distance D is measured from the origin as presented in **Figure 3**. Mass *M* can be written as a product of the mass density ρ of the galaxies inside the shell and the volume of the spherical shell with the radius D: $V_K = 4\pi D^3/3 = 4\pi x^3 a(t)^3/3$. Eq. (6) is thus transformed into:

$$x^2\dot{a}(t)^2 - \frac{8G\rho\pi x^2 a(t)^2}{3} = \frac{2E}{m}\ , \tag{7}$$

where the mass density ρ is changing when the universe is expanding. Lefthand side of Eq. (7) is proportional to x^2. The equation can be solved if we assume that also the righthand side is proportional to x^2, which is reasonable because the energy of the galaxies further away should be larger since they are moving away from us faster. We define constant *k*:

$$k = -\frac{2E}{mx^2}\ . \tag{8}$$

Energy has to be proportional to x^2 for *k* to be constant. With this assumption, the result does not depend on the chosen pair of galaxies because all terms with x^2 cancel out. If equation (8) is considered in Eq. (7), we get the Friedmann equation:

$$H^2 = \frac{\dot{a}(t)^2}{a(t)^2} = \frac{8}{3}G\rho\pi - \frac{k}{a(t)^2}\ , \tag{9}$$

which tells us how $a(t)$ is changing with time. Solutions of Eq. (9) are presented in the next section.

6. Results

Solutions of equation (9) depend on the value of the constant *k*. There are three qualitatively different solutions. If $k > 0$, the absolute value of gravitational energy is larger than kinetic energy. In this case, gravity stops the expansion and the universe starts to shrink back after some time (**Figure 4**, blue line). When $k < 0$, the kinetic energy is larger compared to the absolute value of gravitational energy and the expansion of the universe never stops (**Figure 4**, green line). And lastly, for $k = 0$, the absolute value of gravitational

energy is the same as kinetic energy. In this case, the velocity of expansion is always decreasing and the expansion stops in infinity (**Figure 4**, red line). Observations show that our universe is close to the critical case $k = 0$ (Liddle, 2003). To solve the differential Eq. (9), we write the mass density as:

$$\rho = \frac{M}{a(t)^3}\,, \tag{10}$$

where the mass M inside the volume element $a(t)^3$ is constant. If Eq. (10) is considered in Eq. (9), we obtain the following differential equation for $a(t)$:

$$\frac{\dot{a}(t)^2}{a(t)^2} = \frac{8GM\pi}{3a(t)^3} - \frac{k}{a(t)^2}\,. \tag{11}$$

Solutions of Eq. (11) for different values of k are presented in **Figure 4**.

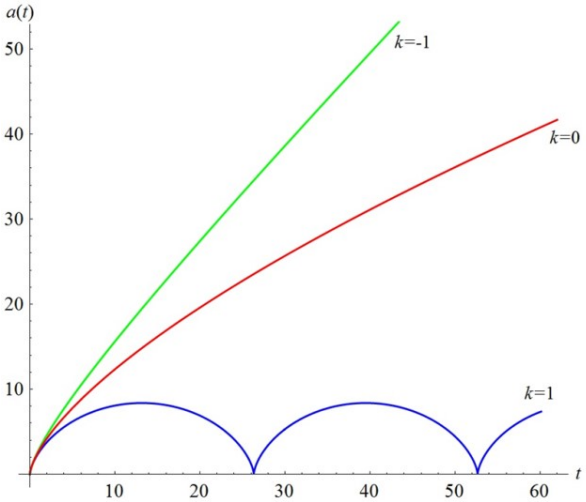

Figure 4. Time dependence of the scale factor $a(t)$ obtained by solving the differential Eq. (11) for different values of the constant k. Blue line represents the evolution of the closed universe ($k > 0$). Red line represents the evolution of the critical universe ($k = 0$). Green line represents the evolution of the open universe ($k < 0$). Other parameters in Eq. (11): $G = 1$, $M = 1$.

To estimate the age of our universe, we will write the solution of the differential Eq. (11) for $k = 0$. The equation can be solved by assuming the solution:

$$a(t) = Ct^p, \tag{12}$$

where C and p are constants, which are determined by inserting Eq. (12) into Eq. (11). We obtain the following solution:

$$a(t) = \sqrt[3]{6\pi MG}\; t^{2/3} \propto t^{2/3}. \tag{13}$$

At the time $t = 0$ the scale factor $a(t) = 0$ and the whole universe is concentrated in a single point. This is the time of the Big Bang and from that point the universe starts to expand and has been expanding ever since. Therefore, time t is measured from the Big

Bang. This solution is presented as a red line in Figure 4. If we plug the solution from Eq. (13) into the Eq. (3), we get the time dependence of the Hubble's constant for our universe:

$$H = \frac{2}{3t} \propto \frac{1}{t} . \tag{14}$$

By measuring the Hubble's constant, we can estimate the age of our universe:

$$t_V = \frac{2}{3H} . \tag{15}$$

The age of our universe is approximately 14 billion years (Hawley et al., 2005). Hubble's constant can be measured by measuring the distance to different galaxies and their velocity relative to us. In **Figure 1**, Hubble's constant *H* is the slope of the line presented in the graph.

7. Discussion

This contribution presents the description of the universe within the Newton's law of gravitation, which assumes that gravitation is the only force that governs the evolution of the universe. Today, the expansion of the universe is actually dictated by the dark energy, while in the early stages the radiation played the most important role (Liddle, 2003). Nevertheless, the main part of the evolution of our universe was governed by gravitational forces (Liddle, 2003). We derived the equation, which tells us how the size of the universe has been changing with time since the Big Bang, which allowed us to estimate the age of our universe. For more accurate and comprehensive description, we would have to use the Einstein's theory of general relativity. Our universe is close to the critical universe, which means that the absolute value of gravitational energy has a similar value as kinetic energy. Considering only this fact, the velocity of the expansion of our universe should decrease over time. Nevertheless, the accelerated expansion has been observed. This is a consequence of the dark energy effect, which causes the exponential expansion of the universe. We are now in the dark energy dominated era and our universe will expand even faster in the future (Hawley et al. 2005).

Funding: This research was supported by Slovenian Research Agency through the grant no. P2-0232.

Conflicts of Interest: The authors declare no conflict of interest.

References

1. Hawley JF, Holcomb KA. Foundations of Modern Cosmology. New York, Oxford University Press. Second Edition. 2005.
2. Liddle A. An Introduction to Modern Cosmology, Second Edition. Chichester, John Wiley and Sons Ltd. 2003.
3. Osterbrock DE, Gwinn JA, Brashear RS. Edwin Hubble and the Expanding Universe. Scientific American. 1993; 148: 84–89. DOI: 10.1038/scientificamerican0793-84
4. Peebles PJE, Schramm DN, Turner EL, Kron RG. The Evolution of the Universe. Sci Am. 1994; 271: 53–57. DOI: 10.1038/scientificamerican1094-52

Scientific contribution/Original research

The Pioneering Research Practices of Designer Janja Lap

Predan B [1], Šubic Š [2,*]

1. University of Ljubljana, Academy of Fine Arts and Design, Ljubljana, Slovenia
2. Museum of Architecture and Design, Ljubljana, Slovenia

* Correspondence: Špela Šubic spela.subic@mao.si

Abstract:
Janja Lap (1929–2004) is known to the Slovenian professional public as a first-rate glass designer and industrial designer in the field of electro-optical device development. For most of her professional life she was also a devoted researcher in the field of design, yet this facet of her work remained largely overlooked by both the professional and general public until the beginning of 2021, when the Museum of Architecture and Design acquired her archive. In this text we attempt to show that what sets her research apart is the way it thoughtfully weaves together two scientific approaches to design that each characterise a different school: one the Faculty of Architecture in Ljubljana and the other the Royal College of Art (RCA) in London. In other words, we can trace in her work the intertwining of two threads of knowledge: one arising from the architectural and urbanistic background she acquired during her studies under the mentorship of Edvard Ravnikar in what was then Yugoslavia, and the other obtained at the RCA under the mentorship of Bruce Archer, the British mechanical engineer and the first professor to devote himself to systems-level research in design, and Sir Misha Black, a pioneer in the development of scientific research approaches in the field of design.

Keywords: Janja Lap; Slovene design; Ljubljana School of Architecture; Edvard Ravnikar, Sir Misha Black**;**

Citation: Predan B, Šubic Š. The pioneering research practices of designer Janja Lap. Proceedings of Socratic Lectures. 2021; 6: 138-146. https://doi.org/10.55295/PSL.2021.D.018

1. Introduction

After the Second World War, the Yugoslav economy was in a process of massive industrial expansion. Slovenia was undergoing an intensive transformation from an agricultural society to an industrial one. The political-economic system had transitioned from the pre-war capitalism to socialism. Nationalisation and the consolidation of individual production facilities into larger factories geared towards mass production required a different development direction with modified approaches and different results. The large-scale push towards industrialisation had the most success in those industries that had a tradition going back to the pre-war period, among them the wood, textile and glass industries. All industries had to maintain a level of productivity that allowed meeting the country's need for foreign currency, while at the same time reorienting themselves towards a new way of developing and manufacturing modern industrial products.

Figure 1. The Yugoslav pavilion at the XI. Triennale in Milano, 1957, photo: Janez Kališnik. (From MAO photo library, F1110)

In addition to the above, there is another factor crucial for the understanding of the Yugoslav path towards industrialisation paved with socialism, namely the active integration of society with the aim of establishing an alternative to the prevailing ideology of the time, which entailed the division of the world into blocs in a perpetual state of Cold War. After 1948, Yugoslavians chose to reject both of the major blocs' ideologies—the ideology of Western capitalism, as well as the state socialism of the East. In the former, the problem they identified was that in capitalism, the integration of society is mostly carried out by the market, with partial assistance from the state. In centrally planned socialist societies, by contrast, this integration is predominantly a responsibility of the state, with partial assistance from the market (Kavčič, 1987). Consequently, in Yugoslavia in the 50s and especially the 60s, the path beyond bloc politics was represented by the non-aligned movement, while the alternative in the area of the sociology of work was built on the idea of socialist self-management. All of the above also proved vital for the further professionalisation and development of Slovenian design.

There was at the time a growing awareness among the designers of the urgent need to bring about the conditions for developing, designing and manufacturing higher-quality everyday products, joined by a desire for their profession to have a role in industrial production. The furniture pieces exhibited by domestic producers at fairs were

criticised by the young architects as ill-suited to modern types of housing. The only producer to stand out was the Stol factory, the first in Yugoslavia to employ a designer (in 1952), followed by manufacturers such as Iskra, Gorenje and others. In the same period —beginning with 1948—a need to establish a system of higher education for industrial designers became apparent. One of the main initiators of this movement was Edvard Ravnikar, an architect and a professor to the protagonist of this text, the designer and architect Janja Lap.

2. The background of the study and research methods

After the Second World War, the foremost researchers in the field of design in Slovenia included the architect Branka Tancig, whose research involved, among other topics, the concept of the "laboratory" kitchen (Tancig-Novak, 1958; 1971), architects France and Marta Ivanšek, whose research focused on dwellings and their furnishings (Ivanšek, 1959; 1960), and the sculptor and industrial designer Ciril Cesar, who, inspired by the design research institutes at The Ulm School of Design (Hochschule für Gestaltung Ulm) in Germany, sought ways to introduce research into the economy, which in his case meant the producer of household appliances Gorenje (Berg et al., 1978).

Figure 2. The "laboratory" kitchen of designer Branka Tancig with a study into the patterns of movement within the kitchen, 1958, photo: Janez Kališnik. (From MAO photo library, F7, and Tancig 1953).

In contrast to the researchers listed above, Janja Lap and her work remained largely unknown until today. The only record of her research can be found in a 1980 issue of the Belgrade magazine *Industrial Design*, where Lap summarised the research that had been carried out and the potential it held (Lap, 1980). Yet further investigation and intensive examination of the archives led to the discovery of the rest of her extensive and systematically preserved scientific research. The present text is based on the analysis and interpretation of the impact of her research studies and personal documents. Between January and October 2021, we also conducted a series of semi-structured interviews with her son, as well as with students from the period when she was teaching and researching in the UK, as we wished to understand the broader context of her work and research. In this text we focus in particular on her unpublished research studies and other unpublished documents in the archive, such as study materials, preparatory materials for research, detailed research funding applications, and numerous biographical and bibliographical records. These bear witness to the restless spirit of a designer who constantly sought out new opportunities that would allow her to carve out a niche for herself, as well as challenge her to pursue further research.

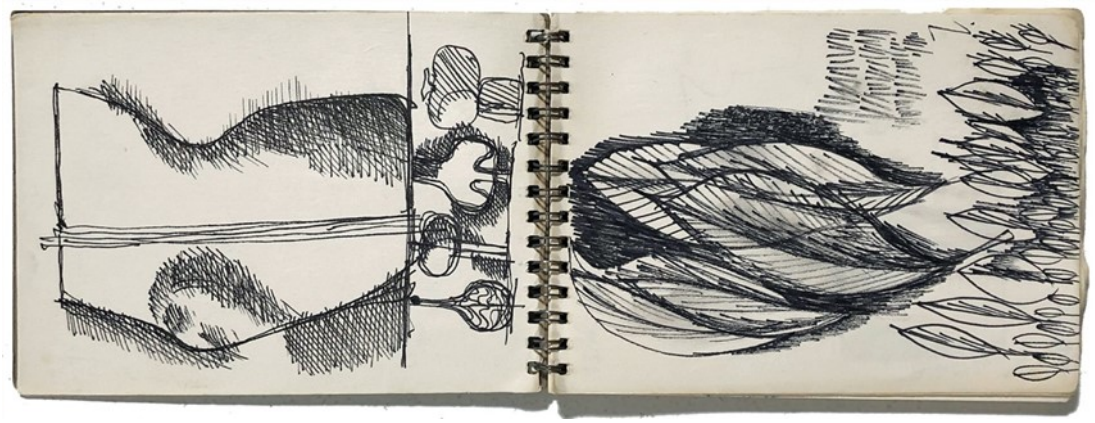

Figure 3. Janja Lap's sketchbook.

The results of the study, which lasted for several months, paint a picture of an exceedingly astute researcher and a first-rate designer. She was born in 1929 in Ljubljana, in what was then the Kingdom of Yugoslavia; Janja Lap's father was Anton Lap, an engineer, who was the head of landscaping in Ljubljana and a close associate of the domestically and internationally acclaimed architect Jože Plečnik. He collaborated with the latter in practically all of his projects in Ljubljana that involved planting and landscaping. Her childhood admiration for Plečnik as a master of his craft ended up influencing her decision to study architecture. During her studies at the Faculty of Architecture, Civil and Geodetic Engineering in what had by then become the Socialist Federal Republic of Yugoslavia, Lap soon proved to be a diligent student, becoming first an assistant to the architect and professor Edvard Ravnikar and eventually his colleague.

Figure 4. Janja Lap presenting a project for a 7000-person housing estate 1958. Left to right: Večeslav Holjevac, Josip Broz - Tito, Aleksandar Ranković, Jovanka Broz, Pepca Kardelj, Lidija Šentjurc and Janja Lap. (From Jeffs, XXXX).

In 1956, she graduated with a first degree and five years later with a second. In 1964, following a brief stint at the Secondary School of Design and Photography in Ljubljana, she joined a research team at the Royal College of Art (RCA) in London with a scholarship from the British Council. Until 1977, save for a few short breaks, she remained a permanent resident of the United Kingdom, where, among other things, she completed Master's level studies at the RCA, lectured at the University of Sheffield, engaged in creative work and, above all, researched extensively. Upon her return to Slovenia she first worked as a researcher in the field of social issues in housing construction at the Institute of Sociology and Philosophy at the University of Ljubljana. In 1979, she began a 10-year stint at Iskra as a designer of electro-optical devices. In 1990, she received the title of assistant professor for the subject "Applied Arts: Glass". In the period shortly before Slovenian independence, she lectured at the University of Mosul in Iraq as part of the treaties among the non-aligned countries; afterwards, she worked until her retirement at the Faculty of Education in Ljubljana and at the Slovenian branch of the Open University.

In 1956, she graduated with a first degree and five years later with a second. In 1964, following a brief stint at the Secondary School of Design and Photography in Ljubljana, she joined a research team at the Royal College of Art (RCA) in London with a scholarship from the British Council. Until 1977, save for a few short breaks, she remained a permanent resident of the United Kingdom, where, among other things, she completed Master's level studies at the RCA, lectured at the University of Sheffield, engaged in creative work and, above all, researched extensively. Upon her return to Slovenia she first worked as a researcher in the field of social issues in housing construction at the Institute of Sociology and Philosophy at the University of Ljubljana. In 1979, she began a 10-year stint at Iskra as a designer of electro-optical devices. In 1990, she received the title of assistant professor for the subject "Applied Arts: Glass". In the period shortly before Slovenian independence, she lectured at the University of Mosul in Iraq as part of the treaties among the non-aligned countries; afterwards, she worked until her retirement at the Faculty of Education in Ljubljana and at the Slovenian branch of the Open University.

Even this brief and highly abbreviated overview of her life attests to her exceptional learning capacity, highly pronounced curiosity and ability to identify new challenges. It is no wonder, then, that on her arrival in London (1964) she integrated so well into the research community at the RCA, which at the time was a pioneering one. It was then that she first demonstrated a desire and aptitude for researching and designing complex systems—systems that go beyond the mere transformation of products and services for a single entity; she continuously focused on understanding and designing a holistic approach in the broader social and geographical space. Our study revealed that her work demonstrates a commingling of two approaches to design research, each characteristic of a particular school: one the Faculty of Architecture in Ljubljana and the other the RCA in London. In other words, we can trace in her work the intertwining of two threads of knowledge: one arising from the architectural and urbanistic background she acquired during her studies and later through her close collaboration with the architect Edvard Ravnikar, and the other obtained at the RCA under the mentorship of Bruce Archer, the British mechanical engineer and the first professor to devote himself to systems-level research in design. What was crucial for the development of scientific research approaches in design, however, was the work of Sir Misha Black, who had an immense influence on the education approaches in the field of industrial design at the RCA; his work served as the foundation of the new academic discipline of design research. During her time in Great Britain, Janja Lap was a close associate of both of these scholars. She worked with Professor Black in a research group that focused on hospitals; six years later, Professor Archer was her thesis advisor when she was writing her Master's thesis with the title *Communal Feeding System* (Lap, 1973).

In the preface to the article titled *Communal Feeding*, which was published in 1980 in the magazine *Industrial Design*, Janja Lap articulated her interest in the field of research in design. She wrote that her central interest was "in the impact of industrial design on the systems-level issues of a given social standard" (Lap, 1980). With this she secures her place in a noble tradition of architects and designers who worked and studied in the years

after the Second World War and who consciously chose as the central mission of their work the gradual modernisation of the living environment, raising the standard of living and contributing to the development of technical culture (Ivanšek, 1951). Her subsequent efforts should all be interpreted in this light. For instance, when she undertook research into communal feeding systems in hospitals within the research group led by Professor Misha Black, she focused her efforts on the critical analysis and understanding of the advantages and disadvantages of existing hospital feeding schemes. During her in-depth research into the topic she not only identified numerous deficiencies in the existing systems; she also discovered that in the established systems, the time between the preparation and consumption of food led to a loss of its nutritional value in terms of vitamins and other nutrients. She found this was not only due to the time factor, but also because of the need for reheating and transfer of food, as well as inappropriate means of transport and meal serving. These discoveries forced her to come up with a unique approach to solving a recognised problem that she had first very precisely and systematically analysed.

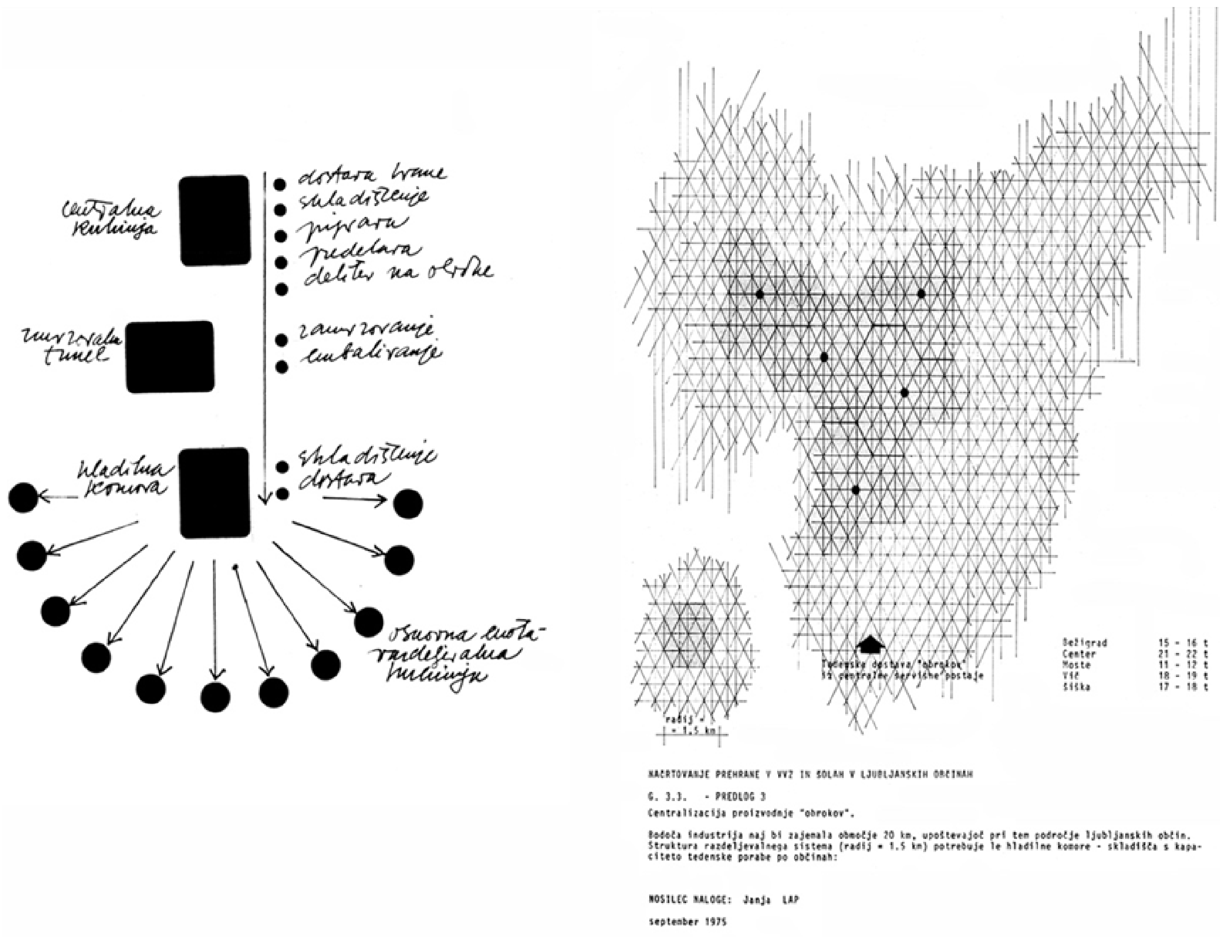

Figure 5. Janja Lap, proposal for the introduction of central kitchens for the purpose of meal planning in kindergartens and schools in the municipality of Ljubljana, schematic illustrations.

Let us briefly illustrate two premises. She carefully elaborated the identified issue—transport in the context of addressing the complex problem of increasing the quality of food provided in community programmes to the most vulnerable groups (the young, elderly and sick)—on the basis of Ravnikar's conception of the functionalist city, an idea that "strived towards order and good organisation in all the vital functions of the city. According to these principles, all the operations of the city can be categorised into one of

the four functions: habitation, work, leisure and traffic, the latter as the junction of the first three" (Žnidaršič, 2004). Through careful planning of the use of urban road networks, Janja Lap devised a system for rapid and efficient delivery of meals to designated institutions, which allowed for the relocation of the main food preparation facilities to the outskirts of the city. For her, however, the organisational matrix of the city served only as the basic premise for a further expansion of systems-level design principles.

In the course of the research, her findings compelled Janja Lap to change her approach. Whereas initially she focused on the design of an adaptable container that would enable transporting the meal rapidly and safely, in the subsequent steps the idea of the service as a system assumed an increasingly central role in her research and redesign efforts. In her research and design, she focused on the end user—whose desire is to receive a healthy and quality meal—as well as all those involved in preparing and serving the meal (from the cooks and those who dispensed the food into pots, to the delivery workers). In doing so, Lap approached the design process in a way typical of a service designer; it is necessary to note, however, that while such systems-level approaches to problem solving had already begun to be introduced at the time, the discipline of service design would only begin to be discussed at a formal level in 1995 in Germany (Mager, 2021). Janja Lap, by contrast, underwent this shift in thinking in the early 1970s; this clarifies the claim she made in her master's thesis—that in her research "she devised a new approach to a recognised design problem" (Lap, 1974).

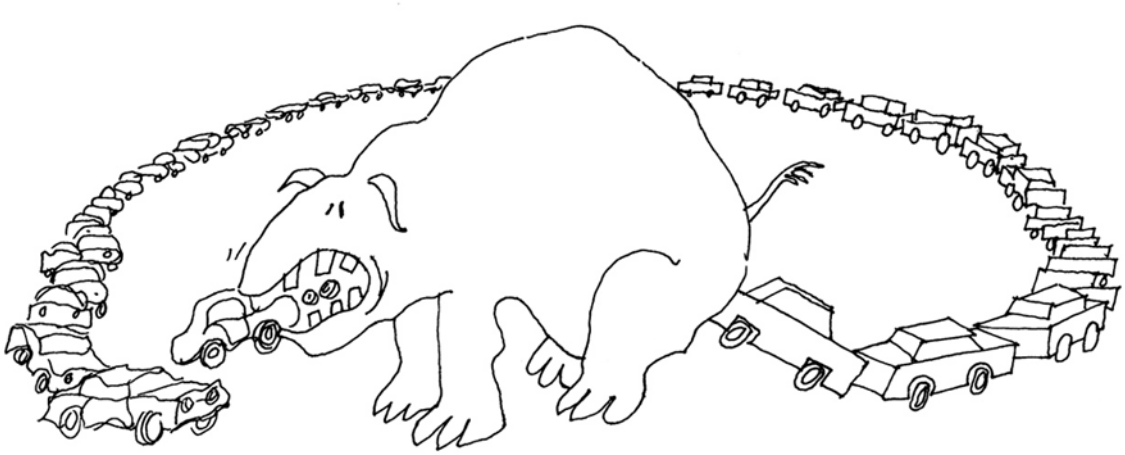

Figure 6. Janja, Lap's, illustration of circular design in the master's thesis.

It was this transition from the micro- to the macro level that facilitated another one of Janja Lap's insights into systems-level issues: in 1971, on the basis of in-depth studies, she astutely recognised the social problem, nowadays of acute importance, of the world's dependence on single-use packaging (Lap, 1971). Wishing to overcome this problem, she devised a container that could handle rapid freezing and reheating of food while also being suitable for serving and eating the food. But she did not stop there. She also highlighted the urgent need to have a system in place for the time when the container wears out and needs to be discarded. She was convinced that as the community feeding system is introduced, a system should be instituted that would involve the collection of discarded containers and cleaning of the material, as well as its further processing (Lap, 1971; 1980). With this proposal, she entered the nowadays highly relevant fields of circular economy and reverse logistics.

4. Discussion

Tangible results of her research can be encountered in Slovenia as well. In 1972, under the auspices of the Central Institute for Home Economics, she was commissioned by the Chamber of Commerce of the then Socialist Republic of Slovenia (SR Slovenia) to prepare a programme for a research study titled *Certain Transport and Distribution Systems for Collective Feeding* (Lap, 1972). The proposal included the results of her research at RCA, adapted, for the Slovenian milieu. Three years later, the Union of Child Care Associations of the SR Slovenia commissioned her to prepare the research study *The Introduction of an Industrial-style Catering System in Education-Day Care Institutions and Schools in the Municipality of Ljubljana* (Lap, 1975). With this analysis she provided a concrete view of the problems encountered on the ground and used them to identify what the needs were. She looked at them from three perspectives (ideal situation, existing situation, an adaptation of the existing situation).

Partial results of her research were later published in Polde Maček's article Community Feeding in the SR Slovenia, Central Preparation and Distribution and in the Official Gazette at the end of 1979 in the article Views, conclusions and recommendations for the formulation and implementation of policy in the field of community feeding and provisioning in the SR Slovenia (Arhiv Republike Slovenije 1277, 1979). The 1978 document included, among other things, proposals for an externally located facility for centralised thermal processing of meals, with consideration given to distribution routes and delivery, as well as the possibility of deep-freezing food. These are not the work of Janja Lap alone, but her efforts have undoubtedly been an important piece of the puzzle in the development of an understanding that there is a need for a sensible and systemic upgrade of the existing infrastructure.

5. Conclusions

It is important to point out that, building on long years of research in the field of design, Janja Lap eventually developed a unique analytical approach to addressing a previously identified problem. She succeeded in incorporating the principles of systems-level, service and circular design, all highly relevant nowadays, in her research and planning, while placing everything firmly into the context of Ravnikar's conception of the functionalist city. In light of today's remarkable expansion of methodological approaches in the aforementioned areas of research in design, the methods described in her pioneering research work seem exceptionally progressive for the mid-1960s and early 1970s period and retain their relevance today.

Acknowledgements: The article is a result of the research project J7-2606, Models and practices of international cultural exchange within the Non-Aligned Movement: researching the spatio- temporal cultural dynamics, and the research and exhibition project of the Museum of Architecture and Design of Ljubljana.

Conflicts of Interest: The authors declare no conflict of interest.

References

1. Arhiv Republike Slovenije 1277 Kardelj Edvard - Krištof, 1926–1990, 158–367. Maček, P., Družbena prehrana v SR Sloveniji, centralna priprava in distribucija, I. faza. [Community Feeding in the SR Slovenia, Central Preparation and Distribution, phase 1] Ljubljana, Združena podjetja živilske industrije, 1978.
2. Arhiv Republike Slovenije 1277 Kardelj Edvard - Krištof, 1926–1990, 158–370. A photocopy of the article Views, conclusions and recommendations for the formulation and implementation of policy in the field of community feeding and provisioning in the SR Slovenia. Official Gazette of the SR Slovenia, no 1, 13 January 1979
3. Berg F, Wolf K, Maser S, Cesar C. DE-institut '80. Aufgaben und Organisation eines Design Institutes in der Industrie. Braunschweig, SHFBK, 1978.
4. Ivanšek F. Stanovanjsko raziskovanje na Švedskem [Housing Research in Sweden]. Ljubljana, Stanovanjsko komunalni center, 1959.
5. Ivanšek F. Stanovanje in potrošnik (rezultati ankete stanovanjskih želja 1960) [The Dwelling and Its Buyer (results of the 1960 survey of housing preferences)]. Ljubljana, Urbanistični inštitut LR Slovenije, 1960.

6. Ivanšek F.Oblikovanje v industriji [Design in Industry]. Arhitekt, 1951, 1/1: 26–29.
7. Jeffs N. Personal archive.
8. Kavčič B. Sociologija dela [Sociology of Work]. Ljubljana, Delavska enotnost, 1987, pp. 325.
9. Lap J. Application to take a Master's Degree by Project in the School of Industrial Design (Engineering). London, RCA, 1971.
10. Lap J. Določeni transportni in razdeljevalni sistemi kolektivne prehrane, typed manuscript [Certain Transport and Distribution Systems for Collective Feeding]. Ljubljana, CZNG, 1972.
11. Lap J. Master's Degree by Project: Communal Feeding System. Department of Design Research, Royal College of Art, 1973. The archive of Nikolai Jeffs.
12. Lap J. Whittlestone, P. Way to Community Catering, typed manuscript. Architectural Association School of Architecture, 1974.
13. Lap J. Uvedba industrijskega načina preskrbe prehrane v vzgojno-varstvenih zavodih in šolah v ljubljanskih občinah [The Introduction of Industrial-style Catering System in Education-Day Care Institutions and Schools in the Municipality of Ljubljana]. Ljubljana, Zveza skupnosti otroškega varstva SR Slovenije, 1975.
14. Lap J. Objekti društvene ishrane – Polazne osnove za rešenje dizajn problema. Industrijsko oblikovanje, 1980, 11/57–58: 37–39.
15. Mager B. My Journey with Service Design. 2019. Accessed 28 April 2021. Available from www.service-design-network.org/community/birgit-mager-4178.
16. MAO photo library, F1110. Accessed XXXX.
17. Tancig - Novak B. Kuhinja: načrtovanje in oprema [Kitchen: Planning and Furnishing]. Ljubljana, Centralni zavod za napredek gospodinjstva, 1958.
18. Tancig - Novak B. Načela za oblikovanje kuhinjskega kompleta in kuhinjskega prostora v stanovanju: Raziskovalna naloga s področja industrijskega oblikovanja stanovanjske opreme in s področja racionalizacije gradnje stanovanj [Principles for the design of the kitchen suite and kitchen space in a residence: a research assignment in the fields of industrial design of furnishings and rationalisation of housing construction]. Ljubljana, Centralni zavod za napredek gospodinjstva, 1971.
19. Žnidaršič R. Edvard Ravnikar's Design Method: the Architect's Procedures for Adapting to Changing Planning Conditions. AB, 2004, 34/165–166: 8–33.

Scientific contribution/Original research/Invited lecture

Transcultural Aspects in Lili Novy's Life and Work

Griessler L.*

1. University of Ljubljana, The Faculty of Arts, Aškerčeva cesta 2, 1000 Ljubljana, Slovenia
* Correspondence: Larina Griessler; larina.griessler@gmail.com

Abstract

The life and work of the German-Slovenian poet Lili Novy is most often presented in Slovenia in the context of dualism because of her German-Slovenian biography. However, the central thesis is that her life and work should be understood in terms of transculturality, as a meeting place, as an area of interaction, overlapping, intertwining and mutual influence of her two identities and languages, as a process that eludes univocal definitions and requires a different angle of observation. This process and a different angle of observation result in a deeper and better understanding of her self, her essence, her linguistic multi-domain and her (literary) work.

Keywords Lili Novy; Transculturality; Poetry; Translation; German-Slovene Literature

Citation: Griessler L. On Love. Transcultural aspects in Lili Novy's life and work. Proceedings of Socratic Lectures. 2021; 6: 148-155. https://doi.org/10.55295/PSL.2021.D.019

Publisher's Note: UL ZF stays neutral with regard to jurisdictional claims in published maps and institutional affiliations.

1. Introduction

In the fields of research in the humanities and cultural studies, there have been several upheavals and turning points, as new concepts developed in recent decades that triggered a paradigm shift in literary studies (Iljasova-Morger, 2009). In the nineties of the 20th century Wolfgang Welsch (1994) developed the concept of transculturality, which views cultures and their interferences not as isolated and delimited islands, but as a heterogeneous dynamic network. In the present work, it is first explained whether and how the transcultural processes can also be traced in authors with bicultural biographies (Žigon et al., 2020). The lyricist Lili Novy, who had both a German and a Slovenian identity and consequently found artistic expression in both languages (Mugerli, 2003), serves as the object of research. However, the aim of this paper is not to describe Lili Novy's life in detail, nor to present a detailed analysis of her lyrical texts or to search for differences between her German and Slovenian identities regarding the binary concept. Instead, it explores the transcultural elements and traces in Lili Novy's life, in her translational activity and in her poetic work.

2. The concept of transculturality

The concept of transculturality has become increasingly established in academic disciplines in recent decades (Iljasova-Morger, 2009). In Germany, the new concept of culture was introduced into the discussion by the German philosopher Wolfgang Welsch in the early 1990s (Iljasova-Morger, 2009). Welsch (1994) describes it as a concept of culture that is not abandoned, but merely reworked and changed by presenting the observer with a completely new perspective. This perspective enables an "integrative understanding of culture" (Welsch, 1995). In his theory, Welsch (1994) sketches a different picture of the relationship between cultures. Not one of isolation and conflict, but one of interweaving and intermingling. It does not promote separation but understanding and interaction. The transculturality concept thus distances itself from the isolation and demarcation of the foreign and the familiar, the foreign culture and the own culture. This creates a new wholeness (Nünning, 2013). The question now arises as to what significance the concept of transculturality has for literary studies and what new perspectives arise from embedding the transcultural discourse in literary studies work. On the one hand, the transcultural process itself is an important starting point: "In this process, which consists of losses, selections, new discoveries and adoptions, the result is something unprecedented." explains Nünning (2013). Literature is thus suitable for the application of the transculturality concept in many ways, since the "unprecedented" (Nünning, 2013; Pfeifer, 1993) can be explored on different levels: on the linguistic, formal and content level - the level of "textual analysis" (Iljasova-Morger, 2009) - and on the level of "literary production and reception" (Iljasova-Morger, 2009). Indeed, literature can also be understood as a transit space where cultural and literary contexts are mixed and interpenetrated through overlaps and entanglements, thereby breaking down any cultural boundaries (Welsch, 1995; Žigon et al., 2020). Literature thus serves as a place where cultural differences are not perceived as problematic or disturbing (Iljasova-Morger, 2009), but as art itself (Žigon et al., 2020). A good example of transcultural analysis is the German-Slovenian lyricist and translator Lili Novy (**Figure 1**), who never separated her German and Slovenian identities in her life as well as in her lyrical and translational work (Žigon et al., 2020). According to Žigon, Kondrič Horvat and Udovič (Žigon et al., 2020), transcultural identities appear in literary works among authors who have bi- or pluricultural biographies. Indeed, these texts can be understood as interweaving of cultural diversity through which knowledge and understanding of cultural differences and overlaps can be disseminated and preserved (Samide, 2017). The following sections will explore in more detail and explain why addressing "two worlds" (Lončar, 2020), the German and the Slovenian, makes less sense in the case of Lili Novy.

Figure 1. Lili Novy in her early years. From (Javoršek,1984).

3. Lili Novy's Life

The poet Lili Novy was born as Elizabeta Haumeder on 24 December 1885 in Graz. Her father was an Austrian colonel, her mother was Slovenian (Mugerli, 2003). Javoršek (1984) reports that only German was spoken in the aristocratic officer's family, as the mother, Ludovika Ahačič, conversed only with the servants in her mother tongue. After only three years, the family moved to Ljubljana, although it must be emphasised that the new language environment did not yet have any influence on Lili Novy's Slovene language identity (Javoršek,1984). Public life took place in the German language: German was used not only in the higher social circles, but also in schools, offices and in court (Mugerli, 2003). The lyricist's Slovenian language identity only began to develop in Vikrče (**Figure 2**), a small town northwest of Ljubljana, where she spent most of the summer days of her childhood (Javoršek,1984). It was on her grandfathers' estate that she was first confronted in depth with the Slovenian language (Vidmar, 1979). The children from the village with whom she played conversed with her exclusively in Slovenian, as they did not know German (Javoršek,1984). Lili Novy was therefore not only in a new language environment, but became a part of a different and, for her, completely new cultural environment (Mugerli, 2003).

Life in the countryside was in great contrast to the life she led at home, in the baroque house in Stari trg 11a in Ljubljana (**Figure 3)** (Mugerli, 2003). There, she received a strict, almost Spartan upbringing that was strongly based on the values and lifestyles of the German-Austrian aristocracy and the militarism of the Habsburg monarchy (Javoršek, 1984). Vikrče, on the other hand, was a place where she could be free of rules and norms and come closer to the Slovenian language and culture (Vidmar, 1979). Nevertheless, her German identity was much more dominant in her teenage years (Mugerli, 2003).

Figure 2. Grandfather's estate in Vikrče (2).

Figure 3. The baroque house in Stari trg 11a, Ljubljana (Tripadvisor, 2022).

4. Lili Novy's Translation

She only encountered Slovene literature for the first time after 1919 (Javoršek,1984). Although her translations are often overlooked, they are an important starting point in the poet's life regarding the concept of transculturality (Stančić, 2013). It was through her translations that she made her breakthrough into the Slovenian literary scene, which was becoming more and more established at the time between the two world wars, and was thus an important milestone in the development of her Slovenian identity (Vidmar, 1979). Therefore, translating can be seen as a transit space that enabled her to perceive her Slovenian identity more clearly and to be able to develop it further, which later resulted in overlaps of both cultural worlds (Žigon et al., 2020). But firstly, it is important to under-

stand what was happening during the Second world war. The news and reports about deportations, forced resettlements, mistreatment, torture and mass murder under the occupying German rule, triggered an inner breakdown in Lili Novy (Javoršek,1984). Although she was never tortured or taken to a concentration camp, she could never really overcome the traumatic experiences of the Second World War (Javoršek,1984). The values and ideals of her German homeland, her belief in humanity, cosmopolitanism, memories of her childhood with which she identified so strongly, were destroyed, resulting in an existential crisis (Javoršek,1984; Mugerli, 2003; Vidmar, 1979). Her German identity was severely violated precisely because of her transcultural biography (Žigon et al., 2020). Although she was unable to write poetry in German for a long time after the war, she did not give up translating (Javoršek,1984). She even started translating from German into Slovenian (Mugerli, 2003). Thus, translation could serve as a kind of healing process to bridge traumatic experiences (Žigon et al., 2020).

5. Lili Novy's Poetic Work

In the context of the transculturality concept, Lili Novy's poetic work can also be seen as a whole. Lili Novy began writing her first verses in her youth (Stančić, 2013). She wrote them in German and even in French (Javoršek,1984). In the years that followed, German remained the language of her artistic expression (Vidmar, 1979). In these poems she expressed her thoughts about transience, loneliness, pain, loss, love, nature, life and death (Mugerli, 2003). Only much later, in her more mature years, she began to write poetry in the Slovenian language (Javoršek, 1984) (**Figure 4**). She did not write in German or Slovenian to pursue ideological or national goals, but to enter new spaces through the languages and to find new forms of expression within which she could combine her two identities (Žigon et al., 2020). Indeed, for her, the Slovene language was never a closed space, but a means to live, think and create (Žigon et al., 2020): an important aspect of language in the context of the concept of transculturality (Iljasova-Morger, 2009).

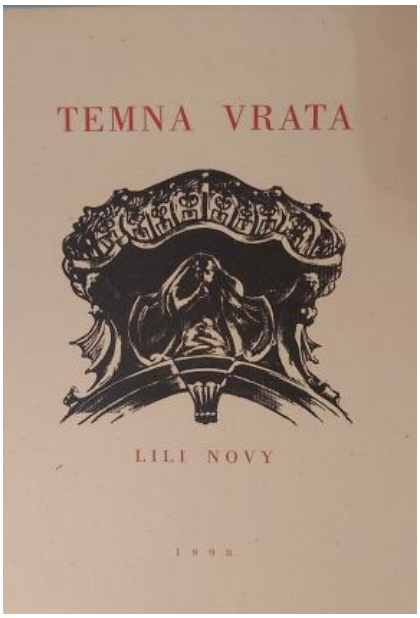

Figure 4. The front page of Lili Novy's first poetry collection in Slovenian language Temna vrata (Novy, 1998).

When asked in which language she preferred to express herself, Lili Novy's grandson Ingo Paš replied that it was not the language that was decisive for the poet, but the "how" and the "what" (Žigon et al., 2020), thus the poetry itself. Indeed, many of her colleagues and researchers, such as Javoršek (1984) or Vidmar (1959; 1979), wrote in their texts that they regretted that Lili Novy's knowledge of Slovenian was insufficient, which is why her poetry contains many outdated or rarely used phrases (Javoršek,1984,

Vidmar, 1959; 1979). The rhythm and sentence structure are also "unusual" in some poems (Vidmar, 1959). If the alienations are seen as an expression of their transculturality, one can no longer speak of exclusively Slovenian poetry or exclusively German poetry (Žigon et al., 2020). Her art exists precisely in this space of overlaps and intertwining of her two identities or languages, and thus the alienations stand for what her poetry is (Žigon et al., 2020). For in her lyrical texts, the poet interweaves personal experiences and feelings (Mugerli, 2003) as well as experiences from both homelands that have shaped her (Iljasova-Morger, 2009; Žigon et al., 2020), thus linking her original culture with the culture of the country where she later lived (Mugerli, 2003). This can be proven by the following poem "Svit" (Novy, 1998), which creates the strong linguistic effect (Žigon et al., 2020) precisely through the outdated Slovenian formulations and the unusual rhythm (Vidmar, 1959). The beauty of the poem lies in the strangeness of her art.

SVIT

Roké in usta, pôgled, v mesečini
kot sij vodé mehak;
zrak ves lahak,
drgèt rastočih vej, ščebèt v tišini,
srebrn oblak -

Beseda nežna kot dotik nečésa,
kar pride in zbeži,
predrami kri,
dotik njen, plah kot ptičjega peresa,
kot dih noči -

Krajina vsa začarana in druga:
nikoli še poprej
biló ni v njej
te ceste, zvezdnobele kot vijuga
do zadnjih mej -

Zrak bolj hladan in prvi svit v daljini,
neblag, prodiren znak;
korak na tlak
predmestni, trdi. Vso sladkost razblini
okus grenak. –

6. Conclusions

Nevertheless, many authors write of the duality in Lili Novy's life (Lončar, 2020), which on closer examination seems less meaningful and is not in harmony with Lili Novy's self-image. In Lili Novy's case, two forms of identity can be identified, the German and the Slovenian identity (Mugerli, 2003), which she skilfully combined by letting them flow together and thereby opening herself up to completely new perspectives (Žigon et al., 2020), which can be seen as a clear element of the transcultural processes (Welsch, 1995). Indeed, Lili Novy understood her different identities not as dividing lines but as points of intersection within which she could express herself and emphasise her artistic self-understanding as a whole (Žigon et al., 2020). Lili Novy never separated her Slovenian and German identities, even more, she even stood out from the nationality labels and rather understood herself as a European, as a world person (Vidmar, 1979). Therefore, the question of which identity she preferred to identify with would not

be appropriate, as she lived across cultures, beyond any boundaries that could constrict her (Welsch, 1994). Therefore, the transculturality concept is more appropriate for the deeper understanding of Lili Novy than the classical binary system that presents the two identities as isolated, delimited entities (Welsch, 1994, 1995). It is in this context that her translations and poetological work were formed within these two identities that permeated and impacted on her simultaneously (Žigon et al., 2020). Indeed, translating enabled her to perceive her Slovenian identity more clearly (Javoršek,1984), to connect it with the German (Vidmar, 1979) and even to partially overcome the wounded places in her German identity left by the experiences of the Second World War (Samide, 2017). The alienations found in her outdated and unusual formulations (Vidmar, 1959) are not linguistic gaps or errors, but an expression of her art (Žigon et al., 2020). Lili Novy (**Figure 5**) can therefore be described as a phenomenon in that. In order to intertwine the two identities, she demonstrated a great deal of courage, cosmopolitanism and maturity - and that as a woman.

Figure 5. Lili Novy in her later years. From (Javoršek,1984).

Acknowledgements
The author thanks Irena Samide for the idea to study transcultural aspects in Lily Novy's life and work and for the support in research writing.
Conflicts of Interest: The authors declare no conflict of interest.

References

1. Iljassova-Morger O. Transkulturalität als Herausforderung für die Literaturwissenschaft und Literaturdidaktik, Das Wort, Ger-manistisches Jahrbuch Russland 2009, pp. 37–57.
2. Javoršek J. Lili Novy. Partizanska knjiga, Ljubljana. 1984.
3. Lončar N. Analiza in recepcija slovenskih pesmi Lili Novy. Diplomsko delo, Filozofska fakulteta Ljubljana. 2020.
4. Mugerli M. Nemške pesmi Lili Novy. Diplomsko delo, Filozofska fakulteta, Ljubljana, 2003, pp. 121.
5. Novy L. Temna vrata. Samozal. D. Petek, Ljubljana. 1998.

6. Nünning A. (Ed.) Metzler Lexikon. Literatur- und Kulturtheorie. Ansätze – Personen – Kulturbegriffe, Verlag J. B. Metzler, Stuttgart. 2013, pp. 759–760.
7. Pfeifer W. (Ed.) Etymologisches Wörterbuch des Deutschen. Digitalisierte und von Wolfgang Pfeifer überarbeitete Version im Digitalen Wörterbuch der deutschen Sprache. 1993.
8. Samide I. Luiza Pesjak, eine Mittlerin zwischen zwei Welten, (Ed. Kramberger P, Samide I, Žigon T, Und die Brücke hat gezogen, die vom Ost zum West sich schwingt: literarische, kulturelle und sprachliche Vernetzungen und Grenzüberschreitungen: Festschrift für Mira Miladinović Zalaznik), Znanstvena založba Filozofske fakultete, Ljubljana. 2017, pp. 117–131.
9. Stančić M. Verschüttete Literatur. Die deutschsprachige Dichtung auf dem Gebiet des ehemaligen Jugoslawien von 1800 bis 1945, Böhlau Verlag, Vienna. 2013.
10. Tripadvisor, Schweigerjeva House. Accessed 13.1.2022. Available at https://www.tripadvisor.com/Attraction_Review-g274873-d8261763-Reviews-Schweigerjeva_House-Ljubljana_Upper_Carniola_Region.html
11. Vidmar J. Oboki: Lili Novy. Državna založba Slovenije, Ljubljana. 1959, pp. 5–26.
12. Vidmar J. Obrazi. Državna založba Slovenije, Ljubljana, 1979.
13. Welsch W. Transkulturalität – die veränderte Verfassung heutiger Kulturen. Ein Diskurs mit Johann Gottfried Herder, VIA REGIA – Blätter für internationale kulturelle Kommunikation. 1994; 20: 1–19.
14. Welsch W. Transkulturalität. Zur veränderten Verfaßtheit heutiger Kulturen, Zeitschrift für Kulturaustausch. 1995; 45: 39–44.
15. Žigon T, Kondrič Horvat V, Udovič B. Vprašanja identitet, migracij in transkulturnosti. Dve domovini. 2020; 51: 185–200. DOI:10.3986/dd.2020.1.11

Reflection

Archaeological Treasures of Dolenjski muzej Novo mesto

Stipančić P [1], Dokl-Osolnik J [1]

1. Dolenjski muzej Novo mesto, Slovenia
* Correspondence: Petra Stipančič petra.stipancic@dolenjskimuzej.si, Jasna Dokl Osolnik jasna.dokl.osolnik@dolenjskimuzej.si

Abstract:
Dolenjski muzej Novo mesto takes care of very rich cultural heritage. Even since the beginning, Dolenjski muzej has been best known for its permanent archaeological exhibition. A short overview of enormous, very prestige archaeological heritage is presented with special effort on the Early Iron Age.

Keywords: Dolenjski muzej Novo mesto; Archaeology; Prehistory; Early Iron Age

Citation: Stipančić P, Dokl Osolnik J. Archaeological treasures of Dolenjski muzej Novo mesto. Proceedings of Socratic Lectures. 2021; 6: 157-163. https://doi.org/10.55295/PSL.2021.D.020

1. Geographical position of Novo mesto

Slovenia is a Central European Country with two million inhabitants, bordered by Italy in the west, Austria in the north, Hungary in the northeast and Croatia in the east and south. It lies at the point where the Alps, the Mediterranean, the Pannonian Plain and the Dinaric Alps meet. The diversity of its geographical features in the past fostered human endeavour, dwelling, commerce and the adoption of cultures from neighbours near and far.

The highly distinctive landscape of the Dolenjska region lies in the south-eastern part of Slovenia, and is centred around Novo mesto, which has around 25,000 residents and plays an important commercial, cultural and educational role not just in the region, but also further afield (**Figures 1, 2**).

Figure 1. Position of Slovenia and Novo mesto.

Figure 2. Novo mesto as town was established in 14th century but archaeological evidences of first human presence are much older.

2. Dolenjski muzej Novo mesto and Archaeology

Dolenjski muzej Novo mesto was founded on 1 June 1950, and is a museum of regional type with archaeological, ethnological, cultural history and art history departments, a department for contemporary history and an education department, along with two separate units, the Jakčev Dom (an artist's collection) and the Kočevski Rog (World War II sites) (**Figure 3**).

Figure 3. View on the Dolenjski muzej Novo mesto.

The first permanent archaeological exhibition was set up by staff at Dolenjski muzej in 1953, with material that was borrowed from private collections. Tone Knez, the first archaeologist at the museum, set up the first permanent archaeological exhibition in 1983, displaying material collected by the museum through its intensive and multiple archaeological research projects throughout Dolenjska, especially in Novo mesto. Even when the museum opened the space for the permanent exhibition was too cramped for all the exhibits, so the majority of the material stayed stored in repositories.

Evidence of the first settlement or use of the physical space in the area of Novo mesto dates back to the 6th–5th millennium BC. The settlement pattern begins to change in the Late Bronze Age (9th century BC) and reaches a high point in the Early Iron Age (8th to 4th centuries BC). The Early Iron Age is the period of Greek culture in the Mediterranean, with the flourishing of city states contrasting with what contemporary Greeks saw as 'Barbarian' Europe. The Early Iron Age or Hallstatt culture, named after the archaeological site of Hallstatt in Austria, is subdivided geographically, and Slovenia was a part of its south-eastern sub-Alpine area.

The Dolenjska Hallstatt group plays a central role in Slovenia with its wealth of archaeological sites, including Novo mesto. One of the most important economic sectors of the Early Iron Age in Dolenjska was ironworking, which allowed the extraordinary development and flourishing of all of society. Iron ore in the form of lumps of manganese-rich limonite lies on the surface and was easily accessible (**Figure 4**). The iron ore was worked into iron products which were traded. Despite the lack of written sources, we can study and familiarise ourselves with this extraordinarily interesting and important period for our ancestors, by studying the rich and exceptional archaeological material heritage kept at the Dolenjski muzej.

Figure 4. The most important raw material in the Iron Age was iron ore**.**

3. Archaeological Image of Dolenjska

Since 2008, a new permanent exhibition on the "Archaeological Image of Dolenjska" has been on display. It was created by museum archaeology curator Borut Križ and showcases events in archaeological periods in Dolenjska, from the first few traces of humans in the Stone Age right through to the end of the early Middle Ages and the dense settlement of the area. Only five percent of rich and amazing archaeological heritage is presented on the exhibition while the rest is kept in our depositories. The introductory part of the exhibition presents the natural heritage of Dolenjska, complete with the major bedrocks and fossils. The main part of the exhibition, occupying three rooms, is devoted to the Early Iron Age. (**Figure 5**) The exhibition contains numerous high-quality, significant and attractive archaeological objects. Among the most important of these are bronze, figurally decorated situlae found in the cemeteries at Kandija and in Kapiteljska njiva in Novo mesto. (**Figure 6**) There is also an exceptional range of variously coloured glass beads, supplemented by amber and bronze jewellery. Testifying to the elaborate equipment of important figures in the Early Iron Age are the mass of bronze and iron weapons, including outstanding bronze helmets and bronze armour. The rich archaeological material on display in the permanent exhibition enhances our knowledge of life in the wider Dolenjska area from prehistory through to the early Middle Ages (Križ et al., 2009).

Figure 5. The main room on archaeological exhibition is dedicated to the richest princely graves of Hallstatt period.

Figure 6. Figurally decorated bronze situlae from Novo mesto.

4. Closer overview will be done on archaeological heritage from the Early Iron Age

The Early Iron Age period was a time of prosperity, progress and blossoming of the whole society, which expressed its success in the cult of the dead by burying the deceased under the earthen barrows, which can be seen even today on the field. The upper classes of the socially ranked society are represented by the notables, who have been called Hallstatt princes by researchers. Rich and special grave goods were found in such princely graves.

Very sophisticated and artistic objects are bronze vessels called situlae. In the area of Slovenia, we have no written sources from the Early Iron Age but we have some scenes with human and animal figures curved in bronze sheet that can be read almost like a book. The archaeological excavations in Novo mesto that have taken place since 1890s until today have resulted in the discovery of sixteen bronze situlae, nine of which have been decorated in the figural Situla Art style (Križ, 2012). Bronze situlae in Novo mesto were found in graves with grave goods which date to the end of fifth and to the fourth century BC.

In the archaeological collection of Dolenjski muzej special point is put on huge amount of multicoloured glass beads of varied decorations and shapes (**Figure 7**).

Figure 7. Multicoloured glass beads of necklace. Novo mesto, Kapiteljska njiva, various graves. 6th-4th century BC.

Very often they are complemented by orange-red amber beads (Križ, 2017). In the Early Iron Age, the trade with amber increased greatly and it came on Dolenjska region by the Amber Road from the area of the Baltic coast (**Figure 8**).

Figure 8. Amber bead necklaces from the Early Iron Age. Novo mesto, Kapiteljska njiva, various graves, &th-4th century BC.

The impressive equipment of Early Iron Age chiefs is attested by the many bronze and iron weapons found, with bronze helmets and breastplates being particularly outstanding (**Figure 9**).

Figure 9. Grave VII/19 from Kapiteljska njiva is one of the most richly equipped graves in the South-eastern Alpine region. Two Greco-Illyrian helmets were in the grave. 5th-4th century BC.

5. Fields of work

Our professional work involves considerable collaboration with external institutions. We work together with the Chemical Institute in Ljubljana, the Institute of Archaeology at the Slovenian Academy of Arts and Science in Ljubljana, the Institute of Mediterranean Heritage, the National Museum of Slovenia, the archaeology departments at the Faculty of Arts in Ljubljana and in Zagreb, the restoration and conservation workshop at the Roman-Germanic central Museum in Mainz, and many similar institutions in Slovenia and abroad. We closely cooperate with the novo mesto regional unit of the heritage protection institute. We also regularly prepare popular and academic science article, lectures, and actively cooperate in international symposiums (Bregar et al., 2010).

Our special focus is also on filed work, especially for the last thirty years on the excavations at the Kapiteljska njiva site in Novo mesto (**Figure 10**). The systematic, annual archaeological research has produced excellent results that not only enrich our archaeological knowledge of Dolenjska and Slovenia in the first millennium BC, but also our knowledge of Europe as a whole in that epoch (Križ and Stipančić, 2016).

5. Conclusions

Our work is not only to research, study and take care of the heritage. Our role is also to present and promote. To make archaeology more understandable and closer to our public. One of the projects how to closer our common heritage is Situlae Festival. Every year for the last six years we prepare it at the end of June. It is a festival of iron age life, cuisine and culture. With reconstructions, craftsmen, cuisine and music the town changes into a Hallsttat town (**Figure 11**). Our main work and role are to develop common consciousness of meaning of heritage, on which national identity is standing and to help growing museum public from the earliest time.

Figure 11. Scene from the Situlae Festival which is held at the end of June.

Figure 12. Bronze fibula with two ducks. Novo mesto, Kapiteljska njiva, Grave XVI/12. 6th century BC.

Acknowledgements: All photo images (Figure 1-12) are from archive of Dolenjski muzej Novo mesto.
Conflicts of Interest: The authors declare no conflict of interest.

References

1. Bregar M, et al. 60 let Dolenjskega muzeja Novo mesto. Novo mesto. 2010.
2. Križ B. Reflections of Prehistory in Bronze. The Situla Art of Novo mesto. Novo mesto. 2012.
3. Križ B. Amber Jewels of the Baltic in Novo mesto. Catalogue of temporary exhibition. Novo mesto. 2017.
4. Križ B, Stipančić P, Škedelj Petrič A. Archaeological Image of Dolenjska. Catalogue of permanent exhibition. Novo mesto. 2009.
5. Križ B, Stipančić P. A thousand-year necropolis. Catalogue of temporary exhibition. Novo mesto. 2016.

Scientific contribution/Original research

Biomechanics of Joints at 6th Socratic Lectures

Bambič U[1], Bujanović E[1], Cibula M[1], Jakin PA[1], Lipovec S[1], Novak Š[1], Pražnikar E[1]*, Zmazek J[1], Romolo A[2], Kralj-Iglič V[2,3]

1. University of Ljubljana, Faculty of Medicine, Ljubljana, Slovenia
2. University of Ljubljana, Faculty of Health Sciences, Ljubljana, Slovenia
3. National Research Council of Italy, Naples, Italy

* Correspondence: eva.praznikar@gmail.com

Abstract:
Traditionally, Socratic Lectures are mainly devoted to students and young scientists. To optimize the transfer of knowledge from excellence to youth, curricula and examination procedures were being updated since the initiation of this process in 2008. This year, 8 students of Medicine taking place at the Faculty of Medicine, University of Ljubljana have participated in the elective subject Biomechanics of joints. Within this contribution we report on the subject and the examination process and results.

Keywords: Extracellular vesicles; Neuropathy; Brachycephaly; Stem cells; Microalgae; Nanoplastics

Citation: Bambič U, Bujanović E, Cibula M, et al. Biomechanics of joints at 6th Socratic lectures. Proceedings of Socratic Lectures. 2021; 6: 165-177. https://doi.org/10.55295/PSL.2021.D.021

1. Curriculum

In the academic year 2021/2022, the elective subject Biomechanics of joints took part of the winter semester. The lectures were organized in the second half of November followed by analysis of the biomechanical parameters of hips and Socratic Lectures with the examination. The lecturers were prof. Vane Antolič, prof. Matej Drobnič and the leading author of this contribution. Due to positive experience with online teaching from 2020/2021, we decided to continue with online curricula also in the future, regardless of the COVID-19. Namely, a significant part of the subject is devoted to the HIPSTRESS method for determination of biomechanical parameters of hips (resultant hip force and distribution of contact hip stress). For that, digitized X-ray images are used and analyzed by an appropriate graphical software. It is convenient for the students to immediately use the software during the lectures and follow the method by screen sharing. Furthermore, the number of students that chose the subject this year (8) allowed individual consultations which increased the quality of the analysis made by the students. This year, the students continued with the analysis of a series of periacetabular osteotomies which started a year ago. To calculate biomechanical parameters, a new HIPSTRESS model for resultant hip force is being tested (Uršič et al., 2021). The new model is dimensionless at the expense of simplification to only one effective muscle. This simplification has been introduced because the newer digitized X ray images do not contain a unit length, therefore scaling of reference muscle attachment points that was included in the original 3-dimensional HIPSTRESS model (Iglič et al., 1993) could lead to large errors. Each student analyzed 8 – 12 X ray images. In testing the method, all participants simultaneously analyzed the same X ray image and inserted the measurements as well as calculations in a common google drive excel document. This allowed for immediate checking of the results and finding the errors in formulas and measurements. Furthermore, the students inserted analysis of the X-ray images directly to the excel document which made the averaging over the populations fast and easy. The student Jan Zmazek has previously graduated from the Faculty of Physics and is presently also a PhD student. As he is skilled with computer as well as with mathematical modeling, he introduced his own improvements in the method by using the software Geogebra and inserting in it the solution of a nonlinear algebraic equation which is obligatory to determine the hip stress distribution. The students cooperated successfully between each other to share the skills and contribute the knowledge that they acquired previously.

2. Examination

The examination questions were sent to the students a day before. A group of questions addressed the plenary lecture. As there were 7 scientific sections and 8 students, each student was assigned to one section and the corresponding questions. The students were advised to get acknowledged with the subjects and to ask the participants of the symposium for help in answering the questions. All tools and social networks were allowed to be used for answering the questions. The questions were posed according to the state of the art in the respective fields; therefore, no decisive answers are yet available, and the students were obliged to consider the available arguments and take a standpoint. This symposium's plenary lecture was given by prof. Antonella Bongiovanni from Palermo, Italy, on green extracellular vesicles which are being considered as carriers of substances in medical applications. The scientific sections covered the fields of medicine, veterinary medicine, orthopedics, biomaterials, ecology, physics, and extracellular vesicles. After the end of the scientific section the students have assembled the answers into one MS Word document and have submitted it to an official mail of the Socratic Lectures within the limited time.

3. Results

Below we present the revised version of the document created by the students in which the answers to the questions were sought.

3.1. What are extracellular vesicles (EVs)?

EVs are sub-micron sized membrane-enclosed entities shed or secreted by cells that cannot replicate (Théry et al., 2018). They can be shed from the plasma membrane or from internal departments of the cell. They are called microvesicles and exosomes, respectively (**Figure 1**)

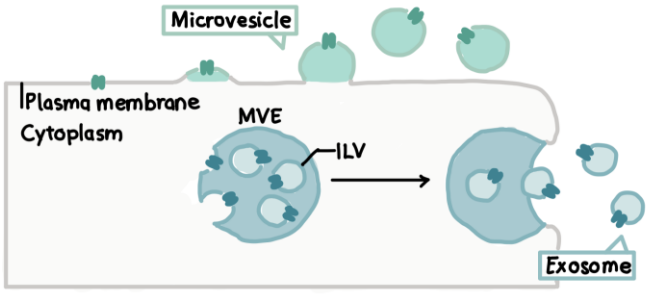

Figure 1. Scheme of microvesicle and exosome shedding. Adapted from van Niel et al. (2018).

EVs can be isolated in vitro from cultured media or from different biological samples (blood, urine, saliva, cerebrospinal fluid, tissue, wastewater). EVs are intrinsic mediators of intercellular communication in the body, allowing functional transfer of biomolecules (lipids, proteins, DNA, mRNA, microRNAs, and other noncoding RNA) between diverse locations (Yáñez-Mó et al., 2015). EVs have diverse biologic roles in different tissues as biomarkers for different diseases and as potential therapeutic agents (Svenson, 2012, Yáñez-Mó et al., 2015, Fais et al., 2016). They are involved in the modulation of genetically encoded messages via miRNA trafficking (Ullah et al., 2019) and in regeneration of tissue (Taverna et al., 2017). Due to these pleiotropic effects, EVs are hypothesized to play an influential role in modulating the tissue microenvironment as it relates to the repair and regeneration of damaged or diseased tissues, as well as for the removal of unwanted proteins and toxic materials (Ullah et al., 2019).

The role of EVs in different pathophysiological conditions (cancer, cardiovascular disease, infectious diseases, and neurodegenerative disorders) is being investigated (Ullah et al, 2019). It was suggested that EVs may act in synergy with bone marrow-derived stem cells in inflammation, immunomodulation, and cellular reprogramming, and that they interact with stem cells and cancer cells in the process of oncogenesis (Ullah et al., 2019). The advantages of the EV delivery compared to liposome delivery include simpler technical manufacturing and delivery and reduced cost (Gepstein et al., 2019, Çağdaş et al., 2021).

3.2. How are EVs identified?

EVs can be identified based on size, morphology, shape, membrane presence, structure, proteins, density, topology, etc. (Adamo et al., 2021). The size of plant vesicles is between 30 and 150 nanometers in diameter (Bongiovanni, 2021). Experimental methods for EV identification (pointing to their origin and mechanism of formation) are electron microscopy and diverse omics (Kralj-Iglič et al., 2020). Furthermore, EVs are characterized by immunoblotting, density determination by gUC, fluorescamine assays, stability

testing, testing resistance to detergents, light scattering, flow cytometry, different spectrometric assays and nanotracking analysis (Adamo et al., 2021).

3.3. How are EVs experimentally distinguished from viruses?

Taking into account definitions, viruses can take over cellular pathways to replicate inside the cell while EVs cannot (Théry et al., 2018; Bongiovanni, 2021). However, in encapsulated viruses such as SARS-CoV-2 the cargo is enclosed within a bilayer-based membrane (Bongiovanni, 2021), similarly to EVs. Such virions structurally resemble EVs, which makes the distinction between them difficult. It was found that retroviruses resemble EVs in size and density (50-100 nm, 1.13–1.18 g/L) (Nolte-'t Hoen et al., 2016). In a HIV study, separation of EVs from HIV virions was based on faster migration of virions than EVs in velocity gradients (Nolte-'t Hoen et al., 2016, Lazarian et al., 2018). Discrimination of EVs from virions included determination of capsid protein p24 in virions and of acetylcholinesterase and lymphocyte common antigen (CD45, CD stands for cluster of differentiation) in EVs (Nolte-'t Hoen et al., 2016). HIV virions were considered not to incorporate acetylcholinesterase and CD45 in their membrane, however, it is unclear whether these molecules are carried by all EVs (Nolte-'t Hoen et al., 2016; Cantin et al., 2008).

3.4. Which are the biological roles of EVs?

Biological roles of EVs are to maintain cellular and tissue homeostasis by transferring critical biological cargos to distal or neighboring recipient cells (Zarà et al., 2011). Because they participate in the pathogenesis of several diseases they can be used as disease biomarkers, as well as therapeutic tools in tissue regeneration and novel options for drug delivery (Zarà et al., 2011).

3.5. How could EVs be used for drug delivery inside the organism?

Drug delivery mechanisms of EVs are currently being investigated for their capability of carrying lipids, proteins, and nucleic acids throughout the human body (Bongiovanni, 2021). Cells communicate with each other by exchanging information through the secretion of soluble factors such as growth agents, cytokines, and genetic material, all of which can be encapsulated within EVs (Ullah et al., 2019).

3.6. Describe the mechanism by which EVs could deliver drugs to recipient cells?

Constituents of the EV membrane can interact with receptors that are present in the plasma membrane of recipient cells (Zaborowski et al., 2015). In addition, EVs were found to be internalized into recipient cells via different endocytic pathways that are characteristic for different cell types (Zaborowski et al., 2015). Endocytosis is the process by which cells take in substances from outside of the cell by engulfing them in a vesicle (Gleichmann, 2020). These can include things like nutrients to support the cell or pathogens that immune cells engulf and destroy (Gleichmann, 2020). EVs can be loaded with drugs after being isolated or during their formation (Elsharkasy et al., 2020).

3.7. From which sources could EVs be harvested for wide use drug delivery?

EVs can be harvested from different human cells (kidney, muscle, cardiac, liver, intestinal, nerve, epithelial, cancer, dendritic, immune and stem cells), bacteria, plants, animals (bovine milk) and microalgae. However, human cells are difficult to obtain in large enough quantities to be widely used, thus the recent fascination with microalgae, which are abundant and show promising results.

3.8. Which methods would be appropriate to produce a sufficient amount of EVs for these means?

Various methods have been developed to isolate EVs from microalgae-conditioned media, differing in yield, purity, and size distribution of isolated EVs (Kang et al., 2017). Nanoalgosomes were harvested by differential ultracentrifugation, gradient ultracentrifugation, and tangential flow filtration (Adamo et al., 2021). In ultracentrifugation the centrifuge rotor attains centripetal accelerations over 100.000 g, where g = 10 m/s^2 (Adamo et al., 2021). Differential centrifugation consists of consecutive centrifugation steps to separate particles with different sizes, while in gradient centrifugation, liquids with different densities are poured on top of each other to collect the particles with matching densities (Adamo et al., 2021). In tangential flow filtration the culture samples pass the filters embedded in cassettes to collect EVs which are further concentrated (Adamo et al., 2021).

3.9. Describe at least one possible mechanism of clinical use of EVs.

Mesenchymal stem cell EVs have high potential for bone and tissue regeneration due to a combination of pro-angiogenic, anti-apoptotic and immunomodulatory factors (Marangon, 2021). While there are preclinical studies using bone marrow MSC to treat bone defects in rats and mice (Marangon, 2021), it is the possibility of isolating EVs from different biofluids that makes them valuable biomarkers to be analyzed for the diagnosis or prognosis of several conditions. Their complex cargo reflects the (patho)physiologic status of the cells from which they originate. Moreover, natural nanoparticles have been investigated as therapeutic tools in many pathological conditions (Ciferri et al., 2021). The methods for harvesting EVs include limitations in the process of conventional invasive tissue biopsies, because the procedure can lead to infection and cannot be used on all tissues. Instead, the minimally invasive 'liquid biopsy' is a better strategy (Allelein et al., 2021).

3.10.Which are the limitations of the methods for harvesting and characterization of EVs?

During centrifugation, filtration, and passage through chromatographic columns, EVs are subjected to shear stresses which may change their morphology and composition or even cause their destruction or aggregation. According to Juares (2021), during processing, EVs may get contaminated by proteins and soluble factors; polymer-based precipitation can lead to co-precipitation of protein contaminants and polymeric materials and immunoaffinity capture-based techniques induce antibody cross-reactivity. Static/dynamic light scattering, tunable resistive pulse sensing and nanoparticle tracking methods can be inaccurate with poly-dispersed and size heterogeneous samples which is often the case with isolates (Chiriacò et al., 2018). Flow cytometry has a detection limit (>100 nm, flow cytometer dependent), a swarming effect (identification of multiple vesicles as a single event) and cannot distinguish EVs from other particles of similar size (i.e., protein/antibody aggregates) (Chiriacò et al., 2018). ELISA/Western Blot can also detect non-EV proteins (Chiriacò et al., 2018). Atomic force microscopy has poor resolution, classical scanning electron microscopy requires fixation and metal sputtering which causes EV shrinking (Chiriacò et al., 2018). The majority of these methods were developed for other systems, e.g., cells or inorganic nanoparticles and are only partially suitable for tiny fragile particles with transient identity (such as EVs).

3.10. What is neuropathy and which are its biomechanical effects?

Peripheral neuropathy is described as damage or dysfunction of one or more nerves within the peripheral nervous system (Cleveland Clinic, 2019). The presented symptoms depend on the type of nerve (sensory, motor, autonomic including digestion and circulation) that is damaged; the most common risk factors include diabetes, trauma, meta-

bolic syndrome, alcoholism, abnormal vitamin levels, particular medications and poisons, cancer treatment with chemotherapy, some inherited disorders, autoimmune disorders, and infections (Cleveland Clinic, 2019). The common signs and symptoms are tingling or numbness (usually in the hands and feet - distal sensory loss that spreads proximally), sharp, burning pain, changes in sensation, falling, loss of coordination, muscle weakness, twitching, cramps, spasms and/or paralysis (Cleveland Clinic, 2019). The symptoms can appear suddenly (acute neuropathy) or develop slowly over time (chronic neuropathy) (Schara, 2021). Distal symmetric polyneuropathy is a chronic complication of diabetes mellitus with prevalence of 6.3% – 50% (Mankowsky, 2021). It usually starts with lesions on peripheral sensitive nerves and progresses to motor and autonomic nerves (Sartor et al., 2012). It causes progressive loss of vibratory, thermal, tactile, and proprioceptive sensitivities (Sartor et al., 2012). Muscle atrophy, musculoskeletal impairments, and autonomic dysfunction can be established in later stages of the disease, mainly due to impairment of the larger diameter neural fibers (Sartor et al., 2012).
The biomechanical effects of neuropathy are limitation of mobility of the foot and ankle joints, alterations in spatial-temporal patterns of gait (velocity, step length, stride length, and time of double support) in delayed leg and thigh muscle activation, resulting in unfavorable alterations of ground reaction forces, and plantar pressure during gait (Sartor et al., 2012). These alterations may lead to foot ulcerations and increase risk for foot amputation (Mankowsky, 2021). The best options for minimizing these problems are wound debridement, dressing and off-loading. Most common and effective tools for off-loading are crutches, healing shoes and total contact cast (Schara, 2021). They reliably reduce plantar pressure, increase healing rate, and time in healing and reduce complications (Schara, 2021).

3.11.Which are the biomechanical effects of wearing the above knee leg prosthesis?

The most common reasons for leg amputations are illness (tumor, infection, frostbite, cardiovascular diseases, diabetes) and accidents (Ipavec, 2021). The above knee prosthesis involves an artificial knee which can be mechanical (based on hydraulic system or locking mechanism) or microprocessor-assisted (Ipavec, 2021). The important parameters are the height of the prosthesis, the prosthetic socket (required comfortable fit) and the prosthetic foot (corresponding to the type of artificial knee and to the shape of artificial heel) (Ipavec, 2021). An above knee prosthesis can have a significant impact on gait, with substantial deviations of symmetry, step length, hip exertion and upper body involvement (Ipavec, 2021). These differences can produce gait that is less efficient and less comfortable, resulting in slower and shorter walking distance (Ipavec, 2021). Other problems that can appear with an above knee amputation and wearing of the prosthesis are phantom pain, poor fit of the prosthetic socket, blisters, tissue thickening on the amputee's residual limb and allergic reactions to the prosthetic socket's material (Ipavec, 2021).

3.12.Which are the biomechanical effects of brachycephaly in dogs? How can brachycephaly affect homeostasis and hemostasis in dogs?

In dogs, brachycephaly causes the shortening of the muzzle, flat facial conformation and widening of the skull, without a corresponding decrease in the size of the soft tissue in the skull (**Figure 2**).

Brachycephaly is perceived as a desirable trait in domesticated dogs, with commonly encountered breeds being English bulldog, French bulldog, pug, Boston terrier, Shih tzu, etc. (Šimundić, 2021). Brachycephaly in dogs causes elongated soft palate, macroglossia, stenotic nares, undersized nasal chambers, malformed and aberrantly growing nasal conchae, and tracheal hypoplasia (Šimundić, 2021). Consequent respiratory signs include dyspnea, stertor, stridor, increased respiratory effort, exercise intolerance, heat, or stress

intolerance and even cyanosis and collapse (Žgank et al., 2021). Biomechanical effect of brachycephaly in dogs is difficulty in breathing, mainly caused by the airway obstruction by soft tissue rather than tracheal diameter (Žgank et al., 2021).

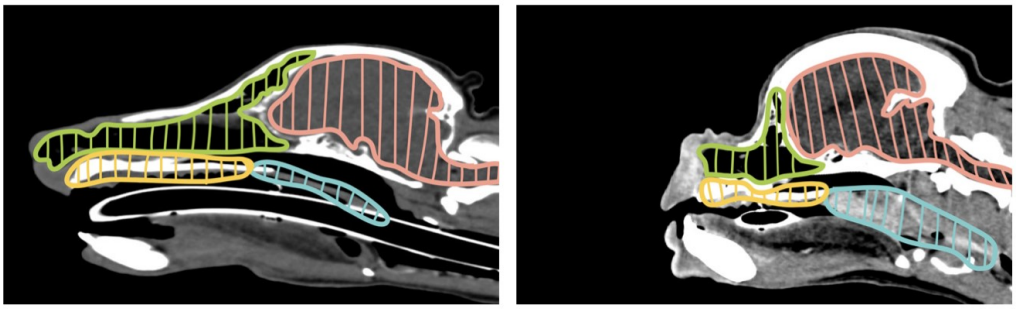

Figure 2. Magnetic resonance image of the cross section of the canine skull. Left: dolichocephalic dog, right: brachycephalic dog. The shape of the elements is marked by shading. Soft tissue is marked by cyan color (Erjavec and Lukanc, 2021).

The homeostasis and hemostasis effects of brachycephaly in dogs are polycythemia, hypercoagulative state, hypomagnesemia, oxidative stress, myocardial damage, and respiratory acidosis (Erjavec and Nemec, 2021). Compensatory sinus tachycardia with weak pulse occurs due to respiratory insufficiency (Smajlović, 2021). The tachypnea is also observed due to laryngeal paralysis, edema, and airway obstruction (Smajlović, 2021). Inflammation might lead to disseminated intravascular coagulation (Smajlović, 2021). Laboratory evaluations also show that brachycephalic breeds are more prone to hemoconcentration (Smajlović, 2021).

3.13.How can we identify and characterize stem cells?

According to reviews by Hongxiang et al. (2011), stem cells are cells with capability of self-renewal and potential to differentiate into many types of cells in the body. There are two main types of stem cells: embryonic stem cells, derived from embryonic blastocysts, and adult stem cells, found among specialized cells within adult tissues or organs (Hongxiang et al., 2011). Embryonic cells are stem cells with full potential to differentiate, they are pluripotent (Hongxiang et al., 2011). Adult stem cells are only partially differentiated stem cells that appear to have a more restricted ability of producing different cell types and self-renewing, they are multipotent (Hongxiang et al., 2011). Adult stem cells are found throughout the body after embryonic development in organs and tissues such as brain, bone marrow, peripheral blood, blood vessels, skeletal muscle, skin, teeth, heart, gut, liver, etc. (Hongxiang et al., 2011). According to their decent, adult stem cells can be hematopoietic, endothelial, olfactory, neural crest, testicular, mammary, neural, and mesenchymal stem cells (Spasovski, 2021). Adipocytes develop from mesenchymal cells and their differentiation is a complex process of events accompanied by changes in cell morphology, hormone sensitivity and gene expression (Bunnell et al., 2008). Stromal cells that have preadipocyte characteristics can be isolated from adipose tissue of adult subjects in large or small quantities, propagated in vitro and induced to differentiate into adipocytes (Bunnell et al., 2008). The term "Adipose-derived Stem Cells" (ASCs) identifies the isolated, plastic-adherent, multipotent cell population (Bunnell et al., 2008). Methods to isolate these cells from the adipose tissue, start with the collection of adipose tissue by needle biopsy or liposuction aspiration (Bunnell et al., 2008). ASCs can then be isolated by washing the tissue sample extensively with phosphate-buffered saline (PBS) containing 5% Penicillin/Streptomycin (P/S) (Bunnell et al., 2008).

3.14.Describe at least one possible mechanism of treatment with stem cells.

Stem cells are used in regenerative medicine in the process of creating living, functional tissues to repair or replace tissue or organ whose function is lost due to several conditions like disease, aging, damage, or congenital defects (Perez-Terzic et al., 2014). The potential use of stem cells in medical therapy is widespread and it can be used to cure various diseases such as blindness, deafness, myocardial infarction, muscular dystrophy, diabetes, Crohn's disease, different types of cancer, spinal cord injury, wound healing, stroke, missing teeth and neurodegenerative diseases, osteoarthritis, and others (Spasovski, 2021). Adipose tissue – derived stem cells are being used for treatment of osteoarthritis (Spasovski, 2021). Samples of fat tissue are first obtained by surgical excision and then processed in vitro, including isolation, propagation, harvesting and phenotyping (Spasovski, 2021). After 15-24 days of growth, the cells are applied to the joint by needle injection (Spasovski, 2021).

3.15.How can the presence of endoprosthesis in the body affect homeostasis and hemostasis?

Table 1. Information related to the key essential metals which are used for different medical implants (U.S Food and Drug Administration, 2019).

Metal	Major Physiological Roles of Proteins Utilizing the Metal	Key Manifestation of Deficiency	Potential Toxicities or Manifestations of Excess
Cobalt (Co)	Metabolism of purines/ pyrimidines, amino acids, fatty acids, folate	Anemia, Neuropathy, Neurocognition changes	ACD*, Cardiomyopathy, Polycythemia, Altered thyroid function
Copper (Cu)	Collagen cross-linking, Bone formation, Iron metabolism, Hemostasis/thrombosis, Neurotransmitter synthesis	Iron-refractory anemia, Neutropenia/infection, Osteoporosis, Neurological dysfunction	GI symptoms, Hemolysis, Cardiac failure, Renal failure, Hepatic dysfunction, Alzheimer's
Iron (Fe)	Oxygen transport/storage, DNA synthesis/repair, RNA transcription, Synthesis of collagen, Immune function	Microcytic anemia, Diminished thyroid function, Impaired neutrophil function, Impaired cognition	Free radical generation, GI symptoms (acute), Hemochromatosis: Cardiomyopathy, Cirrhosis, Diabetes, Arthritis
Manganese (Mn)	Metabolism of carbohydrates, lipids, urea, Neurotransmitter synthesis, Bone/cartilage formation	Dermatitis, Weight loss, Growth retardation, Abnormal bone/cartilage, Dyslipidemia, Glucose intolerance	Headache, Psychiatric symptoms, GI symptoms, Parkinson's-like signs/symptoms
Molybdenum (Mo)	Metabolism of nucleotides, amino acids, neurotransmitters	Urinary tract stones, Acute renal failure, Myositis, Mental changes/coma	Elevated uric acid/gout, Secondary copper deficiency, Reduced testosterone
Zinc (Zn)	Immune function, Wound healing, DNA synthesis and repair, Stabilization of protein structure, Intracellular signaling	Decreased immune function, Delayed wound healing and growth, Neurological and bleeding abnormalities, Osteoporosis	Copper deficiency, Myeloneuropathy
Chromium (Cr)	Glucose metabolism/tolerance, Lipid metabolism	Impaired glucose tolerance, Abnormal lipids profiles, Peripheral neuropathy	Cr3+: Potential liver issues and kidney issues, CR6+: Respiratory and GI symptoms, Dermatitis/ulcerations, Lung cancer
Vanadium (V)	Phosphate metabolism, Insulin enhancement, Lipid metabolism	/	GI symptoms, Headache, Weakness, Tremor

*Abbreviations: ACD: Allergic contact dermatitis; GI: Gastrointestinal; UA: Uric Acid.

The foreign body reaction is an unavoidable process which takes place whenever any material becomes implanted into the body (Carnicer-Lombarte et al., 2021). The process of implantation injures the tissue around the foreign object, which triggers an inflammatory process) (Carnicer-Lombarte et al., 2021). Over a period of weeks to months this inflammatory process develops into a fibrotic response, which envelops and isolates the implanted material (Ullah et al., 2019). When the foreign material is implanted with the aim of delivering a therapy, both the acute (predominantly inflammatory) and chronic (fibrotic) stages of the foreign body reaction pose significant challenges to its integrity and therapeutic function (Ullah et al., 2019). Myeloid cells such as neutrophils and macrophages are the primary cells involved in the expected acute inflammation with subsequent peri-implant wound healing (Ullah et al., 2019). An implant may continue to elicit a chronic inflammatory response, lasting for months or longer and is characterized by a broader immune cell infiltration including both myeloid and lymphoid cells (Ullah et al., 2019). Chronic inflammation by implanted metal devices or metal wear debris may lead to adverse clinical effects (**Table 1**).

3.16.Describe at least one possible mechanism for maintenance of homeostasis of the ecosystem which is based on microalgae.

Microalgae are ecologically important photosynthetic organisms. They inhabit a highly diverse range of habitats (sea ice, sea waters, snow, inland waters, and soil) (Yong et al., 2016). As carbon fixators, primary producers in food chains and food sources for higher trophic organisms, microalgae play a crucial role in maintaining the equilibrium of food webs in the aquatic ecosystem (Yong et al., 2016). Climate change could affect the growth of microalgae, which could have a negative impact on the ecosystem homeostasis (Yong et al., 2016). Moreover, microalgae are sources of materials for biotechnological applications and medical use (Yong et al., 2016).

3.17.What are bisphenols and which are the mechanisms of their translocation between water, air, and soil?

Bisphenols are a group of chemicals that have been used for manufacturing plastics, epoxy resins and other products since the 1960s (Vehar, 2021). Bisphenols can enter the environment either directly from chemical, plastic and staining manufacturers, paper or material recycling companies, enterprises, which use bisphenols in casting sand, or indirectly leaching from plastic, paper, and metal waste in landfills (Vehar, 2021). The mechanism of translocation between water, air and soil mainly depends on bisphenol physical and chemical characteristics (Vehar, 2021). Water soluble bisphenols are more often found in water, those with lower density are more likely to pollute the air (Vehar, 2021).

3.18.Which are biological effects of micro and nanoplastics on cells?

The understanding of the biologic effects of micro - and nanoplastics on cells and the corresponding toxicity mechanisms is still limited. Human cell-based studies provide fundamental and valuable information on the key toxicity mechanisms. In general, toxicity mechanisms of micro - and nanoplastics depend on their size, surface characteristics, polymer type, as well as cell type (Matthews et al., 2021). The toxicity of micro - and nanoplastics on human cells is mainly attributed to nanoplastic particles, since microplastics cannot enter the cells due to their size (Banerjee et al., 2021). Toxicity mechanisms mainly include membrane disruption, extracellular polymeric substance disruption, reactive oxygen species generation, DNA damage, cell pore blockage, lysosome destabilization, and mitochondrial depolarization (Banerjee et al., 2021).

3.19.Describe the photo effect. Some models describe light as particles and some models describe it as a wave. How can we decide which model to use?

The photoelectric effect (**Figure 3**) is a phenomenon in which electrically charged particles are released from or within a material when it absorbs electromagnetic radiation (Encyclopedia Britannica, 2021). The effect is often defined as the emission of photoelectrons from a metal surface when exposed to light (Encyclopedia Britannica, 2021). One inexplicable observation is that the maximum kinetic energy of the emitted photoelectrons does not vary with intensity of the light or duration of exposure (above a certain frequency that is needed for dislodgement of the electrons), as expected according to the wave theory, but is instead proportional to the frequency of light (Encyclopedia Britannica, 2021). However, light intensity did determine the number of electrons released from the metal - measured as an electric current (Encyclopedia Britannica, 2021). That is why Albert Einstein proposed a particle model of light, which describes a beam of light as a swarm of discrete energy packets, known as photons and features particle properties such as momentum and energy (Encyclopedia Britannica, 2021). Such an approach is used when discussing the interaction of light with atoms and molecules, however it cannot explain diffraction, interference and the doppler effect, which are all wave-like phenomena (Cannata, 2021). The wave model of light on the other hand operates with wavelength and frequency and is used in macroscopic phenomena, optometry, and optical instruments (Cannata, 2021).

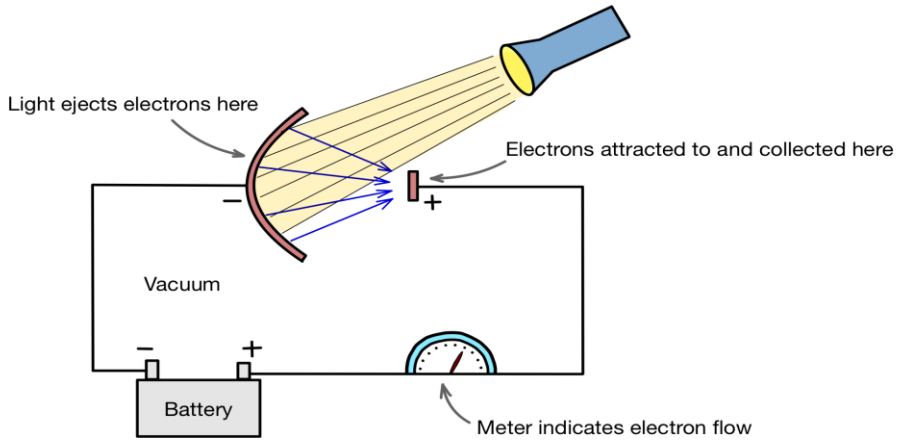

Figure 3. A scheme of the photoelectric effect. Adapted from (Cannata, 2021).

3.20.What was in your opinion the role of Mileva Marič in formulation of the theory of relativity, statistical physics, and quantum mechanics?

Mileva Marič worked closely with Albert Einstein, as she was a mathematician, a physicist, his partner and later his wife (Cannata, 2021). There is no definite proof of her contributions to the theory of relativity, statistical physics, and quantum mechanics, however in his letters to her Einstein refers to his work as "ours" (Cannata, 2021). Some sources also claim Mileva's name was on the first paper about relativity and that as a mathematician she worked on the mathematical basis of Albert's theories, took notes from foreign literature, and wrote scientific essays (Cannata, 2021). Einstein has never acknowledged Mileva's help, but it seems like she was a collaborator to his work during a crucial, however difficult, time in history when women were socially discriminated against and often signed under acknowledgments instead of being co-authors of papers (Cannata, 2021).

3.21.Can you see a connection between black holes and membranous nanostructures?

Black holes are objects characterized by so much gravity pull that even light cannot get away from them (Mesarec, 2021). They are like membranous nanostructures in topological sense, as relativity is all about curvatures, only more complex and in more dimensions than membranes (Mesarec, 2021). Physics and calculations, for example membrane curvature tensors, in both examples are so akin, that we can use these nanostructures as a playground for describing black holes (Mesarec, 2021). Furthermore, the theory of membranes from a mathematical point of view, when applied to more dimensions, can be one of the simplest ways of describing string theory and curvatures of space-time (Mesarec, 2021).

4. Conclusions

It is our intention to continuously improve and update the method, the curriculum, and the examination process to initiate the students in the research process and immediately enable their active involvement in creating new knowledge. Also, it is important that the students enter the scientific society and acknowledge the values of the state of the art. The most important contribution to this is their decision to devote their professional life to consider the emergent problems and support that they provided to the lecturers of the symposium.

Conflicts of Interest: The authors declare no conflict of interest.

References

1. Adamo G, Fierli D, Romancino DP, et al. Nanoalgosomes: Introducing extracellular vesicles produced by microalgae. J Extracell Vesicles. 2021; 10(6)e12081. DOI:10.1002/jev2.12081
2. Allelein S, Medina-Perez P, Lopes A, et al. Potential and challenges of specifically isolating extracellular vesicles from heterogeneous populations. Scientific Reports. 2021; 11(1). DOI: 10.1038/s41598-021-91129-y
3. Banerjee A, Shelver W. Micro- and nanoplastic induced cellular toxicity in mammals: A review. Science of The Total Environment. 2021; 755(2):142518. DOI: 10.1016/j.scitotenv.2020.142518
4. Bongiovanni A. Green bioparticles for cross-kingdom communication: a drug delivery platform designed by nature, 6.th Socratic Lectures, online. 2021.
5. Bunnell BA, Flaat M, Gagliardi C, Patel B, Ripoll C. Adipose-derived stem cells: isolation, expansion and differentiation. Methods. 2008; 45(2):115-120. DOI:10.1016/j.ymeth.2008.03.006
6. Çağdaş M, Sezer A and Bucak S. Liposomes as Potential Drug Carrier Systems for Drug Delivery. Accessed 10.12.2021. Available from https://www.intechopen.com/chapters/46983
7. Cannata I. Hundred years from the Nobel prize for the discovery of the law of photoelectric effect, 6.th Socratic Lectures, online. 2021.
8. Cantin R, Diou J, Bélanger D, et al. Discrimination between exosomes and HIV-1: purification of both vesicles from cell-free supernatants. J Immunol Methods. 2008; 338:21-30. DOI: 10.1016/j.jim.2008.07.007
9. Carnicer-Lombarte A, Chen ST, Malliaras GG, Barone DG. Foreign Body Reaction to Implanted Biomaterials and Its Impact in Nerve Neuroprosthetics. Front Bioeng Biotechnol. 2021; 9:622524. DOI:10.3389/fbioe.2021.622524
10. Chiriacò M, Bianco M, Nigro A, et al. Lab-on-Chip for Exosomes and Microvesicles Detection and Characterization. Sensors. 2018; 18: 3175. DOI: 10.3390/s18103175
11. Ciferri MC, Quarto R, Tasso R. Extracellular Vesicles as Biomarkers and Therapeutic Tools: From Pre-Clinical to Clinical Applications. Biology (Basel). 2021; 10:359. DOI: 10.3390/biology10050359
12. Cleveland Clinic (2019), Neuropathy (Peripheral Neuropathy). Accessed 10.12.2021. Available from https://my.clevelandclinic.org/health/diseases/14737-neuropathy
13. Elsharkasy O, Nordinbc J, Hagey D, et al (2020), Extracellular vesicles as drug delivery systems: Why and how? Accessed 10.12.2021. Available from https://www.sciencedirect.com/science/article/pii/S0169409X20300247
14. Encyclopaedia Britannica. Photoelectric effect. Accessed 11.12.2021. Available from https://www.britannica.com/science/photoelectric-effect
15. Erjavec V, Lukanc B. Surgical treatment of brachycephalic syndrome, 6.th Socratic Lectures, online. 2021.
16. Erjavec V, Nemec A. Selected parameters of venous blood gas analysis in brachycephalic dogs with brachycephalic obstructive airway syndrome before and after surgical treatment, 6.th Socratic Lectures, online. 2021.

17. Fais S, O'Driscoll L, Borras FE, et al. Evidence-Based Clinical Use of Nanoscale Extracellular Vesicles in Nanomedicine. ACS Nano. 2016; 10:3886-3899. DOI:10.1021/acsnano.5b08015
18. Gepstein L, Skorecki K, Regenerative medicine, cell, and genet. In: Goldman-Cecil Medicine, Goldman L, Schafer AI. New York, NY, Elsevier, 26th edition. 2019; pp. 183-195, e2.
19. Gleichmann N (2020), Endocytosis and Exocytosis: Differences and Similarities. Technology Networks. Accessed 10.12.2021. Available from https://www.technologynetworks.com/immunology/articles/endocytosis-and-exocytosis-differences-and-similarities-334059
20. Hongxiang H, Yongming T, Min H, Xiaoning Z (2011), Stem Cells: General Features and Characteristics. Accessed 10.12.2021. Available from https://www.intechopen.com/chapters/18217
21. Iglič A, Antolič V, Srakar F. Biomechanical analysis of various operative hip joint rotation center shifts. Arch Orthop Trauma Surg. 1993; 112. DOI: 10.1007/BF00449986
22. Ipavec M. Experience with above knee endoprosthesis, 6.th Socratic Lectures, online. 2021.
23. Juares Ramos AP. Heterogeneity of plasma derived extracellular vesicles and their separation into discrete subpopulations, 6.th Socratic Lectures, online. 2021.
24. Kang H, Kim J, Park J. Methods to isolate extracellular vesicles for diagnosis. Micro and Nano Systems Letters. 2017; 5. DOI: 10.1186/s40486-017-0049-7
25. Kralj-Iglič V, Pocsfalvi G, Mesarec L, Šuštar V, Hägerstrand H, Iglič A. Minimizing isotropic and deviatoric membrane energy - An unifying formation mechanism of different cellular membrane nanovesicle types. PLoS One. 2020; 15:e0244796. DOI:10.1371/journal.pone.0244796
26. Kralj-Iglič V. Exams at Socratic lectures in the time of COVID-19, Proceedings of the 4th International Symposium Socratic Lectures, Ljubljana, 2021; 202-207.
27. Lazarian A, Yuen KH, Ho KW, et al. Distribution of Velocity Gradient Orientations: Mapping Magnetization with the Velocity Gradient Technique. The Astrophysical Journal. 2018; 865. Accessed 10.12.2021. Available from https://iopscience.iop.org/article/10.3847/1538-4357/aad7ff
28. Mankowsky B. Neuropathy and the brain, 6.th Socratic Lectures, online. 2021.
29. Marangon T. Mesenchymal Stem cell derived EVs and their role in bone regeneration, 6.th Socratic Lectures, online. 2021.
30. Matthews S, Mai L, Jeong CB, Lee JS, Zeng EY, Xu EG. Key mechanisms of micro- and nanoplastic (MNP) toxicity across taxonomic groups. Comp Biochem Physiol C Toxicol Pharmacol. 2021; 247:109056. DOI: 10.1016/j.cbpc.2021.109056
31. Mesarec L. The Big Bang theory, 6.th Socratic Lectures, online. 2021.
32. Nolte-'t Hoen E, Cremer T, Gallo RC, Margolis LB. Extracellular vesicles and viruses: Are they close relatives? Proc Natl Acad Sci USA. 2016; 113:9155- 61. Accessed 10.12.2021. Available from https://www.pnas.org/content/pnas/113/33/9155.full.pdf
33. Perez-Terzic C, Childers MK. Regenerative rehabilitation: a new future?. Am J Phys Med Rehabil. 2014; 93 (11 Suppl 3). DOI: 10.1097/PHM.0000000000000211
34. Sartor CD, Watari R, Pássaro AC, et al. Effects of a combined strengthening, stretching and functional training program versus usual-care on gait biomechanics and foot function for diabetic neuropathy: a randomized controlled trial. BMC Musculoskelet Disord. 2012; 13. DOI: 10.1186/1471-2474-13-36
35. Schara K. Neuropathic diabetic foot, 6.th Socratic Lectures, online. 2021.
36. Šimundić M. Internistic problems of brachycephalic dogs, 6.th Socratic Lectures, online. 2021.
37. Smajlović A. Heat stroke in brachycephalic dogs, 6.th Socratic Lectures, online. 2021.
38. Spasovski D. Treatment of cartilage degeneration with stem cells, 6.th Socratic Lectures, online. 2021.
39. Svenson S. Clinical translation of nanomedicines. Curr Opin Solid State Mat Sci. 2012;16:287-294. DOI:10.1016/j.cossms.2012.10.001
40. Taverna S, Pucci M, Alessandro R. Extracellular vesicles: small bricks for tissue repair/regeneration. Ann Transl Med. 2017; 5:83. DOI:10.21037/atm.2017.01.53
41. Théry C, Witwer KW, Aikawa E, et al. Minimal information for studies of extracellular vesicles 2018 (MISEV2018): a position statement of the International Society for Extracellular Vesicles and update of the MISEV2014 guidelines. J Extracell Vesicles. 2018; 7:1535750. DOI:10.1080/20013078.2018.1535750
42. U.S. Food and drug administration (2019), Biological Responses to Metal Implants. Accessed 11.12.2021. Available from https://www.fda.gov/media/131150/download
43. Ullah M, Qiao Y, Concepcion W, Thakor AS. Stem cell-derived extracellular vesicles: role in oncogenic processes, bioengineering potential, and technical challenges. Stem Cell Res Ther. 2019; 10: 347. DOI: 10.1186/s13287-019-1468-6
44. Uršič B, Kocjančič B, Romolo A, Iglič A, et al. Assessment of coxarthritis risk with dimensionless biomechanical parameters. Acta Bioeng Biomech. 2021; 23:25-34. DOI: 10.37190/ABB-01738-2020-03
45. van Niel G, D'Angelo G, Raposo G. Shedding light on the cell biology of extracellular vesicles. Nat Rev Mol Cell Biol. 2018; 19:213-228. DOI:10.1038/nrm.2017.125
46. Vehar A. Fate of bisphenols during conventional wastewater, 6.th Socratic Lectures, online. 2021.
47. Yáñez-Mó M, Siljander PR, Andreu Z, et al. Biological properties of extracellular vesicles and their physiological functions. J Extracell Vesicles. 2015; 4:27066. DOI:10.3402/jev.v4.27066

48. Yong W, Tan Y, Poong S, Lim P. Response of microalgae in a changing climate and environment. Malaysian Journal of Science. 2016; 35:167-187. DOI:10.22452/mjs.vol35no2.7
35. Zaborowski MP, Balaj L, Breakefield XO, Lai CP. Extracellular Vesicles: Composition, Biological Relevance, and Methods of Study. Bioscience. 2015; 65:783-797. DOI:10.1093/biosci/biv084
36. Zarà M, Guidetti GF, Camera M, et al. Biology and Role of Extracellular Vesicles (EVs) in the Pathogenesis of Thrombosis. Int J Mol Sci. 2019; 20:2840. DOI: 10.3390/ijms20112840
37. Žgank Ž, Nemec A, Erjavec V. Blood lactate, body temperature and pulse before, during and after submaximal exercise in dogs with brachycephalic obstructive syndrome, 6.th Socratic Lectures, online. 2021.

Reflection

Schooling During COVID-19 Pandemic: A High School Student's Perspective

Kocjančič E[1,*], Kocjančič B[2]

1. International School Gimnazija Bežigrad, Ljubljana, Slovenia
2. Department of Orthopaedic Surgery, University Medical Centre Ljubljana, Ljubljana, Slovenia

* Correspondence: ema.kocjancic@gmail.com

Abstract:
As the COVID-19 pandemic was declared on March 11th, 2020, numerous health restrictions were put into place to help slow down the spread of the infectious disease. One of those safety measures was online school which replaced the traditional in-school learning. While distance learning meant a safer and innovative alternative to traditional schooling during the pandemic, it severely impacted a number of students, especially those from a lower socioeconomic background. This is because those students very often did not have access to functioning electronic devices and stable network connections and therefore could not participate in online schooling. Additionally, learning from home greatly limited students' ability to socialise with their classmates, something that in-person schooling allowed for every day.

Keywords: On-line learning; Lockdown; Socialization; Digital platforms

Citation: Kocjančič E, Kocjančič B. Schooling during COVID-19 pandemic: a high school student's perspective.Proceedings of Socratic Lectures. 2021; 6: 179-183. https://doi.org/10.55295/PSL.2021.D.022

1. COVID-19 and schooling

1.1. COVID-19 pandemic

On January 31st, 2020, with the global death toll by COVID-19 (caused by SARS-CoV-2 virus; Severe Acute Respiratory Syndrome (SARS)) surpassing 200 and the quickly growing number of daily confirmed cases, the World Health Organisation (WHO) declared the infectious disease a public health emergency (AJMC, 2021). Throughout February, the number of confirmed infections exponentially grew, most visibly in China, where the infectious disease was first detected and described as unusual pneumonia at the end of 2019 (WHO, 2021). By February 10th, 2020, the number of deaths by COVID-19 in China surpassed the total number of deaths by the believed predecessor virus SARS-CoV-1 from 2004 (AJMC, 2021). Worldwide spread of the virus to 114 countries by air travel and cruising (AJMC, 2021) led to WHO declaring a pandemic on March 11th 2020, and encouraging world country leaders to do everything in their power to find a balance between protecting the public health, minimising socioeconomic consequences of health restrictions and respecting human rights (WHO, 2020).

Almost two years later, the number of all confirmed cases is nearing 277 million and the number of deaths 5.5 million (WHO, 2021). Several regulations that had been put into place at the beginning of the pandemic are still in use today, such as maintaining personal hygiene, wearing protective masks and, in some countries, online schooling.

1.2. Lockdown of schools and online learning

In a matter of weeks from the declaration of COVID-19 being a public health emergency, as many as 1.5 billion students worldwide were affected by the lockdowns that followed. Schools were opened and functioning as they normally had been one day, and the next day pupils found themselves learning from home in front of a computer screen with schools closed. The traditional face-to-face learning was replaced by online learning with the only means of communication between students and teachers being school-provided emails and digital platforms (OECD, 2021, p. 5), such as Zoom and Microsoft Teams. With their children staying at home all day, the proportion of adults working from home increased significantly and many workers, especially those with the youngest children, had to adjust their working hours to help their children take part in online learning and provide them support they needed for studying and doing homework (Thorn et al., 2021).

There was also a great difference between the accessibility of education to students of different social backgrounds. Rates of infections and COVID-19-related deaths were notably higher in areas with lower socioeconomic status which has put additional stress on students from such backgrounds or regions. In addition, many of those students also had difficulties with accessing network connections, as well as devices required for online learning, such as functioning computers and printers (OECD, 2021, p. 5). This was especially highlighted in lower income countries, such as sub-Saharan Africa where as many as 45% of students had no exposure to remote learning, and the rest were only exposed to such information via radio or TV (Saavedra, 2021). In Latin America, the situation was slightly better. For instance, in Mexico, about 60% students had access to remote lessons via television or radio (McMahan, 2021). In other middle-income countries, education accessibility differences were significant within the same country, with the elite minority receiving several hours of online lectures daily, while the rest settled for a few lessons via TV or radio. Such differences are also seen in the recent evaluations of the loss of expected learning with the poorest quintile losing over 20% more of the expected learning than the richest quintile (Saavedra, 2021).

The sudden and unexpected transition to online learning or a combination of online and in-person learning not only put a strain on students, but also teachers who were mostly not familiar with online learning platforms but had to master them in a matter of days. Additionally, a lot of materials were not suited to online learning and classes, such as arts, language and physical education classes were seemingly impossible to conduct online (OECD, 2021, p. 5). Most countries provided teachers support during the transition between in-person learning and online learning in terms of training programs and courses on online teaching. Teaching content was also adapted with opening education resources and providing lesson plans (OECD, 2021, p. 34). Teachers' access to technology was one of the most frequently stated challenges among European teachers. The majority of countries resolved this by providing them ICT (Information and Communication Technologies) tools and network connectivity (OECD, 2021, p. 36).

1.2. Outcomes and the future of learning

To our best knowledge, extensive objective analyses of the effect of the COVID-19 on education have not yet been elaborated. However, subjective experiences and evaluations shared by countries and educational institutions have been performed. Publicly available online sources are consequently very mixed; on one hand, the transition from the well-established in-person learning to online hybrid learning was very rapid and thus allowed very little time for planning and training of personnel. Many teachers and students thus did not have access to technologies which would allow for them to participate in online schooling, or they did not know how to properly use the equipment that they had. In addition, technology is subjected to limitations - poor internet connections and non-working cameras and microphones. Most of all, some hands-on courses, such as physical education, dental hygiene etc. could not be taught online (University of Illinois Springfield, 2021). On the other hand, this new way of learning has introduced new, innovative models which also focus on integrating technology with education, modernising the school system (Li et al., 2020). Some experts even claim that forms of hybrid online learning are the future of education. Many universities, such as Zhejian University, managed to move over 5000 courses completely online in a matter of two weeks (Zhaohui, 2020). Other experts (Li et al., 2020) even argue that a long-awaited new way of teaching which makes student-teacher interactions, document sharing and online research much faster and more efficient, has been discovered and will, even after the pandemic is over, become part of schooling.

2. Reflection

When schools in Slovenia abruptly closed in March 2020, I was in my second year of high school. When lockdown was announced, students and teachers were told that we would stay at home for the next two weeks as a precautionary measure against the spread of COVID-19. As the concept of online learning was almost completely foreign to us, it seemed to be an exciting new experience - we did not have to wake up as early as we usually would, and we could follow classes from the comfort of our homes. Back then, none of us thought that the pandemic was just starting, and that online schooling would actually become a long-term experience.

The primary form of communication with our teachers was school email that every student was assigned as they enrolled in high school. This form of communication was efficient, but sometimes, in the flood of emails received daily, information about online classes or homework or additional resources got lost. However, this was always resolved with communication among students, mostly over previously created social media class group chats.

At first, neither the students not the majority of teachers knew how online school would look like. This gave most teachers the freedom to come up with their own system

that we were introduced to during the first week of online classes. Generally, we had one online lesson weekly per subject and in between those lessons we studied textbooks and completed worksheet by ourselves. After the first two weeks of lockdown quickly passed and there was no talk of returning to school in-person, we soon realised that online learning had become a new reality and we had no choice but to get used to it. I believe it was this realisation that encouraged us students, as well as teachers, to do our best communicating and helping each other - after all, we were all in this together. After about one month, everyone was used to online schooling and had their own rhythm and system of working. Until the end of the school year we were graded at least once per subject, most often by written examinations during which we had to turn on our cameras and place them so that our workspace was seen. Meanwhile, classes then continued in a similar manner as before, that is, one or two online lessons per subject per week in addition to textbooks and worksheet.

We started the next school year, my third year of high school, in person. As I had just joined the two-year International Baccalaureate Diploma programme at my school, I started the year in a new classroom filled with students who did not know each other, so the seven weeks we spent physically in school were very valuable to us, as we were just getting to know each other. Since the beginning of the year, we were all prepared for the possibility of online school, so we mostly got instructions as to how online classes would look like for each subject in advance. When the state of the pandemic did indeed get worse a few weeks after the school year began, we once again switched to online schooling. Having spent prolonged periods of time at home the previous year too, it felt as if the time spent in schooling online was the time when socialisation was put on pause. This was mostly due to the lack of breaks in-between lessons that we would otherwise spend in a classroom together. At home the breaks were spent with the computer camera turned off. So, for the duration of online schooling which lasted for about five months, my classmates and I spent little to no time getting to know each other and mostly stayed in contact with our other acquaintances and friends. This lack of connection between us is still seen today; while we are classmates who see each other every day, we have not formed many meaningful friendships among each other.

During the second lockdown, schooling was a bit different and more organised; all classes that we would have at school in person were held online, following the same schedule. This made keeping track of assignments and online lectures much easier than during the first year, however, it was also much more time consuming, and I had often found myself finishing classes at 5 pm when it was already dark outside. This combined with the fact that my bedroom had essentially become my classroom and the room I wrote my exams in, both contributed to my overall lack of motivation to do school-related work after class, and my increased need to go outside multiple times per day to get away from the computer screen. I often had headaches and strained eyes following the entire day of online lectures attended with a computer screen.

To sum up, online schooling was a very interesting experience which allowed for the safest way of learning during the pandemic. However, the lack of socialisation and changing of my everyday environment is what had me hoping every day that things would finally return back to the old normal, and that I would again be able to attend school in-person again.

Conflicts of Interest: The authors declare no conflict of interest.

References

1. AJMC Staff (2021), A Timeline of COVID-19 Developments in 2020. Updated 2021. Accessed 26.12.2021. Available from https://www.ajmc.com/view/a-timeline-of-covid19-developments-in-2020
2. University of Illinois Springfield (2021), Strengths and Weaknesses of Online Learning. Accessed 28.12.2021. Available from https://www.uis.edu/ion/resources/tutorials/online-education-overview/strengths-and-weaknesses/

3. Li C, Lalani F (2020). The COVID-19 pandemic has changed education forever. This is how. Accessed 28.12.2021. Available from https://www.weforum.org/agenda/2020/04/coronavirus-education-global-covid19-online-digital-learning/
4. McMahan B (2021), Education in Latin America after the pandemic. Accessed 29.12.2021. Available from https://news.mit.edu/2021/education-latin-america-after-pandemic-1029
5. OECD, The state of school education: One year into the COVID pandemic. 2021; pp. 5-36. Updated April 2021. Accessed 27.12.2021. Available from https://read.oecd-ilibrary.org/education/the-state-of-school-education_201dde84-en#page1
6. Saavedra J (2021), A silent and unequal education crisis. And the seeds for its solution. Accessed 28.12.2021. Available from https://blogs.worldbank.org/education/silent-and-unequal-education-crisis-and-seeds-its-solution
7. Thorn W, Vincent-Lancrin S. Executive Summary. In: Schooling During a Pandemic: The Experience and Outcomes of Schoolchildren During the First Round of COVID-19 Lockdowns. OECD Publishing 2021. https://doi.org/10.1787/d106fff3-en.
8. WHO (2020), WHO Director-General's opening remarks at the media briefing on COVID-19 - 11 March 2020. Accessed 27.12.2021. Available from https://www.who.int/director-general/speeches/detail/who-director-general-s-opening-remarks-at-the-media-briefing-on-covid-19---11-march-2020
9. WHO (2021), WHO Coronavirus (COVID-19) Dashboard. Accessed 26.12.2021. Available from https://covid19.who.int
10. WHO Team (2021), WHO-convened global study of origins of SARS-CoV-2: China Part. Accessed 26.12.2021. Available from https://www.who.int/publications/i/item/who-convened-global-study-of-origins-of-sars-cov-2-china-part
11. Zhaohui W (2020), How a top Chinese university is responding to coronavirus. Accessed 28.12.2021. Available from https://www.weforum.org/agenda/2020/03/coronavirus-china-the-challenges-of-online-learning-for-universities/


I. Klepetář
Prag.

Scientific contribution/Original research/Invited lecture

Semiotics and Transcultural Aspects of J. S. Bach's St John Passion

Komarova E[1]

[1] F. M. Dostoevsky Omsk State University, Omsk, Russia

* Correspondence: Elena E. Komarova: komarova_elena63@mail.ru

Abstract:
This article deals with the music of Bach as both a perfect theological, scientific and art phenomenon. On the example of his work «St John Passion» a hypothesis is put forward about the reflection of the symbolism of the Gospel Word in musical form.

Keywords: St John Passion; Chorale preludes; Symbol of eternity; Rhetorical figures; Rainbow music of Bach.

Citation: Komarova E. Semiotics and transcultural aspects of J.S. Bach's St John passion. Proceedings of Socratic Lectures. 2021; 6: 185-188. https://doi.org/10.55295/PSL.2021.D.023

1. Introduction

In modern views on transculture, the human race on its moves "nature - culture - transculture" has been breaking free of customs, conventions, unconscious typical behavior, native culture gravitation. On this road, the dialogue with Johann Sebastian Bach's music is an asset. He like the keystone of vault as much holds apart as unites pre classical (for example, Baroque) and classical music, stretching out his influence on today's composers. His music is both a perfect theological, scientific and art phenomenon.

2. Religious influences in Bach's music

Eisenach, the land of Luther and birthplace of J. S. Bach, produced protestant national tradition for further Bach work, especially in ecclesiastical genres. It means he not only refers to protestant chorale resources as the foundation of thematic and melody invention (melopoeia [melə'pē(y)ə]), but builds all his technique of composition and musical way of thinking in accordance with the law of the gospel of Christ and protestant chorale. Therefore, one may understand Bach both through learning of polyphonic music, theology, philosophy.

A special music function in a protestant church is an evangelic (kerygmatic) preaching. In the days of Bach and earlier the ecclesiastical music was to address artistic issues, and even more to search for narratives the Holy Scriptures offered and then to embody them in sounds. The gospel of Christ sang by the congregation in chorales *was immediately followed by* non-verbal interpretation by a church organist. For example, in chorale preludes Bach adds to the tune of a protestant chant other counterpoint lines, which includes melodic idioms, rhetoric figures as they present Christian symbols in accordance with the text of the service prayer, i.e. the text of chorale the congregation has just sung. A Baroque music vocabulary, based on highly developed theory, widely uses affects, melody and rhythm configurations as rhetoric figures. That's why the Baroque period got the name the Age of Ready Word in science musical literature. Bach's preludes for organ contain commonly used musical rhetoric figures of "Cross," "katabasis" (a descent), "anabasis" (an ascent), "circulation" etc - one may see in improvised parts, which set off the melody of wordless chorale relevant to the narrative of a prayer's verbal content. While a chorale is a sermon in musical sounds, Bach's preludes for organ become wonderful reflection over sacraments as far as author's unique artistic fantasy goes.

In bigger genres of his ecclesiastic music, oratorial like Passions, we may see the influence of Dutch contrapuntists, operatic Italian contemporaries, and Baroque instrumentalists. At the same time, Bach expanded the "variations on chorale" principles with a dramatic composition, the polyphonic way of thinking, symbolic musical language.

On one hand, his St Matthew Passion and St John Passion present author's pieces of arias, ariosos, choruses sung on the Passion Week's protestant service where we can hear an evangelist's recitation and congregation's chants of the Book of Gospels. On the other hand, it is an independent artistic phenomenon, the author's original piece.

3. St. John Passion

Attentive listeners of St John Passion created in 1724 for Good Friday Vespers may notice strange frequent repetitions of some musical text. Its structure and St Matthew's reminds the arched-shape structure of a cathedral, interconnected by vaults, divided by pillars and interspaces. In St Matthew Passion, arched-shape and replication principles are applied to chorales, in St John Passion replications or tune imitation - to choruses and arias. There are so many of replications that the certain author design obviously, besides pure musical aims, should be understood through theological, symbolic context.

All arias in the first part of St John Passion have key and tonal relationship or reflections within the second part. For example, aria 11 of alto echoes in aria 65 of soprano, soprano aria 13 you may recognize in chorus 34 and 50, tenor aria 19 resounds in alto aria 58 (both, with a motif of mourning, are typical lamento arias). But most repetitions at a short periods between them appear in the second part, the scene of Pontius Pilate's court, the climax for both St Matthew and St John Passions. So: St John Passion: the tone of chorus 36 Kreuzige is similar to 44, and 38 to 42. Therefore, chorus-replicas of vengeful crowd make the outer structural shapes of chorus 40, the most important, sense bearing, chorale, revealing an assignment of Christ Passions.

According to Baroque symbolism this chorale differs because of juxtaposed chorus repetitions that create the shape of chalice – a symbol of Martyrdom - Jesus Christ is going to drink for purpose of redemption of human sins. In the outer structural shapes of chorus 40 one may see another symbol: the Eternity, a religious narrative of that historical period. Vanitas i.e. Eternity, is Bach's favorite symbol in music.

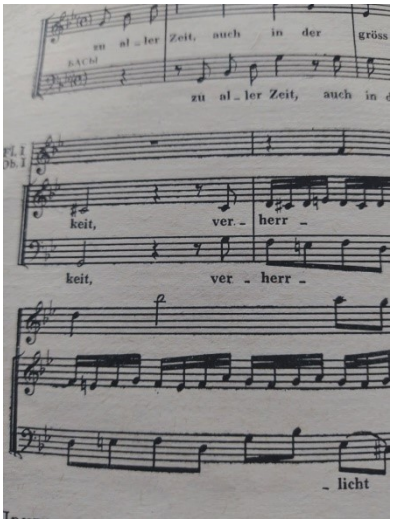

Figure 1: Opening choir. Figures of eternity.

Such numerically organized climax as well as the whole composition of St John Passion means contemplation of *arched-shape* repetitions, because circle is a symbol of Eternity in German protestant musical vocabulary. Eternity is already verbally and musically declared at the opening chorus of the Passion. Voices sing about eternal worshiping of Christ at his mortal torments: orchestra part includes figures of "circulation" as Baroque music specifies a Bible definition of Eternity.

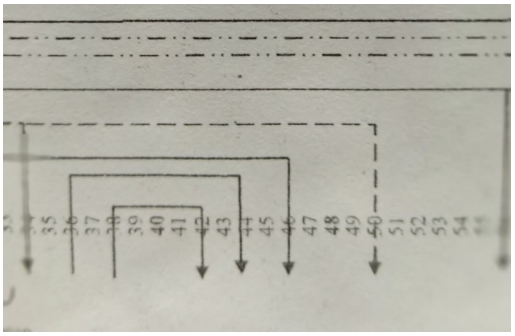

Figure 2: Scheme of repetitions around the chorale № 40.

This rhetoric figure functions not only as was common after the Baroque era, or as a leading motif of a symphony or opera's general melodic pattern and dramatic part, but as a leading symbol St John Passion's structure itself establishes. Moreover, the symbol is of both religious and earthly source. Eternity on the verbal and musical level was first announced already in the opening choir of passions. «The moment words are involved the attention is deflected away from form and towards meaning and interpretation» - wrote in a book about Bach the famous interpreter and researcher of his music J. E. Gardiner [1, p. 19]. But in the Passion according to John, the form influences the interpretation of the meaning, the interpretation of the key words of the text of this work. The religious one enters at the opening chorus, religious chorale texts, but the earthly one in aria 32 – is the symbol of a rainbow in verses by an unclerical author, Christian Weise. The aria says that over torrents of our sins similar to the Old Testament's Flood the Rainbow of the God's Blessing will rise. A. Schweitzer described this aria as "a smile through the tears of the redeemed world"[2]. Same, the Rainbow of the Old Testament, the sign of an agreement between the God and people, foresees the New Testament's Rainbow. The aria's woodwind gliding passages are the symbol of purification, waves of the Flood washing out human sins.

4. Conclusion

An arched-shape musical organization of Passions, especially repetitions, the circumference of chorale 40, builds up an X-shape so called chiasmatic rhythm one can meet in Bible, more often in the Gospel of St John. Once inspired by the most poetic of Testaments, J. S. Bach also assumed its poetic rhythm.

Thus, the principles of arched-shape, thematic, tonal cross-talk through the whole piece of work can be explained that on compositional level he wanted to reveal off-beat symbol which is Rainbow rather than more established in spiritual practice of his time symbols of the Cup of Suffering and Eternity, and in order to do it, he took a poetic text, not the canonic, organized semantic culmination in line with chiasmatic rhythm (ABCBA) pertaining to the Gospel of St John.

Therefore, a coherent analysis and an interpretation of J. S. Bach's work, St John Passion in particular, is not simple and lays in the field of multiple music practices, art, science, theology, i.e. in the field of transculture.

Acknowledgements: Author is indebted to Alla Ozdural for translation from Russian to English language.

References

1. Gardiner JE. Music in the castle of heaven: A portrait of Johann Sebastian Bach. Penguin UK. 2013, pp. 629.
2. Schweitzer A. J.S. Bach. Dover Publications, Mineola, New York, U.S.A. 2012, pp. 727.

Scientific contribution/Original research

Samuel Gmelin (18th century): Inspiration from the Past through Science, Technology, Engineering, the Arts, and Mathematics Approach

Istileulova Y*

* Correspondence: Yelena Istileulova yelena.istileulova@fulbrightmail.org

Abstract:
Samuel Gmelin, the German physician, explorer and botanist is known for two books, a "Historia Fucorum" in 1786, and "Travels through Russia to Investigate the Three Natural Realms" between 1770-1774. The new method of SMS (Stories based on Music about Scientists) is introduced under the umbrella of STEAM (Science, Technology, Engineering, the Arts, and Mathematics) approach inspiring an interest towards scientists of the Past and their innovations. The method is illustrated on the example of Samuel Gmelin´s life and represents the new learning and teaching method.

Keywords: STEAM;

Citation: Istileulova Y. Samuel Gmelin (18th century): Inspiration from the past through science, technology, engineering, the arts, and mathematics approach. Proceedings of Socratic Lectures. 2021; 6: 190-193. https://doi.org/10.55295/PSL.2021.D.024

Publisher's Note: UL ZF stays neutral with regard to jurisdictional claims in published maps and institutional affiliations.

1. Introduction

The discoveries and innovations are very often coming from the inspiration of stories and life of scientists of the Past perceived through a prism of the Present. The goal of this article is to demonstrate the new method SMS (Stories based on Music about Scientists) which can be applied under the STEAM approach on the example of inspiring life of Samuel Gmelin (1744, Tübingen, Germany - 1774, Dagestan (Derbent), Russia).

Samuel Gottlieb Gmelin, the German physician, explorer and botanist, was a member of celebrated family of German naturalists with Russian connections thanks to his uncle Johann Georg Gmelin (1709-1755) (Silva et al.,1996) Gmelin is known for two books, "Historia Fucorum" (1786), the first book published in Russia on marine biology where he described 20 types of algae in the Russian seas, and "Reisen durch Russland zur Untersuchung der drei Naturreiche" (Travels through Russia to Investigate the Three Natural Realms) (between 1770-1774) (Gmelin, 1770-1774).

In 1770, he embarked on a journey on behalf of the Russian Academy of Sciences and in the service of Catherine the Great. The interesting fact is that he was accompanied not only by the other 8-9 professionals, soldiers, but also the flutist and drummer (Darwin Museum, 2021). He researched flora and fauna of the western part of the Caspian Sea. He was also visiting the east coast (present day Kazakhstan), making interesting ethnographic observations there.

The tragic event took place on February 5, 1774 in Dagestan, when Gmelin was taken as a prisoner by the Kaitag Khan, and all attempts by the Russian authorities to influence the khan on the extradition of a scientist were not successful. Catherine II wanted to release the scientist by force, but the Pugachev uprising prevented this step. Gmelin died in captivity in July 1774 from anxiety, unrest, malnutrition, exhaustion and dysentery, and he was only thirty years old (Gokhnadel 2017).

Research of Samuel Gmelin covers the broad spectre - from the Caspian birds, fish as well as mammoth remains described by him in 1769 with a flora and fauna of the Caspian Sea´s region (Chernykh, 2015). That is why his books could be inspiration for many scientists of different disciplines – from botanics up to the biology of marine life. The STEAM (Science, Technology, Engineering, Arts, and Mathematics) approach with the power of the art can re-create the life of scientists with their innovations and resides in its ability to represent nature. In the ancient Greece people believed the creativity artists possessed came to them from a muse, a personification of knowledge and the arts that inspired them to write, sculpt, or compose (OECR 2019).

2. Methodology with STEAM approach

The method which is demonstrated here is entitled SMS (Stories based on Music about Scientists). It was first introduced in 2013 in the Russian Center of Science and Culture in Ljubljana by the author (under the name of Aleona Sultanova) with the song written about a Russian and Soviet rocket scientist who pioneered astronautic theory - Konstantin Tsiolkovsky. Methodology is based on the experimental design of author´s Poetry, Music as well as Visual Arts (video with pictures or compiled documentaries when is placed in video presentation during the performance) incorporating the elements of aesthetics, creativity, and a research discourse about scientists´ discoveries from the Age of Enlightenment (17th-18th century) up to the present days.

SMS method is well-incorporated in STEAM (STEM + Art) approach under Art (Music and poem) with "complex problem solving, creativity, critical thinking, people management and cognitive flexibility" (OECR 2019). In addition, the incorporation of elements like SMS related to poem and music provides STE(A)M with real opportunities for innovation in teaching, training as a new learning method. Thus,

STEAM SMS method is based on research delivered in the form of song – with a poem where its context can be enriched through the means of music. The example is published in the 2nd Proceedings of International Symposium Socratic Lectures 2019 about Baron Valvazor, a natural historian and polymath from Carniola (present-day Slovenia), and the story (poem) about him with the music score (Sultanova, 2019). The song "Baron Valvazor" was also performed by Duo "Al-Chemy" during Symposium in 2019 with some accompanying pictures. This story about life of Gmelin is based on research and became the source of inspiration to create a song. Here we publish the poem in Russian with its translation in English.

3. Methodology with STEAM approach

SMS method – stories based on music about scientists is presented here through the song entitled „Дорога длиной на всю жизнь" (The road of a lifetime) and dedicated to Samuel (George) Gottlieb Gmelin, the scientist of the 18th century. The original is in Russian language, and translation in English is also provided. The music scores are not attached here (due to the lengths) but can be performed. Both lyrics and music are written by Aleona Sultanova, and this pseudonym used by the author of this article for her compositions and poems.

Дорога длиной на всю жизнь Посвящено Гмелин, Самуил Готлиб (1744-1774).
Восемнадцатый век. Тюбинген... Ты отсюда отправишься в путь,
И дорога длиной на всю жизнь, твой красивый недолгий путь
Чтоб узнать величие морей, и как водоросли растут,
Ты в Голландию путь держал, чтоб в России себя воплотить

Припев
Вода-Вода, горы-берега, степь бескрайних равнин и пустынных долин
Вода-Вода, «трёх царств естества», дикой лошади след в «царские луга»

Кистяной колокольчик в пуху на лугах у Валдайских гор
Ты открыл здесь свою главу из растений, птиц, рыб и цветов
И на западе Каспия, где ты проложишь чудесный след
Барабанщик твой дух пробудит, а флейтист на птиц чары пустит

Припев
Вода-Вода, горы-берега, степь бескрайних равнин и пустынных долин
Вода-Вода, «трёх царств естества», дикой лошади

The road of a lifetime dedicated to Gmelin, Samuel Gotlieb (1744-1774) (translation)
Eighteenth century. Tübingen...You will start your journey from here,
And this road is a lifetime, your beautiful short journey
To know the majesty of seas, and how algae will grow,
You made your way to Holland in order to realise yourself in Russia

Chorus
Water-Water, Mountains-Shores, steppe of endless plains and desert valleys
Water-Water, "of three kingdoms of nature", a wild horse trail in the "royal meadows"

Flower bell in fluff in the meadows near the Valdai Mountains
You opened your chapter here from plants, flowers and birds
And in the west of the Caspian Sea, where you will lay a wonderful trail
Your drummer will awake your spirit and flutist will cast spells on birds

Chorus
Water-Water, Mountains-Shores, steppe of endless plains and desert valleys
Water-Water, "of the three kingdoms of nature", a wild horse trail in the "royal meadows"

The song refers to the concepts and names used in the original books of Gmelin. SMS method might rise different questions, and requires some small initial discussion what was so stimulating to write about it. For instance, the "white horse" used to be named "tarpan", a Kazakh or Kyrgyz name meaning "wild horse" which is derived from a Turkic language - The horse was named after Gmelin, but it disappeared or almost disappeared by the end of 18th century.

Conclusions

SMS method has a motivational focus to stimulate interests to learn, understand and innovate as well as ask questions. It is well suited under umbrella of STEAM, where art is presented by music and poem, and brings their power of influence (Sachant and Tekippe, 2022). So far it has not been discovered in any publications related to songs about scientists and their innovations. Therefore, it can potentially bring the new research and innovations. The discoveries and innovations are very often coming from the inspiration of stories from the life of such scientists of the Past as Samuel Gmelin.

Conflicts of Interest: The author declares no conflict of interest.

References:

1. Chernykh E. (Елена Черных) 2015, июль. Как ученый Гмелин исследовал под Воронежем «скелеты слонов» https://infovoronezh.ru/News/Kak-uchenyiy-Gmelin-issledoval-pod-Voronejem-skeletyi-slonov-39539.html
2. Darwin Museum (2021), Дарвиновский музей. Видеорепортаж из фондов музея «Трагическая история научной экспедиции второй половины XVIII века на юг России» Available at: http://www.darwinmuseum.ru/projects/event/den-istoricheskogo-i-kul-turnogo-naslediya-moskvy
3. Gmelin, Samuel Gottlieb (1743-1774) Global plants. Available at: https://plants.jstor.org/stable/10.5555/al.ap.person.bm000374049
4. Gokhnadel V.Виктор Гохнадель (2017, март). Талантливый и дерзкий путешественник . Available at: https://daz.asia/ru/talantlivyj-i-derzkij-puteshestvennik/
5. OECR (Opinion of the of the European Committee of the Regions — Strengthening STE(A)M education in the EU (2019/C 404/06)
6. Sachant PJ, Tekippe R. Art and Power. Available at: https://alg.manifoldapp.org/read/introduction-to-art-design-context-and-meaning/section/54129c96-ca5a-4108-832b-9e3180e85cc8
7. Silva PC, Basson P, Moe RL. Catalogue of the benthic marine algae of the Indian Ocean .Univ of California Press. 1996.
8. Sultanova A. Baron Valvazor. International Symposium Socratic Lectures 2019,110-112 . Available at: https://repozitorij.uni-lj.si/IzpisGradiva.php?id=113109


CARL DÖRR WIEN

Reflection

Music at 6th Socratic Lectures: Organ Concert of Roberta Schmid

Prelovšek A[1], Kralj-Iglič V[1],*

1. Univresity of Ljubljana, Faculty of Health Sciences, Laboratory of Clinical Biophysics, Ljubljana, Slovenia
* Correspondence: Veronika Kralj-Iglic: veronika.kralj-iglic@fe.uni-lj.si

Abstract: Description of the social event accompanying 6th Socratic Lectures is presented. This event consisted of a concert by organist Roberta Schmid from Naples, Italy in the Church of the Assumption of Mary, Ljubljana at the evening of the day of symposium. The connection of the concert to the Socratic Lectures, the biography of the artist, the description of the organ with the list of the stops, the program of the concert and the critics of the concert are presented.

Keywords: Organ music; JS Bach Choral Ich ruf zu dir, Herr Jesu Christ BWV 639; JS Bach Toccata and Fugue in D minor BWV 565; J Pachelbel Ciacona in F minor; PA Yon Toccatina for flute; E Gigout Toccata in B minor; JG Rheinberger Passacaglia; L Boellmann Suite Gothique op.25

Citation: Prelovšek A, Kralj-Iglič V. Music at 6th Socratic Lectures: organ concert of Roberta Schmid. Proceedings of Socratic Lectures. 2021; 6: 195-201. https://doi.org/10.55295/PSL.2021.D.025

1. Social event at 6th Socratic Lectures

Traditionally, an important part of Socratic Lectures is the accompanying social event that features also art, in any kind connected to science. Roberta Schmid collaborated with the members of the project Ves4us already at a concert that took place in Naples, Italy in 2019 (Prelovšek, 2020). Then, it was planned that this collaboration will continue within the social events of the Socratic Lectures in Ljubljana. Due to pandemic, in 2020 and in April 2021, 4th and 5th Socratic Lectures took place online. There were no social events in person, but music was nevertheless included by performances online, yet an organ concert was considered to be performed in the church, in particular in the Church of the Assumption of Mary, therefore it was postponed for later. The situation in December 2021 indicated a possibility to have concert in person at the church, however with restrictions that minimized the risk for possible transmission of COVID-19. Organized by the Franciscan p. Vid Lisjak, the concert of Roberta Schmid from Naples, Italy, took place at the evening of the symposium, 11.12.2021.

2. The organist Roberta Schmid

Roberta Schmid was born in Naples in 1964. She took her diploma in Organ and Organ Composition at the Musical Conservatoire "S. Pietro a Maiella" in Naples with the mentorship of prof. A.M.Robilotta and then improved her technique with maestros of international standing such as L. Ghielmi, E. Kooiman, M. Radulescu, D. Roth, K, Schnorr, L. F. Tagliavini, M. Torrent, P. Westerbrinck, W. Zerer, specializing her executive practice in different organ repertoires. After getting through a national examination she attended a three year course in Professional training as an Organist at the Musical Academy in Pistoia and took a diploma in "Italian and German Organ Music Interpretation". She attended a three year course in Gregorian Chant at the International Study Centre of Gregorian Chant in Cremona. She also took diplomas in Piano and in Musical Didactics, and, lately, the second level degree specializing in Organ interpretation and composition, recently introduced in Italian Music Conservatoires. She has a very busy professional life performing at concerts as a soloist and in chamber formations. As a soloist, she has been invited to take part in numerous international organ festivals - in Europe and in Mexico - and she has always been highly acclaimed by public and critics alike. She also performs for: Quarto Festival Internacional de Organo de Zamora Michoacàn (Mexico), Primer Ciclo Internacional de Conciertos en el Organo Barroco de la Parroquia de Santiago de Querétaro (Mexico), International Organ Summer Festival in Rome, XXVIII Festival Internazionale di Noale, Rassegna Antichi organi di Piacenza, Associazione Alessandro Scarlatti di Napoli, Associazione Studi Mezzogiorno, Associazione Ricercare, Accademia Organistica Campana, Rassegna organistica internazionale di Avezzano, Rassegna organistica di Pescara, Settembre Organistico Fabrianese, Rassegna organistica veneta "Musica nell'Agordino" , Rassegna "Musicalia" in Pavia, Festival Organistico Internazionale Città di Senigallia, Rassegna Organistica di Fiemme (Trento), Rassegna organistica della Svizzera italiana and for the International festivals performed at Notre Dame de Compassion in Paris, Merano Cathedral, Amalfi Cathedral, S. Vitale's Basilica in Ravenna, S. Ambrogio's Basilica in Milan and in Mexico City. She has recorded a Cd of Bach and pre-Bach music sponsored by the Goethe-Institut Italien. She is Artistic Director of the Festival "Musica intorno all'organo" at the St. Maria della Rotonda Church in Naples with the contralto Daniela Del Monaco. She was Artistic Director of the Concorso Organistico Nazionale Città di Napoli "11 Fiori del Melarancio". She taught "Organ and Organ composition" at F. Vittadini Civic Institute in Pavia and Organ at High School Alfano I in Salerno and at High School Palizzi in Naples. She is the official organist of Mascioni mechanical organ at St. Maria della Rotonda Church and at Santa Chiara's Basilica in Naples.

3. The organ

The organ in the Church of the Assumption (**Figure 1**) was built by Franc Goršič in 1870. The organ had originally two manuals and 32 stops. However, the Franciscans, in particular p. Hugolin Sattner (1851 – 1934) wished a more powerful instrument. Therefore, the organ was upgraded by an Austrian masters Mauracher in 1902 to add another manual and 12 more stops (Župnija Marijino oznanjenje – frančiškani, 2021). The list of present stops is given in **Table 1**.

Table 1. Stops of the organ at the Church of the Assumption of Mary, Ljubljana.

Manual I		Manual II		Manual III		Pedal	
I.71	Principal 8	II.31	Bells	III.51	Tremolo Bourdon 16	P.11	Violon 16
I.72	Vox Humana 8	II.32	Gamba 8	III.52	Salicional 8	P.12	Subbass 16
I.73	Octave 4	II.33	Tubular flute 8	III.53	Vox Coelestis 8	P.13	Covered bass 8
I.74	Quint 2 2/3	II.34	Conical flute 4	III.54	Violin Principal 8	P.14	Cello 8
I.75	Superoctave 2	II.35	Cornet V8	III.55	Octave 4	P.15	Nachthorn 2
I.76	Tierce 1 3/5	II.36	Trumpet 16	III.56	Viole 4	P.16	Contra bombarde 32
I.77	Cimbel 2/3 IV-V	II.37	Trumpet 8	III.57	Nasat 2 2/3	P.17	Bombarde 16
I.78	Connection III-I	II.38	Clairon 4	III.58	Tierce 1 3/5	P.18	Trombone 8
I.81	Tremolo	II.41	Principal 16	III.59	Mixture 2 IV-VI	P.19	Schalmei 4
I.82	Copula 8	II.42	Principal 8	III.61	Soft Bourdon 16	P.21	Contrabourdon 32
I.83	Woudfluit 4	II.43	Octave 4	III.62	Bourdon 8	P.22	Principalbass 16
I.84	Blockflute 2	II.44	Quint 2 2/3	III.63	Harmonic flute 4	P.23	Octavbass 8
I.85	Larigot 1 1/3	II.45	Super Octave 2	III.64	Small flute 2	P.24	Coralbass 4
I.86	Dulcian 16	II.46	Mixture Minor 1 1/3	III.65	Piccolo 1	P.25	Mixture 2 2/3 IV
I.87	Bent horn 8	II.47	Mixture Major 2	III.66	Fagotto 16	P.26	III-P
		II.48	Connection III-II	III.67	Harmonic trumpet 8	P.27	II-P
		II.49	Connection I-II	III.68	Oboe 8	P.28	I-P
				III.69	Vox Humana 8		

Figure 1. The organ in the Church of the Assumption of Mary, Ljubljana.

4. The program

JS Bach: Choral Ich ruf zu dir, Herr Jesu Christ BWV 639
JS Bach: Toccata and Fugue in D minor BWV 565
J Pachelbel: Ciacona in F minor
PA Yon: Toccatina for flute
E Gigout: Toccata in B minor
JG Rheinberger: Passacaglia
L Boellmann: Suite Gothique op.25

The program opened with a Choral by J.S. Bach (1685 – 1750) taken from Orgelbuchlein "Ich ruf zu dir, Herr Jesu Christ" BWV 639 (Bach, 17--), conceived in F minor, the key, according to Mattheson (1958) as passionate:

"F minor is felt to be mild and relaxed, yet at the same time profound and heavy with despair and fatal anxiety. It is very moving in its beautiful expression of black, helpless melancholy which occasionally causes the listener to shudder."

The choral is included in a collection of 46 choral preludes for organ written during the 1708-1717 period, while Bach was a court organist in Weimar. The collection is defined by Bach himself as 'Orgel-Büchlein, Worinne einem anfahenden Organisten Anleitung gegeben wird, auff allerhand Arth einen Choral durchzuführen…' (Little organ book, in which an organist is taught to arrange a chorale in all sorts of ways). The text of the choral (in German language) reads:

Ich ruf zu dir, Herr Jesu Christ

1. Ich ruf zu dir, Herr Jesu Christ, ich bitt, erhör mein Klagen; verleih mir Gnad zu dieser Frist, lass mich doch nicht verzagen.
2. Den rechten Glauben, Herr, ich mein, den wollest du mir geben, dir zu leben, meim Nächsten nütz zu sein, dein Wort zu halten eben.
3. Ich bitt noch mehr, o Herre Gott – du kannst es mir wohl geben –, dass ich nicht wieder werd zu Spott; die Hoffnung gib daneben; voraus, wenn ich muss hier davon, dass ich dir mög vertrauen und nicht bauen auf all mein eigen Tun, sonst wird's mich ewig reuen.
4. Verleih, dass ich aus Herzensgrund den Feinden mög vergeben; verzeih mir auch zu dieser Stund, schaff mir ein neues Leben; dein Wort mein Speis lass allweg sein, damit mein Seel zu nähren, mich zu wehren, wenn Unglück schlägt herein, das mich bald möcht verkehren.
5. Lass mich kein Lust noch Furcht von dir in dieser Welt abwenden; beständig sein ans End gib mir, du hast's allein in Händen; und wem du's gibst, der hat's umsonst, es mag niemand erwerben noch ererben durch Werke deine Gunst, die uns errett' vom Sterben.
6. Ich lieg im Streit und widerstreb, hilf, o Herr Christ, dem Schwachen; an deiner Gnad allein ich kleb, du kannst mich stärker machen. Kommt nun Anfechtung her, so wehr, dass sie mich nicht umstoße du kannst machen, dass mir's nicht bringt Gefähr.
7. Ich weiß, du wirst's nicht lassen.

.

It can be seen that the first two parts address the faith and the hope that are also the subject of the Letter of St. Paul to the Romans (Corynthians). However, it stands there that (Corynthians):

13 And now abide faith, hope, love, these three; but the greatest of these is love."
2 And though I have the gift of prophecy, and can understand all mysteries and all knowledge, and though I have faith, that can move mountains, but have not love, I am nothing."

According to Schmid, the three values (faith, hope and love) are symbolically represented by a three-part writing throughout the Orgelbuchlein. She considered this particularly important due to a dark time that our world is going through. She wished to to open with a message that became crucial in pandemic: Without faith, hope and love, and without even the concrete possibility of expressing it we remain separated and sad, deprived of

the greatest values, the ones that truly makes us "human". Yet, the music has the power to warm everyone's heart.

To contrast the intimacy and sweetness of the first piece, Toccata and Fugue in D minor BWV 565 by J.S. Bach presents extraordinary rhythmic incisiveness and the impressive effectiveness of the sound which should affirm the strength, determination and also the joy that must never abandon us. Despite its dubious authenticity, the Toccata and Fugue BWV 565 remains among the most celebrated compositions of J.S. Bach. The Toccata, characterized by a virtuosic writing far from the rigid contrapuntal style and rather much closer to the art of improvisation, is followed by the famous Fugue, which also includes a toccatistic section (bars 59-85) and a concluding section in highly effective recitative style.

With the third piece - J. Pachelbel's (1653 – 1706) Chaconne - we return to the initial key, F minor, the same "passionate" key of Bach's Choral BWV 639. The cantability of the melodic line reveals the influence of the Italian school. Great is the poetry of this page, also intimate and intense, built on a theme and 22 variations, the last of which is an integral repetition of the theme itself. The ostinato bass (that is the short melodic line enunciated by the bass and which, repeated continuously in the form of variations) occasionally undergoes changes and interruptions throughout the piece. A similar form can be perceived in the famous and monumental Passacaglia BWV 582 by J.S. Bach.

The Chaconne - a form that originates in the Baroque period - is in fact a musical form very similar to that of the Passacaglia, also built on an ostinato bass and therefore on a series of rhythmic-melodic variations. It is no coincidence that the seventh piece proposed within the program was a Passacaglia, the Passacaglia in B minor taken from the eighth Sonata op. 132 for Organ by J. Rheinberger (1839 – 1901), and considered one of the best Passacaglie written in the nineteenth century for its masterful use of counterpoint pervaded by a profound romantic spirit. The theme, in 8 bars, as always is enunciated by the pedal, and immediately reveals the intense and sometimes poignant character of this wonderful piece.

On the other hand, the piece that preceded the performance of Rheinberger's Passacaglia was also an intense and touching piece: "The Old Castle", taken from "Pictures at the exhibition", a famous composition for piano by M. Mussorgsky (1839 – 1881), later also orchestrated by M. Ravel. Here the proposed piece was a beautiful transcription for organ by J. Gillou. It is known that M. Mussorgsky's original composition is a suite with a subject inspired by drawings and watercolors produced by V. Hartmann to which the composer had been linked by deep friendship. After Hartmann's sudden death, an exhibition was dedicated to the famous painter at the Academy of Fine Arts in St. Petersburg in which 400 of his works were exhibited. Mussorgsky's Piano Suite includes 15 pieces inspired by some of the paintings present at the exhibition and 5 "promenades" that represent the movement of the observer from one canvas to another. That of the Old Castle is a scene that takes place in France where a troubadour sings his touching love song in front of the walls of a medieval castle. Mussorgsky's music is also intimate and touching.

Table 2. Registrations applied in some of the pieces of the program

Composition	Registration
JS Bach: Choral Ich ruf zu dir, Herr Jesu Christ BWV 639	P.12,P.28/II.33/III.57,III.62,III.63/I.82
J Pachelbel: Ciacona in F minor	P.28/II.42/III.62,III.64/I.82,I.83
PA Yon: Toccatina for flute	P.12,P.14/II.33,II.49/I.83
M. Mussorgsky: Old castle (from Pictures at an exhibition – trancription of J. Guillou)	P.12,P.14/II.33,II.42,II.49/III.52,III.62,III.63,III.68/I.82
L Boellmann: Suite Gothique op.25; Priere a Notre Dame	P.12,P.28/II.48,II.49/III.53,III.62,III.63/I.82

Among the many intense, intimate, sometimes poignant contents, moments of lightness and lively energy could not be missing, such as a very delicate Toccatina for flute by P.A. Yon (1886 – 1943), the brilliant and virtuosic Toccata in B minor by E. Gigout (1844 – 1925) (fourth and fifth piece of the program, respectively) and the final piece of the entire concert, the Suite Gothique by L. Boellmann (1862 – 1897). Composed in 1895 - two years before the death of its author. The Suite is divided into 4 parts, within different tonalities and with different characteristics (Introduction, Menuet, Prière à Notre Dame, Toccata). All the parts are evocative and exciting, but certainly the most engaging, for virtuosity and sound impact, is the final Toccata.
The registration of the selected parts of the pieces chosen by Schmid for the concert at the Church of the Assumption in Ljubljana is given in Table 2.

5. The performance

Schmid performed all registration by herself. She used the advantage of pre-programing the combinations of stops which she chose at rehearsals the previous two days. She sought for the timbric colors to represent the character of the respective pieces in the best possible way.

The serene introduction by Bach's Choral Ich ruf zu dir, Herr Jesu Christ BWV 639 was delivered as a message of faith, hope and love, which supports the spirit of Socratic Lectures. The choral as well as its interpretation up-graded by Schmid's message was clearly presented by the choice of the pace and registration. The acoustic properties of the church imposed an echo that blended the notes to some extent, but allowed for their resolution.

The tempo of the Bach's Toccata was taken fast from the beginning, with rather short pauses between the phrases, which created rich energy flow. The diminished 7 acord in bar 2 initiated by the pedal exhibited the power of the instrument to extend over its acoustic possibility within the church body. It gave an impression of an eagle spreading over the sky. The pedal solo in bars 28-30 caused no hesitation to proceed with the fugue which was pursuing forward with equilibrated pace and un-ceased energy, and culminated in technical complexity in the 3 voice sequence within bars 87-95. This piece which can be considered representative for organ potentials was performed with precision and elegance.

Pachelbell's Chiaccona was played after the Bach's pieces although it was created before them, supposedly giving the advantage to the Bach's message indicated by the composition as well as the performance. This was the first piece of the program built on the variations, the variations being used also in Rheinberger's Passacaglia. Registration was markedly different from the one used for the previous piece (Bach's fugue), together with the melancholic and contemplative theme contrasting the joyful character of the former.

Following were two pieces similarly structured as to accompaniment of the melody: Yon: Toccatina for flute and E Gigout: Toccata in B minor. The author of the first one was of the most recent lifespan of all authors that were presented in the concert, therefore the composition takes more liberty in melody as well as rhythm. Schmid took full advantage of this liberty with sudden stops. The presentation was joyful. The latter technically very demanding piece of E. Gigout was attacked from the beginning and building up in volume while retaining the pace to end in a victorious B major. Schmid presented a strong interpretation of this piece that has often been chosen by her for concerts.

The 6/8 rhythm of Musorgsky's Old castle presented a pleasant change with respect to previously played Toccatina and Toccata, as well as registration that exposed the melody in a soft mode, accompanied by a pedal that crated a basso continuo effect. The choice of registration was excellent and presented the diverse acoustic effects of manuals as well as allowed for clear recognition of the pedal continuo

To proceed, Schmid was able to transcend the ostinato of the Rheinberger's Passacaglia from the Sonata VII, OP 132 into a forward developing masterpiece. She employed the ingenious counterpoint and the potential of the registration of the organ to create a developing spiral rather than variations, that presented the ostinato as newly emerging phrases. In that, she exposed in certain time intervals besides the main theme also the other voices which were equivocally revealed as a choice of the interpretation. However, she retained a firm backbone of the piece by the continuous simple and clear rhythm. In this, she leaded the composition in graded intensity to reach the magnificence of the acoustic possibilities of the space.

In Maestoso of the Introduction-Choral of the Boellmann's Suite Gothique Schmid's energy has reached the point from which she flew like an eagle and interpreted almost effortless. The closing Toccata outlined again the elements that connected it with the Yon's Toccatina, Gigout's Toccata and Rheinsberger's Passacaglia in a majestic finale that rocked the Church of assumption for moments even after the organ ceased to cause vibration of sound. The audience thanked the artist with appreciation and accompanied her 35 stairs descend with a warm applause.

References

1. Bach JS, Deutsche Staatsbibliothek. (n.d.). Orgel-Büchlein worinne einem anfahenden Organisten Anleitung gegeben wird, auff allerhand Arth einen choral durchzuführen, an bey auch sich im Pedalstudio zu habilitiren, indem in solchen darinne befindlichen Choralen das Pedal ganz obligat tractiret wird. Dem Höchsten Gott allein' zu Ehren, dem Nechsten, draus sich zu belehren. 17--. Schmeider, BWV 599-644.
2. **Corinthians 1;13:1 –** Bible Gateway. www.biblegateway.com.
3. Mattheson J, Lenneberg H. Johann Mattheson on Affect and Rhetoric in Music. J Music Theor 1958; 2:: 47-84.
4. Prelovšek A, Musical programme accompanying the Naples symposium and 2020 Socrates Lectures. Proceedings of the 3.rd International Symposium Socratic Lectures, Ljubljana, April 2020, pp 143–172. https://www.zf.uni-lj.si/si/predstavitev/zalozba/sokratska-predavanja-2020
5. The Holy Bible, New King James Version. *Nashville: Nelson. 1982.*
6. Župnija Marijino oznanjenje - frančiškani. Accessed 27.12.2021. Available from: http://www.marijino-oznanjenje.si/index.php/content/display/83/20/20

INTERDISCIPLINARY APPROACH TO AIRBONE PARTICULATE MATTER ACTIVITY ON RED BLOOD CELLS

Urška Skube[1], Manca Orel[2], Kristina Berglez[2], Marjan Bele[3], Darja Božič[2,4], Ana Kroflič[1], Marko Jeran[2,4,*]

[1]National Institute of Chemistry, Department of Analytical Chemistry, Ljubljana, Slovenia; [2]University of Ljubljana, Faculty of Electrical Engineering, Laboratory of Physics, Ljubljana, Slovenia; [3]National Institute of Chemistry, Department of Materials Chemistry, Ljubljana, Slovenia; [4]University of Ljubljana, Faculty of Health Sciences, Laboratory of Clinical Biophysics, Ljubljana, Slovenia

*Correspondence: marko.jeran@fe.uni-lj.si | @marko_jeran | www.lkbf.si

PM stands for *particulate matter*, the term used for a mixture of solid particles and liquid droplets found in the air – *aerosol*. PM is classified as one of the most dangerous air pollutants, which cause numerous adverse health effects. Prolonged exposure to high PM concentrations can lead to serious health complications and severe chronic conditions.

PM_{10} ~ inhalable particles, with diameters that are generally 10 µm and smaller.

$PM_{2.5}$ ~ fine inhalable particles, with diameters that are generally 2.5 µm and smaller.

This study started with **air quality analysis** with the focus on differences between **summer and autumn** air samples. The activity of phosphate-citrate buffer **suspended PM** particles on **human red blood cells** was further studied.

EXPERIMENTAL METHODS

AIRBORNE PM DETERMINATION

Figure 1: Particulate Matter (PMx) Sampler.

PM mass concentration in the air was monitored every day from 9 August 2020 to 15 August 2020, and from 22 November 2020 to 28 November 2020. Samples were collected on the premises of the National Institute of Chemistry (Ljubljana, Slovenia). In order to determine the difference in filter mass before and after sampling, every filter was weighed already before sampling. In this way, we determined the mass of PM particles deposited on the filter in a 24-hour step. Prior to use, the filters were pre-baked at 450 °C for 4 hours to remove potential organic contaminants. Airborne PM particles were captured on filters using a $PM_{2.5}$ sampler (Dado lab, Giano). The filters with a diameter of 47 mm are made of *quartz*-SiO_2 fibers and were loaded with a constant air flow through the sampler at 2.3 m^3/h for 24 h.

FLOW CYTOMETRY

Samples treated with PM_{10} particles were prepared in three parallels. After 1, 8 and 24 hours, the prepared samples were quantitatively evaluated by flow cytometry to determine the concentration of erythrocytes.

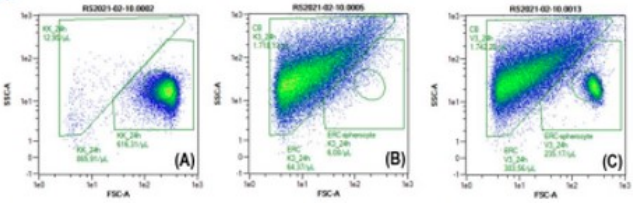

Figure 3: Scatter plots after 24 hours: (**A**) diluted blood, (**B**) PM_{10} of 200 µg/mL concentration, (**C**) treated blood sample with 200 µg/mL PM_{10}. The triangular region in the upper left corner represents the scattering region of PM_{10} particles. The region resembling the shape of a rectangle belongs to erythrocytes (ERC) and the region in the central part (circle) covers the spherocyte forms of erythrocytes (ERC-*spherocyte*). Measurements were performed using Macs Quant flow cytometer (Miltenyi, Bergisch-Gladbach, Germany).

SCANNING MOBILITY PARTICLE SIZE SPECTROMETERY

Figure 2: Scanning Mobility Particle Sizer (SMPS).

In parallel with PM sampling, outside air was drawn into an SMPS (TSI-SMPS Spectrometer, 3936L75). Before the measurement, dehydrated silica gel was filled in the instrument to prepare it for operation. The measurement range of the SMPS covers particle sizes from 14.1 to 736.5 nm. A measuring cycle in which the device counts all particles in the set measuring range was 5 minutes.

MORPHOLOGICAL ANALYSIS (MICROSCOPY)

After 1, 8 and 24 hours of blood treatment, morphological examination was performed. Blood samples, PM_{10} particles, and their mixtures were examined with a Nikon EM CCD inverted light microscope (Eclipse TE2000-S, Tokyo, Japan; coupled with a digital camera system: spot boost, Visitron Systems) at 100× magnification using immersion oil. Afterwards, 200 µL of diluted blood, particle suspension, and a mixture of PM_{10} particles with blood were pipetted into experimental perfusion chambers (26 mm × 43 mm, CoverWell™, PC4L-0.5, Grace Bio-Labs) for efficient analysis and analytical image acquisition under the microscope.

A scanning electron microscopy (SEM) image of ambient PM deposited on a quartz fiber filter was carried out using a Zeiss Supra 35 VP (Carl Zeiss, Oberkochen, Germany) microscope. The operating voltage was at 1 kV.

RESULTS

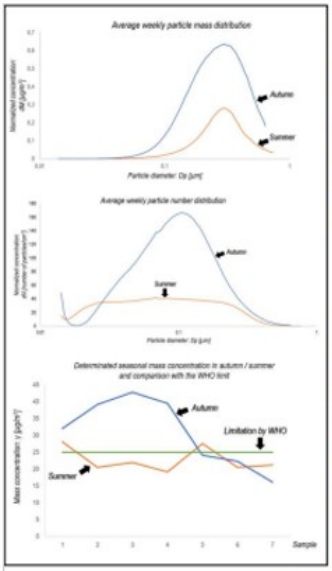

Figure 4: The graph (**A**) shows that the average weekly mass concentration of particles in summer is lower than the average weekly mass concentration of particles in autumn. In autumn, the value of maximum mass concentration was 225% higher than the value of maximum mass concentration in summer. Measurement (**B**) shows that the highest weekly number concentration of particles in summer is much lower than the weekly number of particles in autumn. From the graph we can see that in autumn there were most particles with size about 100 nm. There were significantly fewer larger particles (up to 736 nm) and smaller particles. A plateau can be seen in the curve of the summer campaign. The number of particles of different sizes is constant (between 38 and 41 particles/cm^3). For the largest and smallest particles, a decrease in the number of particles in the air can also be seen. Graph (**C**) shows the mass concentrations of $PM_{2.5}$ in summer and autumn. Measurement shows that the mass concentrations of PM particles in the air are usually lower in summer than in autumn. Autumn concentrations are 159% higher than summer concentrations. The average mass concentration of PM particles in the air was 22.71 µg/m^3 in summer and 30.85 µg/m^3 in autumn. The average mass concentration of particles in the air was also higher in winter (136%).

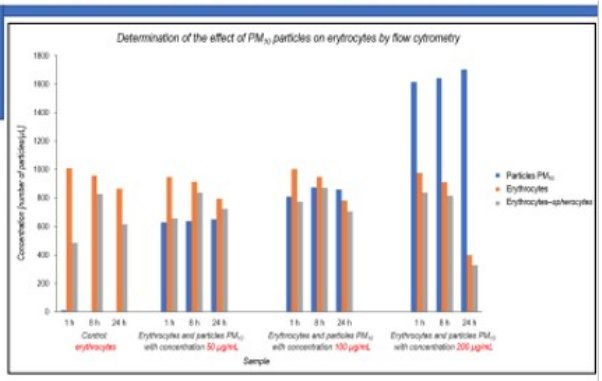

Figure 5: The graph shows the variation over time of the population (cell number) in the negative control (blood) and in the samples treated with PM_{10} particles (c = 50, 100 and 200 µg/mL). The main trend observed with respect to the increasing time component indicates a decrease in the population of erythrocytes when treated with PM_{10}. The particle concentration added to the sample plays an important role. After *24-hour* exposure, the greatest effect is observed at particle concentration of 200 µg/mL. It can be concluded that the highest concentration of PM_{10} particles has the most negative effects on erythrocytes. In the samples with lower particle concentration, the effect is visible only after 8 hours treatment.

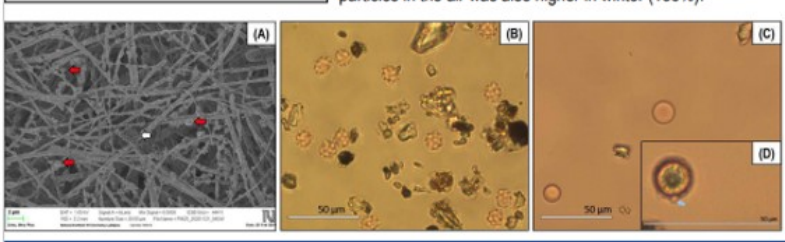

Figure 6: (**A**) Shows a SEM image of a sample collected in autumn 2020. The fibers in the image represent the filter. A large soot aggregate (white arrow) can be seen in the center of the image, and smaller accumulations of other PM particles (red arrows) can be seen all around the sample. (**B**)-(**D**): Present treated erythrocytes with PM_{10} particles (ERM–CZ100 PM_{10}, *fine dust*, c = 200 µg/mL). In the first hour of exposure (**B**), erythrocytes retain the original echinocyte shape, which begins to increase significantly after 8 hours. After 24 hours (**C**), most of the erythrocytes in the sample burst, and only the stomatal form can be detected in the preserved samples. After 24-h exposure of erythrocytes to particles (**D**), the appearance of external vesicles (arrow *D*) on the erythrocyte membrane was noted. The erythrocyte cells recognize the presence of PM particles as foreigners and consequently trigger vesicle synthesis. Namely, PM particles cause damage to the membrane so that smaller membrane fragments are released into the surrounding solution where they are converted into vesicles.

Funding: European Union's Horizon 2020 research and innovation program under grant agreement No. 801338 (VES4US project) & Slovenian Research Agency (ARRS) grants: P3-0388, P1-0034, L3-2621 and J1-1707.

Anaesthetic management for dogs treated surgically for brachycephalic syndrome: preliminary study

Barbara Lukanc[1], Alenka Nemec Svete[1], Vladimira Erjavec[1]
[1] Veterinary faculty, University of Ljubljana, Ljubljana, Slovenia
Contact: Barbara Lukanc: Barbara.lukanc@vf.uni-lj.si

OUTLINE

Brachycephalic dogs characterized by severe shortening of the muzzle and underlying bones, resulting in deformation of the upper airway:

- stenotic nares,
- an elongated soft palate,
- a hypoplastic trachea,
- laryngeal collapse,
- an inversion of the laryngeal saccules.

These anatomic features result in upper airway obstruction and represent brachycephalic obstructive airway syndrome (BOAS):

- dyspnea,
- stridor,
- snoring,
- disturbed sleep patterns,
- exercise intolerance,
- syncope.
- 2/3 hirds of BOAS dogs stridor even at rest
- 90% snore during sleep.
- surgical treatment (resection of the ala nasi and of the soft palate) is often required.
- This procedure is performed under general anaesthesia of the dogs.

Due to difficult breathing BOAS patients often have gastrointestinal abnormalities:

- regurgitation,
- vomiting,
- gastroesophageal reflux,
- distal oesophagitis
- cardial atony,
- gastritis, gastric retention,
- pyloric hyperplasia, stenosis and atony,
- duodenal inflammation.

EXPERIMENTAL METHODS

- 30 brachycephalic dogs (BOAS group), 21M, 9F, including 14 French bulldogs (FB), 9 Boston terriers (BST) and 7 pugs for surgical treatment of BOAS (folded flap palatoplasty and vertical edge alaplasty)
- two control groups
  - a group of non-brachycephalic dogs (7M, 8F)
  - control group of 11 (6M, 5F) brachycephalic dogs (FB, BST and pugs) undergoing surgery not related to BOAS
- fasting 14 hours, water deprivation two hours prior to anaesthesia.
- Statistical analysis (IBM SPSS, 25 Statistics): a one-way ANOVA with Tukey HSD post-hoc test (normal distribution) or Kruskal-Wallis test followed by multiple comparisons and Bonferroni correction (non-normal distribution) of the data, were used. A value of $P<0.05$ was considered significant

Anaesthesia for brachycephalic dogs

- premedication maropitant 1 mg/kg i.v.
- pantoprazole 0.78 – 1.18 mg/kg i.v.
- metoclopramide 0.17 – 0.26 mg/kg s.c.
- dexamethasone 0.09 – 0.16 mg/kg i.m.
- preoxygenation 100% O_2
- butorphanol 0.12 – 0.33 mg/kg i.v.
- midazolam 0.045 – 0.14 mg/kg i.v.
- propofol (2.1 – 13.1 mg/kg) i.v.
- intubated cuffed endotracheal tube
- isoflurane in 100% oxygen
- carprofen 3.2 – 4.1 mg/kg i.v.
- After recovery:
  - buprenorphine 0.01 - 0.02 mg/kg i.v.
  - carprofen 2 mg/kg for 5 to 7 days p.o.
  - metoclopramide 0,2 mg/kg BID 14 days p.o.
  - esomeprazol 1 mg/kg BID 14 days p.o.

CONCLUSION

Guidelines to choose the endotracheal tube size in dogs are based on normal body weight. However, these guidelines cannot be used for brachycephalic dogs, which is consistent with our findings that the internal diameter of the endotracheal tube was significantly smaller in all brachycephalic dog breeds.

Thus, we can assume that difficult breathing in certain brachycephalic dogs is mainly caused by airway obstruction by soft tissue rather than tracheal diameter. This was confirmed by the markedly improved breathing of brachycephalic dogs after nose and soft palate surgery.

The severity of respiratory and gastrointestinal signs were positively correlated in French bulldogs, males, and heavy brachycephalic dogs.

Because of the respiratory and associated gastrointestinal problems, all dogs undergoing surgical treatment for brachycephalic syndrome should receive gastroprotective drugs and antiemetics before and for at least 10 days after surgery to prevent vomiting, regurgitation, and aspiration pneumonia.

It is important that the anesthesiologist allow for a longer recovery time after anaesthesia in brachycephalic dogs and not overbook anaesthesia times.

When a brachycephalic dog is treated surgically for brachycephalic syndrome, an even longer recovery time is expected.

RESULTS

BOAS group had significantly higher body temperature in comparison to control group of brachycephalic dogs that underwent surgery not related to BOAS ($P = 0.024$).
Internal diameter of endotracheal tube was significantly smaller in BOAS group ($P < 0.001$) and control group of brachycephalic dogs ($P = 0.002$) in comparison to group of non-brachycephalic dogs. But there was no significant difference in endotracheal tube size between BOAS group and control group of brachycephalic dogs.

The time of extubation after general anaesthesia was significantly longer in BOAS group compared to group of non-brachycephalic dogs ($P < 0.001$) and control group of brachycephalic dogs ($P = 0.029$).
(table).

		Age (month)	Weight (kg)	Dogs n (M/F)	Temperature (°C)	HR (bpm)	ID endotracheal tube (mm)	Extubation time (min) after end of surgery	Duration time of anaesthesia (min)
		median (IQR)	mean ± SD		mean ± SD	median (IQR)	median (IQR)	median (IQR)	median (IQR)
FB		16.0 (11.0 - 35.5)	11.7 ± 2.2	14 (11/3)	38.8 ± 0.5	126 (100 - 131)	6.0 (5.5 - 6.0)	23 (19 - 31)	65 (54 - 80)
BST		55.0 (36.5 - 86.0)	9.2 ± 1,6	9 (7/3)	38.5 ± 0.5	120 (100 - 139)	5.5 (5.0 - 5.8)	20 (15 -30)	85 (60 - 98)
Pug		73.0 (33.0 - 93.0)	8.9 ± 1.4	7 (3/4)	38.5 ± 0.6	120 (110 - 172)	6.0 (5.5 - 6.0)	20 (15 - 20)	60 (50 - 65)
BOAS group (14 FB+9 BST+7 pugs)		38.0 (15.0 - 73.8)	10.3 ± 2.2	30 (21/9)	38.7 ± 0.5[a]	120 (100 - 136)	5.8 (5.5 - 6.0)	20 (16 - 30)[c]	65 (55 -80)
Group of non brachycephalic dogs		117.0 (14.0 - 148.0)	8.9 ± 1.9	15 (7/8)	38.6 ± 0.4	110 (88 - 122)	7.5 (7.0 – 8.0)[b]	7.0 (5 - 13)	55 (40 - 90)
Control group of brachycephalic dogs		86.0 (42.0 - 118.0)	10.5 ± 2.0	11 (6/5)	38.2 ± 0.6	120 (92 - 120)	6.0 (5.4 - 6.6)	12 (10 -17)	90 (60 - 100)

ID – internal diameter in mm; IQR interquartile range - 25th-75th percentile, F-female, M-male, FB-French bulldog, BST-Boston terrier, n-number of dogs, HR-hearth rate, bpm-beats per minute, a-significantly ($P = 0.0024$) higher compared to control group of brachycephalic dogs; b - significantly bigger compared to BOAS group ($P < 0.001$) and compared to control group of brachycephalic dogs ($P = 0.002$); c – significantly longer compared to group of non-brachycephalic dogs ($P < 0.001$) and compared to control group of brachycephalic dogs ($P = 0.029$).

LITERATURE

1. Aron DN, Crowe DT. Upper airway obstruction. General principles and selected conditions in the dog and cat. Vet Clin North Am Small Anim Pract. 1985; 891.
2. Doxey S, Boswood A. Differences between breeds of dog in a measure of heart rate variability. Vet Record. 2004; 154:713–717.
3. Downing F, Gibson S. Anaesthesia of brachycephalic dogs. J Small Anim Pract. 2018; 59:725–733.
4. Gruenheid M, Aarnes TK, McLoughlin A, et al. Risk of anesthesia-related complications in brachycephalic dogs. JAVMA 2018; 253: 301-6.
5. Roedler FS, Pohl S, Oechtering GU. How does severe brachycephaly affect dog's lives? Results of a structured preoperative owner questionnaire. Vet J. 2013; 198:606-10.
6. O'Dwyer L, Anaesthesia for the Brachicephalic Patient. WSAVA Congress proceedings 2017, Copenhagen, Denmark 25th - 28th September.
7. Poncet CM, Dupre GP, Freiche VG., et al. Long-term results of upper respiratory syndrome surgery and gastrointestinal tract medical treatment in 51 brachycephalic dogs. J Small Anim Pract. 2006; 47: 137-42.
8. Poncet C. M., Dupré G., Freiche V. G., et al. Prevalence of gastrointestinal tract lesions in 73 brachycephalic dogs with upper respiratory syndrome. *J Small Anim Pract* 2005; 46: 273–9.
9. Remingа C, King LG. Oxigenation and Ventilation. In: Kirby R, Linklater A, eds. Monitoring and intervention for the critically ill small animal. The rule of 20. Wiley Blackwell,UK 2017:109-136.

ACKNOWLEDGEMENTS

The authors acknowledge the financial support of the Slovenian Research Agency (Research program P4-0053).

Moreira, F. D., Oliveira Dias, E. H. 2020. Constructed wetlands in rural sanitation: A review. *Environmental Research*, 190: 110016
Ofori, S., Puškáčová, A., Ružíková, I., Wanner, J. 2021. Treated wastewater reuse: Pros and cons. *Science of The Total Environment*, 760: 14

Results of colorectal cancer treatment in General Hospital of Izola

Bojana Uršič[1], Tomaž Jakomin[2], Valentin Sojar[3]
[1]University Medical Center Ljubljana, Slovenia; [2]General Hospital of Izola, Slovenia; [3] MC Iatros, Ljubljana, Slovenia.

BACKGROUND

Colorectal cancer is the third most commonly diagnosed malignancy and the second leading cause of death from malignancy in the world (1). Due to this, it is necessary to raise awareness among people of the disease itself, provide early and rapid diagnostic approaches and appropriate surgical treatment. From 2009 an important impact on the number of colorectal cancer patients has Slovenian national screening program named Svit.

METHODS

We have performed a retrograde analysis of the data from patients with colorectal cancer admitted to General Hospital of Izola (GHI) for surgical treatment in the period from 1.1.2019 to 31.12.2020. According to International Classification of Diseases Tenth Revision (ICD-10) diagnoses for colorectal carcinoma patients were sorted by gender, age and type of operation (emergent/elective, laparoscopic/open). Furthermore, the type of operative resection and early postoperative complications were also assessed.

CONCLUSIONS

Colorectal cancer predominantly affects men in their 7th decade. In GHI, carcinoma of the rectum, sigmoid colon and ascending colon are the three most common locations that require surgery. Due to good and rapid diagnostics, only 10% of patients needed emergent surgery. In electively operated patients, laparoscopic resection was performed in a high percentage. In GHI, the percent of laparoscopic rectum resection is relatively high in comparison with some other health institutions.

RESULTS

- From 1.1.2019 to 31.12.2020, 201 patients with confirmed colorectal cancer were operated in GHI. 59% of them were male and 41% female, with an average age of 68.5 (68.1 male, 69.1 female).
- The three most prevalent sites for colorectal carcinoma according to ICD-10 were malignant neoplasm of the rectum (29.4%), malignant neoplasm of the sigmoid colon (22.9%), and malignant neoplasm of ascending colon (19.9%). Other 27.8% is mainly represented with malignant neoplasm of the caecum (C18.0), malignant neoplasm of the hepatic flexure (C18.3), malignant neoplasm of the transverse colon (C18.4), malignant neoplasm of splenic flexure (C18.5), malignant neoplasm of descending colon (C18.6) and malignant neoplasm of the rectosigmoid junction (C19.0).
- In 90% of cases, elective surgery was performed. Only 10% of patients needed emergent surgery. Laparoscopic resection was feasible in only 14% of the emergently operated patients. On the other hand, in the group of electively operated patients, laparoscopic resection was performed in 77%.
- Early postoperative complications were present in 10% of all operated patients (8% after elective surgery, 29% after emergent surgery).

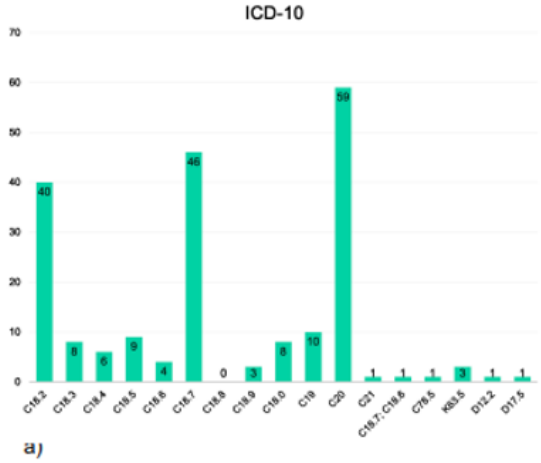

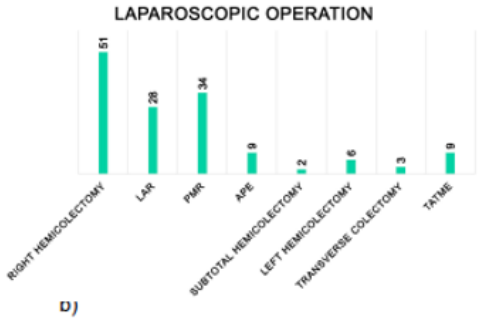

Figure 1: The number of patients with colorectal carcinoma according to ICD-10 (a), types and numbers of performed laparoscopic resections (b), types and numbers of performed open resections (c). Abbreviations: low anterior resection (LAR), parcial mesorectal resection (PMR), Abdominoperineal excision (APE), transanal total mesorectal excision (TATME).

1.) Sung H, Ferlay J, Siegel RL, Laversanne M, Soerjomataram I, Jemal A, et al. Global Cancer Statistics 2020: GLOBOCAN Estimates of Incidence and Mortality Worldwide for 36 Cancers in 185 Countries. CA Cancer J Clin. 2021;71(3):209–49.

Univerza v Ljubljani
Zdravstvena fakulteta

Univerza v Ljubljani
Fakulteta za kemijo in kemijsko tehnologijo

6th 2021 SOCRATIC LECTURES

Treatment wetland as a source of water and nutrients for agriculture

Anja Volk[1], Andreja Gotvajn Žgajnar[1], Darja Istenič[2,3]

[1]Faculty of Chemistry and Chemical Technology, Večna pot 113, 1000 Ljubljana, Slovenia; [2]Faculty of Health Sciences, Zdravstvena pot 5, 1000 Ljubljana, Slovenia; [3]Faculty of Civil and Geodetic Engineering, Jamova cesta 2, 1000 Ljubljana, Slovenia
Contact: Anja Volk: anja.volk1@gmail.com

OUTLINE

Nowadays, in accordance with the principles of the circular economy and the re-use of resources, we want to use treated water from treatment wetlands (TW) for the needs of fertilization and irrigation in agriculture. Wetlands usually operate to meet effluent discharge limits given in the legislation and release the treated water into a nearby watercourse or to the underground. If obliged by legislation, TW remove nutrients. In the case of reuse of treated water in agriculture, the removal of nutrients is undesirable, as it can replace part of the mineral fertilizers. Therefore the operation of the TW needs to be adjusted so that nutrients are not removed in the treatment process during the growing season, while removal must be ensured during winter.

In this research we monitored changes in efficiency of nutrient removal from municipal wastewater in TW with vertical flow by changing the operation mode of the wetland. Namely, by changing the flow through the TW we induced aerobic or aerobic-anaerobic conditions thus changing the removal of total nitrogen according to the seasonal dynamics of irrigation and fertilization in agriculture. Hereby the results from summer period are reported.

EXPERIMENTAL METHODS

The experiment was carried out on a pilot TW with vertical flow in the city of Ajdovščina, Slovenia. The TW (69.3 m^2) was intermittedly loaded with primary treated municipal wastewater. Total nitrogen, Kjeldahl N, NH_4-N, NO_2-N, NO_3-N, chemical oxygen demand (COD), biochemical oxygen demand (BOD), total suspended solids (TSS), pH, O_2, and electric conductivity were monitored at the inflow of the sedimentation tank, inflow and outflow from TW 3-times per week in July 2021. Summer mode of operation was the classical operation of a TW while winter mode will include recirculation of outflow to anaerobic pumping chamber.

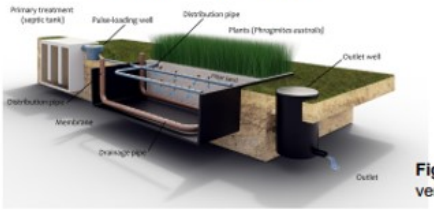

Figure 1: Scheme of treatment wetland with vertical flow.

CONCLUSION

- Vertical flow treatment wetland enables efficient removal of organic matter.
- Denitrification also takes place in the treatment wetland with vertical flow.
- Due to efficient nitrification, high levels of nitrate are present in the effluent, which is desirable for its application as fertilizer in the agriculture.
- Suspended solids are retained and degraded in the substrate of the treatment wetland.

RESULTS

The results are presented as „box and whiskers" plots for the three sampling points. Statistically significant differences were determined using single factor analysis of variance followed by t-test and are marked with a star in Figures 2-5.

Regarding **COD and TSS concentrations**, there was no statistically significant difference between the inflow to sedimentation tank and inflow to TW meaning that sedimentation tank does not provide efficient sedimentation of suspended solids. This is most probably due to high amount of accumulated sludge which should be removed from the system (Moreira and Oliveira Dias, 2020). Despite this, the TW enabled efficient removal of TSS and COD; the effluent concentrations were statistically significantly lower than the inflow concentrations (Figures 2 and 3) and were also below the legislation limits for discharge of treated water to the environment (EU Directive 91/271/EEC).

Regarding **nutrients**, TW enabled efficient nitrification; the effluent concentrations of NH_4-N were statistically significantly lower than the inflow concentrations. As expected, there was no nitrification in anaerobic sedimentation tank (Figure 4). The main advantage of TW with vertical flow is their high ability to oxygenate and thus the ability to nitrify (Brix and Arias 2005), so they have high concentrations of nitrate in the effluents (Figure 5). Statistically, the outflow concentrations were significantly higher than inflow concentrations. There were no statistically significant differences between sedimentation tank and inflow. Use of such treated water for crop irrigation can improve nitrogen content of soil by acting as a good source of inorganic nitrogen thus increasing the crop production (Ofori et al., 2021).

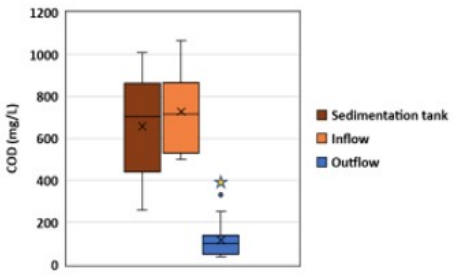

Figure 2: Chemical oxygen demand (COD) in the sedimentation tank, inflow and outflow from the treatment wetland.

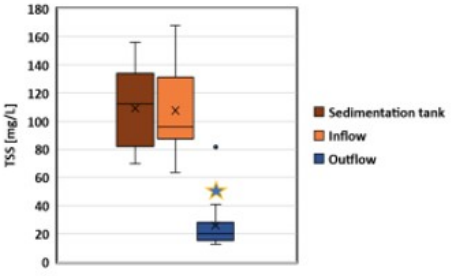

Figure 3: Total suspended solids (TSS) in the sedimentation tank, inflow and outflow from the treatment wetland.

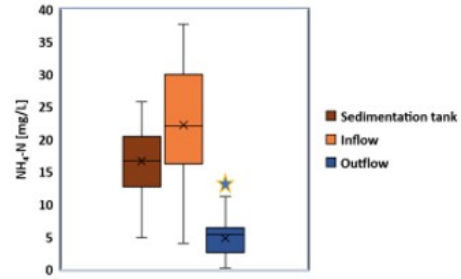

Figure 4: Ammonia nitrogen (NH_4-N) concentrations in the sedimentation tank, inflow and outflow from the treatment wetland.

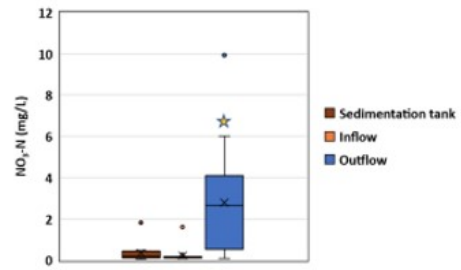

Figure 5: Nitrate nitrogen (NO_3-N) concentrations in the sedimentation tank, inflow and outflow from the treatment wetland.

REFEREFNCES

Arias, C. A., Brix, H. 2005. The use of vertical flow constructed wetlands for on-site treatment of domestic wastewater: New Danish guidelines *Ecological Engineering*, 25(5): 491–500.

Moreira, F. D., Oliveria Dias, E. H. 2020. Constructed wetlands in rural sanitation: A review. *Environmental* Researcsh, 190: 110016

Ofori, S., Puškáčová, A., Ružiková, I., Wanner, J. 2021. Treated wastewater reuse: Pros and cons. *Science of The Total Environment*, 760: 14

Scanning electron microscopy of microorganisms growing in co-cultures with microalgae

Božič D[1,2], Hočevar M[3], Jeran M[1], Matos T[4], Tomazin R[4], Pocsfalvi G[5], Iglič A[2,6], Kralj-Iglič V[1]

[1]University of Ljubljana, Faculty of Health Sciences, Laboratory of Clinical Biophysics, Ljubljana, Slovenia; [2]University of Ljubljana, Faculty of Electrical Engineering, Laboratory of Physics, Ljubljana, Slovenia; [3]Institute of Metals and Technology, Department of Physics and Chemistry of Materials, Ljubljana, Slovenia; [4]University of Ljubljana, Faculty of Medicine, Institute of Microbiology and Immunology, Ljubljana, Slovenia; [5] Extracellular Vesicles and Mass Spectrometry Laboratory, Institute of Biosciences and BioResources, National Research Council of Italy, Naples, Italy; [6] University of Ljubljana, Faculty of Medicine, Laboratory of Clynical Biophysics, Ljubljana, Slovenia.
Contact: Darja Božič: darja.bozic@zf.uni-lj.si

OUTLINE

Microalgae often grow in co-culture with different kinds of bacteria. While axenic cultures are hard to maintain, the co-cultured microorganisms are often not known. Many of the bacteria/archaea from the environmental samples cannot easily be cultivated.

In our study several microalgal cultures were analysed by scanning electron microscopy (SEM). The bacteria that could be isolated on standard solid media were analysed by matrix assisted laser desorption ionization-time of flight mass spectrometry (MALDI-TOF-MS).

EXPERIMENTAL METHODS

Microalgae cultures were grown at 20°C with 12h/12h light/dark ilumination cycle. Selected samples were subjected to antibiotic treatment (gentamycin, penicillin-streptomycin, and their combination).
SEM: Samples were osmium-fixed, ethanol-dehydrated, treated with hexamethyldisilazane and air-dried. Before visualization with a JSM-6500F Field Emission Scanning Electron Microscope (JEOL Ltd., Tokyo, Japan), the samples were Au/Pd coated (PECS Gatan 682).
Bacteria identification: Bacteria were isolated on standard solid media and analysed by MALDI-TOF-MS (Bruker Daltonik, Germany).

CONCLUSION

SEM analysis revealed a great heterogeneity of microorganisms in the samples. Many of them were found to be antibiotic-resistant. Some of bacteria were identified by MALDI-TOF-MS. Interestingly, the identified type of bacteria often did not mach the morphology of the prevailing microorganisms in the starting microalgal culture.

RESULTS

Microorganisms of diverse shapes were found in microalgal cultures. Only few of them efficiently grew on standard bacteriological solid media and could be identified by MALDI-TOF MS. Among the identified strains, there were no typical human-related ones. Often, the MALDI-TOF-MS-identified strain was not the one prevailing in the initial sample according to the SEM. E.g., *Microbacterium liquefaciens* and unidentified Gram-positive cocci were found after standard cultivation and MALDI-TOF-MS in the sample of microalgae culture shown in Figure 1. In the culture of *Dunaliella tertiolecta*, long-rodded strain prevailed according to the SEM (Figure 1) while *Staphylococcus felis* was the one identified by MALDI-TOF-MS. Many of the bacteria growing in the co-cultures with microalgae were found resistant to gentamicin and/or ampicillin/streptomycin treatment (e.g. Figure 2, and results not-shown). The number of particular morphologies of microorganisms regularly exceeded the number of different bacteria identified in them (e.g. only Gram-positive bacilli were recovered from *Tetraselmis chuii* culture shown in Figure 4). A question remains, which of the observed different morphologies pertain to different microorganisms and which to a single-strain shape plasticity and environmental adaptation. SEM imaging reveals the heterogeneity of microorganisms in the samples. However, sometimes, distinguishing between an organism, a part of an organism and a vesicle is hard even by visualization (Figures 5 and 6).

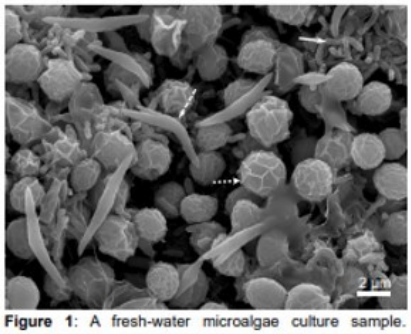

Figure 1: A fresh-water microalgae culture sample. Dotted arrow – a microalgae cell; full-line arrows – bacteria; dashed arrow – unidentified microorganism.

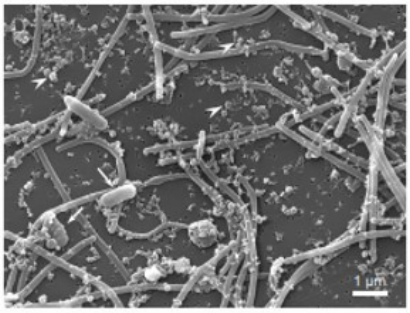

Figure 2: Bacteria from a culture of *Dunaliella tertiolecta*. Arrows – bacteria of various morphology; arrow-heads – vesicles.

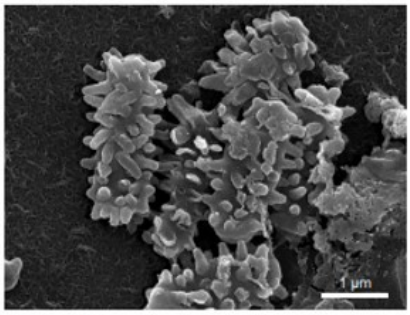

Figure 3: Bacteria/archaea in an isolate of EVs from the culture of *Phaeodactylum tricornutum*.

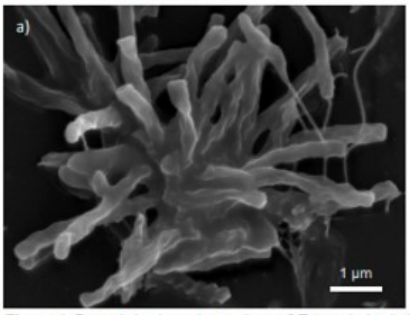

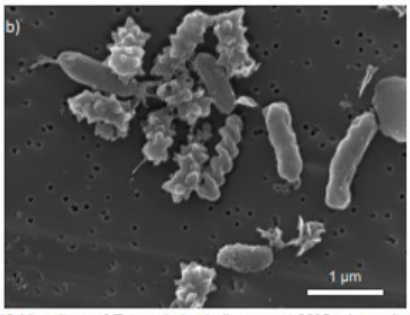

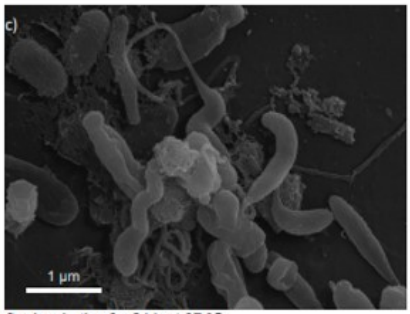

Figure 4: Bacteria/archaea in a culture of *Tetraselmis chuii*. a)& b): culture of *Tetraselmis chuii* grown at 20°C; c): a culture after incubation for 24 h at 37 °C.

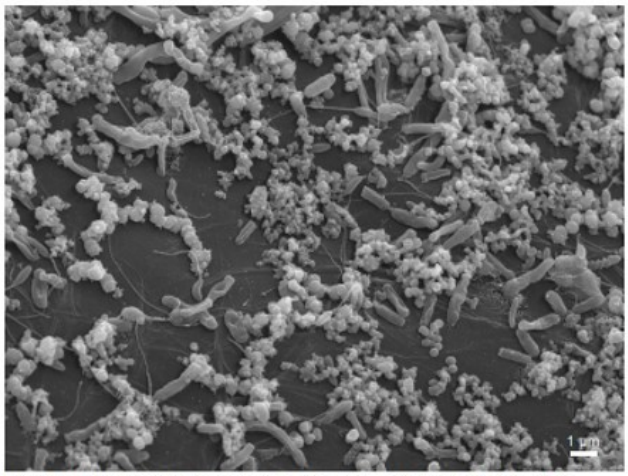

Figure 5: Bacteria and numerous vesicles in a sample of *Tetraselmis chuii* culture, incubated 24 h at 37 °C.

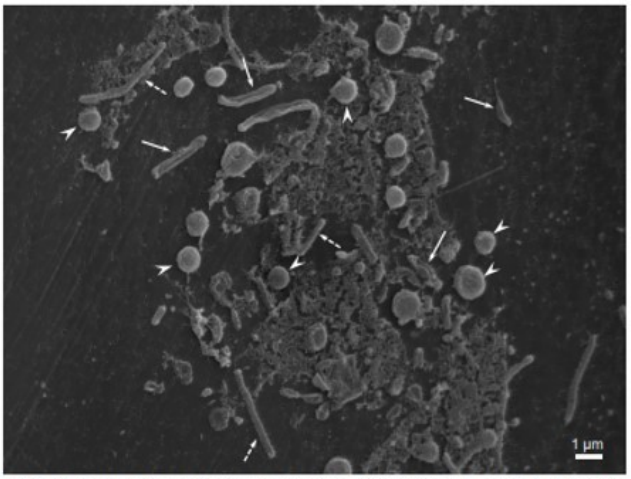

Figure 6: Bacteria, flagella remnants and vesicles in a sample of *Tetraselmis chuii* culture where flagellae amputation was induced by pH-shock. Full-line arrows – bacteria; dashed arrows – flagella remnants, arrowheads – micro-sized vesicles formed from the shedded flagella.

This research was supported by the European Union's Horizon 2020 Research and Innovation Program under Grant Agreement No. 801338 and by the Slovenian Research Agency through the core Fundings No. P2-0232, P3-0388, P2-0132, and Projects No. L3-2621 and J3-3066.

Removal of contaminants of emerging concern in algal photobioreactors: from lab-scale to pilot-scale

David Škufca[1,2], Franja Prosenc[3], Ana Kovačič[1,2], Gianluiggi Buttiglieri[4], David Heath[1,2], Tjaša Griessler Bulc[3*], Ester Heath[1,2*]

[1]Jožef Stefan Institute, Ljubljana, Slovenia; [2] Jožef Stefan International Postgraduate School, Ljubljana, Slovenia; [3] Faculty of Health Sciences, University of Ljubljana, Ljubljana, Slovenia; [4] Catalan Institute for Water Research, Girona, Spain.
* Contact: Prof Dr Ester Heath - ester.heath@ijs.si, Prof Dr Tjaša Griessler Bulc - tjasa.bulc@zf.uni-lj.si

OUTLINE

Contaminants of emerging concern (CEC) are organic pollutants occurring in wastewater which enter the environment due to insufficient removal during treatment. An alternative to conventional wastewater treatment are algal photobioreactors, which treat wastewater with low energy input. An important advantage is the production of nutrient- and energy-rich algal biomass and treated water, which both have the potential to be reused (e.g., agriculture and energy production). However, further studies are needed to perform risk assessment, future regulation and good practices for the safe reuse of algal biomass and reclaimed water in a circular economy.

EXPERIMENTAL METHODS

Chlorella vulgaris and a mixed algal culture from a high-rate algal pond (HRAP) were cultivated in small photobioreactors for laboratory experiments under Osram Fluora lights in BBM medium. A pilot-scale HRAP with a volume of 3000 L was fed with municipal wastewater and operated with a hydraulic retention time (HRT) of 5 days. CEC were extracted and purified by solid-phase extraction (SPE) and analysed by either GC-MS, GC-MS/MS or LC-MS/MS. Physicochemical properties of CEC were calculated by Marvin Suite. Acquired data was analysed and visualised using R in RStudio environment.

CONCLUSION

Most CEC removals in algal photobioreactors are comparable to conventional biological wastewater treatment, while algal photobioreactors offer the potential of water and biomass reuse. As some CEC remain recalcitrant, optimisation of operating parameters of algal photobioreactors, along with the development of suitable pre- or post-treatment to supplement algal wastewater treatment, is vital. Algae-based wastewater treatment shows promise for CEC removal and re-use of water and biomass. Efficient wastewater treatment with algal photobioreactors and regulation in the future will be established with continued study of CEC and their occurrence, removal, fate, and toxicity.

RESULTS

1 METHOD DEVELOPMENT

Analytical methods for sample preparation and GC-MS/MS analysis of 18 bisphenols in algal biomass and treated water were developed, optimised and validated.

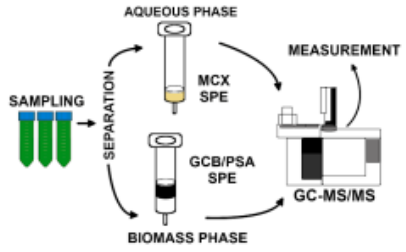

Publication: https://doi.org/10.1016/j.chemosphere.2021.129786

2 REMOVAL OF BISPHENOLS

Removal of 18 bisphenols ranged from 25% to 99%. Total removal was generally influenced by algae growth, compound hydrophobicity and in some cases by pH of the medium.

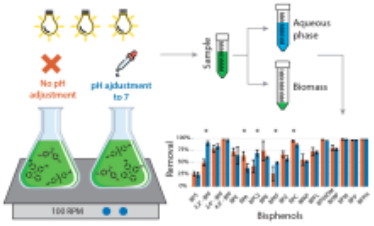

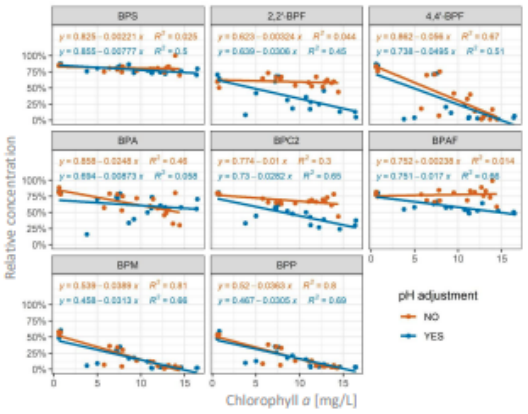

Publication: https://doi.org/10.1016/j.scitotenv.2021.149878

3 INCREASING COMPLEXITY

Removal of bisphenols, pharmaceuticals and pesticides (28 CEC) was studied and compared in pure and mixed cultures. Removal of individual compounds ranged from 2% to 99%. Average removal was 67% in the pure and 83% in the mixed culture.

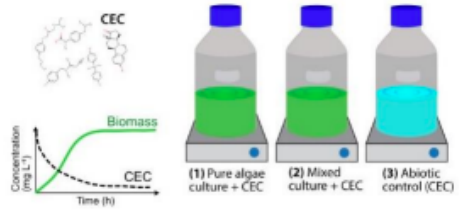

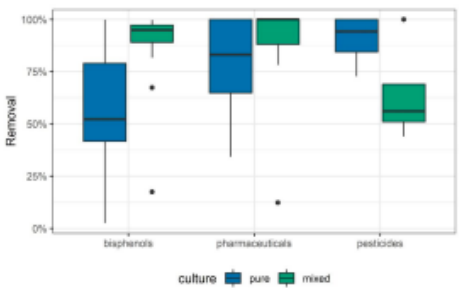

Publication: https://doi.org/10.1016/j.jhazmat.2021.126284

4 PILOT-SCALE HIGH-RATE ALGAL POND

Removal of nutrients and 7 CEC was studied in a HRAP fed by primary wastewater. CEC removal ranged from 32% to 92%.

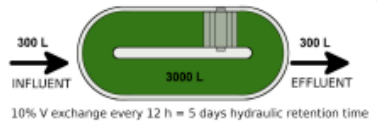

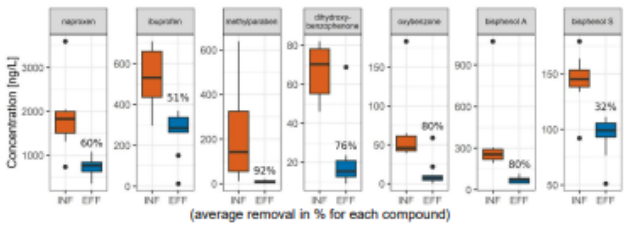

Publication: https://doi.org/10.1016/j.scitotenv.2021.146949

The study was performed with the financial support of the Slovenian Research Agency, namely Program Groups P1-0143, P3-0388 and Projects J2-8162, N1-0047, L1-9191, N1-0143 and L7-1848. This work was supported by project 18NMR01 that has received funding from the EMPIR program co-financed by the Participating States and from the European Union's Horizon 2020 research and innovation program.